US Army Corps of Engineers

HYDRAULICS LABORATORY

TECHNICAL REPORT HL-92-14

OUTLET WORKS FOR SEVEN OAKS DAM, SANTA ANA RIVER, SAN BERNARDINO COUNTY, CALIFORNIA

Hydraulic Model Investigation

by

Deborah R. Cooper

Hydraulics Laboratory

DEPARTMENT OF THE ARMY
Waterways Experiment Station, Corps of Engineers
3909 Halls Ferry Road, Vicksburg, Mississippi 39180-6199

October 1992

Final Report

Approved For Public Release; Distribution Is Unlimited

Prepared for US Army Engineer District, Los Angeles
Los Angeles, California 90053-2325

Destroy this report when no longer needed. Do not return it to the originator.

The findings in this report are not to be construed as an official Department of the Army position unless so designated by other authorized documents.

The contents of this report are not to be used for advertising, publication, or promotional purposes. Citation of trade names does not constitute an official endorsement or approval of the use of such commercial products.

REPORT DOCUMENTATION PAGE

Form Approved
OMB No. 0704-0188

1. AGENCY USE ONLY (Leave blank)	2. REPORT DATE	3. REPORT TYPE AND DATES COVERED
	October 1992	Final report

4. TITLE AND SUBTITLE
Outlet Works for Seven Oaks Dam,
Santa Ana River, San Bernardino County, California;
Hydraulic Model Investigation

5. FUNDING NUMBERS

6. AUTHOR(S)
Deborah R. Cooper

7. PERFORMING ORGANIZATION NAME(S) AND ADDRESS(ES)
USAE Waterways Experiment Station, Hydraulics Laboratory, 3909 Halls Ferry Road, Vicksburg, MS 39180-6199

8. PERFORMING ORGANIZATION REPORT NUMBER
Technical Report
HL-92-14

9. SPONSORING/MONITORING AGENCY NAME(S) AND ADDRESS(ES)
USAE District, Los Angeles, PO Box 2711,
Los Angeles, CA 90053-2325

10. SPONSORING/MONITORING AGENCY REPORT NUMBER

11. SUPPLEMENTARY NOTES
Available from National Technical Information Service, 5285 Port Royal Road, Springfield, VA 22161.

12a. DISTRIBUTION/AVAILABILITY STATEMENT
Approved for public release; distribution is unlimited.

12b. DISTRIBUTION CODE

13. ABSTRACT (Maximum 200 words)

A 1:25-scale physical model reproduced 225 ft of the surrounding topography upstream of the outlet works tower of Seven Oaks Dam, San Bernardino County, CA; the main tower with trash structure and the multilevel withdrawal tower; 50 ft of the 9-ft-diameter air vent shaft; and 748 ft of the 18-ft-wide by 9-ft-high rectangular open channel conduit. The model conduit discharged into a flume where the topography representing 1,600 ft of the exit channel was later installed. The main and multilevel withdrawal towers laid back into the mountainous terrain at a 4V on 1H slope and were connected by a 5-ft-wide by 7-ft-high gated passageway. Average and dynamic hydrostatic pressures in the outlet works structure, air demand in the midtunnel flow control section, average velocities in the open channel conduit, and scour potential downstream of the outlet works exit portal were measured. An energy dissipator at the exit portal was designed. Return velocities and wave heights in the plunge pool energy dissipator, the plunge pool apron stability, water-surface differentials across the apron, and uplift pressures along the roof of the midtunnel control section were obtained.

14. SUBJECT TERMS			15. NUMBER OF PAGES
Aeration	Hydraulic model	Seven Oaks Dam	194
Apron stability	Outlet works	Scour	16. PRICE CODE
Energy dissipator	Riprap		

17. SECURITY CLASSIFICATION OF REPORT	18. SECURITY CLASSIFICATION OF THIS PAGE	19. SECURITY CLASSIFICATION OF ABSTRACT	20. LIMITATION OF ABSTRACT
UNCLASSIFIED	UNCLASSIFIED		

PREFACE

The model investigation reported herein was authorized by the Headquarters, US Army Corps of Engineers (HQUSACE), on 12 April 1988 at the request of the US Army Engineer District, Los Angeles.

The studies were conducted in the Hydraulics Laboratory (HL) of the US Army Engineer Waterways Experiment Station (WES) during the period April 1988 to April 1991 under the direction of Messrs. F. A. Herrmann, Jr., Director of the Hydraulics Laboratory; R. A. Sager, Assistant Director of the Hydraulics Laboratory; and G. A. Pickering, Chief of the Hydraulic Structures Division (HSD), HL. The tests were conducted by Mrs. D. R. Cooper and Messrs. E. L. Jefferson and R. Bryant, Jr., of the Spillways and Channels Branch, HSD, under the direct supervision of Mr. N. R. Oswalt, Chief of the Spillways and Channels Branch. This report was prepared by Mrs. Cooper.

During the course of the investigation Messrs. F. Khroun, S. Bhamidipaty, and J. Leong of the US Army Engineer Division, South Pacific; D. Cozakos, B. Tracy, J. Evelyn, A. Jung, and M. Carlassare of the US Army Engineer District, Los Angeles; J. Stow, P. Etzel, B. Bird, T. Edminster, B. Branch, E. Daugherty, D. Chambers, L. Berre, and D. Illias of the US Army Engineer District, Portland; S. Powell and T. Munsey of HQUSACE; and Dr. H. T. Falvey, a consultant on cavitation and instrumentation, Conifer, CO, under contract to WES visited WES to discuss test results and correlate test results with current design studies that were under way by the Portland District.

Messrs. W. Landers, M. Simmons, and J. Lyons, Engineering and Construction Services Division, WES, constructed the outlet works tower, midtunnel flow control section, and conduit. Mrs. M. C. Gay, Information Technology Laboratory, WES, edited this report.

At the time of publication of this report, Director of WES was Dr. Robert W. Whalin. Commander was COL Leonard G. Hassell, EN.

CONTENTS

CONVERSION FACTORS, NON-SI TO SI (METRIC)
UNITS OF MEASUREMENT

Non-SI units of measurement used in this report can be converted to SI (metric) units as follows:

Multiply	By	To Obtain
cubic feet	0.02831685	cubic metres
Fahrenheit degrees	5/9*	Celsius degrees or kelvins
feet	0.3048	metres
feet of water (39.2 °F)	2.98898	kilopascals
inches	25.4	millimetres
miles (US statute)	1.609344	kilometres
pounds (force) per square inch	6.894757	kilograms
pounds (mass) per cubic foot	16.01846	kilopascals
square feet	0.09290304	square metres

* To obtain Celsius (C) temperature readings from Fahrenheit (F) readings, use the following formula: $C = (5/9)(F - 32)$. To obtain Kelvin (K) readings, use: $K = (5/9)(F - 32) + 273.15$.

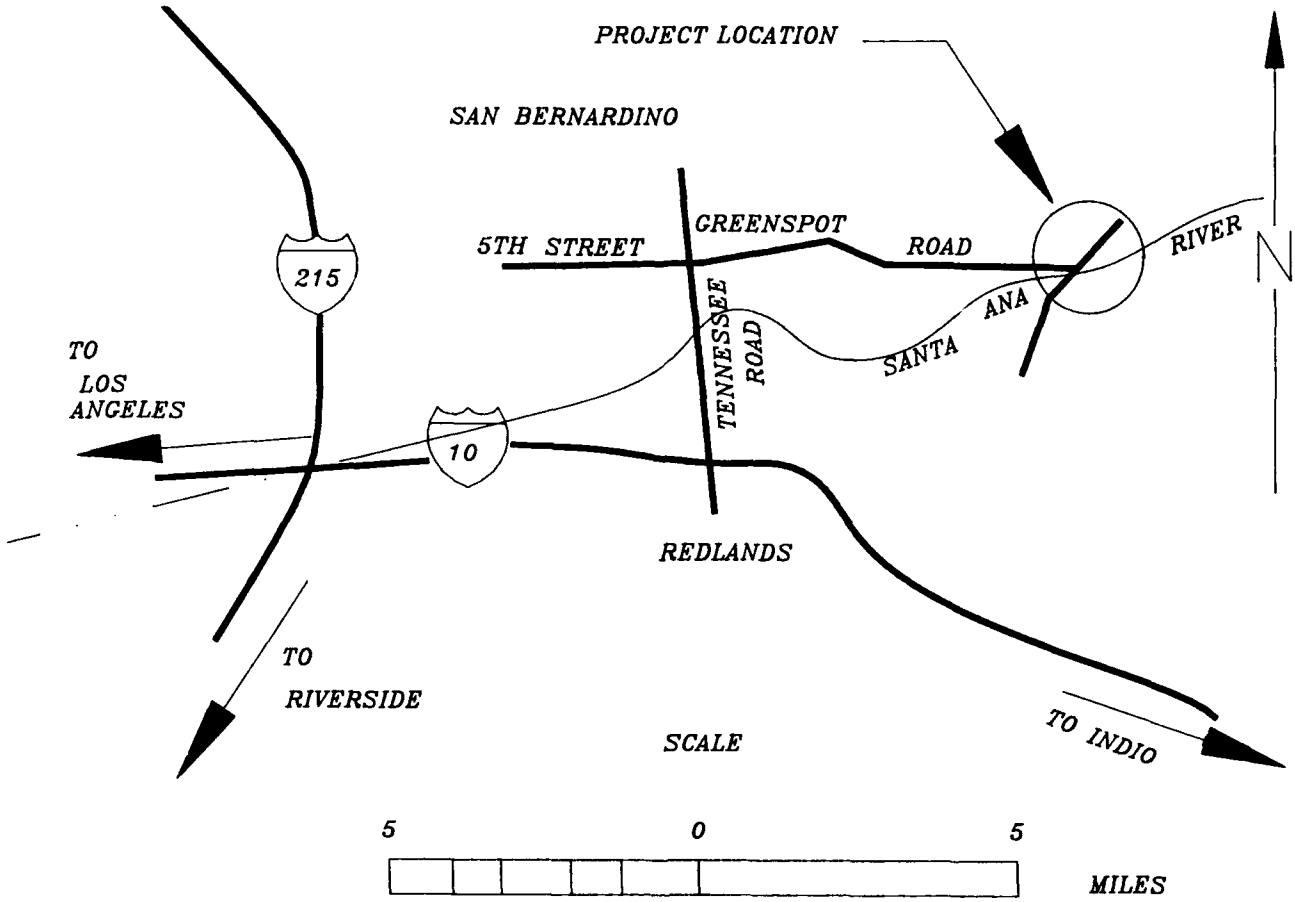

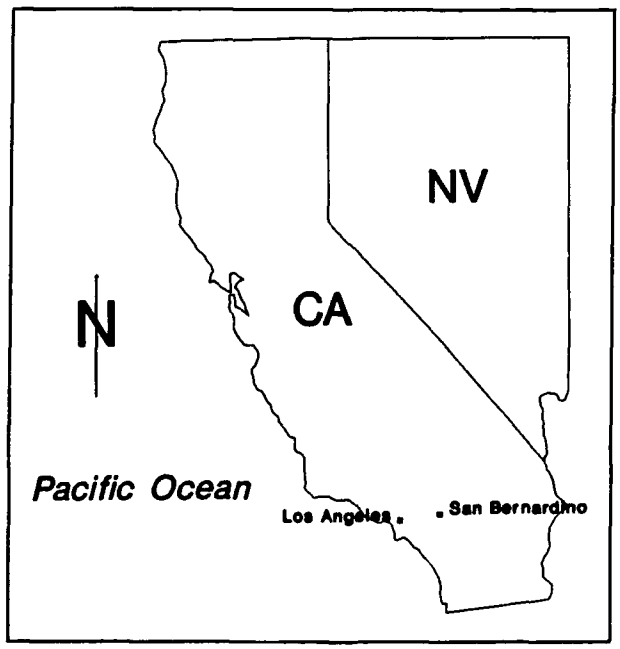

Figure 1. Location and vicinity maps

OUTLET WORKS FOR SEVEN OAKS DAM, SANTA ANA RIVER, SAN BERNARDINO COUNTY, CALIFORNIA

Hydraulic Model Investigation

PART I: INTRODUCTION

The Prototype

1. Seven Oaks Dam and Outlet Works is part of the Santa Ana Flood Protection Project to be located in the upper Santa Ana Canyon approximately 1 mile* from the canyon mouth. The site is 8 miles northeast of the city of Redlands, CA, in San Bernardino County on the Santa Ana River (Figure 1). The proposed dam will trap sediment and provide temporary storage during floods. The 18-ft-diameter outlet works tunnel will allow regulated flow release after major flood flows.

2. The outlet works, located within the east (left) abutment, will consist of an approach channel, a multilevel withdrawal intake structure inclined and anchored to foundation rock abutment (Plates 1 and 2), a pressurized diversion/outlet tunnel with a midtunnel control structure equipped with outlet works gates (Plate 3), and a downstream horseshoe diversion/outlet tunnel that will include an access passage, an exit channel, a valve structure, and a preexcavated plunge pool for energy dissipation. Maximum vertical height of the intake structure will be 225.5 ft, extending from el 2080** at the foundation to el 2305.5 at the top of the parapet. The high-level intake height will be 165 ft based on an expected sediment deposition over the project life from el 2100 to el 2265. The sill of the intake structure for flood flows (normal operating maximum of 8,000 cfs) will be located at el 2265. The structure was designed for operation under submerged conditions. Below el 2276, on the right side of the structure, will be the Multilevel Withdrawal System (MWS). This system will consist of 18 pairs of 27-in.-diameter intakes used to regulate the lower debris pool. The debris pool, after years of

---

* A table of factors for converting non-SI units of measurement to SI (metric) units is presented on page 3.

** All elevations (el) and stages cited herein are in feet referred to the National Geodetic Vertical Datum (NGVD).

reservoir sedimentation or a flood event at year zero, will submerge the intake structure. The high-level intake will consist of a concrete trash structure with 111 openings 3 ft 4 in. square covering the circular area from el 2265 to el 2295.5. The concrete-lined tunnel excavated through rock will be 1,656 ft long with a slope of 0.026. The tunnel, without gates and access, will be used to pass diversion flows. Regulating outlet gates will be located in a concrete-lined dome chamber approximately 600 ft upstream of the downstream portal. Air supply to the tunnel downstream of the gates will be provided through a shotcrete vertical shaft with an air supply structure at the surface approximately 1,000 ft downstream of the tunnel entrance. Access roads will be provided to the intake structure deck, the air supply structure, and the downstream access structure.

Purpose and Scope of the Model Study

3. Because of the high head and complicated design of the structure, this model study was conducted at the US Army Engineer Waterways Experiment Station (WES) to evaluate the hydraulic design by measuring dynamic hydrostatic pressures in the outlet structure. Zones of potential cavitation and air demand at the midtunnel were determined. The adequacy of the intake tower, the outlet plunge pool, and the exit channel design was also evaluated. Determination of the extent of scour and the need for protection downstream of the structure was of interest. Discharge characteristics of the regulating outlet (RO) gates with various operating scenarios were determined from the model.

Presentation of Data

4. In the presentation of test results, no attempt is made to introduce the data in the chronological order in which the tests were conducted on the model. Instead, as each element of the structure is considered, all tests conducted thereon are discussed in detail. All model data are presented in terms of prototype equivalents. All tests are discussed in Part III.

PART II: THE MODEL AND TEST PROCEDURE

Description

Type 1 design

5. Initially the 1:25-scale model (Figure 2) reproduced the following features:

a. 225 ft (prototype) of the surrounding topography upstream of the outlet works tower (Plate 1).

b. The 200-ft-high main tower with trash structure and the multilevel withdrawal tower (Plate 2).

c. The 60-ft-long transition from the 7-ft-wide by 13.75-ft-high conduit to an 18-ft-diameter conduit.

d. 895.5 ft of the 18-ft-diameter pressure conduit.

e. The 45-ft-long transition from the 18-ft-diameter conduit to the midtunnel flow control section.

f. The 158.5-ft-long midtunnel flow control section (Figure 3) with two 5-ft-wide by 9-ft-high vertical slide gates in the regulating outlets; the 5-ft-wide by 9-ft-high regulating outlet emergency gate slots; one 2-ft-wide by 3.5-ft-high vertical slide gate in the low-flow discharge conduit; two 60-ft-long piers; and the 1-ft vertical and 0.5-ft horizontal offsets downstream of the gates.

g. 50 ft of the 9-ft-diameter air vent shaft (Plate 3).

h. 748 ft of the 18-ft-wide by 9-ft-high rectangular open channel conduit.

The model conduit discharged into a 1,600-ft-long by 875-ft-wide flume where the topography was later installed. The main and multilevel withdrawal towers were laid back into the mountainous terrain at a 4V on 1H slope and were connected by a 5-ft-wide by 7-ft-high gated passageway (Plate 2) that remained closed during rising pool tests and was opened during falling pool tests. The portion of the model representing the upstream topography was molded in screen wire to plywood templates and painted with waterproof paint. The model tower, conduit, gates, and midtunnel flow control section were constructed of transparent plastic to allow for visual observation of hydraulic flow conditions. The original design is referred to as the type 1 design midtunnel.

Type 2 design

6. Operation of the model through the full range of discharges Q indicated loss of aeration under the gates at gate openings G_o of 7 ft and

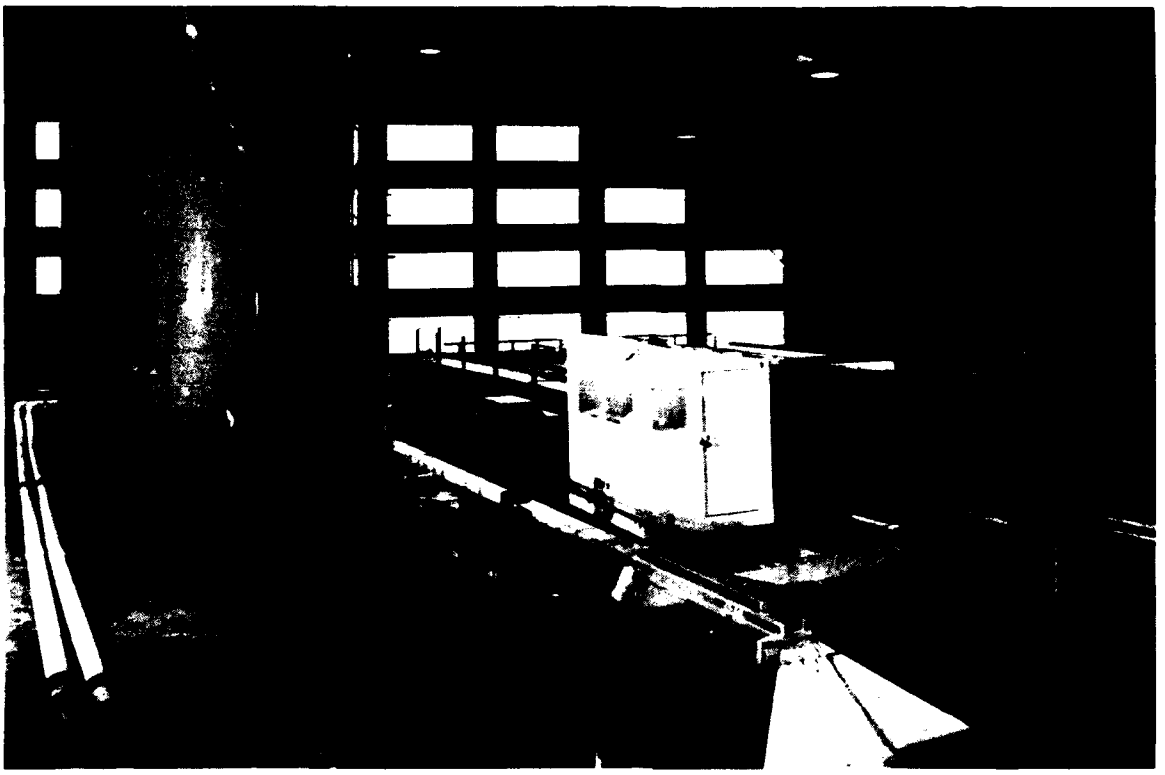

Figure 2. 1:25-scale model

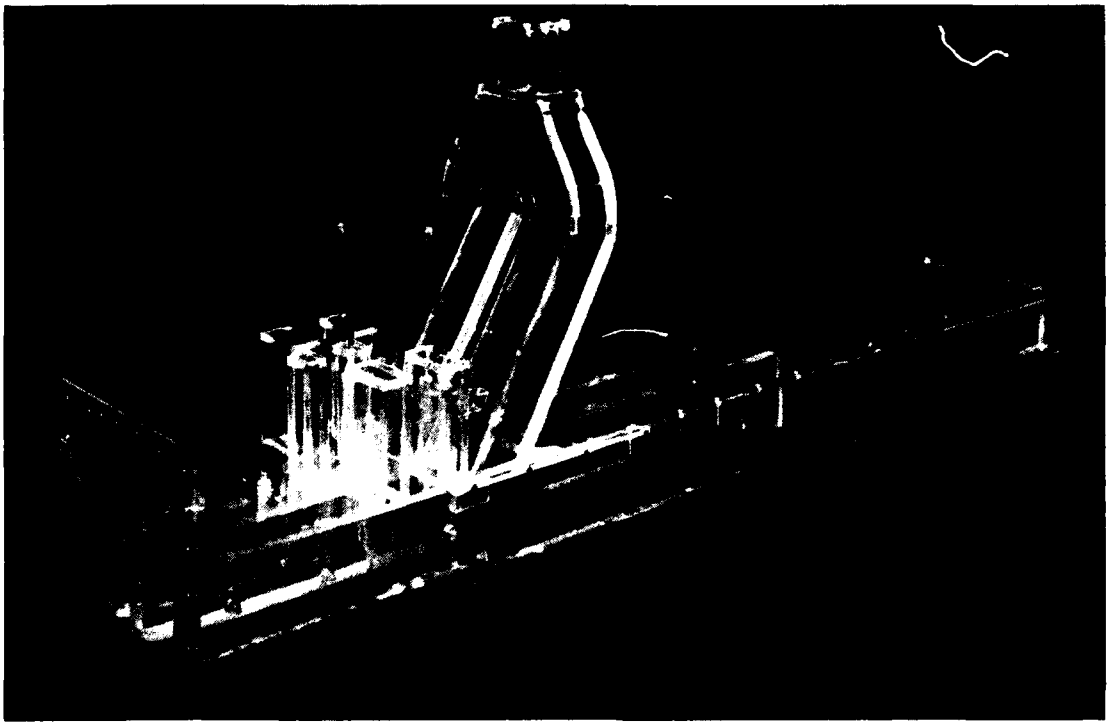

Figure 3. Midtunnel flow control section

above. The type 1 (original) design was modified to the type 2 design midtunnel control section (Plate 4). The model floor in the gate chambers and at the offset was raised 0.5 ft (effectively decreasing the regulating outlet gate to 8.5 ft high) and the piers were shortened 60 ft upon the recommendation of Dr. Henry T. Falvey* and engineers from the US Army Engineer Districts, Portland and Los Angeles.

Type 3 design

7. A 0.52-ft-square mesh of 0.05-ft-diameter wire was mounted for added roughness on the sides, crowns, and inverts of both regulating gate chambers between the gate and the offset of the type 2 design midtunnel flow control section in the type 3 design (Plate 5) to evaluate air demand at the gate offsets.

Type 4 design

8. Because of the need for structural support of the midtunnel roof, the type 2 design midtunnel flow control section was modified to include 9-ft-long pier extensions in the type 4 design midtunnel shown in Plate 6.

Appurtenances and Instrumentation

9. Water used in the operation of the model was supplied by pumps, and discharges were measured with orifice meters. The tailwater in the downstream end of the model was controlled by an adjustable tailgate. Steel rails set to grade provided reference planes. Water-surface elevations were obtained with point gages. Velocities were measured with a pitot tube and an electromagnetic velocity meter. Load cells and a voltmeter were used to measure and record the magnitude and frequency of the total forces acting on the sides and crown of the conduit.

Scale Relations

10. The accepted equations of similitude, based upon the Froudian relations, were used to express the mathematical relations between the dimensions and hydraulic quantities of the model and the prototype. General relations

---

* Personal Communication, 12 June 1990, Dr. Henry T. Falvey, Consultant, Conifer, CO.

for the transference of model data to prototype equivalents are presented in the following tabulation.

Characteristic	Dimension*	Scale Relation Model:Prototype
Length	$L_r = L$	1:25
Area	$A_r = L_r^2$	1:625
Velocity	$V_r = L_r^{1/2}$	1:5
Discharge	$Q_r = L_r^{5/2}$	1:3,125
Time	$T_r = L_r^{1/2}$	1:5
Weight	$W_r = L_r^3$	1:15,625
Force	$F_r = L_r^3$	1:15,625

* Dimensions are in terms of length.

Friction Losses

11. The model was constructed of plastic with an absolute roughness height of less than 0.00005 ft. Initially, as a best approximation, the smooth pipe curve from the US Army Corps of Engineers Hydraulic Design Criteria (HDC) Chart 224-1* was used to calculate friction coefficients to be used in head loss computations. Losses through individual components were later calculated by Falvey** from dimensionless coefficients derived from model data, which will be discussed in paragraph 32.

12. The ability to predict the behavior of the prototype with the model, or the similitude of the two structures, varies. Discharge and changes in cross-sectional area (velocity) along the structure will vary the degree of similitude. The model was expected to be rougher than the prototype throughout the dischar ⁵ range, particularly for flows greater than 4,000 cfs. To

* US Army Corps of Engineers. "Hydraulic Design Criteria," prepared for Headquarters, US Army Corps of Engineers, by US Army Engineer Waterways Experiment Station, Vicksburg, MS, issued serially since 1952.

** Personal Communication, 16 January 1991, Dr. Henry T. Falvey, Consultant, Conifer, CO.

compare model data against analytical data, WES computed the head loss across the 18-ft-diameter pipe using the energy equation. The Reynolds number was computed for the model at 8,000 cfs using the following equation:

$$Re_m = \frac{V_m D_m}{\nu} = 3.74 \times 10^5 \qquad (1)$$

where

Re_m = Reynolds number in the model

V_m = velocity in the model as calculated by

$$\frac{8000 \div \frac{\pi(18)^2}{4}}{\sqrt{25}}$$

D_m = diameter of model pipe = 18/25, ft

ν = kinematic viscosity of water at 60 °F = 1.21 x 10^{-5}, ft^2/sec

Using HDC Chart 224-1 gives a friction factor of 0.014. Head loss in model equivalents was then computed using the Darcy-Weisbach formula as

$$h_{l_m} = \frac{fL_m}{D_m}\frac{V_m^2}{2g} = \frac{(0.014)\left[\frac{821.76}{25}\right]}{\left[\frac{18}{25}\right]}\frac{(31.44)^2}{(2)(32.2)} = 0.392 \qquad (2)$$

where

h_{l_m} = head loss in model pipe

f = Darcy-Weisbach friction factor = 0.014

L_m = model pipe length = (821.76/25), ft

D_m = model pipe diameter = 18/25, ft

V_m = velocity in the model pipe = 31.44 ft/sec

g = acceleration of gravity = 32.2 ft/sec^2

The model head loss over the 18-ft-diameter pipe was found to be 8.83 ft, equivalent to 0.3532 ft in the model. The difference between the computed values and the model value of 0.0388 ft represented approximately 0.2 percent of the 20.15 ft of head on the gate in the model. This demonstrated a high

degree of similitude. Therefore, it was concluded that the model would adequately simulate the head losses over the entire range of discharges studied and there was no need to change the length of the tunnel section in the model to better reproduce the energy grade line at the midtunnel section.

Test Procedure

13. Average hydrostatic pressures in the conduit were measured in the model with Bourdon gages and piezometers. The pressure taps were located as shown in Plates 7-9. Hydrostatic pressures were measured with Bourdon gages at pressure tap locations 1-52 and with piezometers at pressure tap locations 53-120 and A-E. Dynamic pressures were measured with electronic pressure cells mounted flush with the floor and left sidewall of the midtunnel flow control section as shown in Plate 9. The elevation of the hydraulic gradient was determined using the differential pressures detected by seven pressure cells connected to piezometers in the pressure conduit and upstream of the gates as shown in Plates 7-9. The locations of the dynamic and differential pressure cells are tabulated in Tables 1 and 2. The differential pressures were subtracted from the pool elevation to obtain the hydraulic gradient elevations. The electronic pressure cells were used to measure instantaneous pressure fluctuations due to hydraulic forces that occurred due to the high-velocity flow passing over offsets in the boundary of the conduit. The differential pressure cells were used to measure the losses in the pressure conduit and develop a hydraulic grade line for each test condition.

14. Prior to the start of a test, the force-measuring equipment was checked to ensure that it was working properly and the water level of the upper pool was properly adjusted. The force-measuring device, having been previously zeroed, was then placed in operation. All force data presented in tables were measured in this manner.

PART III: TESTS AND RESULTS

Outlet Works

Type 1 (original) design

15. Initial tests were conducted to determine the discharge rating curves for the type 1 (original) design midtunnel control section (Plate 3) for 2-, 4-, and 6-ft gate openings. During these tests a bulkhead was sealed in the low-flow emergency gate slot (Plate 3). The reservoir pool elevation was measured using an electronic pressure cell mounted flush with the steel tank housing the reservoir and verified using a Tygon tube water level indicator. Various constant discharges were introduced into the model, and the upper pool was allowed to stabilize. Basic model calibration curves for flow through both regulating outlet gates were developed and are compared to the gate calibration curves computed by the Portland District in Plate 10. The basic calibration data for the type 1 (original) design are tabulated in Table 3. For gate openings of 4 ft and less, the model discharge coefficients were within 3 percent of the values recommended in HDC Chart 320-1* (Plate 11) as shown in Table 3. The high discharge coefficients for gate openings of 6 ft and greater were caused by the location of the piezometers, which determined the upstream energy grade line. Due to these piezometers being out of the stagnation zone at gate openings of 6 ft and above, the total energy measured just upstream of the midtunnel gates was not precise.

16. An underwater camera was installed in the model immediately downstream of the outlet works intake, and visual observations were made from an observation deck inside the steel headbay tank above the outlet works tower. Observations were made for any vortex formation in the outlet works intake, at the trash structure intakes, in the main wet well, or MWS wet well through the full range of operation. The upper pool elevation was set at el 2580 and was allowed to fall to el 2150 with the 5- by 7-ft passageway connecting the wet wells open. No vortices were observed during these tests. The 5- by 7-ft passageway connecting the wet wells was closed and the pool was raised from el 2150 to el 2580. No vortices were observed during these tests.

---

* US Army Corps of Engineers, op. cit.

17. Hydrostatic pressures in the outlet works intake roof and along the center line indicated no zones of potential cavitation.

18. Hydrostatic pressure measurements, recorded in feet of water, are shown in Table 4. The elevations of the hydraulic gradient plotted from the differential cell data and the corresponding pressure coefficients for various flow conditions are shown in Plates 12-14. The basic differential pressure data are tabulated in Table 5.

Type 2 design

19. During the operation of the model through the full range of discharges, a reduction in aeration under the gates at gate openings of 7 ft and above was indicated. The type 1 (original) design midtunnel was modified, at the recommendation of Dr. Falvey* and engineers from the Los Angeles and Portland Districts to the type 2 design midtunnel (Plate 4) by elevating the invert in the gate chambers 0.5 ft (effectively decreasing the regulating outlet gate to 8.5 ft high and the low-flow gate to 3.0 ft high) and shortening the piers 60 ft. This increased the bottom offset at station 22+12 to 1.5 ft. Also, the differential pressure cell at station 20+00 was moved to station 21+00; two additional differential pressure cells were installed at pressure tap locations 16 and 17 (Plate 15) to measure losses through the transition from the 7-ft-wide by 13.75-ft-high to 18-ft-diameter conduit; and an additional pressure tap, 63A (Plate 16), was installed 9.3 ft upstream of the right regulating outlet gate in the crown.

20. Tests were conducted to determine what effect the modifications in the type 2 design had on discharge calibration curves. Results of these tests are shown in Table 6. These data are also shown in Plate 10. As can be seen from the data obtained with the types 1 and 2 designs (Plate 10), raising the floor 0.5 ft and shortening the piers 60 ft had no significant effect on the gate rating curves.

21. Hydrostatic pressure measurements obtained with the type 2 design are tabulated in Table 7. Dynamic pressure transducer data, recorded in feet of water, are tabulated in Tables 8-11. As shown in these tables, the minimum pressure P_{min} was extremely low for some of the cells. Actual time-history plots of the dynamic pressures detected by each pressure cell are shown in

---

* Personal Communication, 13 June 1990, Dr. Henry T. Falvey, Consultant, Conifer, CO.

Plate 17 for one test condition. Plate 18 shows a typical time-history plot and the various tabulated values. The actual time-history plots show large negative pressure spikes in some of the transducers.

22. The dynamic pressure measurements were made with piezoresistive transducers. The conventional piezoelectric transducer is not capable of measuring static head; however, it can measure dynamic pressure fluctuations accurately. The piezoresistive transducer is a new development, designed to determine both static and dynamic pressure fluctuations. The model investigations indicated that the piezoresistive transducers were extremely sensitive to temperature. During a test, the zero was observed to drift by 65 ft (prototype). To eliminate the effect of the zero drift, measurements of the static pressure were made with a piezometer at each transducer location. Then the data were adjusted so that the mean output from the piezoresistive transducer coincided with the average reading of the piezometer. It was assumed that the dynamic fluctuations would be accurate. Interpretation of the output from transducers located in a region of intermittent contact with the water is difficult. All of the measurements in this zone are characterized by large negative spikes. The maximum value of the pressure fluctuation is normally within two to four standard deviations of the mean value. However, the magnitude of the negative spikes varied between 6 and 15 standard deviations from the mean value. For transducers that are always covered with water, both the positive and negative peak values are within two to four standard deviations from the mean value. As will be discussed later, the value of the cavitation index σ , not absolute values of pressure, is important with respect to the prediction of cavitation damage. The transducers were located downstream from the service gates (Plate 9) in an environment subject to severe turbulence, high velocity, and high air entrainment. Falvey indicated that the large negative pressures could have been caused by the sudden change in temperature between the water and air as the probe was alternately immersed in the water and then exposed to the air.* Also, the random impact of water on the cells could generate these spikes. In any event, the large subatmospheric pressures indicated in Tables 8-11 are not representative of the actual minimum pressures and should be disregarded. These spikes had little effect on the

* Personal Communication, 16 January 1991, Dr. Henry T. Falvey, Consultant, Conifer, CO.

average dynamic pressures since they were of such short duration. The average pressure readings indicated no zones of potential cavitation.

23. The elevations of the hydraulic gradient plotted from the differential cell data for various flow conditions with the type 2 design are shown in Plates 19-21. The basic data are tabulated in Table 12.

24. Although the quantity of air cannot be precisely scaled in a model of the scale used in this study because of the difference in turbulence in the model and prototype, a qualitative analysis can be conducted to determine if modifications are effective in increasing air demand and to predict if aeration will occur in the prototype. Although the velocity of air flow in the air shaft was not measured with the original design, the air flow was felt by hand and observed from streaks of injected smoke. For the type 2 design, air velocities in the air shaft were measured with an anemometer in addition to observing the air flow as was done for the original design. These observations and test results showed that air demand was increased by the modifications in the type 2 design. The test results (Plate 22) indicated that air demand increased with increasing gate openings, peaked at a 6-ft gate opening, and declined with increasing gate openings greater than 6 ft. The basic data are tabulated in Table 13.

25. Dynamic pressure cell data were collected for gate openings of 2, 4, 6, and 7 ft at higher pool elevations and higher Reynolds numbers. Pressure cell data are tabulated in Tables 14-20. Three tests were repeated to verify the average dynamic pressure data and the stability of the instrumentation as the temperature changed. The average dynamic pressures were very close for all repeat tests. Tables 15, 17, and 19 are repeat pressure measurement tests.

Type 3 design

26. In order to evaluate the capability of a model to simulate air demand and air bulking in the prototype, the model friction can be artificially increased and tests conducted to determine if there is a significant difference in air demand. If the model is not capable of estimating the air demand for the prototype, there will be a significant difference in air demand with different levels of turbulence (boundary roughness) in the model. As described in paragraph 7, a 0.52-ft-square mesh of 0.05-ft-diameter wire was mounted on the sides, crowns, and inverts of both regulating gate chambers between the gate and the offset (type 3 design midtunnel) to determine if the

added model roughness would affect the air demand. Air demand in the model air vent did not significantly change due to the artificial roughness in the model as indicated by comparing the type 2 and 3 designs in Plate 22. The air velocity data are tabulated in Table 13. Thus, it was concluded that the model was properly estimating the air demand and that aeration will occur in the prototype.

Type 4 design

27. Because of the need for structural support of the midtunnel roof, the type 2 design midtunnel flow control section was modified to include 9-ft-long pier extensions in the type 4 design midtunnel shown in Plate 6. The 0.52-ft-square mesh of 0.05-ft-diameter wire was removed from the sides, crowns, and inverts of both regulating gate chambers between the gate and the offset.

28. Hydrostatic pressure measurements obtained with the type 4 design midtunnel flow control section are recorded in feet of water in Table 21. Dynamic pressure data, recorded in feet of water, are tabulated in Tables 22-25. Again, note the minimum pressure P_{min} was extremely low at some locations (10P and 12P) similar to the type 2 design (Table 14). This phenomenon was previously discussed in paragraphs 21 and 22. The elevations of the hydraulic gradient plotted from the differential cell data for various flow conditions are shown in Plate 23. The basic differential pressure data are tabulated in Table 26.

29. Six dynamic pressure transducers were mounted flush with the midtunnel roof to measure uplift forces where the water jet impacts the roof (Plate 24). The locations of the pressure transducers are listed in the following tabulation:

Cell	Station
1	22+68.25
2	22+76.75
3	22+83.25
4	22+92
5	23+05.5
6	23+18

Dynamic pressure fluctuations along the midtunnel flow control section roof were measured for 5,000, 6,000, 7,000 and 8,000 cfs using the maximum

operating rating curve provided by the Portland District (Plate 10). Impact points of the jet along the roof are listed in the following tabulation:

Q	Pool El	Station
5,000	2300	23+08.25
6,000	2370	22+95.75
7,000	2500	22+93.25
8,000	2580	22+92

Pressure fluctuations are tabulated in Table 27. The maximum uplift pressure on the midtunnel roof was 23 ft of water, which occurred at station 22+92 with a pool elevation of 2580 and a discharge of 8,000 cfs. Hydrostatic pressure measurements obtained with the type 4 design and dynamic pressure data, recorded in feet of water, indicated no zones of potential cavitation; therefore, the type 4 design midtunnel flow control section was recommended for prototype construction.

Losses through the system*

30. The rugosity used for the prototype roughness was 0.00035 ft. The Darcy-Weisbach friction factor in the prototype is 0.009. In terms of the velocity head at the gates, the loss coefficient is 0.0547. The Darcy-Weisbach friction factor in the model was determined from the differential transducers located at stations 15+00 and 20+00. The results are given in the following tabulation:

Discharge cfs	Reynolds Number	f_{smooth}	f_{model}
2,000	8×10^4	0.019	0.022
5,000	2×10^5	0.016	0.021
8,000	3.2×10^5	0.014	0.016

These results indicated that the model was actually rougher than a smooth pipe. The increased roughness over that of a smooth pipe may have been due to the pipe being made in sections. Each joint produced an irregularity in the boundary that led to singular losses.

31. The effect of the higher friction in the model on the total head loss in the model, on the head across the gate, and on the discharge in the model was estimated from several discharges. The percent error in these

* Personal Communication, 16 January 1991, Dr. Henry T. Falvey, Conifer, CO.

various quantities, caused by the increased friction in the model, are given in the following tabulation:

Discharge cfs	Reservoir El	Percent Error: Head Loss	Percent Error: Head Across Gate	Percent Error: Discharge
2,000	2300	8	-0.2	-0.1
5,000	2300	6	-2	-1
8,000	2577	4	-1	-0.5

The percent losses are expressed as a percent of the total head loss in the tunnel and across the gate, respectively. It can be seen that the effect of the higher friction losses in the model is negligible with respect to the rating curves for the structure. This small effect is caused by the loss coefficient for the 18-ft-diameter conduit being only 7 percent of the total loss coefficient between the reservoir and the gates.

32. The losses through individual components of the outlet works were calculated from dimensionless pressure drop coefficients C_p derived from the differential head measurements. The equation for the differential head is given by

$$\Delta H_x = (K_x + 1) \frac{V_x^2}{2g} = C_{px} \frac{V_x^2}{2g} = E_r - E_x \tag{3}$$

where

ΔH_x = differential head between reservoir and station x, ft

K_x = head loss coefficient

V_x = average velocity at station x or the mean velocity at some reference station, ft/sec

g = gravitational acceleration, ft/sec^2

C_{px} = pressure coefficient = $(2g\Delta H_x)/V_x^2$

E_r = potential head at reservoir (pressure plus elevation head), ft

E_x = potential head at station x, ft

The loss across any component of the outlet works, such as a transition, is given in terms of the pressure coefficients as

$$h_{lt} = \left[C_{pd} - C_{pu}(A_d/A_u)^2 - 1(A_d/A_u)^2\right] \frac{V_d^2}{2g} \quad (4)$$

where

h_{lt} = head loss across transition, ft

C_{pd} = pressure coefficient downstream of transition

C_{pu} = pressure coefficient upstream of transition

A_d = cross-sectional area downstream of transition, ft^2

A_u = cross-sectional area upstream of transition, ft^2

V_d = mean velocity at some reference station, ft/sec

In Equation 3, the pressure coefficients were determined based on the mean velocity at their respective reference stations.

33. The intake loss coefficient for the multilevel intake is 1.727 ± 0.283 from differential head tests listed in Table 28. The intake loss includes all of the losses between the reservoir and the beginning of the 18-ft-diameter tunnel. The loss is based on the velocity head in the 18-ft-diameter tunnel. In terms of the velocity head immediately upstream of the midtunnel gates (8.5 ft high and 5.0 ft wide), the intake loss coefficient is 0.193 ± 0.032. The value used by the Portland District was 0.179.

34. The model contains three form losses that will not be found in the prototype: a 10-in. gate valve, a propeller flowmeter, and construction joints between the Plexiglas sections. The valve is located at station 14+55 and the flowmeter is located at station 17+27. The gate valve includes a 1:1.157 expansion upstream of the valve and a 1:0.864 contraction downstream of the valve. The expansion and contraction couple the 8.64-in. Plexiglas section to the 10-in. valve. The effect of the valve cannot be determined from measurements in the model. However, the losses caused by the construction joints and the propeller flowmeter can be estimated by assuming the flow in the Plexiglas section conforms to the smooth pipe curve. The measured loss coefficient will be offset from the smooth pipe curve by a constant value that represents the combined effect of the singular or form losses of the flowmeter and the construction joints.

35. The friction measurements should be made over the length of the Plexiglas pipe only from stations 15+00 to 20+00. The losses determined between stations 15+00 and 20+00 are very reasonable as shown in Table 29 and Plate 25. The magnitude of the singular losses can be determined by

extrapolating the best-fit equations of the data to a common Reynolds number range as shown in the following tabulation:

Station	Reynolds No.	Darcy-Weisbach	Form Loss*
15+00	1×10^5	0.0233	0.0053
20+00	1×10^6	0.0154	0.0038

* The smooth pipe values for Reynolds numbers of 1×10^5 and 1×10^6 are 0.0180 and 0.0116, respectively.

The best-fit equation is:

$$f = 0.380\ Re^{-0.233} \tag{5}$$

36. The discharges for the two extremes of the Reynolds number correspond to 1,760 and 17,600 cfs, respectively. By eliminating friction factors below the smooth pipe curve, a correlation coefficient of 0.58 was obtained for the data. The average form loss coefficient for the flowmeter is 0.0052.

37. The midtunnel losses as determined from the computations were considered to consist of the following components: the friction in the transition, the transition losses, the entrance form losses to the gate passage, the friction losses in the gate passage, and the emergency gate slots. The coefficients used for the individual components were taken from references based on tests with axially symmetric models. The two gate outlets exit on opposite sides of the transition. They are symmetric with respect to a plane through the vertical center line of the upstream tunnel. However, they are not axially symmetric relative to a horizontal plane through the center line of the upstream tunnel. The effect of this nonsymmetry is a very strong horseshoe vortex that forms in the upper half of the transition. The vortex indicates the existence of a large stagnation area in the top of the transition. Because of the vortex, midtunnel losses in the model (and in the prototype) will be larger than estimated values.

38. The midtunnel losses in the model, shown in Table 30, were determined from differential transducers located at station 20+00 and in the crown of the gate passage, immediately upstream of the gates (station 22+07). The differential pressure tap, upstream of the gate, was in a stagnation zone for

gate openings less than about 7 ft. Therefore, the loss coefficient was determined from Equation 4, neglecting the factor 1.0. Data points for gate openings greater than 7 ft were not considered because the pressure taps were no longer in the stagnation zone. For gate openings greater than 7 ft, determination of the total energy at the cross section was not possible. The average loss coefficient measured in the model was 0.68 ± 0.12. This value is about 70 percent larger than the estimated coefficient of 0.399.

Pressures in the outlet works

39. In Equation 3, the pressure drop coefficients were determined based on the mean velocity at their respective reference stations. For the multilevel intake, the reference station was the end of the transition. For the tunnel, the reference station was the end of the tunnel. For the midtunnel transition, the gate section, and the downstream chute, the reference station was immediately upstream of the control gates.

40. The friction factor over a length of constant diameter is given by

$$f = \frac{(C_{pd} - C_{pu})D}{L} \tag{6}$$

where

D = diameter of section

L = length between measurements

Over lengths where friction losses are small relative to singular losses, the pressure drop coefficient should be constant as discharge varies. This is the case, for example, in the multilevel intake and the midtunnel transition. In the tunnel section, the losses consist of both singular and friction components. Therefore, the pressure drop coefficients will not be constant as discharge varies in the tunnel section.

41. The piezometric pressure measurements can be analyzed by converting each reading into a pressure coefficient as defined in Equation 3. All of the data sets can be lumped together for analysis because the pressure coefficients are not dependent upon the design changes made in the model. Table 31 presents the mean pressure coefficient, the standard deviation from the mean, and values equal to one standard deviation away from the mean ($C_{p_{max}}$). The pressure coefficients can then be used to determine the probability of cavitation occurring. Cavitation will begin when the local pressure drops to vapor

pressure. Referencing the cavitation index to the local pressure head gives

$$\sigma = \text{cavitation index} = 2g \frac{(H_x + H_a + H_v)}{V_x^2} \quad (7)$$

where

H_x = pressure head at station x

H_a = atmospheric head = 31 ft water at el 2100

H_v = vapor pressure head = 0.4 ft water at 50 °F

Cavitation damage has not been observed with flows that produce cavitation indices greater than 0.2 if the prototype structure is constructed from concrete, with 28-day compressive strength of 3,000 psi.* Therefore, for this design, minimum cavitation indices σ_{min} of 0.2 or more indicate that cavitation damage will not likely occur. The minimum values of σ_{min} occurred for a discharge of 8,000 cfs.

42. All pressure coefficients in the multilevel intake were referenced to the velocity at the beginning of the transition at station 11+73. At this station the flow area was equal to 96.25 ft^2 (13.75 × 7 ft). Piezometer taps 1 through 7 were located in the intake tower. Tap 5 was on the reservoir side of the tower. The value of the pressure coefficient was 0.015 ± 0.02. This value is essentially equal to zero, which is its theoretical value. Taps 8-11 were located on the crown of the bell-mouthed intake. The pressure coefficients for all of these taps were positive, so cavitation at the intake was not probable. Measurements were made with differential transducers at piezometer taps 8 and 10. The values of the measurements with the two different methods are as follows:

Tap	Piezometer	Differential Transducer
8	0.14 ± 0.13	0.105 ± 0.026
10	1.69 ± 0.26	1.728 ± 0.164

These readings confirm the assertions regarding the reliability of the two measurement methods and show that the mean values determined by either method

* Falvey, H. T. 1990 (Apr). "Cavitation in Chutes and Spillways," Engineering Monograph No. 42, US Department of the Interior, Bureau of Reclamation, Denver, CO.

compared favorably. Pressure drop coefficients are tabulated in Table 28.

43. All pressure coefficients in the tunnel section were referenced to the mean velocity in the tunnel. The flow area was equal to 254.47 ft^2 ($\pi \times 18^2/4$). The pressure coefficients increased nonlinearly from station 12+38.5 to station 15+00. Between the end of the transition (station 12+38.5) and station 15+00 a uniform velocity distribution was being established. Since the kinetic energy correction factor is not known in this zone, Equation 7 cannot be applied to determine the loss coefficient for the tunnel between the end of the transition and station 15+00.

44. Between stations 15+00 and 21+28, the pressure coefficients increased linearly. In this section, determination of the friction loss in the model tunnel was possible. The average friction coefficient between stations 15+00 and 21+28, as determined from the pressure coefficients given in Table 31, was 0.0126. This value was determined by a least-squares fit of the pressure coefficients as a function of distance. The slope of the straight-line fit was 0.000697 and the intercept was 2.146. The slope of the straight line is equal to the $(C_{pd} - C_{pu})/L$ term of Equation 6. Therefore, the friction factor is obtained by multiplying the slope by the conduit diameter. The friction factor, as determined from the pressure coefficients, is lower than that determined from the more accurate differential transducers.

45. Measurements were made with differential transducers at piezometer taps 17, 20, and 25. The values of the pressure coefficients as determined with the two different methods are as follows:

Tap	Station	Piezometer	Differential Transducer
17	12+38.5	2.805 ± 0.641	2.685 ± 0.315
20	15+00	3.217 ± 0.407	2.909 ± 0.316
25	20+00	3.666 ± 0.640	3.417 ± 0.368

Again, the differential transducer has a lower value for the standard deviation; that is, the readings with the differential transducers are more accurate. However, the mean values of the pressure coefficients are within 10 percent of each other.

46. All pressure coefficients in the transition section were referenced to the mean velocity in the conduit upstream of the two regulating gates. The flow area was equal to 85.0 ft^2 (2 × 5 × 8.5). Piezometers 40–43, 50–52, 56, 57, and 65–68 were located in the 2- by 3-ft gate section. Since no flow

passed through the gate during the measurements, the piezometers should all read the static head at the end of the transition. The static head is equal to the reservoir elevation less head losses between the intake and the end of the transition. The mean value of the pressure coefficient for the piezometers listed in paragraph 45 is 0.518 ± 0.378. Using Equations 3 and 4 (with the term 1.0 neglected), the loss coefficient for the transition is equal to 0.248 ± 0.380. The very large value of the standard deviation with the loss coefficient demonstrates the difficulty in determining small losses from piezometric readings.

47. All pressure coefficients in the gate section were referenced to the mean velocity upstream of the gates assuming both gates were fully open. The flow area was equal to 85 ft^2 (2 × 5 × 8.5). Piezometers 34, 36, 46–49, 53–55, and 69–74 were located on the invert and walls of the gate section. Piezometers 59–63 were located on the crown of the gate section beginning at the bell-mouthed entrance and continuing almost to the emergency gate. All of the pressure coefficients were larger than 0.3. Therefore, cavitation will not be a problem through the gate section.

48. All pressure coefficients in the downstream chute were referenced to the mean velocity upstream of the gates assuming both gates are fully open. The flow area was equal to 85 ft^2 (2 × 5 × 8.5). Although all of the pressure coefficients were positive, three locations had values less than 0.1. These were as follows:

Tap	Station	Pressure Coefficient
99	20+70.3	0.08
A	20+71	0.04
109	25+00	0.07

Tap A corresponds to the point of tangency of the sidewall transition in the downstream chute. Station 25+00 may correspond to the location of the trough of the supercritical wave that forms in the chute. However, the presence of a supercritical wave in the chute cannot be inferred from taps 110–120.

Open Channel Conduit

49. Water-surface elevations were measured at three critical cross sections in the open channel conduit downstream from the control gates for

discharges of 5,000 and 8,000 cfs to determine average velocities V_{AVG} in the open channel conduit. The critical cross sections were based on the location of the lowest point of flow and the highest point of flow and the end of the exit portal as shown in Plate 26. The water-surface data were used to calculate the average depth Y_{AVG} at each cross section. Average velocities V_{AVG} were determined from the average depth measurements at each cross section. Using the continuity equation:

$$V_{AVG} = \frac{Q}{A} \tag{8}$$

where

V_{AVG} = the average velocity in the conduit, ft/sec

Q = discharge in the conduit, ft^3/sec

A = cross-sectional area of flow in conduit = $Y_{AVG}W$, ft

Y_{AVG} = average depth of flow in conduit, ft

W = width of conduit, ft

The water-surface elevations and average velocities at each cross section are shown in Plates 27-32. The basic data are tabulated in Tables 32 and 33.

Energy Dissipator

Type 1 (original) design

50. The type 1 (original) design energy dissipator consisted of providing a vertical cutoff wall at the end of the open channel conduit and allowing a scour hole to develop downstream. In the type 1 design the natural topography surrounding the exit portal was installed in an area 1,100 ft long by 875 ft wide (Figure 4, Plate 33). The coarsest 80 percent of the bed gradation was reproduced to scale in a 1,000-ft-long by 250-ft-wide test section using the gradation curve provided by the Los Angeles District shown in Plate 34. The larger boulders were omitted. The remaining model topography was molded in large gravel simulating material 1/2 to 2 ft in diameter. Flow was gradually introduced into the model and the resulting scour was recorded. A discharge of 2,000 cfs (Photos 1 and 2) was run for 5 hr (prototype) until the scour hole stabilized at pool el 2300. Material was deposited up to

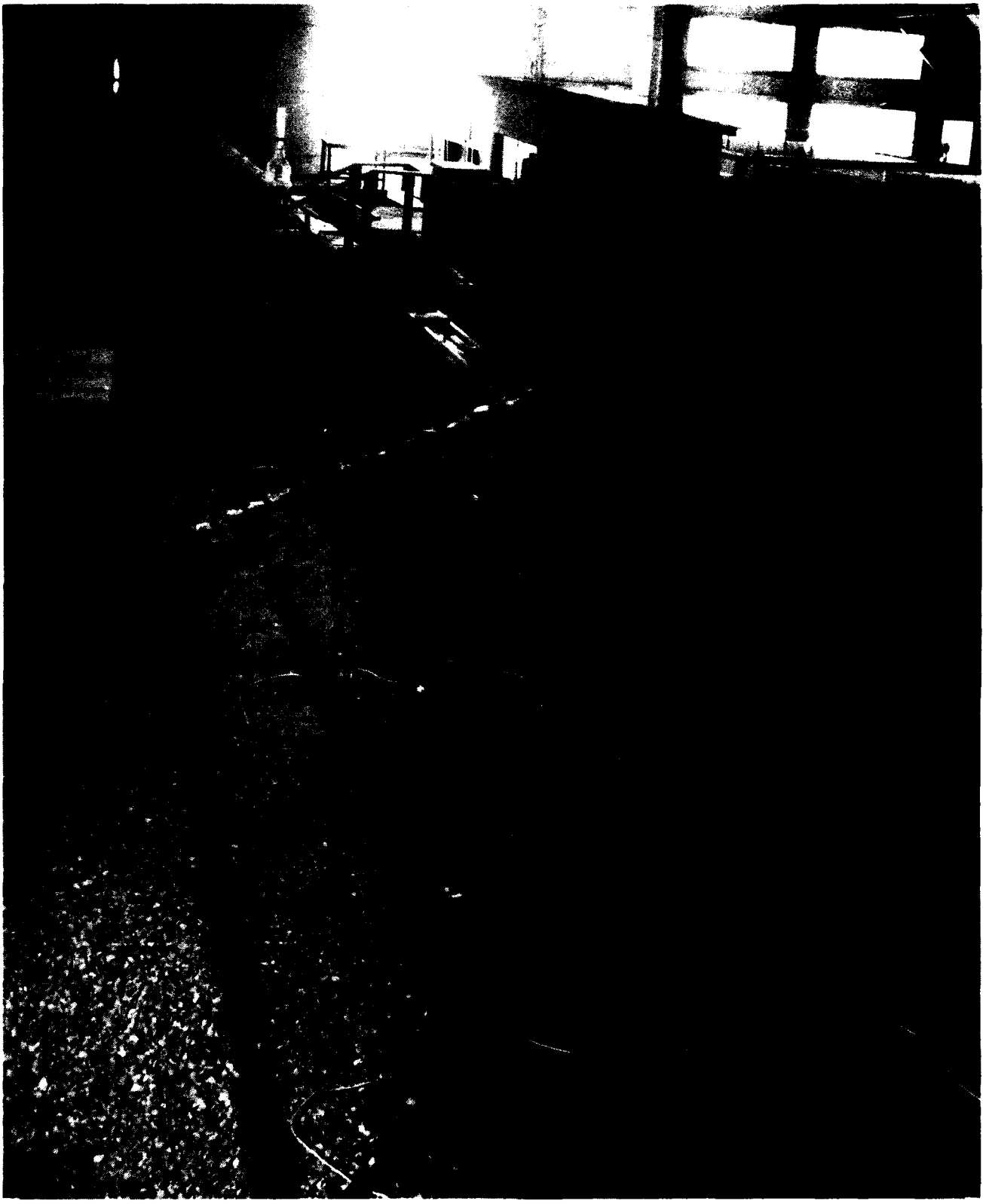

a. Overall view looking upstream

Figure 4. Type 1 (original) energy dissipator (Continued)

b. Closeup looking upstream

Figure 4. (Concluded)

el 2020 at station 34+00 and el 2010 at station 36+50. Maximum scour occurred to el 2007 about 80 ft downstream of the exit portal. The resulting scour contours are shown in Photos 3 and 4. A discharge of 4,000 cfs (Photos 5 and 6) was run for 5 hr (prototype) until the scour hole stabilized at pool el 23-00. Deposition of material up to el 2010 continued to station 38+60. Maximum scour occurred to el 1992 about 140 ft downstream of the exit portal. The resulting scour contours are shown in Photo 7. A discharge of 6,000 cfs (Photos 8 and 9) was run for 5 hr (prototype) until the scour hole stabilized at pool el 2400. Deposition of material up to el 2010 continued downstream to station 39+00. Maximum scour occurred to el 1975 about 140 ft downstream of the exit portal. The resulting scour contours are shown in Photo 10. A discharge of 8,000 cfs (Photos 11 and 12) was run for 4-1/2 hr (prototype) until the scour hole stabilized at pool el 2580. As the discharge was increased to 8,000 cfs, the flow jet was deflected to the right, then to the left, and finally down the center of the scour hole. Deposition of material up to el 2010 continued to station 40+75. Maximum scour occurred to el 1974 about 210 ft downstream of the exit portal. The resulting scour contours are shown in Photo 13.

51. Because of the depth of scour, efforts were made to dissipate some of the energy of the jet plunging out of the exit portal. Deflector blocks were installed in the model to spread the flow exiting the channel These deflectors were effective in spreading the flow and projecting the jet farther downstream while dissipating some of the energy in the jet.

52. During the release of lower flows to flood up the model, there was some headcutting underneath the outlet works exit portal (Photos 3, 4, 7, 10, and 13). It was concluded that some type of apron would be necessary to prevent flow exiting the outlet works exit portal from eroding the supporting ground. The constant deposition of material downstream built a berm that raised the tailwater in the scoured area. The return currents were held in the plunge pool, resulting in a very wide scour hole. It was concluded that some preexcavation was necessary to prevent this from occurring in the prototype. Based on the results of these qualitative scour tests and the headcutting underneath the outlet works exit channel, the type 2 design energy dissipator/preformed scour hole (Figure 5) was designed and tested.

Alternate designs

53. The type 2 design energy dissipator/preformed scour hole consisted

of a 4-ft-thick, 163.2-ft-long by 103-ft-wide, 1V on 3H sloping apron immediately downstream of the exit portal; a 4-ft-thick, 125.2-ft-long by 103-ft-wide horizontal apron; and a 1V on 8H upsloping exit channel. The access road to the outlet works was incorporated in the model along the left perimeter of the preformed scour hole (looking downstream) as shown in Figure 5. The preformed scour hole consisted of 1V on 4.4H side slopes on the left and right sides of the plunge pool sloping up to 16-ft-wide benches at el 2010. The sides sloped up from the 2010 bench to natural ground at a 1V on 2H slope. Plan and profile views of the type 2 design energy dissipator are shown in Plates 35 and 36. Flow was gradually increased to 8,000 cfs and the resulting scour was recorded. The model was operated at a pool el of 2580 with this discharge for 2 hr (prototype) until the scour hole stabilized. Maximum scour occurred to el 1976 about 305 ft downstream of the exit portal. Maximum scour hole width was about 490 ft with the left banks sloughing up to the access road, as shown in Photo 14. The resulting scour contours are shown in Plate 37. Up to 3 ft of material was deposited on the horizontal slab as shown in Photo 14 and Plate 37. Because of potential maintenance problems resulting from deposition of material on the slab and the width of the scour hole encroaching on the access road, the type 2 design was considered unsatisfactory.

54. The 4-ft-thick, 125.2-ft-long horizontal slab was removed in the type 3 design energy dissipator/preformed scour hole. Because the scour width extended outside the test section of graded material with the type 2 design tests, the model bed was remolded to include the bed gradation in a 600-ft-wide by 1,000-ft-long test section. The type 3 design energy dissipator/preformed scour hole consisted of a 4-ft-thick, 163.2-ft-long by 103-ft-wide, 1V on 3H sloping apron immediately downstream of the exit portal; flat natural ground at el 1990; a 1V on 8H upsloping exit channel; and three deflector blocks in the outlet channel to diffuse flow. Plan and profile views of the type 3 design energy dissipator are shown in Plates 38 and 39. Deflector details are also shown in Plates 38 and 39. Flow was gradually increased to 8,000 cfs and the resulting scour was recorded. The model was operated at a pool el of 2580 with this discharge for 5 hr (prototype) until the scour hole stabilized. Maximum scour occurred to el 1973.5 about 180 ft downstream of the exit portal. Maximum scour width was about 463 ft with the left bank

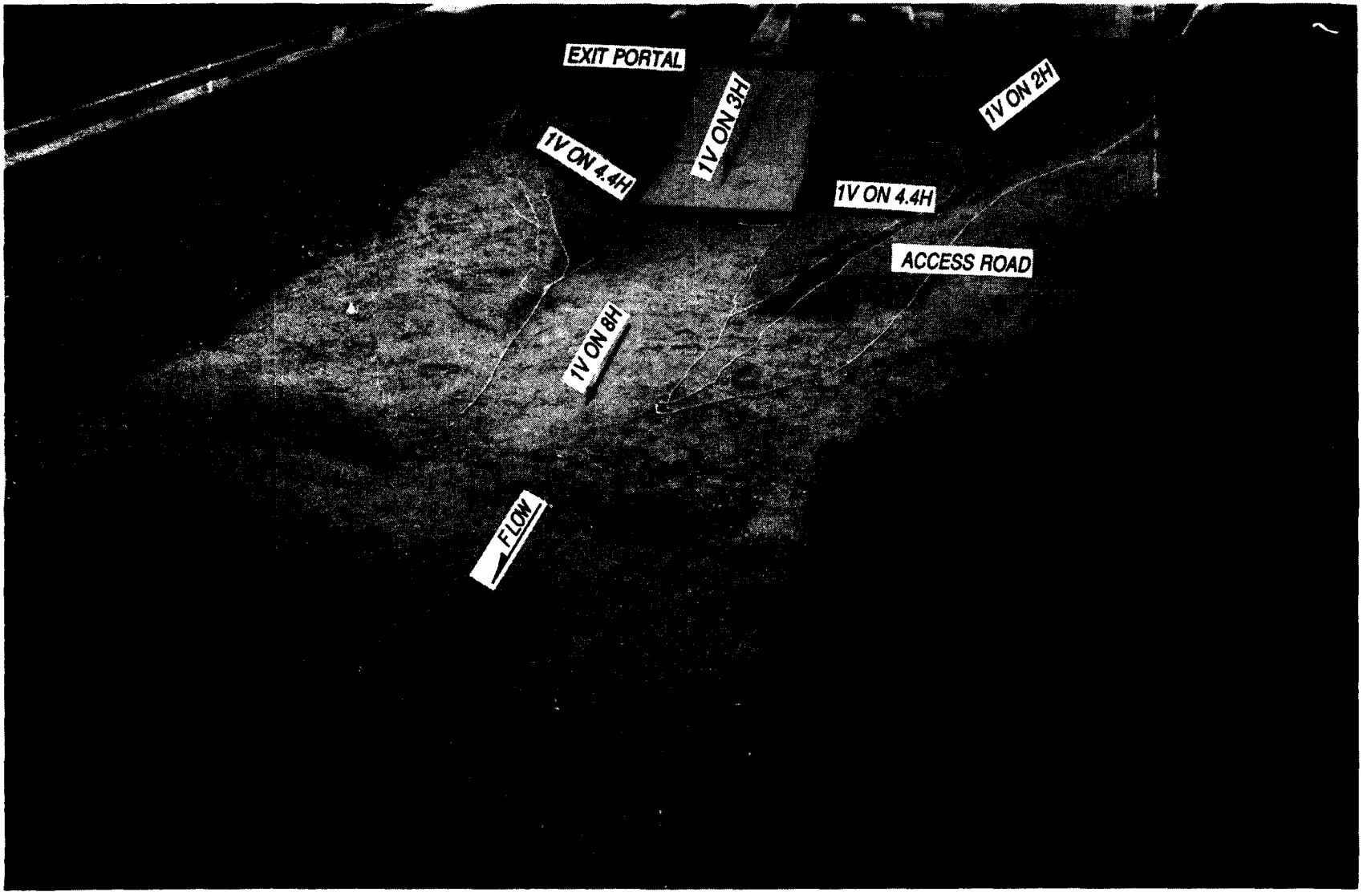

Figure 5. Type 2 energy dissipator/preformed scour hole

sloughing up to the access road as shown in Photo 15. The resulting scour contours are shown in Plate 40.

55. The deflector blocks were removed in an effort to increase scour depth while decreasing scour width in the type 4 design energy dissipator/ preformed scour hole. The left and right 1V on 2H side slopes above el 2010 were remolded. Plan and profile views of the type 4 design energy dissipator are shown in Plates 41 and 42. Flow was gradually increased to 8,000 cfs and the resulting scour was recorded. The model was operated at a pool el of 2580 with this discharge for 1 hr (prototype) until the scour hole stabilized. Maximum scour occurred to el 1964.5 about 150 ft downstream of the exit portal, just downstream of the sloping apron. Maximum scour width was about 478 ft with the left bank sloughing off the edge of the access road as shown in Photo 16. The resulting scour contours are shown in Plate 43. Although the scour hole was deeper, as expected without the deflector blocks installed, the width of the scour hole also increased rather than decreased. The jet was spread and extended farther downstream with the deflectors (Photo 17) than without the deflectors (Photo 18). Thus, the type 4 design was considered unsatisfactory.

56. The type 5 design energy dissipator/preformed scour hole involved using flared deflector blocks in an effort to further spread the exit flow and decrease the extent of scour. The left and right 1V on 2H side slopes above el 2010 were remolded. Plan and profile views of the type 5 design energy dissipator are shown in Plates 44 and 45. Flow was gradually increased to 8,000 cfs and the resulting scour was recorded. The model was operated at a pool el of 2580 with this discharge for 1 hr (prototype) until the scour hole stabilized. Maximum scour occurred to el 1965 about 150 ft downstream of the exit portal, just downstream of the sloping apron. Maximum scour width was about 475 ft with the left bank sloughing up to the access road. The resulting scour contours are shown in Plate 46. The type 5 design provided no improvement over the type 4 design and was considered unsatisfactory.

57. The type 6 design energy dissipator/preformed scour hole involved using flared and tapered deflector blocks in an effort to further spread the exit flow and decrease the extent of scour. Also, a 62.5-ft-wide bench at el 2020 on the left side along the toe of the 1V on 2H side slopes (Figure 6) was added. The bench on the right at el 2010 remained unchanged. Plan and profile views of the type 6 design energy dissipator are shown in Plates 47

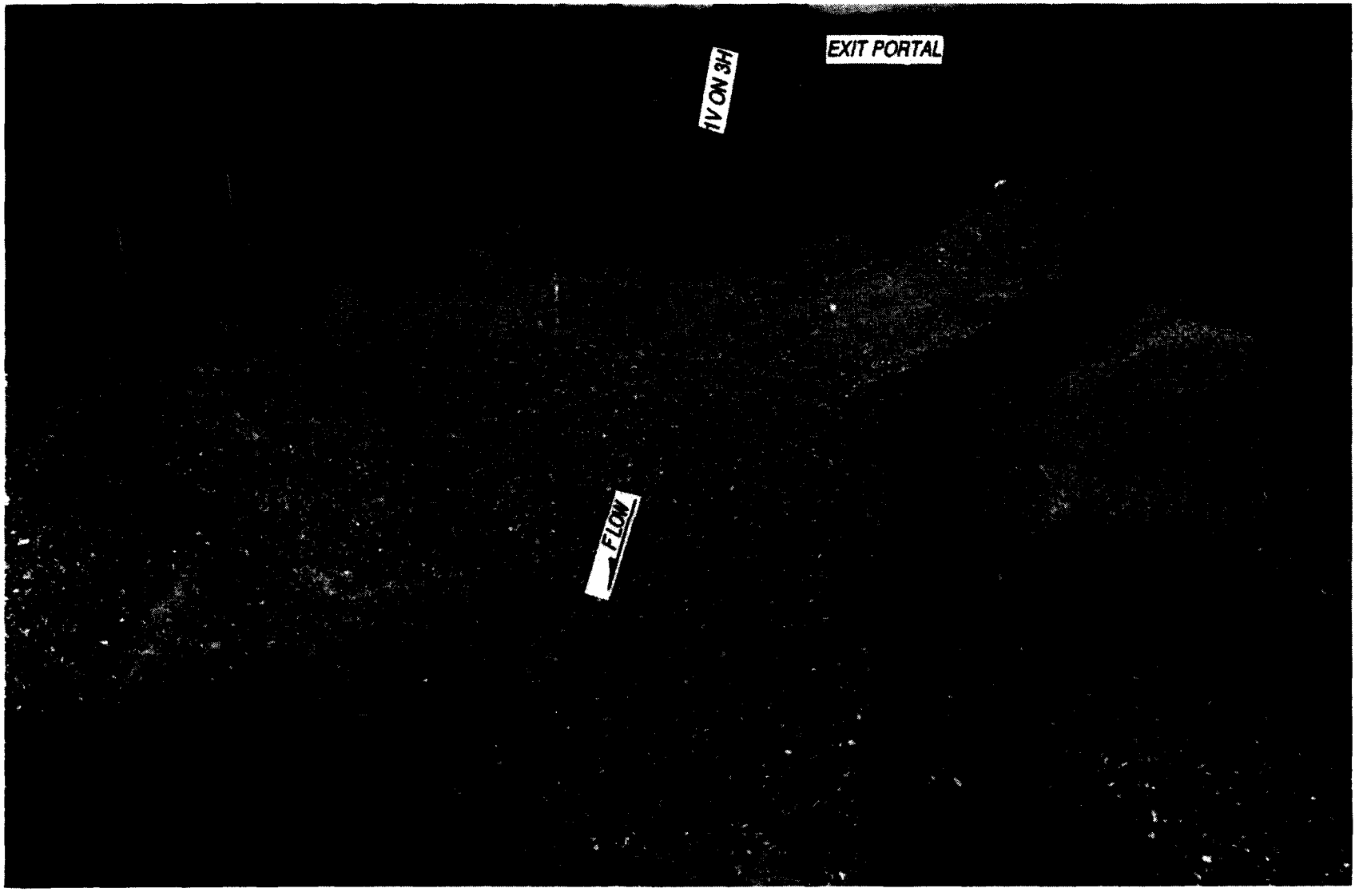

Figure 6. Type 6 design energy dissipator/preformed scour

and 48. Flow was gradually increased to 8,000 cfs and the resulting scour was recorded. The model was operated at a pool el of 2580 with this discharge for 1 hr (prototype) until the scour hole stabilized. Maximum scour occurred to el 1966 about 175 ft downstream of the exit portal, 12 ft downstream of the sloping apron toe. Maximum scour width was about 475 ft. The resulting scour contours are shown in Plate 49. The type 6 design provided no improvement over the type 5 design and was considered unsatisfactory.

58. It was concluded that riprap protection would be necessary to reduce the scour depth and width. The type 7 design energy dissipator/ preformed scour hole involved using the type 6 design energy dissipator/ preformed scour hole with a 75-ft-wide by 75-ft-long by 20-ft-thick blanket of 4- to 6-ft-diameter riprap in the scour hole that developed with the type 6 design immediately downstream of the sloping apron up to el 1986. At the request of the Los Angeles District, scour gages were installed in the model as shown in Plate 50 to monitor scour and material deposition. Plan and profile views of the type 7 design energy dissipator are shown in Plates 51 and 52. The model bed was remolded before the next test. Flow was gradually increased to 8,0^0 cfs and the resulting scour was recorded. The model was operated at a pool el of 2580 with 8,000 cfs for 1 hr (prototype). The scour width was decreased to 435 ft. This test was aborted after 1 hr because the extent of scour that occurred in the first hour in this test exceeded the extent of scour that had occurred in the first hour with previous tests. It was concluded that the extent of scour that would occur with these test conditions after the slopes had stabilized would substantially exceed the extent of scour with previous tests with stable slopes. The riprap downstream of the sloping apron remained stable. The resulting scour contours are shown in Plate 53.

59. The type 8 design energy dissipator/preformed scour hole involved a 60-ft-wide extension of the 1V on 3H sloping apron for an additional 30 ft to el 1980.5. Plan and profile views of the type 8 design energy dissipator are shown in Plates 54 and 55. The model bed was remolded before the flow was gradually increased to 8,000 cfs. The model was operated at a pool el of 2580 with 8,000 cfs for 5 hr (prototype). Operation of the model indicated the need for modifications of the type 7 and 8 design energy dissipator/preformed scour holes and possible realignment of the access road because the banks sloughed up to the access road.

60. The preformed scour hole was redesigned (Figure 7) based on stable contours resulting from previous tests. The realigned access road was also installed in the model. The type 8 design was modified to the type 9 design by extending the 1V on 3H sloping apron down to el 1980 for the entire width of the apron. The preformed scour hole consisted of flat slopes on either side of the channel sloping up to a toe at el 2010 followed by 1V on 2H side slopes up to natural ground. The exit channel sloped up from the toe of the apron (el 1980) on a 1V on 8H slope to el 2017 (Plate 56). Plan and profile views of the type 9 design energy dissipator are shown in Plates 57 and 58. Flow was gradually increased to 8,000 cfs and the resulting scour was recorded. The model was operated at a pool el of 2580 with this discharge for 5 hr (prototype) until the scour hole stabilized. Approximately 6 ft of material was deposited on each downstream corner of the apron for 25 ft. Scour 11 to 12 ft deep occurred along both sides of the apron from about el 2020 and below to the apron toe. Maximum scour occurred to el 1976 about 175 ft downstream of the exit portal and 12 ft downstream of the sloping apron. Maximum scour width was about 460 ft. The resulting scour contours are shown in Plate 59.

61. Following an analysis of the resulting scour from energy dissipator design types 1-9, the type 7 design was reevaluated for its potential to reduce width of scour. The type 7 design was then modified to include a 100-ft-long by 103-ft-wide by 12-ft-thick blanket of 4- to 6-ft-diameter riprap, a 12-ft-thick by 20-ft-wide blanket of 2- to 4-ft-diameter riprap protection along the sides of the sloping apron from contour el 2020 to the toe of the apron, a 6-ft-thick blanket of 2- to 4-ft-diameter riprap protection along the toe of the 1V on 2H side slopes from contour el 2016 to contour el 2006, and a 1V on 10H upsloping exit channel as shown in Figure 8 and Plate 60. This was designated the type 10 design energy dissipator. Plan and profile views of the type 10 design energy dissipator are shown in Plates 61 and 62. Flow was gradually increased to 8,000 cfs (Photos 19-22) and the model was operated at a pool el of 2580 for 5 hr (prototype) until the scour hole stabilized. Although there was minimal launching of the 2- to 4-ft-diameter riprap on the side slopes and the 4- to 6-ft-diameter riprap downstream of the toe of the sloping apron, the type 10 design remained stable during this test (Photo 23). The type 10 design energy dissipator was recommended for prototype construction.

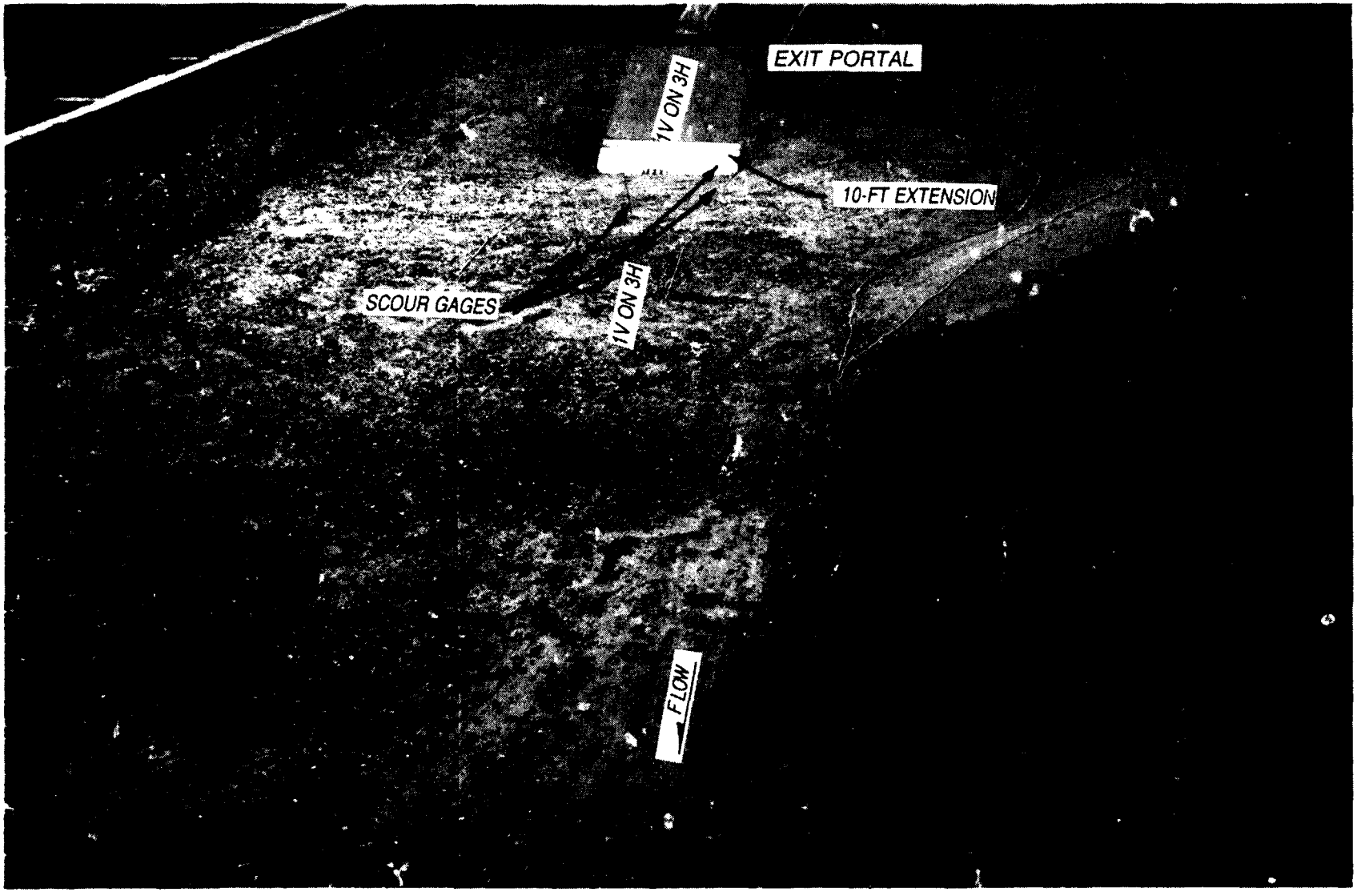

Figure 7. Type 9 design energy dissipator/preformed scour

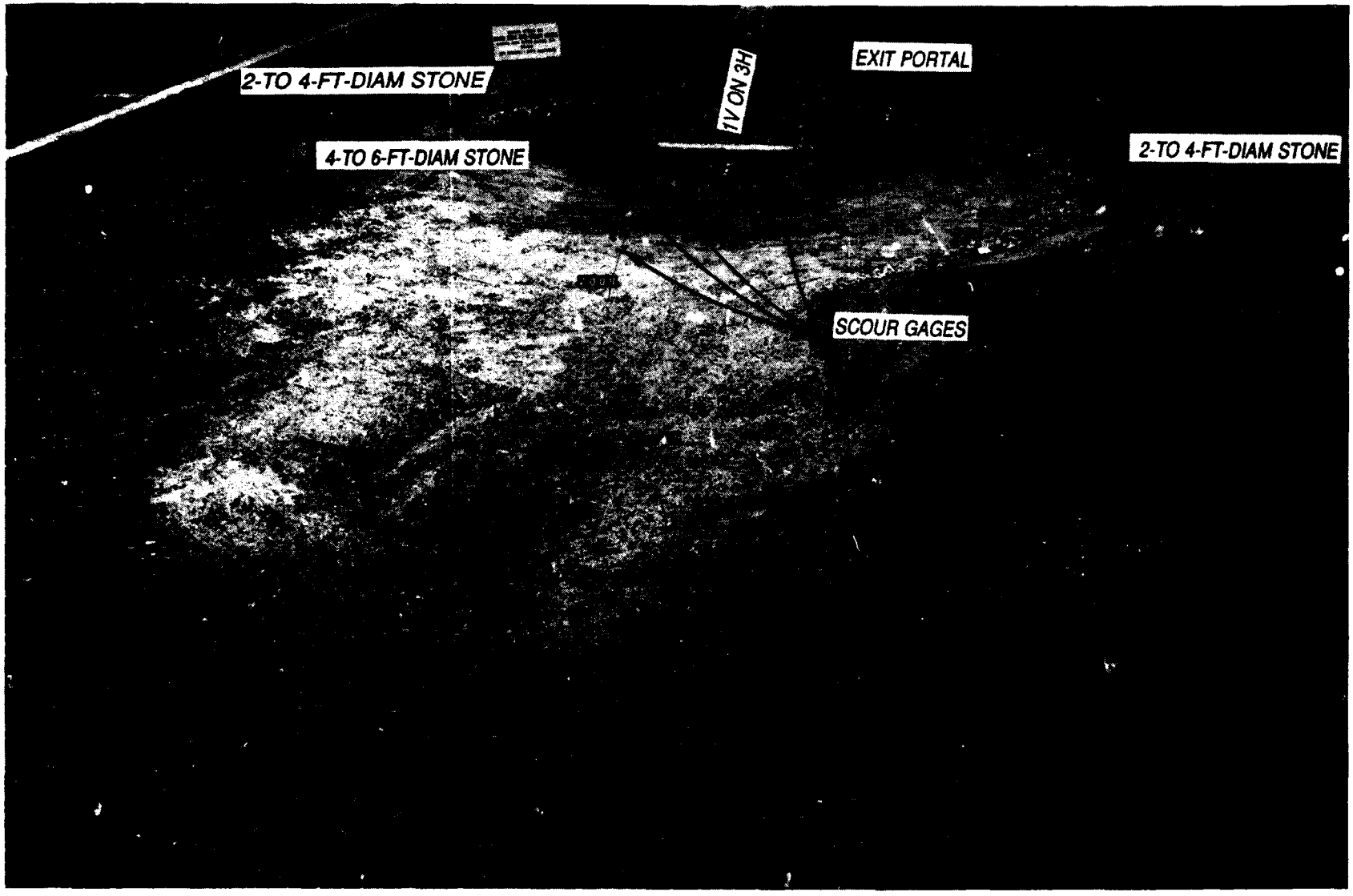

Figure 8. Type 10 design energy dissipator/preformed scour hole

Apron Mat Stability

Type 1 (original) design

62. During tests to develop the optimum energy dissipator, the paved apron downstream from the outlet was simulated with plywood that would not move. After the final design was selected (type 10 design energy dissipator), tests were conducted to determine the stability of the concrete blocks that will be used to protect this area.

63. The type 1 (original) design apron mat consisted of one row of five 16.2-ft-long by 21-ft-wide by 4-ft-thick concrete blocks and seven rows of five 21-ft-long by 21-ft-wide by 4-ft-thick concrete blocks laid on a 1V on 3H slope (Figure 9). The prototype weight of the blocks was reproduced to scale using 150-pcf-strength concrete. Each block was weighed individually and numbered for proper documentation (Plate 63). The type 1 (original) design apron mat was placed in the type 10 design energy dissipator/preformed scour hole and various discharges were run to check its stability. A discharge of 2,000 cfs was run for 5 hr (prototype) at pool el 2300 and plunge pool tailwater el 2012. A discharge of 4,000 cfs was run for 5 hr (prototype) at pool el 2300 and plunge pool tailwater el 2013. The pool elevation and discharge were gradually increased to 2580 and 8,000 cfs, respectively, and the model was operated for 5 hr. The type 1 (original) design apron mat remained stable throughout operation with these conditions (Photo 24).

Alternate designs

64. The 105-ft-wide sloping apron mat was modified to the type 2 design apron mat by decreasing the block thickness to 1 ft. Block lengths and widths remained unchanged. Block 38 (Plate 63) was displaced at about 400 cfs. Failure of the entire apron continued in a "domino" pattern. Blocks 33, 28, and 23 followed. Failure of the type 2 design apron mat is shown in Photo 25.

65. The 105-ft-wide sloping apron mat was modified to the type 3 design apron mat by increasing the block thickness to 3 ft. Block configuration remained unchanged. Block 33 (Plate 63) was displaced at about 2,000 cfs. Failure of the entire apron mat continued in a "domino" pattern. Blocks 28 and 23 followed. Failure of the type 3 design apron mat is shown in Photo 26. Due to the failure of the 3-ft-thick apron, an apron thickness greater than 4 ft was recommended for prototype construction to allow for a factor of safety and settling of the blocks after construction.

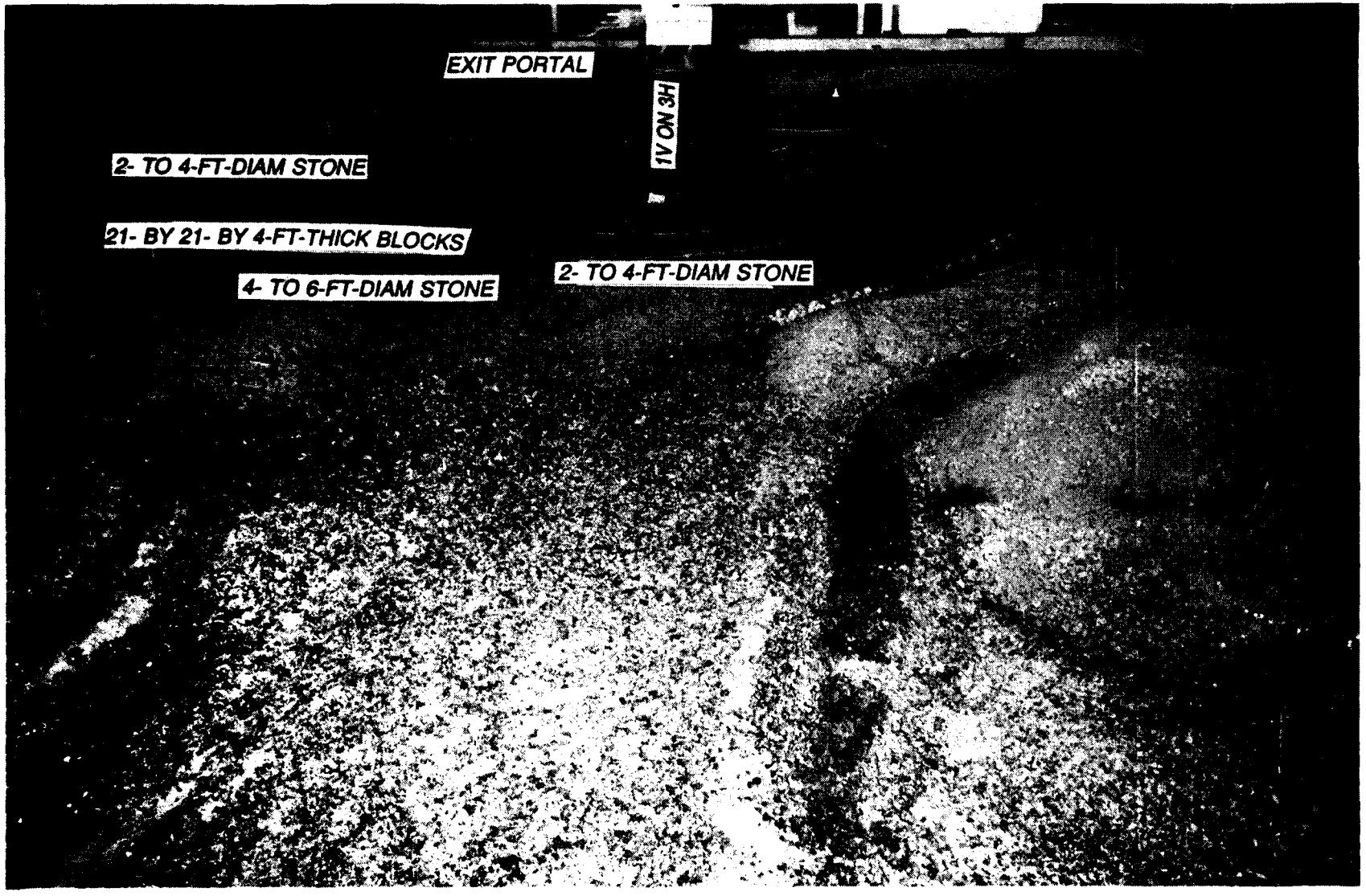

Figure 9. Type 1 design apron mat, 4-ft-thick blocks

Velocity and Wave Heights in Exit Plunge Pool

66. After observation of the model with the type 1 (original) apron mat installed in the type 10 energy dissipator/preformed scour hole configuration, engineers from the Portland District requested velocity and wave height measurements along the toe of the riprap in the plunge pool for design of rounded stone protection for discharges of 4,000, 6,000, and 8,000 cfs, and water-surface contours indicating the water-surface depression by the jet across the face of the sloping apron for calculation of uplift. Velocity measurements are shown in Plates 64-66 for 4,000, 6,000, and 8,000 cfs, respectively. Velocity data and corresponding wave heights are shown in Table 34. Water-surface contours indicating the water-surface depression by the jet are plotted in Plates 67-71 for 4,000, 5,000, 6,000, 7,000, and 8,000 cfs, respectively. The basic data are tabulated in Table 35.

PART IV: DISCUSSION AND RECOMMENDATIONS

67. The general hydraulic design of the outlet works was verified in the model study. Discharge rating curves were determined for various openings of the midtunnel control gates. The rating curves with gate openings less than 6 ft compared favorably with those calculated by the Portland District using existing design criteria. With larger gate openings the discharges measured in the model were more than those computed. This was attributed to the fact that some of the piezometers used to measure the energy grade line in the model were located in a stagnation zone with gate openings above 4 ft. Since the discharge coefficients with the lower gate openings compared very favorably with the existing criteria, the computed discharge rating curves should be used for all gate openings. Raising the invert of the conduit through the control section by 0.50 ft and shortening the piers 51 ft (type 4 design control section) had no significant effect on the gate rating curves.

68. Various modifications were made to the control section to improve flow conditions and increase the amount of air that will be drawn into flow during flood releases. This air is necessary because of the extremely high velocities downstream from the control gates and the potential for cavitation. Although a considerable amount of aeration occurred in the model at gate openings up to 7 ft with the original design, the invert of the gate chamber of the control section was elevated by 0.50 ft, thus increasing the offset downstream by this amount (type 2 design). This modification was somewhat of a safety factor to ensure adequate aeration in the prototype for gate openings of 7 ft and greater. Modeling of air entrainment in models of the size used in this study is not a precise science. However, tests conducted with increased roughness placed on the model immediately downstream from the gates (type 3) indicated that the model was capable of estimating air demand.

69. Pressures were measured throughout the outlet works with piezometers, and pressure cells were placed at critical locations. Although some of the pressure readings downstream from the gates were negative, as expected, there were no zones of potential cavitation, since air entrainment will "cushion" these flows. Thus, the type 4 design midtunnel control section was recommended for prototype construction.

70. The cavitation potential was calculated for all of the flows tested in the model study based on the value of a cavitation index, σ . The minimum

values of σ occurred for a discharge of 8,000 cfs. The lowest values of the cavitation index σ occurred in the downstream chute. However, since none of the values of σ were less than 0.20, cavitation damage should not occur in the outlet works. In addition, the flows in the chute are fully aerated as a result of the floor and sidewall offsets immediately downstream of the gate structure.

71. The tunnel downstream from the control section is designed for free-surface flow, but will contain an access conduit to the control section from the downstream end of the tunnel. This access conduit will be located along the top of the tunnel. Flow downstream from the control gates impacted on the roof of the tunnel (access floor) with some discharges. Pressure transducers were mounted on the roof of the conduit to measure the uplift force created by the impact of the jet. The maximum force measured was 23 ft of water. This occurred with a release discharge of 8,000 cfs. With discharges of 7,000 cfs and less, the maximum force was only 4 ft of water pressure.

72. Initially tests were conducted without an energy dissipator downstream from the exit portal with the natural material simulated in this area. A large scour hole developed as expected. The scoured material deposited downstream in a mound causing an artificial raising of the tailwater. Large eddies formed causing scour in an area wider than desirable. Also, lower flows caused excessive erosion around the end of the open channel outlet and cutoff wall near station 30+80. Thus, it was concluded that some type of protective apron and preformed scour hole (pre-excavation) would be necessary to protect the structure and prevent excessive buildup of material downstream.

73. Results from the scour tests were used for the initial design of an energy dissipator, which consisted of a protective apron at the outlet and a preformed scour hole. After several tests and modification to the design, a satisfactory design was achieved. This design consisted of deflector blocks at the end of the open channel outlet to spread the exiting jet, a sloping apron to absorb the impact of the impinging jet, riprap protection along the sides and at the end of the apron, and a preformed scour hole. This was designated the type 10 design energy dissipator and was recommended for prototype construction.

74. The sloping apron will be constructed of a number of concrete blocks. Each of the blocks in the first row of blocks immediately downstream of the exit channel will be 16.2 ft long and 21 ft wide. The remaining blocks

will be 21 ft long and 21 ft wide. Tests were conducted to determine the stability of these blocks with block thicknesses of 1, 3, and 4 ft. Failure occurred with block thicknesses of 1 and 3 ft. Failure of the apron occurred in a "domino" fashion with blocks flipping out of the bed rapidly after the first block was displaced. Failure did not occur with the 4-ft-thick blocks. Although the 4-ft-thick blocks did not fail, the recommendation was made that consideration be given to increasing the thickness of the prototype blocks. This recommendation was based on problems that could occur during and after construction, such as settling and cracking of blocks, and the mode of failure that could take place if a block becomes displaced.

75. Velocity and wave height measurements were obtained in the exit area where stone protection will be placed. These measurements can be used to determine the size of rounded stone protection should this type of stone be used for the prototype rather than the crushed limestone used in the model.

76. Water-surface differentials across the face of the sloping apron were measured. This information can be used to calculate uplift pressures on the concrete blocks as a check of the stability of the blocks.

BIBLIOGRAPHY

Blaisdell, Fred W., and Anderson, Clayton L. 1991 (Mar). "Pipe Plunge Pool Energy Dissipator," *Journal of Hydraulic Engineering, ASCE*, Vol 117, No. 3, pp 303-323.

Bowers, E. Edward, and Toso, Joel. 1988 (May). "Karnafuli Project, Model Studies of Spillway Damage, *Journal of Hydraulic Engineering, ASCE*, Vol 114, No. 5, pp 469-483.

Coleman, H. W. 1982 (Aug). "Prediction of Scour Depth From Free Falling Jets", *1982 ASCE Conference Proceedings*, pp 298-301.

Farhoudi, Javad, and Narayanan, Rangaswami. 1991 (Jan). "Force on Slab Beneath Hydraulic Jump", *Journal of Hydraulic Engineering, ASCE*, Vol. 117, No. 1, pp 64-81.

Uyumaz, Ali. 1991 (Feb). Discussion of "Effects of Air Entrainment on Plunge Pool Scour," by Peter John Mason, *Journal of Hydraulic Engineering, ASCE*, Vol 117, No. 2, pp 256-258.

Table 1

Pressure Cell Locations

Pressure Cell	Pressure Cell El	Station
1P	2072.2	22+37
2P	2072.5	22+28.5
3P	2072.5	22+28.5
4P	2072.5	22+28.5
5P	2072.7	22+20.5
6P	2074.7	22+37
7P	2077.2	22+37
8P	2074.9	22+30.75
9P	2077.4	22+30.75
10P	2075.1	22+24.5
11P	2077.6	22+24.5
12P	2075.2	22+18.25
13P	2077.7	22+18.25
14P	2072.8	22+14.5

Table 2

Differential Cell Locations

Differential Pressure Cell No.	Differential Pressure Cell El	Station
DPC8	2122.5	11+33
DPC10	2113.8	11+45.9
DPC16	2106.9	11+73.4
DPC17	2116.2	12+38.5
DPC20	2100.4	15+00
DPC25	2087.4	20+00
DPC26	2084.8	21+00
DPC27	2082.9	22+07
DPC28	2082.9	22+07
DPC63A	2082.9	21+98.7

Table 3

Calibration Data

Type 1 Design

Gate Opening ft	Gate Opening percent	Discharge cfs	Pool El	C_d *	C_{dcorp} **
2	0.222	2,030	2362.5	0.754	0.732
		2,380	2485.0	0.741	
		2,580	2560.0	0.738	
4	0.444	3,320	2298.8	0.723	0.746
		3,730	2374.8	0.701	
		4,990	2557.5	0.744	
6	0.667	5,850	2379.8	0.783	0.779
		6,820	2482.8	0.793	
		7,530	2541.3	0.827	

* C_d = model gate discharge coefficient.

** C_{dcorp} = recommended gate discharge coefficients, HDC 320-1.

Table 4

Type 1 (Original) Design

Pressures in Prototype Feet of Water

No.	Pressure Tap El	Station	Q=2,000 cfs Pool El 2300 G_o=2.25 ft	Q=5,000 cfs Pool El 2303.0 G_o=6.00 ft	Q=8,000 cfs Pool El 2577.5 G_o=6.25 ft
1	2103.5	1,113.8	195.8	198.0	473.5
2	2130.0	1,117.5	169.3	171.0	446.4
3	2107.0	1,093.2	192.3	196.3	470.0
4	2180.0	1,111.4	119.8	122.7	393.0
5	2205.0	1,110.5	94.8	98.3	372.0
6	2107.0	1,111.8	192.3	196.3	466.0
7	2182.5	1,130.6	117.3	117.9	389.9
8	2122.5	1,133.0	177.1	176.7	445.6
9	2116.0	1,137.4	175.7	179.7	428.1
10	2113.8	1,145.9	177.5	126.4	318.6
11	2113.8	1,150.4	158.9	158.9	366.8
12	2106.9	1,130.0	164.6	171.6	443.8
13	2106.9	1,132.0	188.9	174.4	445.9
14	2106.9	1,134.0	188.9	177.3	443.0
15	2106.9	1,167.9	188.9	165.8	440.1
16	2106.9	1,173.4	189.5	177.3	437.2
17	2116.2	1,238.5	182.5	176.7	425.0
18	2105.2	1,312.5	192.8	184.7	433.1
19	2103.0	1,400.0	194.5	184.1	432.5
20	2100.4	1,500.0	196.9	184.1	432.4
21	2097.8	1,600.0	198.6	189.9	426.7
22	2095.2	1,700.0	200.6	191.9	428.7
23	2092.6	1,800.0	203.8	183.6	446.3
24	2090.0	1,900.0	205.8	188.5	436.8
25	2087.4	2,000.0	209.3	193.6	438.4
26	2084.8	2,100.0	213.9	196.6	440.3
27	2084.0	2,128.0	214.6	195.6	441.0
28	2084.0	2,128.0	214.6	194.4	442.7
29	2083.5	2,149.5	215.2	192.1	457.7
30	2083.5	2,149.5	215.2	192.1	451.9
31	2082.9	2,171.7	215.7	198.4	441.0
32	2078.4	2,166.9	219.7	208.7	474.3
33	2082.9	2,171.7	212.9	198.4	443.9
34	2078.4	2,179.5	213.9	161.4	318.4
35	2073.9	2,173.5	208.6	182.6	387.6
36	2078.4	2,179.5	209.9	163.7	319.6
37	2078.4	2,173.5	217.4	188.5	367.5
38	2078.4	2,174.5	217.4	202.9	370.4
39	2073.9	2,169.8	221.9	219.0	458.7
40	2075.6	2,175.3	214.4	202.8	428.0

Continued

Table 4 (Continued)

No.	Pressure Tap El	Station	Q=2,000 cfs Pool El 2300 G_o=2.25 ft	Q=5,000 cfs Pool El 2303.0 G_o=6.00 ft	Q=8,000 cfs Pool El 2577.5 G_o=6.25 ft
41	2078.4	2,173.5	209.3	203.5	437.4
42	2073.9	2,173.5	213.2	204.6	441.3
43	2073.9	2,177.3	221.9	210.3	458.7
44	2078.4	2,175.3	214.5	179.8	379.1
45	2073.9	2,176.5	*	*	*
46	2073.9	2,179.5	218.4	157.8	345.5
47	2078.4	2,190.8	*	*	*
48	2073.9	2,190.8	215.5	158.4	337.4
49	2078.4	2,190.8	210.5	148.1	304.0
50	2077.4	2,179.5	*	*	*
51	2077.4	2,182.5	218.4	212.6	463.5
52	2077.4	2,190.8	**	**	**
53	2078.4	2,190.8	210.7	153.1	332.9
54	2073.9	2,190.8	215.3	157.8	337.9
55	2078.4	2,190.8	210.6	152.1	332.4
56	2077.4	2,177.0	220.6	204.1	—†
57	2077.5	2,175.3	221.5	204.0	—†
58	2078.6	2,173.5	221.4	202.9	—†
59	2085.9	2,173.5	208.8	190.1	—†
60	2083.7	2,176.5	206.5	156.8	—†
61	2083.1	2,179.5	203.7	118.9	—†
62	2082.9	2,182.5	204.3	138.4	305.9
63	2082.9	2,190.8	204.1	143.4	313.9
64	2082.9	2,207.0	*	*	*
65	2073.9	2,201.8	**	**	**
66	2077.4	2,201.8	**	**	**
67	2075.6	2,201.8	**	**	**
68	2075.6	2,202.8	**	**	**
69	2078.4	2,207.0	193.9	102.1	224.6
70	2078.4	2,207.0	199.8	101.1	222.1
71	2073.9	2,207.0	158.1	98.6	209.9
72	2078.4	2,206.7	204.8	113.8	218.6
73	2078.4	2,207.0	204.6	112.4	215.9
74	2073.9	2,207.0	155.2	101.6	216.7
75	2072.3	2,272.0	3.1	5.2	15.7
76	2072.3	2,272.0	4.4	6.8	13.4
77	2071.8	2,292.0	4.2	5.9	23.2
78	2070.8	2,292.0	4.7	7.2	15.2
79	2070.8	2,292.0	3.7	6.0	4.7
80	2070.8	2,292.0	1.7	1.9	-0.3

* Air entrained in pressure tap opening.
** Bulkhead inserted in 2- by 3.5-ft emergency gate slot.
† No data recorded.

Table 4 (Continued)

No.	Pressure Tap El	Station	Q=2,000 cfs Pool El 2300 G_o=2.25 ft	Q=5,000 cfs Pool El 2303.0 G_o=6.00 ft	Q=8,000 cfs Pool El 2577.5 G_o=6.25 ft
81	2070.8	2,292.0	2.6	4.2	5.5
82	2070.8	2,292.0	4.2	6.6	9.2
83	2071.8	2,292.0	4.4	5.9	16.2
84	2071.3	2,312.0	3.8	4.2	10.2
85	2070.3	2,312.0	3.4	5.4	12.5
86	2070.3	2,312.0	3.2	4.7	12.1
87	2070.3	2,312.0	2.0	6.7	8.7
88	2070.3	2,312.0	1.2	2.7	2.4
89	2070.3	2,312.0	1.7	3.0	7.3
90	2071.3	2,312.0	3.9	7.7	6.4
91	2070.8	2,332.0	4.2	8.7	16.9
92	2069.8	2,332.0	4.7	7.1	10.2
93	2069.8	2,332.0	3.7	4.9	11.1
94	2069.8	2,332.0	1.5	4.6	4.5
95	2069.8	2,332.0	9.5	11.9	4.9
96	2069.8	2,332.0	4.7	6.5	14.9
97	2070.8	2,332.0	3.7	5.0	7.2
98	2070.3	2,350.0	1.0	2.4	2.4
99	2070.3	2,350.0	*	3.0	5.1
100	2068.6	2,375.0	2.9	4.4	7.2
101	2068.6	2,375.0	0.8	1.9	6.8
102	2068.6	2,375.0	5.8	7.9	14.9
103	2068.6	2,375.0	5.9	8.9	22.9
104	2069.0	2,400.0	6.0	0.9	8.7
105	2068.0	2,400.0	8.3	9.6	19.5
106	2068.0	2,400.0	6.8	8.2	12.4
107	2068.0	2,400.0	1.5	3.0	7.0
108	2069.0	2,400.0	0.9	2.3	7.5
109	2065.4	2,500.0	1.0	2.4	9.3
110	2062.8	2,600.0	2.9	5.9	8.8
111	2062.8	2,600.0	4.5	4.5	11.1
112	2062.8	2,600.0	2.2	4.0	19.2
113	2060.2	2,700.0	3.3	5.4	7.5
114	2057.6	2,800.0	9.2	10.2	7.4
115	2057.6	2,800.0	6.7	4.6	11.9
116	2057.6	2,800.0	2.8	4.9	8.2
117	2055.0	2,900.0	7.5	9.4	5.0
118	2052.4	3,000.0	2.6	4.8	12.0
119	2052.4	3,000.0	6.0	8.4	6.1
120	2052.4	3,000.0	2.6	4.8	13.1
A	2071.0	2,322.0	*	*	*
B	2071.5	2,302.0	*	22.0	4.0

* Air entrained in pressure tap opening.

Table 4 (Concluded)

No.	Pressure Tap El	Station	Q=2,000 cfs Pool El 2300 G_o=2.25 ft	Q=5,000 cfs Pool El 2303.0 G_o=6.00 ft	Q=8,000 cfs Pool El 2577.5 G_o=6.25 ft
C	2072.1	2,282.0	4.7	10.4	12.2
D	2072.7	2,257.0	5.8	6.8	7.3
E	2073.0	2,244.5	*	*	*

* Air entrained in pressure tap opening.

Table 5

Differential Pressure Cell Data

Type 1 (Original) Design

Pressures In Prototype Feet of Water

Differential Cell No.	Q=2,000 cfs Pool El 2300.0 G_o=2.25 ft	Q=5,000 cfs Pool El 2303.0 G_o=6.00 ft	Q=8,000 cfs Pool El 2577.5 G_o=6.25 ft
DPC8	0.4	3.8	9.4
DPC10	8.7	62.8	145.1
DPC20	2.7	18.5	44.7
DPC25	3.3	22.0	51.7
DPC27	7.0	55.8	127.4
DPC28	7.3	51.5	130.9

Note: Differential pressures are referenced to the pool elevation.

Table 6

Calibration Data

Type 2 Design

Gate Opening ft	Q cfs	Pool El
2	2,550	2560.2
	2,200	2453.0
	1,800	2337.2
4	5,050	2581.2
	4,400	2451.2
	3,600	2341.2
6	7,600	2580.0
	6,500	2431.8
	5,500	2329.0

Table 7

Type 2 Design

Pressures in Prototype Feet of Water

No.	Pressure Tap El	Station	Q=2,000 cfs Pool El 2299.5 G_o=2.25 ft	Q=5,000 cfs Pool El 2300.5 G_o=6.00 ft	Q=8,000 cfs Pool El 2583.8 G_o=6.25 ft
1	2103.5	1,113.8	*	*	*
2	2130.0	1,117.5	*	*	*
3	2107.0	1,093.2	*	*	*
4	2180.0	1,111.4	118.6	115.8	398.7
5	2205.0	1,110.5	94.2	95.4	378.4
6	2107.0	1,111.8	*	*	*
7	2182.5	1,130.6	*	*	*
8	2122.5	1,133.0	175.8	172.7	448.9
9	2116.0	1,137.4	179.7	168.2	428.1
10	2113.8	1,145.9	172.0	108.3	269.8
11	2113.8	1,150.4	176.2	132.9	326.4
12	2106.9	1,130.0	*	*	*
13	2106.9	1,132.0	183.1	144.4	333.8
14	2106.9	1,134.0	*	*	*
15	2106.9	1,167.9	183.1	150.8	347.7
16	2106.9	1,173.4	183.0	139.8	333.6
17	2116.2	1,238.5	179.7	166.2	422.3
18	2105.2	1,312.5	*	*	*
19	2103.0	1,400.0	*	*	*
20	2100.4	1,500.0	195.3	180.6	434.9
21	2097.8	1,600.0	*	*	*
22	2095.2	1,700.0	*	*	*
23	2092.6	1,800.0	*	*	*
24	2090.0	1,900.0	*	*	*
25	2087.4	2,000.0	*	*	*
26	2084.8	2,100.0	210.3	192.8	443.8
27	2084.0	2,128.0	211.1	192.7	442.7
28	2084.0	2,128.0	211.1	192.7	442.7
29	2083.5	2,149.5	211.1	192.6	440.4
30	2083.5	2,149.5	211.1	192.6	440.4
31	2082.9	2,171.7	211.1	192.6	446.7
32	2078.4	2,166.9	214.5	202.9	471.5
33	2082.9	2,171.7	211.1	181.1	441.0
34	2078.4	2,179.5	217.4	162.5	315.6
35	2073.9	2,173.5	223.0	191.3	399.2
36	2078.4	2,179.5	215.7	175.2	354.3
37	2078.4	2,173.5	217.4	194.3	373.3
38	2078.4	2,174.5	214.5	197.2	370.4
39	2073.9	2,169.8	225.3	221.9	455.8

(Continued)

* Bourdon gage not read per Portland District request.

Table 7 (Continued)

No.	Pressure Tap El	Station	Q=2,000 cfs Pool El 2299.5 G_o=2.25 ft	Q=5,000 cfs Pool El 2300.5 G_o=6.00 ft	Q=8,000 cfs Pool El 2583.8 G_o=6.25 ft
40	2075.6	2,175.3	194.1	208.6	428.0
41	2078.4	2,173.5	218.0	200.6	434.5
42	2073.9	2,173.5	221.9	213.2	452.9
43	2073.9	2,177.3	224.8	219.0	470.2
44	2078.4	2,175.3	220.3	182.7	376.2
45	2073.9	2,176.5	218.4	172.2	328.1
46	2073.9	2,179.5	*	*	*
47	2078.4	2,190.8	213.5	**	294.3
48	2073.9	2,190.8	245.0	216.1	334.5
49	2078.4	2,190.8	205.8	211.6	292.5
50	2077.4	2,179.5	223.0	**	*
51	2077.4	2,182.5	218.4	209.7	449.4
52	2077.4	2,190.8	†	†	†
53	2078.4	2,190.8	206.7	205.4	205.4
54	2073.9	2,190.8	210.3	210.6	210.6
55	2078.4	2,190.8	206.6	211.6	211.6
56	2077.4	2,177.0	217.2	222.2	222.2
57	2077.5	2,175.3	217.0	222.0	222.0
58	2078.6	2,173.5	216.2	221.2	221.2
59	2085.9	2,173.5	207.5	212.5	212.5
60	2083.7	2,176.5	204.1	209.1	209.1
61	2083.1	2,179.5	200.1	205.1	205.1
62	2082.9	2,182.5	200.8	205.8	205.8
63	2082.9	2,190.8	200.9	205.9	205.9
64	2082.9	2,207.0	**	**	**
65	2073.9	2,201.8	†	†	†
66	2077.4	2,201.8	†	†	†
67	2075.6	2,201.8	†	†	†
68	2075.6	2,202.8	†	†	†
69	2078.4	2,207.0	162.7	95.7	173.0
70	2078.4	2,207.0	171.0	90.9	169.5
71	2073.9	2,207.0	143.1	91.5	166.6
72	2078.4	2,206.7	183.0	105.7	197.9
73	2078.4	2,207.0	173.5	105.7	190.9
74	2073.9	2,207.0	148.1	89.0	167.6
75	2072.3	2,272.0	6.1	6.5	13.6
76	2072.3	2,272.0	12.0	7.2	13.2
77	2071.8	2,292.0	4.8	5.9	8.8
78	2070.8	2,292.0	6.2	8.6	12.7
79	2070.8	2,292.0	2.6	2.8	3.0

(Continued)

* Bourdon gage not read per Portland District request.
** Pressure tap damaged during testing.
† Bulkhead inserted in 2- by 3-ft emergency gate slot.

Table 7 (Continued)

No.	Pressure Tap El	Station	Q=2,000 cfs Pool El 2299.5 G_o=2.25 ft	Q=5,000 cfs Pool El 2300.5 G_o=6.00 ft	Q=8,000 cfs Pool El 2583.8 G_o=6.25 ft
80	2070.8	2,292.0	1.9	6.7	8.7
81	2070.8	2,292.0	13.2	5.7	6.6
82	2070.8	2,292.0	6.1	5.0	7.7
83	2071.8	2,292.0	10.8	5.0	9.6
84	2071.3	2,312.0	17.4	8.1	15.0
85	2070.3	2,312.0	4.2	4.0	5.1
86	2070.3	2,312.0	6.1	6.4	10.1
87	2070.3	2,312.0	4.2	6.5	9.0
88	2070.3	2,312.0	4.2	2.0	1.1
89	2070.3	2,312.0	2.1	4.1	2.4
90	2071.3	2,312.0	5.3	5.7	9.6
91	2070.8	2,332.0	13.7	6.7	14.5
92	2069.8	2,332.0	9.0	6.1	8.6
93	2069.8	2,332.0	4.2	4.8	5.7
94	2069.8	2,332.0	2.0	5.7	6.9
95	2069.8	2,332.0	11.0	8.8	12.4
96	2069.8	2,332.0	9.6	5.5	6.7
97	2070.8	2,332.0	2.0	3.0	6.7
98	2070.3	2,350.0	LOW	7.1	9.4
99	2070.3	2,350.0	LOW	2.0	3.4
100	2068.6	2,375.0	††	††	††
101	2068.6	2,375.0	††	††	††
102	2068.6	2,375.0	††	††	††
103	2068.6	2,375.0	††	††	††
104	2069.0	2,400.0	††	††	††
105	2068.0	2,400.0	††	††	††
106	2068.0	2,400.0	††	††	††
107	2068.0	2,400.0	††	††	††
108	2069.0	2,400.0	††	††	††
109	2065.4	2,500.0	††	††	††
110	2062.8	2,600.0	††	††	††
111	2062.8	2,600.0	††	††	††
112	2062.8	2,600.0	††	††	††
113	2060.2	2,700.0	††	††	††
114	2057.6	2,800.0	††	††	††
115	2057.6	2,800.0	††	††	††
116	2057.6	2,800.0	††	††	††
117	2055.0	2,900.0	††	††	††
118	2052.4	3,000.0	††	††	††
119	2052.4	3,000.0	††	††	††

†† Pressure tap not read per Portland District request.

Table 7 (Concluded)

No.	Pressure Tap El	Station	Q=2,000 cfs Pool El 2299.5 G_o=2.25 ft	Q=5,000 cfs Pool El 2300.5 G_o=6.00 ft	Q=8,000 cfs Pool El 2583.8 G_o=6.25 ft
120	2052.4	3,000.0	††	††	††
A	2071.0	2,322.0	‡	‡	‡
B	2071.5	2,302.0	4.6	3.2	4.0
C	2072.1	2,282.0	6.4	6.4	11.6
D	2072.7	2,257.0	3.8	4.8	8.6
E	2073.0	2,244.5	4.8	3.9	9.0

†† Pressure tap not read per Portland District request.
‡ Air entrained in pressure tap opening.

Table 8

Pressure Data

Type 2 Design, Discharge 2,000 cfs

Pool El 2299.2, Gate Opening 2.25 ft

Pressure Cell Number	P_{min} ft water	P_{mean} ft water	P_{max} ft water	P_{rms} ft water	P_{std} ft water
1P	-17.67	0.74	6.06	2.50	2.39
2P	-22.36	-4.02	1.16	4.83	2.68
3P	-29.36	-5.52	1.89	7.16	4.57
4P	-11.77	-4.48	-2.04	4.60	1.04
5P	-10.04	-4.67	3.74	4.98	1.74
6P	-32.40	-4.77	0.07	6.28	4.09
7P	-33.04	-4.67	14.96	11.08	10.05
8P	-18.30	-4.72	-1.35	5.28	2.37
9P	-24.25	-4.91	2.96	6.48	4.23
10P	-34.11	-4.68	1.80	5.89	3.57
11P	-35.72	-4.80	16.08	11.15	10.07
12P	-20.11	-4.47	4.76	5.14	2.55
13P	-19.04	-3.75	3.28	4.83	3.05
14P	-8.67	-4.33	5.95	4.74	1.92

Note: P_{min} - Minimum pressure fluctuation.
P_{mean} - Mean pressure.
P_{max} - Maximum pressure fluctuation.
P_{rms} - Value of pressure relative to zero pressure.
P_{std} - Pressure one standard deviation from P_{mean}.

Table 9

Pressure Data

Type 2 Design, Discharge 5,000 cfs

Pool El 2300.5, Gate Opening 6.00 ft

Pressure Cell Number	P_{min} ft water	P_{mean} ft water	P_{max} ft water	P_{rms} ft water	P_{std} ft water
1P	0.80	3.91	7.66	3.97	0.70
2P	4.56	23.48	32.92	23.78	3.75
3P	-1.53	24.49	46.85	25.41	6.77
4P	-29.47	20.52	42.23	21.97	7.85
5P	-14.23	-3.72	4.49	4.60	2.71
6P	-7.54	-3.75	-0.67	3.86	0.92
7P	-24.04	-3.77	1.04	5.51	4.02
8P	-7.40	0.06	6.46	1.54	1.54
9P	-11.72	-3.60	-1.21	3.90	1.50
10P	-34.25	-1.36	13.77	3.72	3.46
11P	-19.26	-3.78	-0.52	4.49	2.42
12P	-55.56	-2.45	3.62	3.59	2.61
13P	-9.62	-3.95	-0.68	4.18	1.35
14P	-4.70	3.64	12.79	4.06	1.78

Table 10

Pressure Data

Type 2 Design, Discharge 8,000 cfs

Pool El 2583.8 ft, Gate Opening 6.25 ft

Pressure Cell Number	P_{min} ft water	P_{mean} ft water	P_{max} ft water	P_{rms} ft water	P_{std} ft water
1P	4.19	11.12	19.05	11.24	1.64
2P	-12.01	45.73	87.57	47.15	11.48
3P	-77.81	-0.04	33.95	20.30	20.30
4P	-40.96	0.00	15.77	8.06	8.06
5P	-10.95	-0.01	10.87	2.94	2.94
6P	-11.86	-4.37	1.22	4.65	1.59
7P	-12.07	-3.74	-1.74	3.93	1.21
8P	-6.38	4.04	13.98	5.14	3.18
9P	-8.64	-4.21	-2.37	4.25	0.61
10P	-32.98	-2.07	15.55	5.34	4.92
11P	-11.72	-4.37	-1.11	4.54	1.21
12P	-69.26	-0.84	7.82	5.87	5.81
13P	-18.25	-5.35	2.54	5.77	2.15
14P	-13.98	-5.84	5.38	6.40	2.63

Table 11

Pressure Data

Type 2 Design, Discharge 8,000 cfs

Pool El 2580.0 ft, Gate Opening 6.25 ft

Pressure Cell Number	P_{min} ft water	P_{mean} ft water	P_{max} ft water	P_{rms} ft water	P_{std} ft water
1P	-0.15	11.03	21.01	11.25	2.20
2P	-1.78	45.73	86.27	48.06	14.78
3P	-52.02	-0.06	30.44	14.15	14.15
4P	-29.22	0.03	6.79	3.62	3.62
5P	-9.10	0.00	9.46	2.60	2.60
6P	-9.38	-4.37	0.39	4.55	1.27
7P	-25.11	-3.80	1.67	5.85	4.45
8P	-4.88	4.06	13.32	5.12	3.12
9P	-9.36	-4.23	-1.87	4.33	0.92
10P	-26.33	-2.11	9.70	4.40	3.86
11P	-12.45	-4.42	-1.87	4.54	1.02
12P	-98.30	-.82	5.82	9.55	9.52
13P	-13.91	-5.35	1.61	5.64	1.81
14P	-23.37	-5.90	9.47	6.99	3.76

Table 12

Differential Pressure Data

Type 2 Design

Pressures In Prototype Feet of Water

Differential Cell No.	Q=2,000 cfs Pool El 2299.25 G_o=2.25 ft	Q=5,000 cfs Pool El 2300.5 G_o=6.00 ft	Q=8,000 cfs Pool El 2583.75 G_o=6.25 ft
DPC8	0.9	5.3	12.3
DPC10	13.4	78.4	200.2
DPC16	9.3	53.8	143.3
DPC17	3.3	18.1	45.3
DPC20	3.6	19.5	48.4
DPC26	4.2	22.9	55.2
DPC27	9.8	58.7	161.4
DPC28	9.3	58.7	159.8

Note: Differential pressures are referenced to the pool elevation.

Table 13

Air Velocity in Air Shaft

G_o ft	Q cfs	Pool El	V^*_{avg} ft/sec
	Type 2 Design		
2	2,550	2582.0	148.3
4	5,050	2579.0	167.9
6	7,600	2578.5	208.8
7	9,300	2580.5	195.0
8	11,800	2582.5	152.1
	Type 3 Design		
6.5	8,000	2580.0	202.5

* Average air velocity, ft/sec.

Table 14

Pressure Data

Type 2 Design, Discharge 2,550 cfs

Pool El 2582.0 ft, Gate Opening 2.00 ft

Pressure Cell Number	P_{min} ft water	P_{mean} ft water	P_{max} ft water	P_{rms} ft water	P_{std} ft water
1P	-12.68	-0.26	5.64	2.61	2.60
2P	-13.62	-4.31	1.21	4.66	1.78
3P	-22.10	-3.46	4.25	5.06	3.69
4P	-15.10	-3.71	-1.31	3.83	0.98
5P	-6.42	-0.06	7.53	1.90	1.90
6P	-17.95	-10.77	-1.63	10.83	1.16
7P	-11.79	-4.24	2.81	4.60	1.78
8P	-13.75	-7.91	-4.14	8.09	1.72
9P	-11.06	-4.05	5.40	4.53	2.03
10P	-36.38	-0.04	10.70	4.25	4.25
11P	-17.84	-4.22	8.40	5.46	3.46
12P	-45.42	-3.36	2.49	3.82	1.81
13P	-8.35	-4.13	2.40	4.24	0.99
14P	-11.12	-4.96	4.53	5.36	2.05

Table 15

Pressure Data

Type 2 Design, Discharge 2,550 cfs

Pool El 2577.5 ft, Gate Opening 2.00 ft

Pressure Cell Number	P_{min} ft water	P_{mean} ft water	P_{max} ft water	P_{rms} ft water	P_{std} ft water
1P	-8.96	-0.32	3.82	2.04	2.02
2P	-11.98	-4.31	2.47	4.80	2.12
3P	-25.42	-3.51	6.36	5.84	4.66
4P	-8.83	-3.71	0.76	3.86	1.08
5P	-8.51	-0.02	10.19	2.68	2.68
6P	-14.77	-10.73	-7.50	10.77	0.97
7P	-29.14	-4.30	4.79	6.51	4.89
8P	-14.72	-7.96	-4.66	8.09	1.46
9P	-13.42	-4.03	-1.25	4.24	1.32
10P	-24.56	-0.06	6.08	3.95	3.95
11P	-17.49	-4.17	1.30	4.95	2.66
12P	-30.94	-3.36	5.01	4.24	2.58
13P	-8.52	-4.16	0.00	4.34	1.23
14P	-12.98	-4.93	4.69	5.40	2.20

Table 16

Pressure Data

Type 2 Design, Discharge 5,050 cfs

Pool El 2579.0 ft, Gate Opening 4.00 ft

Pressure Cell Number	P_{min} ft water	P_{mean} ft water	P_{max} ft water	P_{rms} ft water	P_{std} ft water
1P	-5.99	15.25	27.69	16.04	4.99
2P	-56.25	5.50	27.03	11.84	10.49
3P	-24.62	0.54	7.42	3.91	3.88
4P	-13.79	-0.39	2.90	2.17	2.14
5P	-8.86	-0.02	7.61	2.29	2.29
6P	-17.50	-7.95	-1.63	8.06	1.36
7P	-20.70	-4.87	4.32	5.64	2.84
8P	-15.75	-8.73	-5.07	8.94	1.89
9P	-15.11	-4.52	8.63	5.31	2.78
10P	-40.17	-5.10	7.87	7.56	5.58
11P	-19.54	-4.60	10.81	6.22	4.18
12P	-26.24	-4.22	4.91	4.45	1.41
13P	-14.65	-4.16	4.93	4.74	2.27
14P	-16.29	-5.02	1.81	5.89	3.09

Table 17

Pressure Data

Type 2 Design, Discharge 5,050 cfs

Pool El 2572.5 ft, Gate Opening 4.00 ft

Pressure Cell Number	P_{min} ft water	P_{mean} ft water	P_{max} ft water	P_{rms} ft water	P_{std} ft water
1P	-5.88	15.21	26.74	15.85	4.48
2P	-53.34	5.51	9.90	7.27	4.75
3P	-28.72	0.48	7.38	3.94	3.91
4P	-13.42	0.43	5.27	2.26	2.22
5P	-7.71	-0.05	11.35	2.76	2.76
6P	-13.99	-7.94	-4.30	8.00	1.01
7P	-44.13	-4.88	9.66	10.34	9.11
8P	-18.94	-8.70	-5.03	8.91	1.94
9P	-15.92	-4.44	-0.62	4.86	1.98
10P	-51.28	-5.06	3.08	6.89	4.68
11P	-19.11	-4.58	2.93	5.73	3.45
12P	-39.74	-4.22	1.78	4.77	2.22
13P	-10.05	-4.15	0.40	4.35	1.32
14P	-16.25	-5.09	9.63	5.66	2.47

Table 18

Pressure Data

Type 2 Design, Discharge 7,600 cfs

Pool El 2578.5 ft, Gate Opening 6.00 ft

Pressure Cell Number	P_{min} ft water	P_{mean} ft water	P_{max} ft water	P_{rms} ft water	P_{std} ft water
1P	3.52	10.73	20.57	10.84	1.59
2P	-33.76	22.01	63.27	24.01	9.59
3P	-47.81	27.01	57.89	31.80	16.79
4P	-31.78	0.51	10.13	5.05	5.02
5P	-13.22	-0.02	7.46	2.87	2.87
6P	-12.83	-5.56	0.67	5.78	1.60
7P	-15.01	-4.26	0.27	4.75	2.10
8P	-11.61	2.55	11.61	4.07	3.17
9P	-11.33	-3.92	0.40	4.15	1.35
10P	-30.99	-3.12	14.22	5.72	4.79
11P	-14.98	-5.18	-2.41	5.32	1.22
12P	-67.49	-1.25	8.55	3.67	3.45
13P	-17.73	-5.34	7.80	5.70	1.98
14P	-22.24	-5.67	6.08	6.35	2.85

Table 19

Pressure Data

Type 2 Design, Discharge 7,600 cfs

Pool El 2571.5 ft, Gate Opening 6.00 ft

Pressure Cell Number	P_{min} ft water	P_{mean} ft water	P_{max} ft water	P_{rms} ft water	P_{std} ft water
1P	3.53	10.72	19.69	10.91	2.05
2P	-22.42	22.04	65.25	25.43	12.68
3P	-19.07	27.05	66.85	30.78	14.69
4P	-28.71	0.50	7.81	3.87	3.84
5P	-12.15	-0.06	10.19	2.67	2.67
6P	-12.42	-5.54	-1.09	5.69	1.29
7P	-23.20	-4.24	0.99	6.11	4.40
8P	-6.88	2.57	13.17	3.98	3.04
9P	-7.41	-3.82	-1.64	3.90	0.79
10P	-22.33	-3.10	10.93	4.93	3.84
11P	-9.44	-5.20	-3.09	5.28	0.92
12P	-86.99	-1.23	8.08	11.03	10.96
13P	-19.05	-5.39	0.80	5.69	1.82
14P	-14.99	-5.63	17.25	6.56	3.37

Table 20

Pressure Data

Type 2 Design, Discharge 9,300 cfs

Pool El 2580.5 ft, Gate Opening 7.00 ft

Pressure Cell Number	P_{min} ft water	P_{mean} ft water	P_{max} ft water	P_{rms} ft water	P_{std} ft water
1P	8.24	15.74	24.59	15.88	2.13
2P	5.82	46.75	100.30	47.76	9.76
3P	-66.02	14.80	33.98	20.40	14.05
4P	-27.03	-0.46	7.45	4.06	4.03
5P	-8.12	0.00	7.68	2.43	2.43
6P	-8.53	-0.39	4.60	1.51	1.46
7P	-2.67	0.57	2.40	0.84	0.61
8P	-1.87	7.46	20.56	8.02	2.92
9P	-6.07	-0.49	2.16	1.26	1.17
10P	-33.82	-1.61	21.26	5.60	5.36
11P	-10.09	0.02	6.45	1.97	1.97
12P	-84.45	4.75	15.14	8.77	7.37
13P	-16.02	-5.87	1.92	6.15	1.84
14P	-14.48	-5.93	4.01	6.30	2.14

Table 21

Pressures in Type 4 Design Outlet Works Intake Structure and Conduit in Prototype Feet of Water

No.	Pressure Tap El	Station	Q=2,000 cfs Pool El 2298.0 G_o=2.25 ft	Q=5,000 cfs Pool El 2298.0 G_o=6.00 ft	Q=8,000 cfs Pool El 2584.6 G_o=6.25 ft
1	2103.5	1,113.8	194.0	194.4	475.2
2	2130.0	1,117.5	167.5	168.0	445.8
3	2107.0	1,093.2	190.0	190.8	474.6
4	2180.0	1,111.4	117.5	117.8	393.0
5	2205.0	1,110.5	92.5	93.0	379.5
6	2107.0	1,111.8	187.6	191.0	466.0
7	2182.5	1,130.6	112.2	115.5	373.1
8	2122.5	1,133.0	172.1	175.3	450.4
9	2116.0	1,137.4	175.7	179.7	419.4
10	2113.8	1,145.9	173.3	115.6	254.2
11	2113.8	1,150.4	170.5	121.4	335.0
12	2106.9	1,130.0	188.9	157.1	451.7
13	2106.9	1,132.0	183.1	148.5	373.7
14	2106.9	1,134.0	177.3	136.9	362.1
15	2106.9	1,167.9	177.3	134.0	346.0
16	2106.9	1,173.4	171.6	145.6	346.0
17	2116.2	1,238.5	181.3	179.6	421.6
18	2105.2	1,312.5	190.5	184.7	433.1
19	2103.0	1,400.0	189.9	181.2	435.3
20	2100.4	1,500.0	189.6	181.0	426.4
21	2097.8	1,600.0	195.7	184.1	429.6
22	2095.2	1,700.0	197.7	186.2	431.6
23	2092.6	1,800.0	203.8	189.3	443.4
24	2090.0	1,900.0	201.2	188.5	436.8
25	2087.4	2,000.0	*	*	*
26	2084.8	2,100.0	211.0	193.7	437.9
27	2084.0	2,128.0	211.7	195.6	441.0
28	2084.0	2,128.0	211.7	194.4	436.9
29	2083.5	2,149.5	212.3	206.5	457.7
30	2083.5	2,149.5	212.3	200.7	443.3
31	2082.9	2,171.7	212.9	198.4	441.0
32	2078.4	2,166.9	217.9	217.4	471.5
33	2082.9	2,171.7	210.0	195.5	440.4
34	2078.4	2,179.5	211.6	148.1	305.7
35	2073.9	2,173.5	205.7	168.2	370.3
36	2078.4	2,179.5	209.9	137.7	313.8
37	2078.4	2,173.5	218.5	159.6	344.4
38	2078.4	2,174.5	211.6	159.6	341.5
39	2073.9	2,169.8	219.0	210.3	455.8

(Continued)

* Air entrained in pressure tap opening.

Table 21 (Continued)

No.	Pressure Tap El	Station	Q=2,000 cfs Pool El 2298.0 G_o=2.25 ft	Q=5,000 cfs Pool El 2298.0 G_o=6.00 ft	Q=8,000 cfs Pool El 2584.6 G_o=6.25 ft
40	2075.6	2,175.3	211.5	197.0	433.8
41	2078.4	2,173.5	212.2	194.9	437.4
42	2073.9	2,173.5	210.3	198.8	446.0
43	2073.9	2,177.3	219.0	204.6	455.8
44	2078.4	2,175.3	214.5	174.1	378.5
45	2073.9	2,176.5	209.8	154.9	321.8
46	2073.9	2,179.5	209.8	149.1	306.8
47	2078.4	2,190.8	*	*	*
48	2073.9	2,190.8	216.1	141.0	325.8
49	2078.4	2,190.8	211.6	140.0	292.5
50	2077.4	2,179.5	*	*	*
51	2077.4	2,182.5	220.1	201.1	445.9
52	2077.4	2,190.8	**	**	**
53	2078.4	2,190.8	209.1	142.3	306.3
54	2073.9	2,190.8	217.9	148.7	322.4
55	2078.4	2,190.8	213.3	142.3	312.1
56	2077.4	2,177.0	220.6	199.1	448.8
57	2077.5	2,175.3	220.5	199.0	445.8
58	2078.6	2,173.5	219.4	197.9	450.5
59	2085.9	2,173.5	211.7	185.6	425.9
60	2083.7	2,176.5	209.8	151.7	321.3
61	2083.1	2,179.5	206.6	127.4	261.2
62	2082.9	2,182.5	207.6	132.5	278.7
63	2082.9	2,190.8	207.9	133.8	290.3
64	2082.9	2,207.0	168.8	142.6	330.7
65	2073.9	2,201.8	**	**	**
66	2077.4	2,201.8	**	**	**
67	2075.6	2,201.8	**	**	**
68	2075.6	2,202.8	**	**	**
69	2078.4	2,207.0	172.1	96.6	225.5
70	2078.4	2,207.0	172.0	94.3	228.4
71	2073.9	2,207.0	153.1	96.9	212.6
72	2078.4	2,206.7	191.1	102.5	213.9
73	2078.4	2,207.0	160.1	96.0	211.0
74	2073.9	2,207.0	151.6	94.6	212.6
75	2072.3	2,272.0	9.7	11.1	17.0
76	2072.3	2,272.0	8.6	6.2	10.8
77	2071.8	2,292.0	4.2	4.6	8.0
78	2070.8	2,292.0	4.0	4.6	6.4
79	2070.8	2,292.0	2.7	2.9	3.3

(Continued)

* Air entrained in pressure tap opening.
** Bulkhead inserted in 2- by 3-ft emergency gate slot.

Table 21 (Continued)

No.	Pressure Tap El	Station	Q=2,000 cfs Pool El 2298.0 G_o=2.25 ft	Q=5,000 cfs Pool El 2298.0 G_o=6.00 ft	Q=8,000 cfs Pool El 2584.6 G_o=6.25 ft
80	2070.8	2,292.0	1.5	3.7	4.9
81	2070.8	2,292.0	3.0	3.7	4.7
82	2070.8	2,292.0	3.7	4.6	7.2
83	2071.8	2,292.0	3.4	4.7	8.1
84	2071.3	2,312.0	3.3	4.1	4.7
85	2070.3	2,312.0	3.7	4.2	4.3
86	2070.3	2,312.0	2.6	3.2	3.7
87	2070.3	2,312.0	0.3	0.9	-0.3
88	2070.3	2,312.0	0.9	2.2	0.9
89	2070.3	2,312.0	4.3	2.2	0.0
90	2071.3	2,312.0	3.7	5.1	3.1
91	2070.8	2,332.0	3.4	3.9	13.2
92	2069.8	2,332.0	4.9	5.9	7.2
93	2069.8	2,332.0	3.2	4.2	5.1
94	2069.8	2,332.0	1.5	2.7	1.2
95	2069.8	2,332.0	2.9	4.9	5.2
96	2069.8	2,332.0	4.2	5.7	6.2
97	2070.8	2,332.0	2.9	2.2	6.7
98	2070.3	2,350.0	1.0	1.6	4.6
99	2070.3	2,350.0	1.1	2.1	3.7
100	2068.6	2,375.0	7.3	3.2	6.8
101	2068.6	2,375.0	6.4	3.1	4.0
102	2068.6	2,375.0	5.2	8.1	15.6
103	2068.6	2,375.0	3.7	6.9	16.6
104	2069.0	2,400.0	0.8	1.9	2.0
105	2068.0	2,400.0	2.0	3.5	5.0
106	2068.0	2,400.0	3.7	5.7	7.6
107	2068.0	2,400.0	1.3	5.4	6.7
108	2069.0	2,400.0	0.9	4.5	3.2
109	2065.4	2,500.0	0.8	3.6	4.9
110	2062.8	2,600.0	3.3	5.9	8.2
111	2062.8	2,600.0	2.3	4.6	5.3
112	2062.8	2,600.0	1.9	4.6	6.4
113	2060.2	2,700.0	3.0	5.3	7.5
114	2057.6	2,800.0	3.3	6.3	5.7
115	2057.6	2,800.0	2.4	4.3	5.7
116	2057.6	2,800.0	2.6	4.6	5.7
117	2055.0	2,900.0	1.2	4.0	3.8
118	2052.4	3,000.0	2.6	4.6	6.3
119	2052.4	3,000.0	2.7	5.3	6.4
120	2052.4	3,000.0	*	*	*

(Continued)

* Air entrained in pressure tap opening.

Table 21 (Concluded)

No.	Pressure Tap El	Station	Q=2,000 cfs Pool El 2298.0 G_o=2.25 ft	Q=5,000 cfs Pool El 2298.0 G_o=6.00 ft	Q=8,000 cfs Pool El 2584.6 G_o=6.25 ft
A	2071.0	2,322.0	0.8	1.2	1.2
B	2071.5	2,302.0	2.4	3.6	4.3
C	2072.1	2,282.0	3.9	6.0	11.1
D	2072.7	2,257.0	3.1	4.8	8.3
E	2073.0	2,244.5	3.2	4.0	5.5

Table 22

Pressure Data

Type 4 Design, Discharge 2,550 cfs

Pool El 2582.0 ft, Gate Opening 2.00 ft

Pressure Cell Number	P_{min} ft water	P_{mean} ft water	P_{max} ft water	P_{rms} ft water	P_{std} ft water
1P	-12.96	-0.54	5.35	2.65	2.60
2P	-13.26	-3.95	1.56	4.33	1.78
3P	-22.61	-3.96	3.74	5.42	3.69
4P	-14.89	-3.50	-1.10	3.63	0.98
5P	-10.49	-4.13	3.47	4.54	1.90
6P	-17.95	-10.77	-1.63	10.83	1.16
7P	-11.31	-3.76	3.29	4.16	1.78
8P	-14.28	-8.44	-4.67	8.62	1.72
9P	-10.93	-3.92	5.53	4.41	2.03
10P	-36.38	-0.04	10.70	4.25	4.25
11P	-17.39	-3.76	8.86	5.11	3.46
12P	-45.42	-3.36	2.49	3.82	1.81
13P	-8.15	-3.92	2.60	4.05	0.99
14P	-10.47	-4.31	5.17	4.77	2.05

Table 23

Pressure Data

Type 4 Design, Discharge 5,050 cfs

Pool El 2579.0 ft, Gate Opening 4.00 ft

Pressure Cell Number	P_{min} ft water	P_{mean} ft water	P_{max} ft water	P_{rms} ft water	P_{std} ft water
1P	-5.99	15.25	27.69	16.04	4.99
2P	-56.75	5.01	26.53	11.62	10.49
3P	-26.14	-0.98	5.90	4.00	3.88
4P	-15.37	-1.97	1.31	2.91	2.14
5P	-12.85	-4.00	3.62	4.61	2.29
6P	-17.65	-8.10	-1.78	8.21	1.36
7P	-19.87	-4.04	5.14	4.94	2.84
8P	-14.95	-7.93	-4.27	8.15	1.89
9P	-14.70	-4.12	9.04	4.97	2.78
10P	-38.65	-3.58	9.39	6.63	5.58
11P	-19.02	-4.08	11.33	5.84	4.18
12P	-25.77	-3.75	5.38	4.01	1.41
13P	-14.51	-4.03	5.07	4.62	2.27
14P	-15.52	-4.24	2.59	5.25	3.09

Table 24

Pressure Data

Type 4 Design, Discharge 7,600 cfs

Pool El 2578.5 ft, Gate Opening 6.00 ft

Pressure Cell Number	P_{min} ft water	P_{mean} ft water	P_{max} ft water	P_{rms} ft water	P_{std} ft water
1P	3.03	10.23	20.08	10.36	1.59
2P	-6.74	49.03	90.30	49.96	9.59
3P	-47.09	27.73	58.61	32.42	16.79
4P	-30.27	2.03	11.65	5.42	5.02
5P	-17.50	-4.30	3.18	5.17	2.87
6P	-12.54	-5.26	0.96	5.50	1.60
7P	-15.01	-4.26	0.27	4.75	2.10
8P	-11.61	2.55	11.61	4.07	3.17
9P	-11.33	-3.92	0.40	4.15	1.35
10P	-29.34	-1.47	15.88	5.01	4.79
11P	-14.39	-4.59	-1.82	4.75	1.22
12P	-68.50	-2.26	7.54	4.12	3.45
13P	-15.61	-3.22	9.93	3.78	1.98
14P	-21.34	-4.77	6.98	5.55	2.85

Table 25

Pressure Data

Type 4 Design, Discharge 9,300 cfs

Pool El 2580.5 ft, Gate Opening 7.00 ft

Pressure Cell Number	P_{min} ft water	P_{mean} ft water	P_{max} ft water	P_{rms} ft water	P_{std} ft water
1P	9.23	16.73	25.58	16.86	2.13
2P	6.95	47.88	101.44	48.87	9.76
3P	-69.84	10.98	30.17	17.83	14.05
4P	-25.58	0.99	8.89	4.15	4.03
5P	-12.92	-4.80	2.88	5.38	2.43
6P	-5.93	2.21	7.19	2.65	1.46
7P	-0.82	2.42	4.25	2.49	0.61
P	-0.80	8.53	21.63	9.02	2.92
9P	-4.05	1.53	4.18	1.93	1.17
10P	-32.79	-.58	22.29	5.39	5.36
11P	-8.73	1.39	7.82	2.41	1.97
12P	-83.98	5.22	15.61	9.04	7.37
13P	-14.37	-4.23	3.56	4.61	1.84
14P	-13.71	-5.15	4.78	5.58	2.14

Table 26

Differential Pressure Data

Type 4 Design

Differential Cell No.	Q=2,000 cfs Pool El 2302.9 G_o=2.25 ft	Q=5,000 cfs Pool El 2302.5 G_o=6.00 ft	Q=8,000 cfs Pool El 2578.75 G_o=6.25 ft
	Hydraulic Gradient Elevation		
DPC10	2292.4	2219.7	2373.4
DPC63A	2290.9	2210.7	2355.6
	Pressure In Prototype Feet of Water		
DPC10	10.1	82.8	205.4
DPC63A	11.6	91.8	223.1

Note: Differential pressures are referenced to the pool elevation.

Table 27

Pressures on Roof Downstream of Midtunnel

in ft of Water

Test Condition	Cell 1	2	3	4	5	6
8,000 cfs Pool el 2580						
P_{min}	-3	-4	-4	3	-4	-4
P_{max}	-2	-1	-1	23	3	6
7,000 cfs Pool el 2500						
P_{min}	-2	-4	-3	-3	-4	-3
P_{max}	-1	2	3	4	0	7
6,000 cfs Pool el 2370						
P_{min}	-3	-6	-4	-3	-5	-5
P_{max}	6	2	1	3	0	3
5,000 cfs* Pool el 2300	-1	-5	-4	-4	-6	-5
4,000 cfs* Pool el 2300	-1	-3	-7	-3	-5	-3
3,000 cfs* Pool el 2300	0	-4	-4	-3	-6	-3
2,000 cfs* Pool el 2300	-3	-6	-7	-5	-7	-4

Notes: Pressures ±0.5 ft of water.
See paragraph 29 for cell locations.
* No significant pressure fluctuation.

Table 28

Multilevel Intake Pressure Drop and Loss Coefficients

Discharge, cfs	Reservoir El	C_{p8}	C_{p10}	C_{p17}	K_{entr}
2,000	2299.50	0.08	1.29*	2.12	1.12*
2,000	2300.25	0.08	1.29*	2.09	1.09*
2,550	2582.00	0.03*	1.61	3.17	2.17
2,550	2583.00	0.11	1.95	2.87	1.87
2,550	2583.00	0.12	1.95	2.88	1.88
2,550	2582.50	0.02*	1.61	3.18	2.18
5,050	2579.00	0.10	1.76	2.90	1.90
5,050	2579.00	0.10	1.76	2.90	1.90
5,050	2580.75	0.11	1.77	2.69	1.69
5,050	2580.75	0.11	1.77	2.68	1.68
5,200	2297.50	0.11	1.67	2.64	1.64
5,200	2300.50	0.11	1.68	2.63	1.63
7,200	2573.25	0.14	2.10	3.26	2.26
7,200	2574.25	0.14	2.10	3.28	2.28
7,600	2578.50	0.11	1.80	2.87	1.87
7,600	2579.00	0.11	1.80	2.86	1.86
7,700	2579.25	0.12	1.72	2.63	1.63
7,700	2581.00	0.12	1.73	2.64	1.64
9,100	2580.50	0.12	1.80	2.74	1.74
9,100	2581.00	0.12	1.80	2.74	1.74
9,300	2580.00	0.11	1.76	2.78	1.78
9,300	2580.50	0.11	1.76	2.79	1.79
11,600	2581.50	0.11	1.55	2.36	1.36
11,600	2583.75	0.11	1.55	2.37	1.37
11,800	2582.50	0.11	1.58	2.43	1.43
11,800	2583.75	0.11	1.58	2.43	1.43
12,800	2582.50	0.10	1.42	2.19	1.19
12,800	2583.75	0.10	1.40	2.15	1.15*
13,000	2582.50	0.12	1.71	2.65	1.65
13,000	2582.50	0.12	1.71	2.65	2.65
	Average	0.105	1.728	2.685	1.727
	Standard Deviation	0.026	0.164	0.315	0.283

Note: C_{p8} = pressure drop coefficient at DPC8
C_{p10} = pressure drop coefficient at DPC10
C_{p17} = pressure drop coefficient at DPC17
K_{entr} = loss coefficient for the multilevel intake
* Not included in average or standard deviation. Pressure drop coefficients determined from DPC8, DPC10, and DPC17.

Table 29

Pressure Drop Coefficients and Friction Loss in Model Tunnel

C_{p25}	C_{p20}		f_{25-20}	Re
3.38	2.90		0.0173*	2.9E+05
3.40	2.92		0.0174*	2.9E+05
4.24	3.64		0.0216	4.1E+05
4.23	3.63		0.0216	4.1E+05
3.90	3.29		0.0218	1.4E+05
3.92	3.30		0.0223	1.4E+05
3.52	3.01		0.0183	2.9E+05
3.52	3.00		0.0184	2.9E+05
3.43	2.95		0.0173	4.4E+05
3.45	2.96		0.0174	4.4E+05
3.57	3.07		0.0180	5.1E+05
3.57	3.07		0.0181	5.1E+05
3.06	2.63		0.0155	6.6E+05
3.06	2.63		0.0155	6.6E+05
2.77	2.38		0.0140	7.2E+05
2.80	2.41		0.0142	7.2E+05
3.13	2.68		0.0162	6.7E+05
3.14	2.69		0.0162	6.7E+05
3.41	2.90		0.0183	7.4E+05
3.39	2.89		0.0182	7.4E+05
3.59	3.07		0.0185	4.3E+05
3.60	3.08		0.0187	4.3E+05
3.47	2.98		0.0177	5.3E+05
3.48	2.99		0.0178	5.3E+05
3.56	3.02		0.0193	2.9E+05
3.54	3.01		0.0193	2.9E+05
3.32	2.72		0.0216	1.4E+05
3.34	2.74		0.0217	1.4E+05
2.78	2.36		0.0151	1.1E+05
2.76	2.34		0.0151	1.1E+05
3.411	2.909	Mean		
0.368	0.316	Standard Deviation		

Note: C_{p25} = pressure drop coefficient at DPC25
C_{p20} = pressure drop coefficient at DPC20
f_{25-20} = friction loss from DPC25 to DPC20
Re = ynolds number
* Not used in least curve fit. Pressure drop coefficients calculated from differential pressure cells DPC20 and DPC25.

Table 30

Midtunnel Loss Coefficient

Discharge, cfs	Reservoir EL	Gate Opening Percent	C_{p25}	C_{p27+28}	K_t*
2,000	2299.50	26.47	2.78	0.65	0.46
2,000	2300.00	26.47	2.76	0.66	0.46
2,550	2582.00	23.53	3.32	0.89	0.63
2,550	2582.50	23.53	3.34	0.89	0.63
2,550	2583.00	23.53	3.90	0.93	0.61
2,550	2583.00	23.53	3.92	0.94	0.61
5,050	2579.00	47.06	3.54	0.94	0.66
5,050	2579.00	47.06	3.56	0.94	0.65
5,050	2580.75	35.29	3.52	0.91	0.63
5,050	2580.75	35.29	3.52	0.91	0.63
5,200	2297.50	70.59	3.38	0.99	0.72
5,200	2300.50	70.59	3.40	0.99	0.72
7,200	2573.25	73.53	4.23	1.29	0.93
7,200	2574.25	73.53	4.24	1.29	0.93
7,600	2578.50	70.59	3.59	1.05	0.76
7,600	2579.00	70.59	3.60	1.05	0.76
7,700	2579.25	70.59	3.43	1.01	0.73
7,700	2581.00	70.59	3.45	1.01	0.74
9,100	2580.50	82.35	3.57	1.26	0.98**
9,100	2581.00	82.35	3.57	1.29	1.01**
9,300	2580.50	82.35	3.47	1.23	0.96**
9,300	2580.50	82.35	3.48	1.23	0.96**
11,600	2581.50	94.12	3.06	1.24	1.01**
11,600	2583.75	94.12	3.06	1.24	1.01**
11,800	2582.50	94.12	3.13	1.20	0.96**
11,800	2583.75	94.12	3.14	1.20	0.96**
12,800	2583.75	100.00	2.77	1.03	0.84
12,800	2588.50	100.00	2.80	1.03	0.83
13,000	2582.50	100.00	3.39	1.02	0.75
13,000	2582.50	100.00	3.41	1.02	0.75
				Average	0.701
			Standard Deviation		0.122

* K_t = loss coefficient for midtunnel.

** Not used in average or standard deviation. Pressure drop coefficients were determined from differential pressure cell DPC25 and an average of the readings from DPC27 and DPC28.

Table 31

Outlet Works Pressure Drop Coefficients

No.	El	Sta	$C_{p_{mean}}$	Standard Deviation	$C_{p_{max}}$	σ_{min}
			Multilevel Inlet			
1	2103.5	1113.8	0.0457	0.0372	0.0829	4.703
2	2103.0	1117.5	0.0532	0.0382	0.0914	4.451
3	2107.0	1093.2	0.0492	0.0609	0.1101	4.671
4	2180.0	1111.4	0.0602	0.0439	0.1041	3.503
5	2205.0	1110.5	0.0154	0.0233	0.0387	3.016
6	2107.0	1111.8	0.1256	0.1734	0.2990	4.633
7	2182.5	1130.6	0.1506	0.1794	0.3300	3.553
8	2122.5	1133.0	0.1404	0.1343	0.2747	4.443
9	2116.0	1137.4	0.4968	0.3484	0.8452	4.279
10	2113.8	1145.9	1.6904	0.2600	1.9504	2.805
11	2113.8	1150.4	1.3116	0.3737	1.6853	3.332
12	2106.9	1130.0	0.4357	0.2303	0.6659	4.472
13	2106.9	1132.0	0.9433	0.3783	1.3216	3.401
14	2106.9	1134.0	0.9610	0.6041	1.5651	4.419
15	2106.9	1167.9	1.1038	0.4880	1.5918	3.530
16	2106.9	1173.4	1.1767	0.7318	1.9086	3.399
			Tunnel			
17	2116.2	1238.5	2.6058	0.7693	3.3751	29.539
18	2105.2	1312.5	2.2366	0.5137	2.7503	30.238
19	2103.0	1400.0	2.6644	0.2304	2.8948	30.198
20	2100.4	1500.0	3.2174	0.4070	3.6245	30.197
21	2097.8	1600.0	3.2490	0.5284	3.7774	29.822
22	2095.2	1700.0	3.4230	0.6514	4.0744	29.954
23	2092.6	1800.0	3.0662	0.8953	3.9616	31.102
24	2090.0	1900.0	3.7707	0.4472	4.2179	30.481
25	2087.4	2000.0	3.4932	0.1283	3.6215	30.587
26	2084.8	2100.0	3.5834	0.6083	4.1918	30.707
27	2084.0	2128.0	3.5992	0.6173	4.2166	30.755
28	2084.0	2128.0	3.6662	0.6396	4.3058	30.867
			Midtunnel Transition			
29	2083.5	2149.5	0.3461	0.1438	0.4899	3.427
30	2083.5	2149.5	0.3744	0.1280	0.5024	3.427
31	2082.9	2171.7	0.3841	0.1274	0.5115	3.431
32	2078.4	2166.9	0.2854	0.1900	0.4753	3.653
33	2082.9	2171.7	0.4914	0.1113	0.6026	3.431
			Gate Chamber			
34	2078.4	2179.5	1.1147	0.3022	1.4169	2.520

(Continued)

Table 31 (Continued)

No.	El	Sta	$C_{p_{mean}}$	Standard Deviation	$C_{p_{max}}$	σ_{min}
			Gate Chamber (Continued)			
35	2073.9	2173.5	1.0793	0.5785	1.6578	3.043
36	2078.4	2179.5	1.1634	0.2615	1.4249	2.549
37	2078.4	2173.5	0.7171	0.3347	1.0517	2.897
38	2078.4	2174.5	0.8105	0.2770	1.0875	2.918
39	2073.9	2169.8	0.3082	0.1748	0.4830	3.539
40	2075.6	2175.3	0.6663	0.3282	0.9945	3.337
41	2078.4	2173.5	0.5982	0.3268	0.9249	3.384
42	2073.9	2173.5	0.6728	0.4750	1.1478	3.434
43	2073.9	2177.3	0.3399	0.1466	0.4864	3.560
44	2078.4	2175.3	0.7421	0.2479	0.9899	2.960
45	2073.9	2176.5	1.3334	0.2101	1.5435	2.611
46	2073.9	2179.5	1.3205	0.2464	1.5669	2.737
47	2078.4	2190.8	1.2123	0.3224	1.5347	2.365
48	2073.9	2190.8	1.1314	0.3880	1.5193	2.657
49	2078.4	2190.8	1.2925	0.4437	1.7362	2.352
50	2077.4	2179.5	*	*	*	*
51	2077.4	2182.5	0.3299	0.1296	0.4594	3.492
52	2077.4	2190.8	**	**	**	**
53	2078.4	2190.8	1.3434	0.4643	1.8077	2.337
54	2073.9	2190.8	1.2822	0.5127	1.7949	2.360
55	2078.4	2190.8	1.2722	0.5198	1.7920	2.342
56	2077.4	2177.0	0.5142	0.6162	1.1304	3.469
57	2077.5	2175.3	0.5027	0.6237	1.1264	3.474
58	2078.6	2173.5	0.4786	0.6338	1.1123	3.463
59	2085.9	2173.5	0.6265	0.5946	1.2211	3.294
60	2083.7	2176.5	1.1158	0.5479	1.6637	2.599
61	2083.1	2179.5	1.5045	0.5817	2.0862	2.069
62	2082.9	2182.5	1.4019	0.5282	1.9301	2.177
63	2082.9	2190.8	1.3704	0.5268	1.8972	2.223
64	2082.9	2207.0	†	†	†	†
65	2073.9	2201.8	**	**	**	**
66	2077.4	2201.8	**	**	**	**
67	2075.6	2201.8	**	**	**	**
68	2075.6	2202.8	**	**	**	**
69	2078.4	2207.0	2.1949	0.5827	2.7777	1.483
70	2078.4	2207.0	2.1122	0.5213	2.6335	1.458
71	2073.9	2207.0	2.1717	0.2966	2.4683	1.437
72	2078.4	2206.7	2.1020	0.6605	2.7625	1.664
73	2078.4	2207.0	2.0104	0.4899	2.5004	1.613

(Continued)

* Air entrained in pressure tap opening, no data recorded.
** Bulkhead inserted in 2- by 3-ft emergency gate slot, no data recorded.
† Pressure tap damaged during testing, no data recorded.

Table 31 (Continued)

No.	El	Sta	$C_{p_{mean}}$	Standard Deviation	$C_{p_{max}}$	σ_{min}
			Gate Chamber (Continued)			
74	2073.9	2207.0	1.7495	0.8423	2.5918	1.444
			Downstream Chute			
75	2072.3	2272.0	0.1868	0.0835	0.2703	0.324
76	2072.3	2272.0	0.4749	0.4971	0.9721	0.321
77	2071.8	2292.0	0.2906	0.2547	0.5454	0.289
78	2070.8	2292.0	0.2624	0.2331	0.4955	0.318
79	2070.8	2292.0	0.1494	0.1471	0.2964	0.247
80	2070.8	2292.0	0.1020	0.0755	0.1776	0.223
81	2070.8	2292.0	0.2846	0.4556	0.7402	0.265
82	2070.8	2292.0	0.2339	0.2300	0.4639	0.281
83	2071.8	2292.0	0.3409	0.4069	0.7478	0.295
84	2071.3	2312.0	0.4163	0.6327	1.0489	0.300
85	2070.3	2312.0	0.1928	0.1777	0.3705	0.263
86	2070.3	2312.0	0.2052	0.2109	0.4161	0.299
87	2070.3	2312.0	0.1281	0.1448	0.2729	0.289
88	2070.3	2312.0	0.1001	0.1446	0.2448	0.234
89	2070.3	2312.0	0.1327	0.1523	0.2849	0.243
90	2071.3	2312.0	0.1587	0.1646	0.3233	0.272
91	2070.8	2332.0	0.4141	0.5062	0.9203	0.331
92	2069.8	2332.0	0.3027	0.3282	0.6310	0.288
93	2069.8	2332.0	0.1917	0.1751	0.3668	0.267
94	2069.8	2332.0	0.1035	0.0738	0.1774	0.258
95	2069.8	2332.0	0.3754	0.4502	0.8256	0.261
96	2069.8	2332.0	0.3000	0.3411	0.6411	0.274
97	2070.8	2332.0	0.1821	0.1612	0.3433	0.274
98	2070.3	2350.0	0.1089	0.0801	0.1890	0.243
99	2070.3	2350.0	0.0777	0.0697	0.1474	0.250
100	2068.6	2375.0	0.2362	0.2896	0.5259	0.277
101	2068.6	2375.0	0.1661	0.2571	0.4232	0.275
102	2068.6	2375.0	0.2978	0.2396	0.5374	0.333
103	2068.6	2375.0	0.2809	0.2070	0.4879	0.392
104	2069.0	2400.0	0.2012	0.2814	0.4826	0.289
105	2068.0	2400.0	0.2703	0.3182	0.5885	0.367
106	2068.0	2400.0	0.2712	0.2637	0.5349	0.316
107	2068.0	2400.0	0.0973	0.0505	0.1478	0.276
108	2069.0	2400.0	0.1167	0.0772	0.1939	0.280
109	2065.4	2500.0	0.0710	0.0277	0.0988	0.293
110	2062.8	2600.0	0.1777	0.1320	0.3098	0.289
111	2062.8	2600.0	0.1803	0.1704	0.3507	0.306
112	2062.8	2600.0	0.1375	0.0777	0.2152	0.365

(Continued)

Table 31 (Concluded)

No.	El	Sta	$C_{p_{mean}}$	Standard Deviation	$C_{p_{max}}$	σ_{min}
			Downstream Chute			
113	2060.2	2700.0	0.1738	0.1383	0.3122	0.280
114	2057.6	2800.0	0.3097	0.3591	0.6688	0.279
115	2057.6	2800.0	0.2257	0.2596	0.4853	0.312
116	2057.6	2800.0	0.1513	0.1170	0.2683	0.285
117	2055.0	2900.0	0.2212	0.2963	0.5176	0.262
118	2052.4	3000.0	0.1527	0.1078	0.2605	0.313
119	2052.4	3000.0	0.2266	0.2301	0.4567	0.270
120	2052.4	3000.0	0.0813	0.1075	0.1888	0.321
A	2071.0	2322.0	0.0439	0.0743	0.1182	*
B	2071.5	2302.0	0.2173	0.2218	0.4391	0.254
C	2072.1	2282.0	0.3183	0.2827	0.6010	0.310
D	2072.1	2257.0	0.2645	0.2556	0.5201	0.278
E	2073.0	2244.5	0.1619	0.2291	0.3910	0.291
			Standard Deviation	0.3134		

* Air entrained in pressure tap opening, no data recorded.

Table 32

Water-Surface Cross Sections

Q = 5,000 cfs, G_o = 6.0, Pool El 2300

Distance from Left Sidewall ft	Sta 23+86.5 (Low Water Surface) Water Depth ft	Water-Surface El	Sta 24+33.75 (High Water Surface) Water Depth ft	Water-Surface El	Sta 30+80 (Exit Channel) Water Depth ft	Water-Surface El
0.0	3.0	2071.3	5.8	2072.9	4.5	2054.8
2.5	2.9	2071.2	5.0	2072.1	4.4	2054.7
5.0	4.5	2072.8	3.0	2070.1	4.1	2054.4
7.5	4.8	2073.1	2.8	2069.9	4.0	2054.3
10.0	5.0	2073.3	2.9	2070.0	3.6	2053.9
12.5	4.5	2072.8	3.0	2070.1	3.6	2053.9
15.0	3.5	2071.8	3.3	2070.4	4.0	2054.3
18.0	2.8	2071.1	6.0	2073.1	3.9	2054.2

Table 33

Water-Surface Cross Sections

Q = 8,000 cfs, G_o = 6.25, Pool El 2580

Distance from Left Sidewall ft	Sta 24+41.25 (Low Water Surface) Water Depth ft	Water-Surface El	Sta 25+02.5 (High Water Surface) Water Depth ft	Water-Surface El	Sta 30+80 (Exit Channel) Water Depth ft	Water-Surface El
0.0	3.3	2070.2	6.5	2071.8	5.0	2055.3
2.5	4.0	2070.9	4.3	2069.6	5.5	2055.8
5.0	4.0	2070.9	3.8	2069.1	6.0	2056.3
7.5	5.0	2071.9	3.3	2068.6	5.5	2055.8
10.0	5.0	2071.9	3.3	2068.6	5.5	2055.8
12.5	4.5	2071.4	3.6	2068.8	5.8	2056.1
15.0	3.0	2069.9	3.6	2069.8	5.3	2055.6
18.0	2.8	2069.7	3.6	2069.8	4.8	2055.1

Table 34

Velocities and Wave Heights

in Plunge Pool

Station	Dist From ℄ ft	Velocity fps	Wave Height ft	Station	Dist From ℄ ft	Velocity fps	Wave Height ft
4,000 cfs, Pool El 2300, Tailwater El 2003.75				6,000 cfs, Pool El 2400, Tailwater El 2003.75			
32+34.8L	175.0	5.8	0.13	32+34.8L	163.0	8.1	0.25
32+34.8R	175.0	8.6	0.25	32+34.8R	163.0	13.7	0.18
32+50L	192.5	7.0	0.25	32+50L	187.5	7.9	0.28
32+50R	192.5	8.2	0.15	32+50R	187.5	13.3	0.30
32+75L	212.5	5.7	0.12	32+75L	195.0	10.6	0.18
32+75R	212.5	6.7	0.15	32+75R	190.0	12.4	0.18
33+00L	220.0	5.9	0.15	33+00L	220.0	12.2	0.13
33+00R	215.0	6.1	0.13	33+00R	200.0	11.2	0.40
33+25L	220.0	6.2	0.13	33+25L	195.0	12.7	0.30
33+25R	220.0	6.8	0.18	33+25R	200.0	11.8	0.23
33+50L	225.0	7.1	0.17	33+50L	197.5	13.4	0.23
33+50R	220.0	7.2	0.13	33+50R	205.0	11.6	0.25
33+75L	225.0	5.7	0.18	33+75L	197.5	11.5	0.25
33+75R	225.0	6.9	0.12	33+75R	207.5	10.1	0.28
34+00L	222.5	5.7	0.15	34+00L	195.0	13.1	0.15
34+00R	222.5	5.9	0.20	34+00R	205.0	13.4	0.25
34+25L	210.0	5.6	0.10	34+25L	200.0	11.5	0.30
34+25R	200.0	3.9	0.13	34+25R	217.5	13.0	0.13
34+50L	200.0	4.5	0.25	34+50L	200.0	11.0	0.10
34+50R	202.5	3.4	0.12	34+50R	202.5	12.2	0.50
34+75L	205.0	3.2	0.75	34+75L	195.0	9.6	0.08
34+75R	205.0	3.9	0.13	34+75R	207.5	11.6	0.25
35+00L	180.0	3.0	0.18	35+00L	182.5	10.6	0.08
35+00R	185.0	2.6	0.13	35+00R	187.5	8.5	0.30
35+25L	177.5	1.7	0.10	35+25L	175.0	7.8	0.20
35+25R	175.0	2.0	0.20	35+25R	175.0	6.2	0.28
35+50L	147.5	0.9	0.20	35+50L	150.0	5.8	0.25
35+50R	150.0	0.4	0.28	35+50R	150.0	4.4	0.23

(Continued)

Table 34 (Concluded)

Station	Dist From ℄ ft	Velocity fps	Wave Height ft
6,000 cfs, Pool El 2400, Tailwater El 2003.75 (Continued)			
35+75L	87.5	3.0	0.50
35+75R	112.5	1.4	1.35
8,000 cfs, Pool El 2580, Tailwater El 2003			
32+34.8L	125.0	7.4	0.50
32+34.8R	112.5	4.2	0.15
32+50L	160.0	7.5	0.08
32+50R	112.5	15.0	0.25
32+75L	180.0	13.2	0.20
32+75R	150.0	17.6	0.52
33+00L	188.8	11.3	0.25
33+00R	150.0	18.3	0.45
33+25L	200.0	13.2	0.33
33+25R	163.8	18.7	0.28
33+50L	200.0	12.5	0.42
33+50R	175.0	14.4	0.33
33+75L	207.5	16.1	0.30
33+75R	175.0	16.6	0.25
34+00L	200.0	17.9	0.12
34+00R	182.5	14.5	0.42
34+25L	207.5	19.8	0.28
34+25R	187.5	16.7	0.25
34+50L	180.0	17.5	0.47
34+50R	185.0	15.9	0.47
34+75L	175.0	16.4	0.43
34+75R	175.0	16.4	0.32
35+00L	162.5	15.7	0.32
35+00R	155.0	18.2	0.15
35+25L	142.5	15.3	0.48
35+25R	137.5	15.2	0.42
35+50L	147.5	15.9	0.25
35+50R	143.8	15.1	0.25
35+75L	117.5	13.2	0.75
35+75R	75.0	14.5	0.32
36+00L	117.5	13.5	0.75
36+00R	75.0	4.4	0.97

Table 35

Water-Surface Data

1V on 3H Sloping Apron

Dist From ℄	Station	Water-Surface El
Q = 4,000 cfs, Pool El 2300, G_o = 4.75 ft		
Tailwater El = 2012.5		
47.5	31+67.8	2012.3
42.5	31+68	2012.3
37.5	31+68.7	2102.0
32.5	31+68.2	2012.2
27.5	31+71.6	2011.1
22.5	31+74.9	2010.0
17.5	31+76.1	2009.6
12.5	31+77.8	2009.3
7.5	31+77.2	2009.2
2.5	31+77.7	2009.0
0	31+78.4	2008.8
Q = 5,000 cfs, Pool El 2305, G_o = 6.25 ft		
Tailwater El = 2013		
47.5	31+68.2	2012.2
42.5	31+67.8	2012.3
37.5	31+66.8	2012.7
32.5	31+66.8	2012.7
27.5	31+67.5	2012.4
22.5	31+69.6	2011.7
17.5	31+73.0	2010.6
12.5	31+74.2	2010.2
7.5	31+74.4	2010.1
2.5	31+74.9	2010.0
0	31+75.1	2009.9
Q = 6,000 cfs, Pool El 2380, G_o = 6.25 ft		
Tailwater El = 2011		
47.5	31+72.0	2010.9
42.5	31+71.3	2011.2
37.5	31+70.1	2011.5
32.5	31+70.1	2011.5
27.5	31+69.4	2011.8
22.5	31+69.7	2011.7
17.5	31+74.2	2010.2
12.5	31+74.9	2010.0
7.5	31+77.2	2009.2
2.5	31+79.1	2008.6
0	31+80.8	2008.0

(Continued)

Table 35 (Concluded)

Dist From ℄	Station	Water-Surface El
Q = 7,000 cfs, Pool El 2500, G_o = 6.25 ft		
	Tailwater El = 2008	
47.5	31+83.2	2007.2
42.5	31+82.5	2007.4
37.5	31+82.0	2007.6
32.5	31+82.0	2007.6
27.5	31+82.0	2007.6
22.5	31+81.8	2007.7
17.5	31+83.4	2007.1
12.5	31+84.4	2006.8
7.5	31+86.2	2006.2
2.5	31+89.1	2005.2
0	31+89.6	2005.1
Q = 8,000 cfs, Pool El 2580, G_o = 6.25 ft		
	Tailwater El = 2005	
47.5	31+90.3	2004.8
42.5	31+90.8	2004.7
37.5	31+89.1	2005.2
32.5	31+89.1	2005.2
27.5	31+89.1	2005.2
22.5	31+89.1	2005.2
17.5	31+93.8	2003.7
12.5	31+93.8	2003.7
7.5	31+97.9	2002.3
2.5	31+98.6	2002.1
0	31+98.8	2002.0

Photo 1. Flow conditions, type 1 (original) dissipator; discharge 2,000 cfs; pool el 2300; 50 min (prototype)

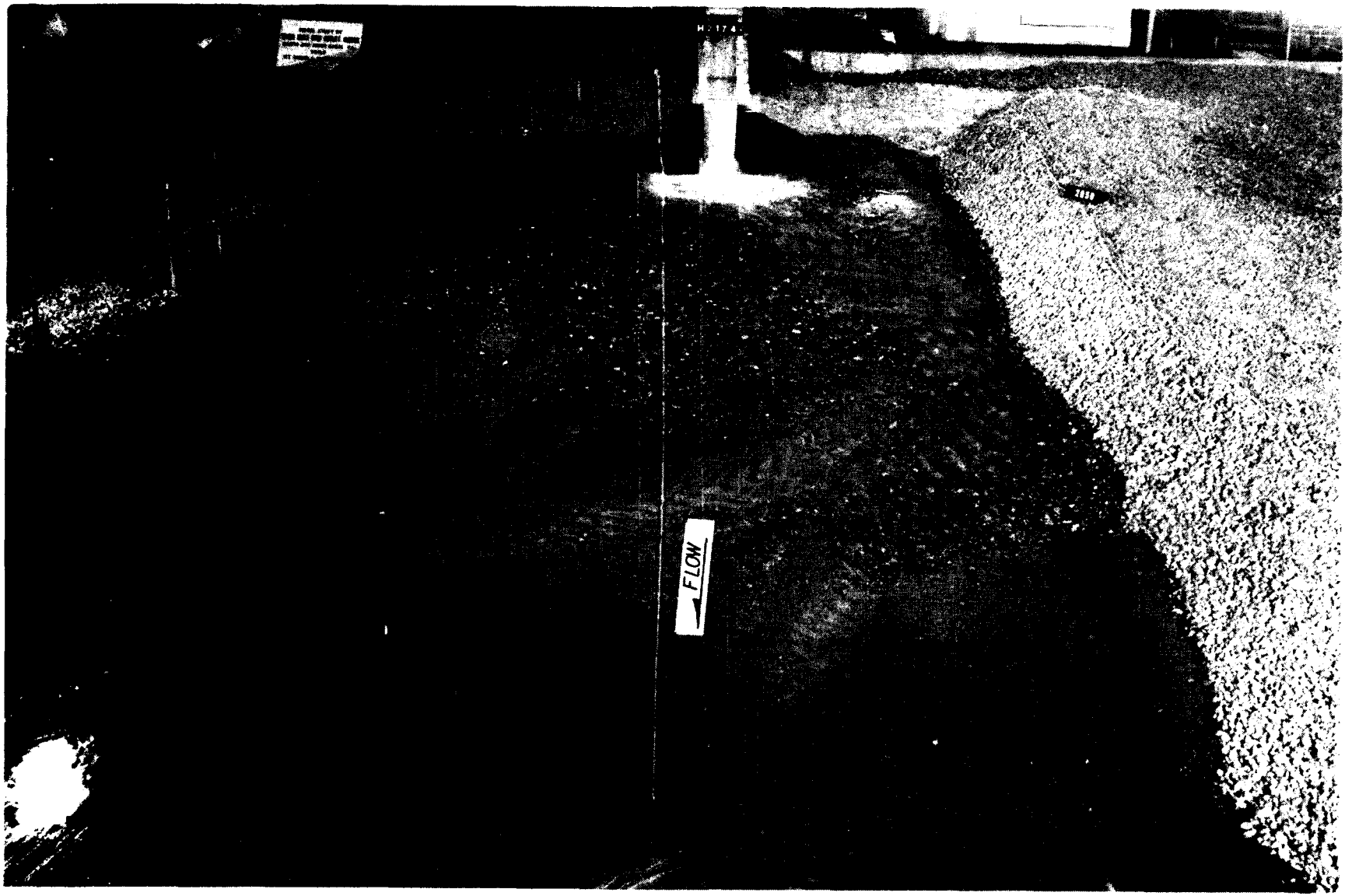

Photo 2. Flow conditions, type 1 (original) dissipator; discharge 2,000 cfs; pool el 2300; 1 hr 40 min (prototype)

Photo 3. Scour contours, type 1 (original) energy dissipator; discharge 2,000 cfs; pool el 2300; 5 hr (prototype)

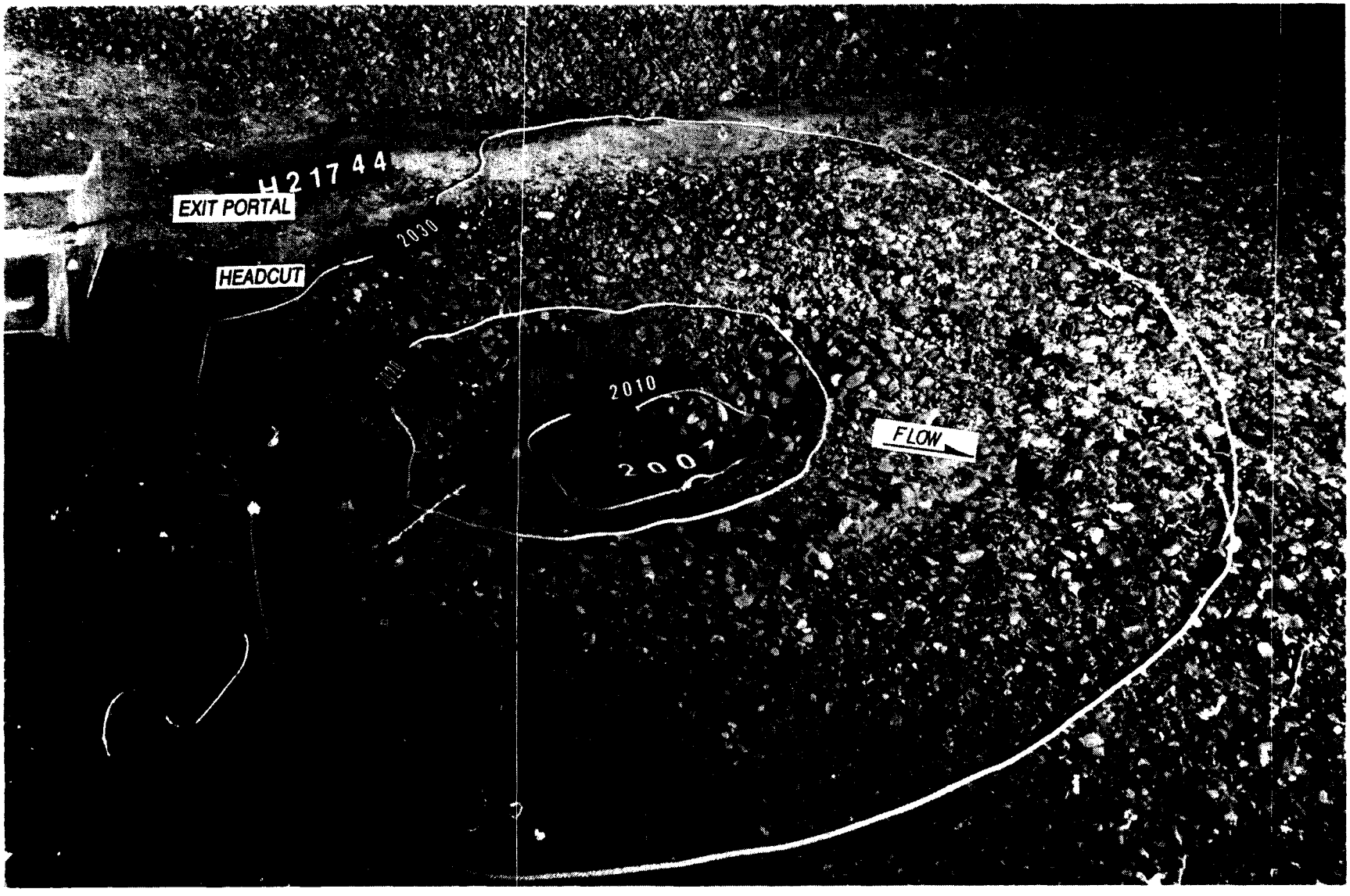

Photo 4. Closeup of scour, type 1 (original) energy dissipator; discharge 2,000 cfs; pool el 2300

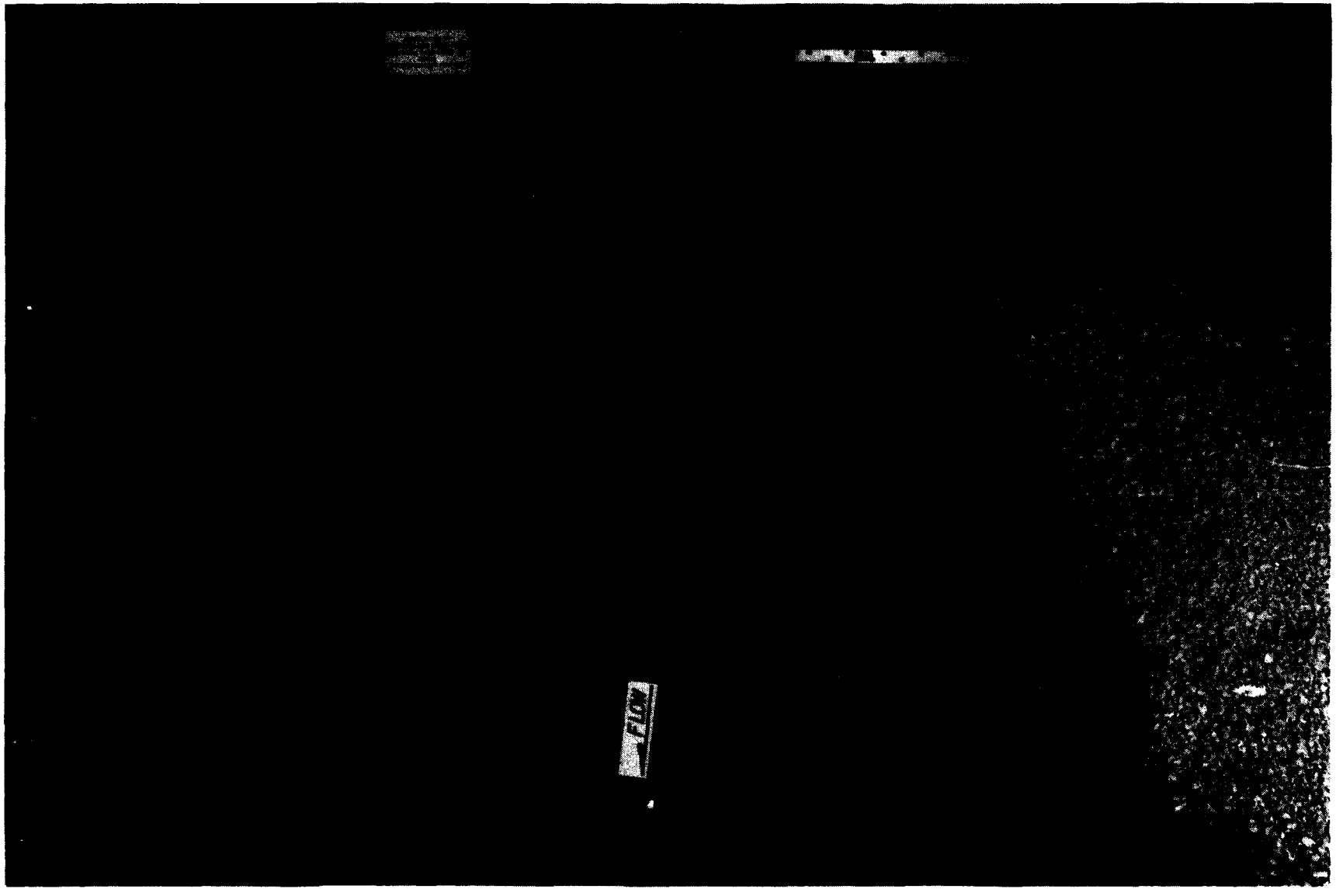

Photo 5. Flow conditions, type 1 (original) dissipator; discharge 4,000 cfs; pool el 2300; 50 min (prototype)

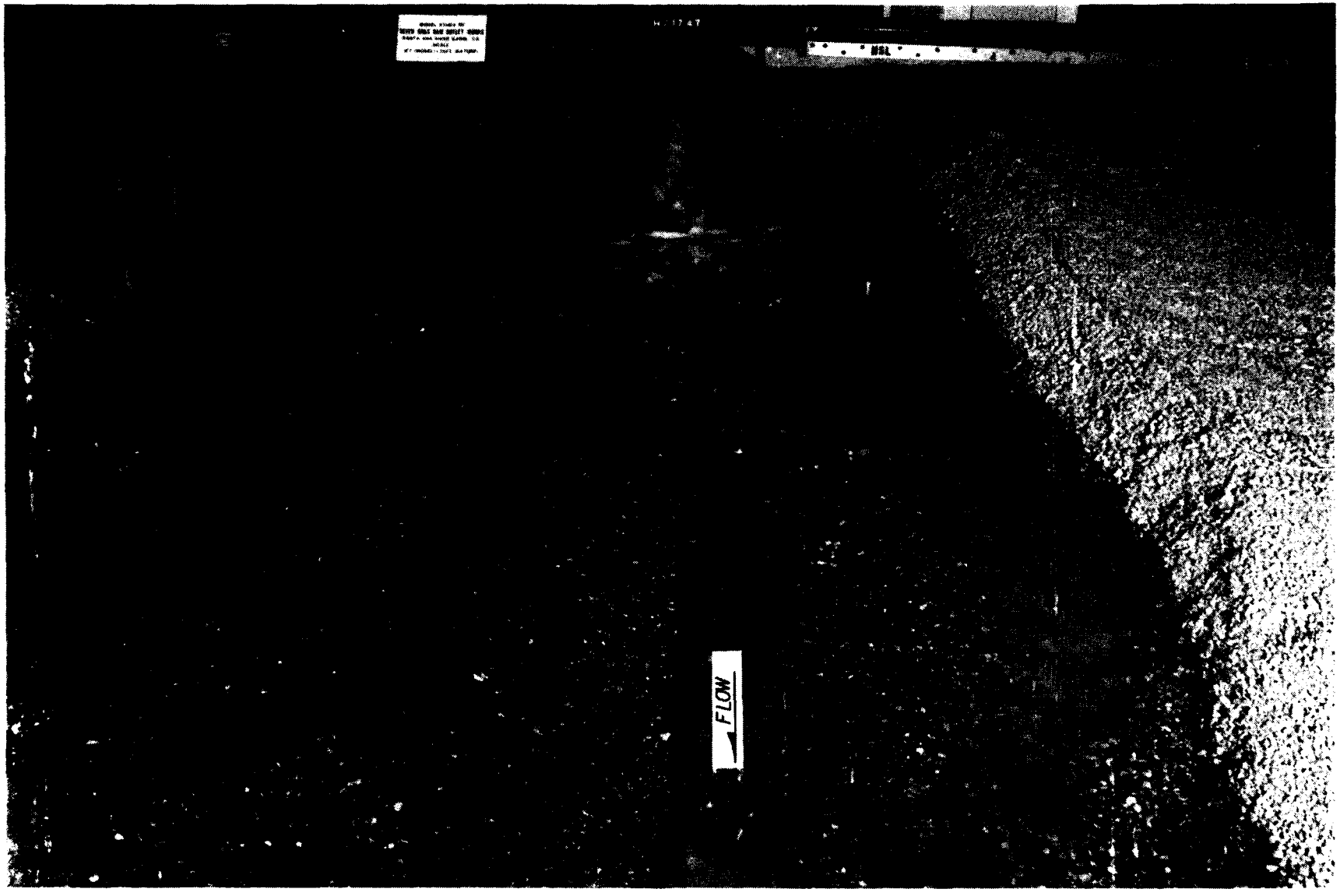

Photo 6. Flow conditions, type 1 (original) dissipator; discharge 4,000 cfs; pool el 2300; 2 hr 30 min (prototype)

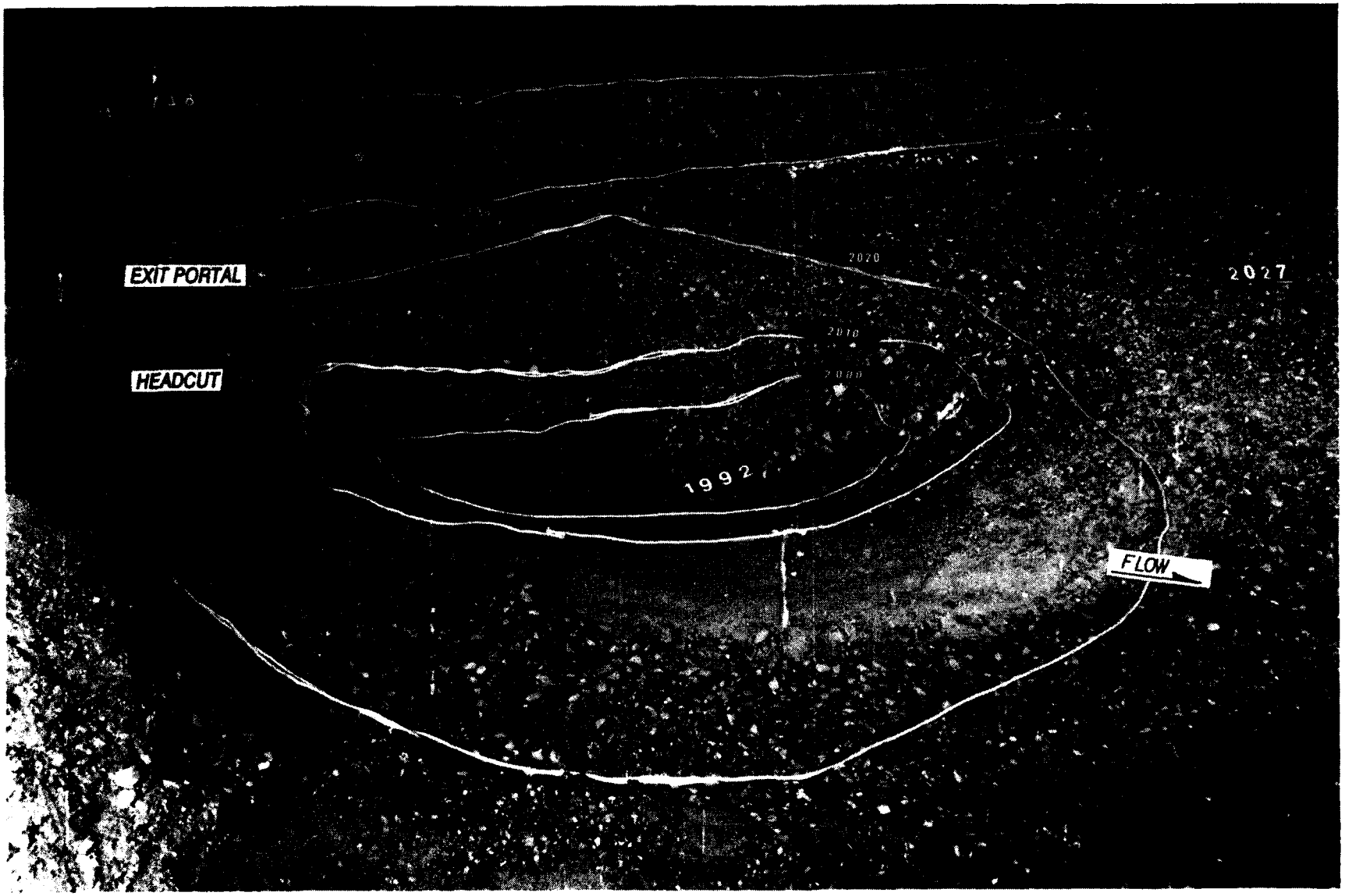

Photo 7. Scour contours, type 1 (original) energy dissipator; discharge 4,000 cfs; pool el 2300; 5 hr (prototype)

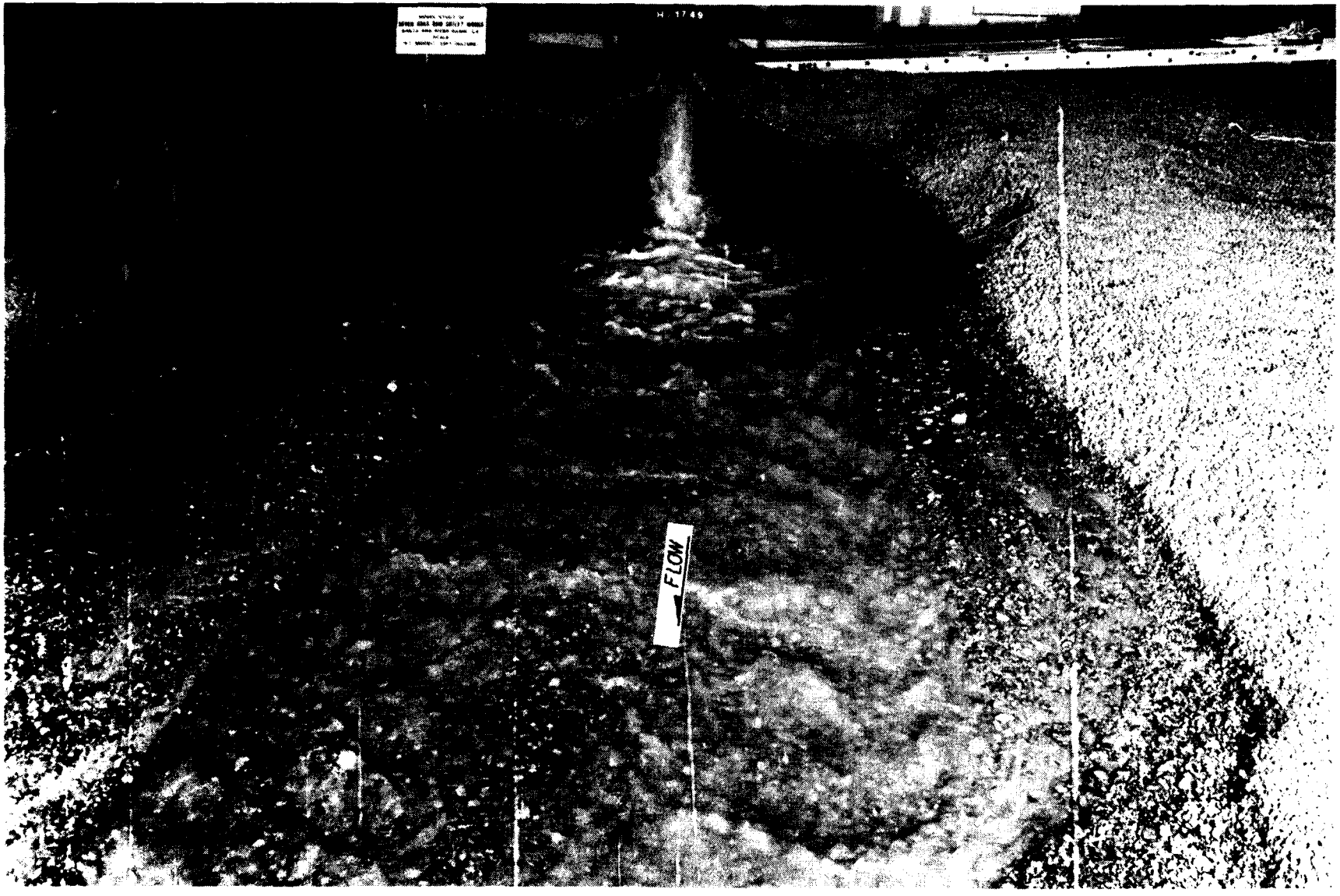

Photo 8. Flow conditions, type 1 (original) dissipator; discharge 6,000 cfs; pool el 2400; 5 hr (prototype)

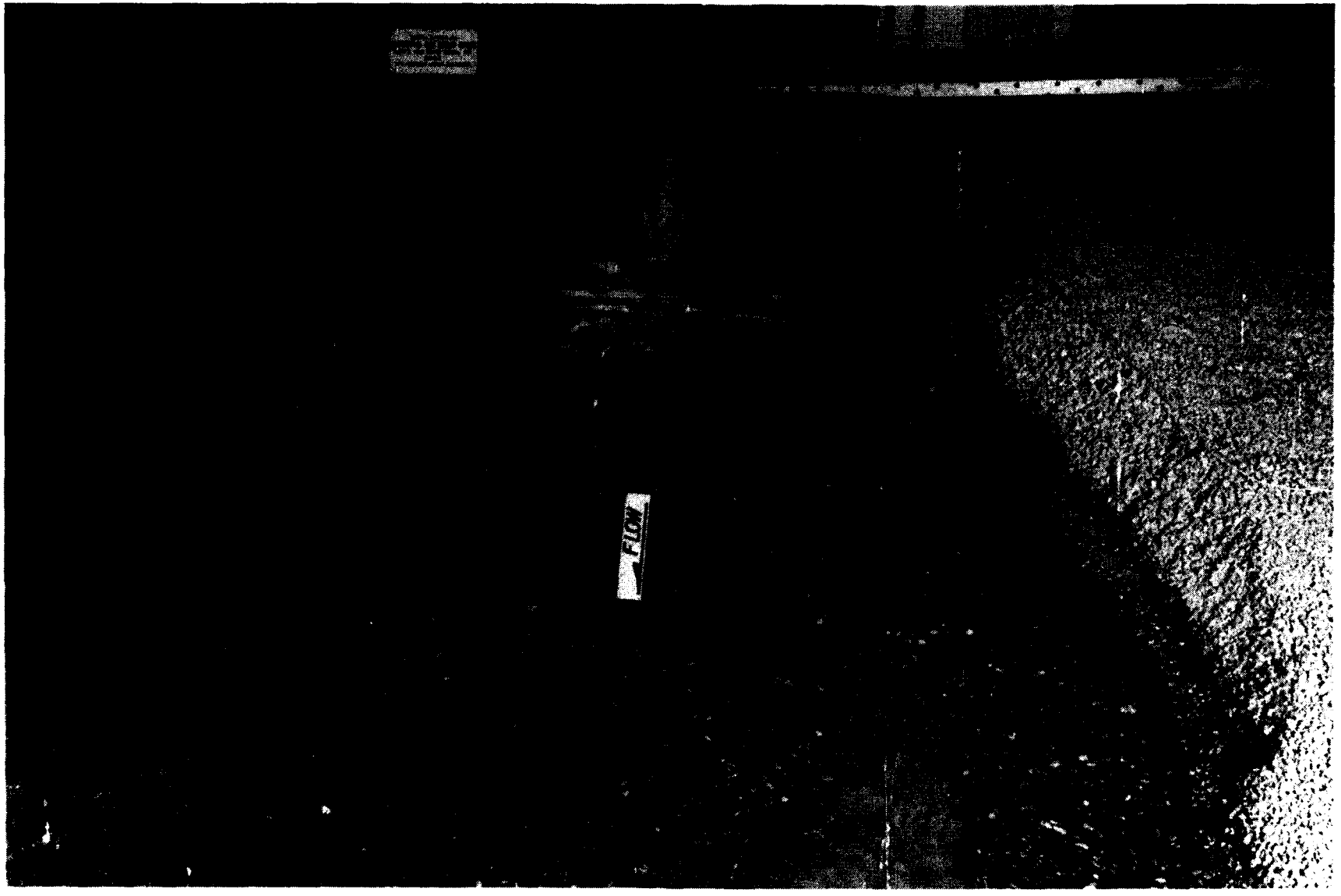

Photo 9. Flow conditions, type 1 (original) dissipator; discharge 6,000 cfs; pool el 2400; 2 hr 30 min (prototype)

Photo 10. Scour contours, type 1 (original) energy dissipator; discharge 6,000 cfs; pool el 2400; 5 hr (prototype)

Photo 11. Flow conditions, type 1 (original) dissipator; discharge 8,000 cfs; pool el 2580; 50 min (prototype)

Photo 12. Flow conditions, type 1 (original) dissipator; discharge 8,000 cfs; pool el 2580; 2 hr 30 min (prototype)

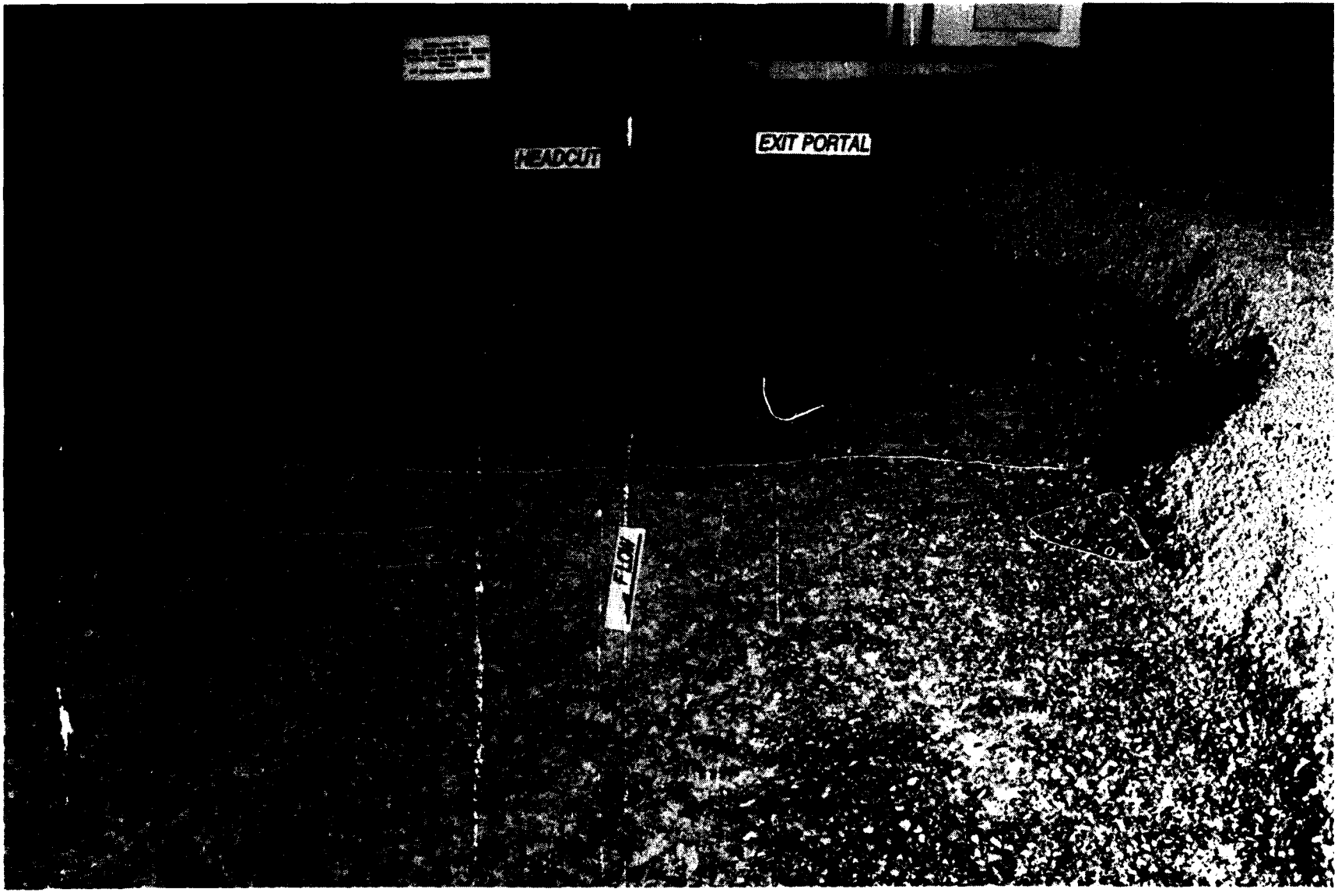

Photo 13. Scour contours, type 1 (original) energy dissipator; discharge 8,000 cfs; pool el 2580; 4 hr 30 min (prototype)

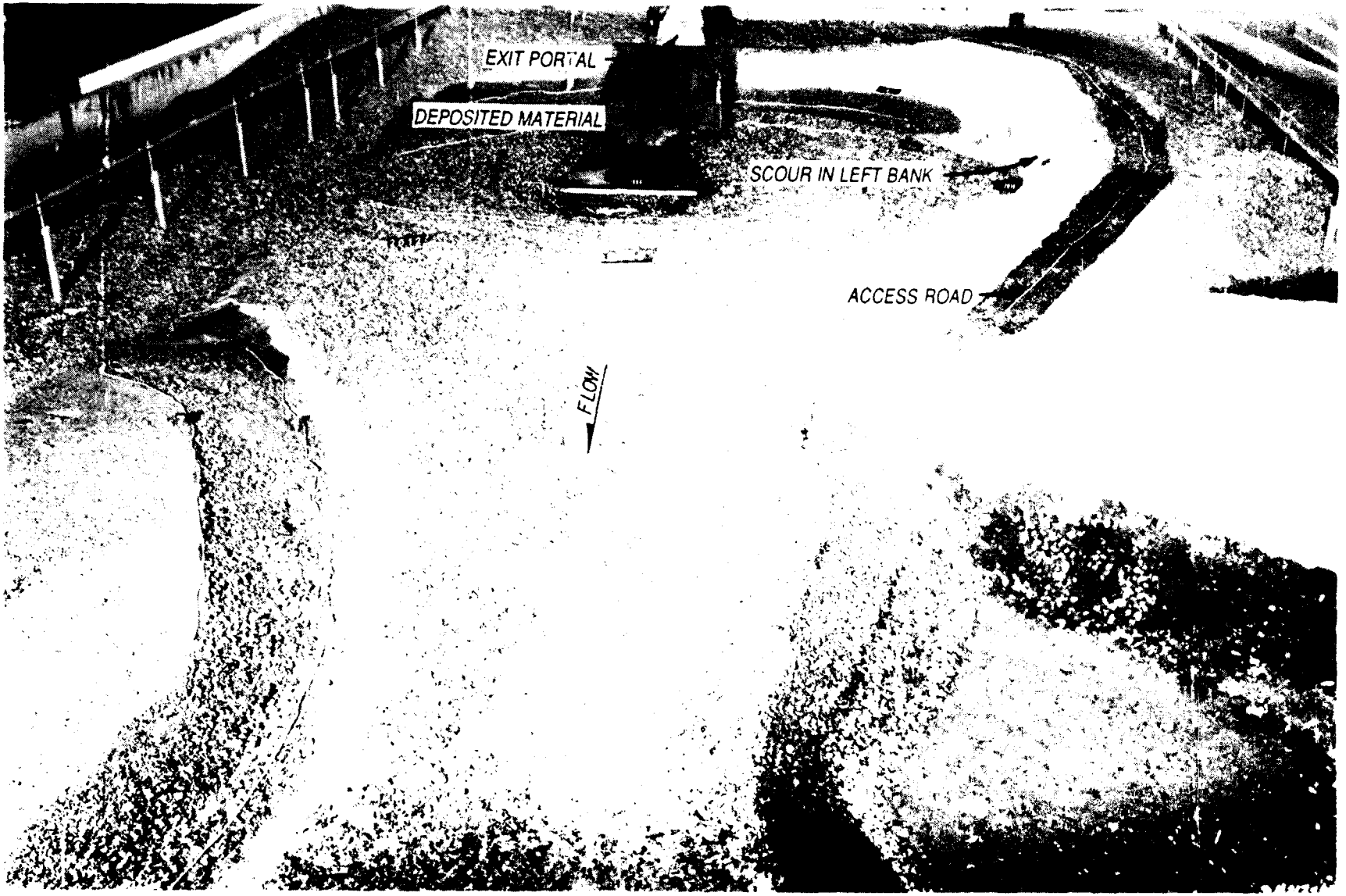

Photo 14. Scour pattern, type 2 design energy dissipator/preformed scour; discharge 8,000 cfs; pool el 2580; 2 hr (prototype)

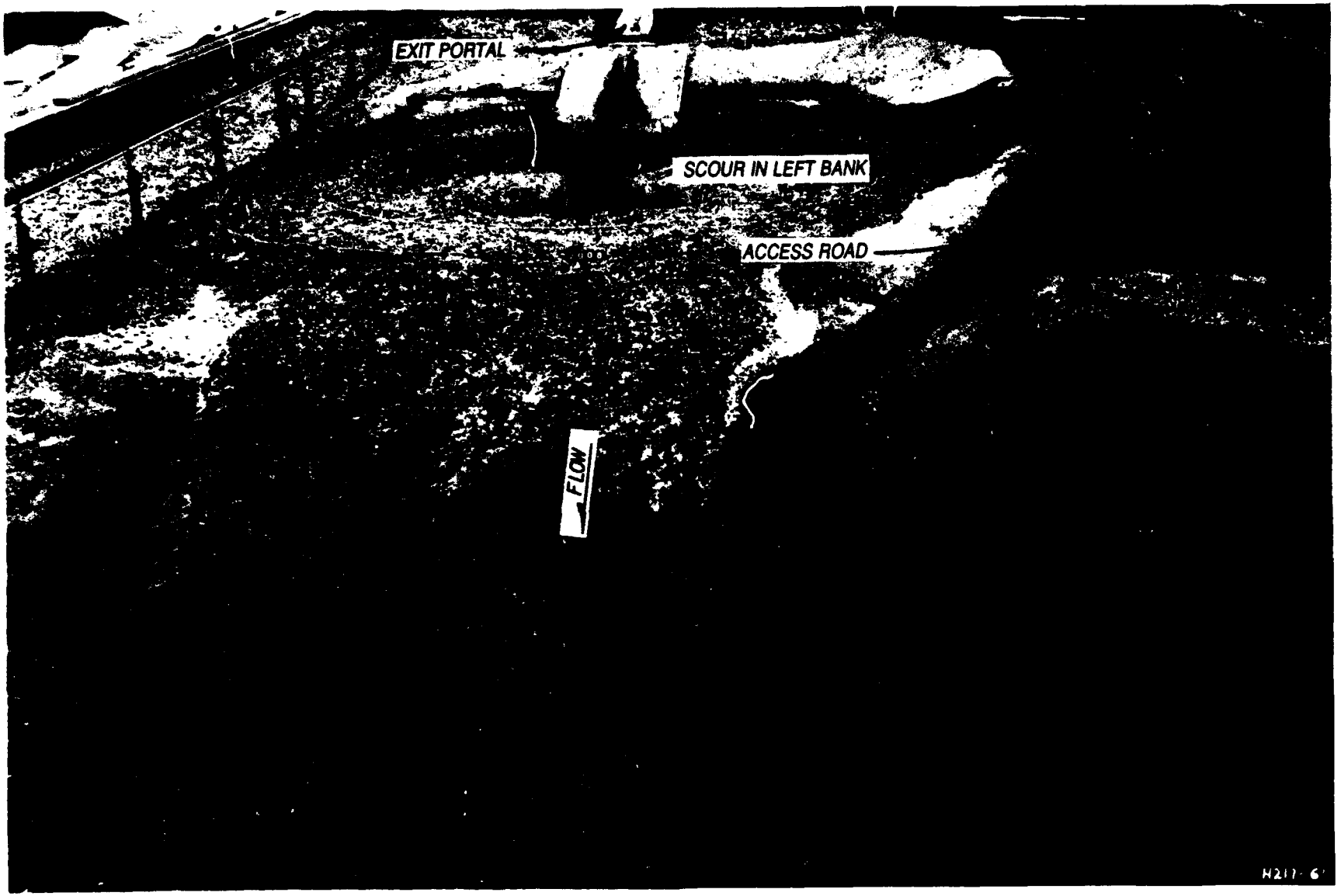

Photo 15. Scour, type 3 design energy dissipator/preformed scour; discharge 8,000 cfs; pool el 2580; 5 hr (prototype)

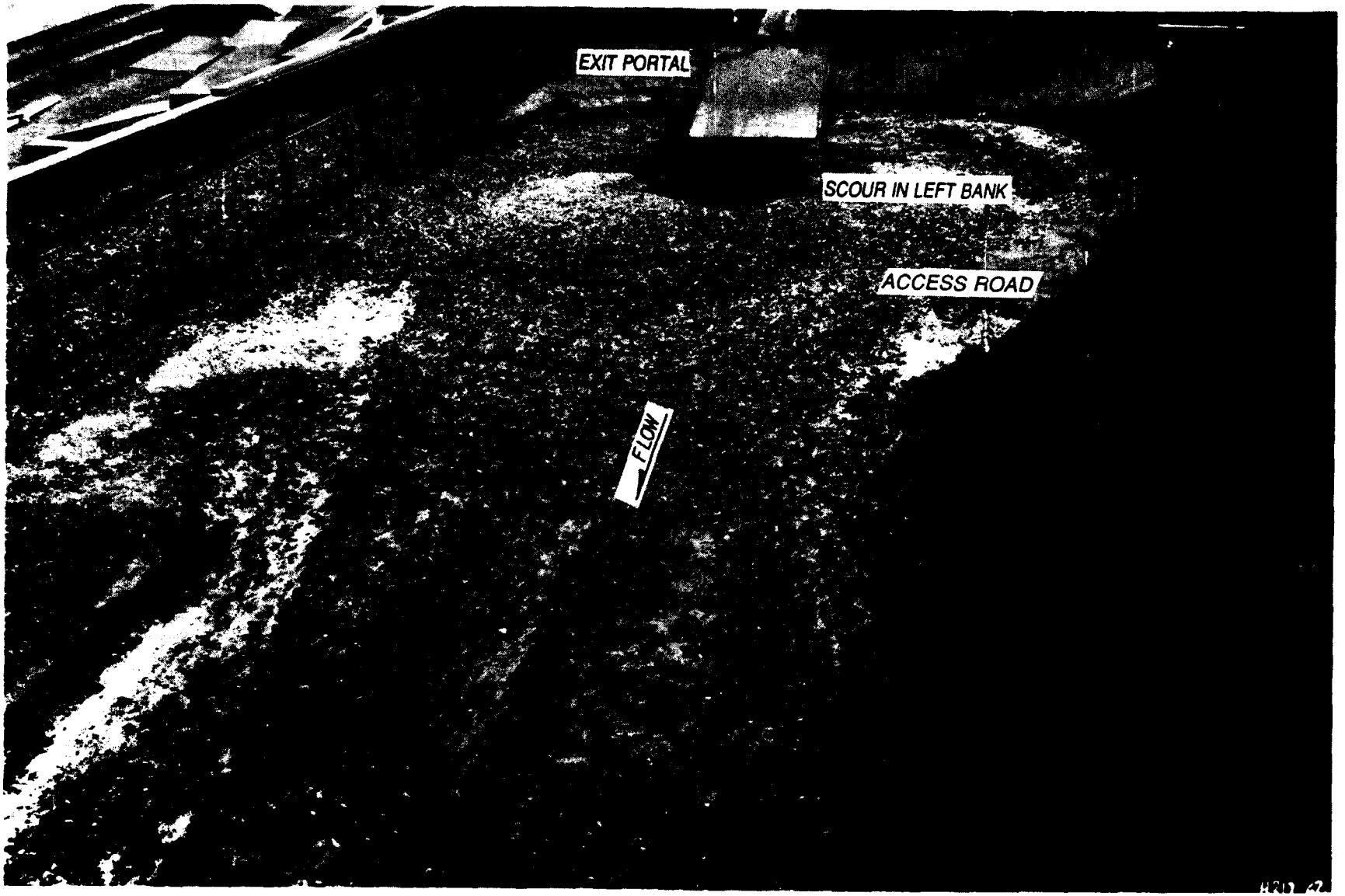

Photo 16. Scour, type 4 design energy dissipator/preformed scour; discharge 8,000; pool el 2580; 1 hr (prototype)

Photo 17. Flow trajectory with deflectors, discharge 8,000 cfs; pool el 2580

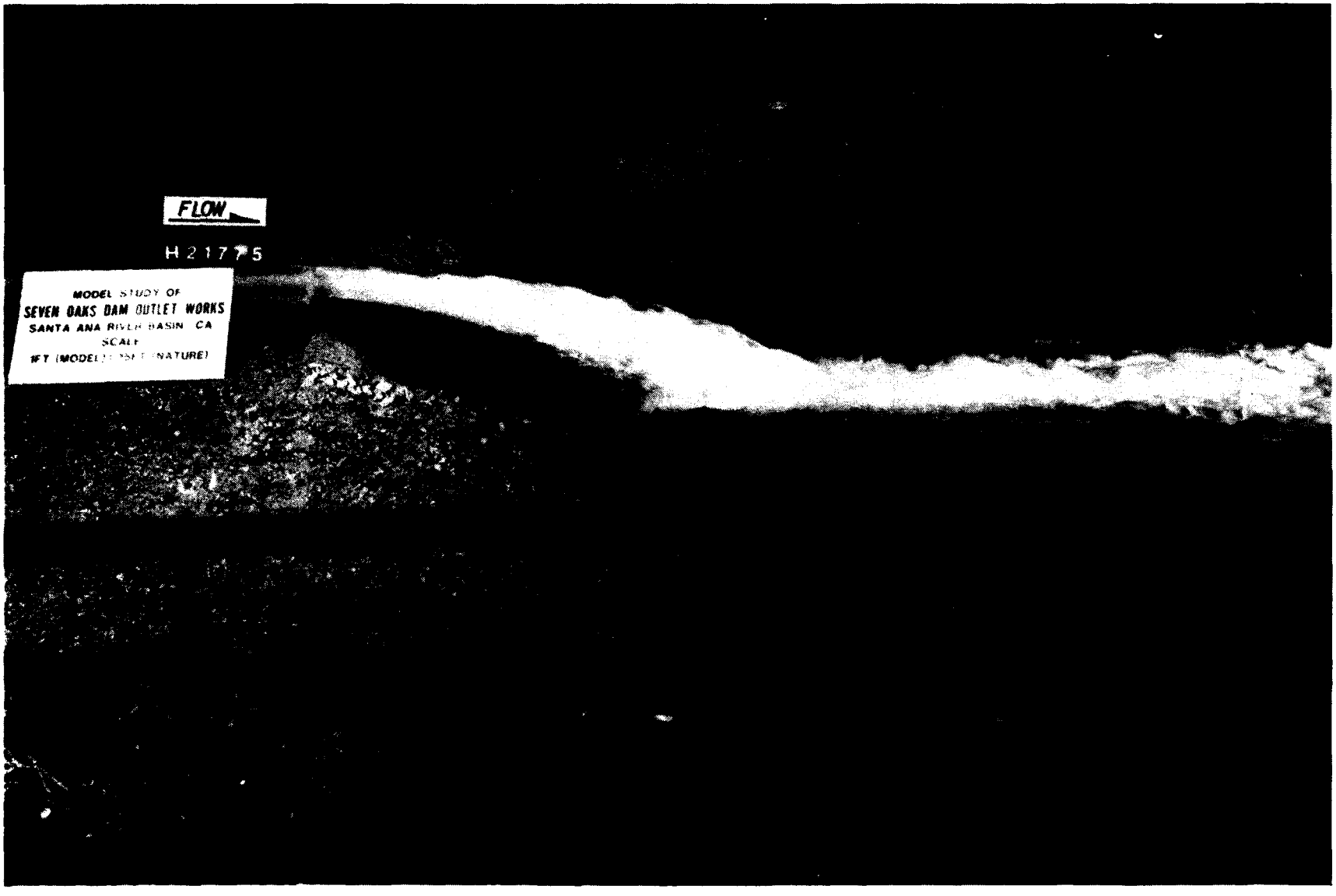

Photo 18. Flow trajectory without deflectors, discharge 8,000 cfs; pool el 2580

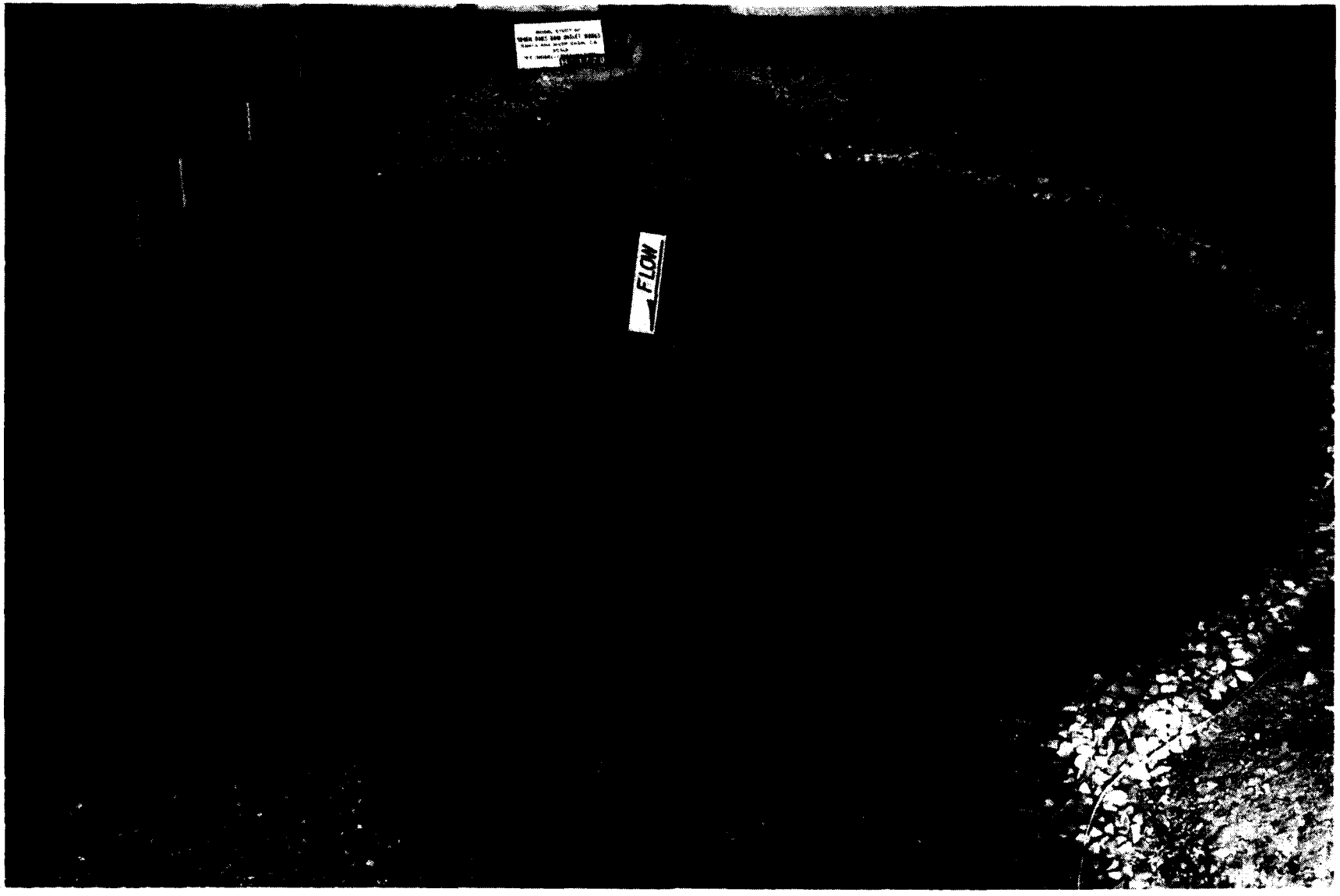

Photo 19. Flow conditions, type 10 energy dissipator; discharge 2,000 cfs; pool el 2300

Photo 20. Flow conditions, type 10 energy dissipator; discharge 4,000 cfs; pool el 2300

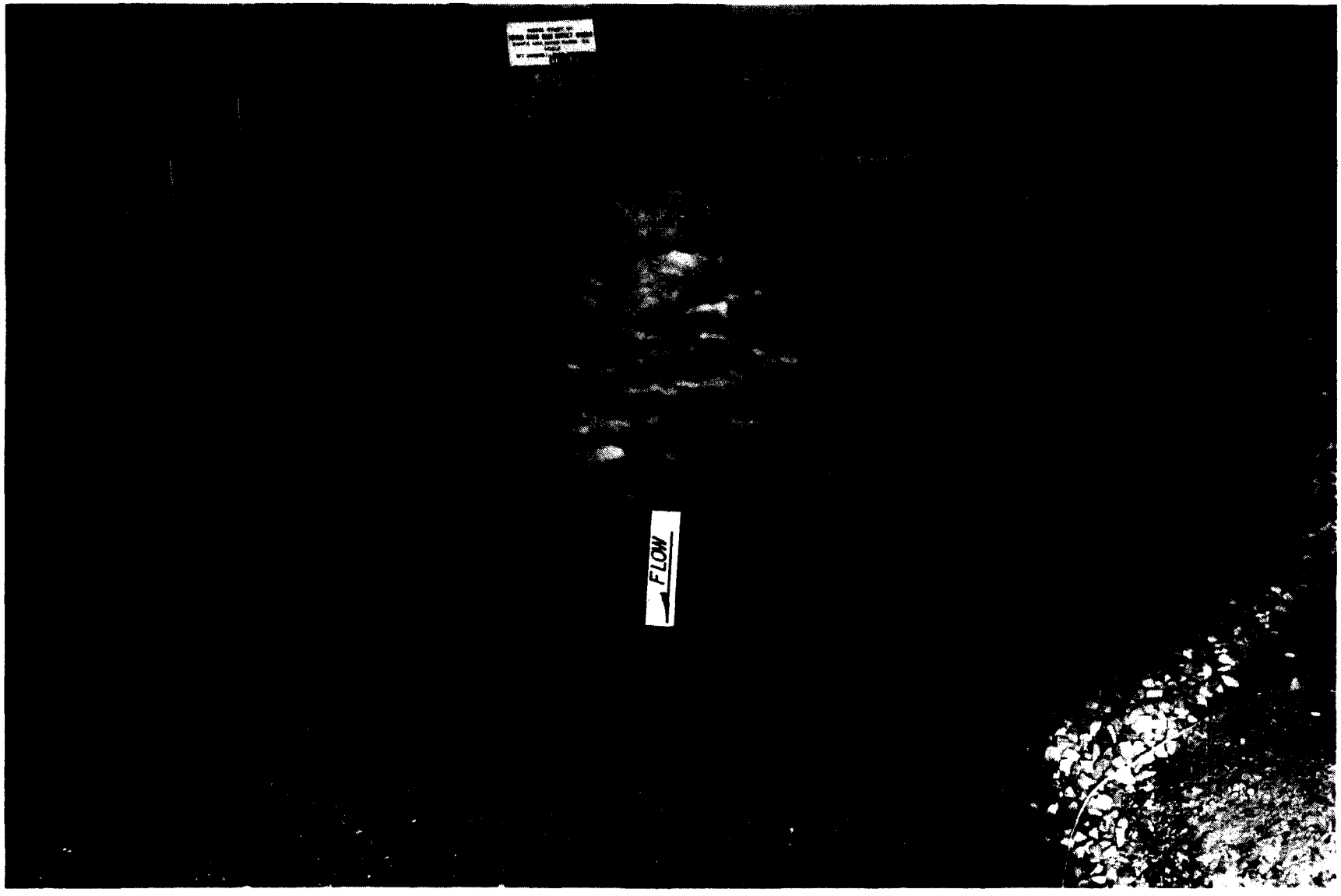

Photo 21. Flow conditions, type 10 energy dissipator; discharge 6,000 cfs; pool el 2400

Photo 22. Flow conditions, type 10 energy dissipator; discharge 8,000 cfs; pool el 2580

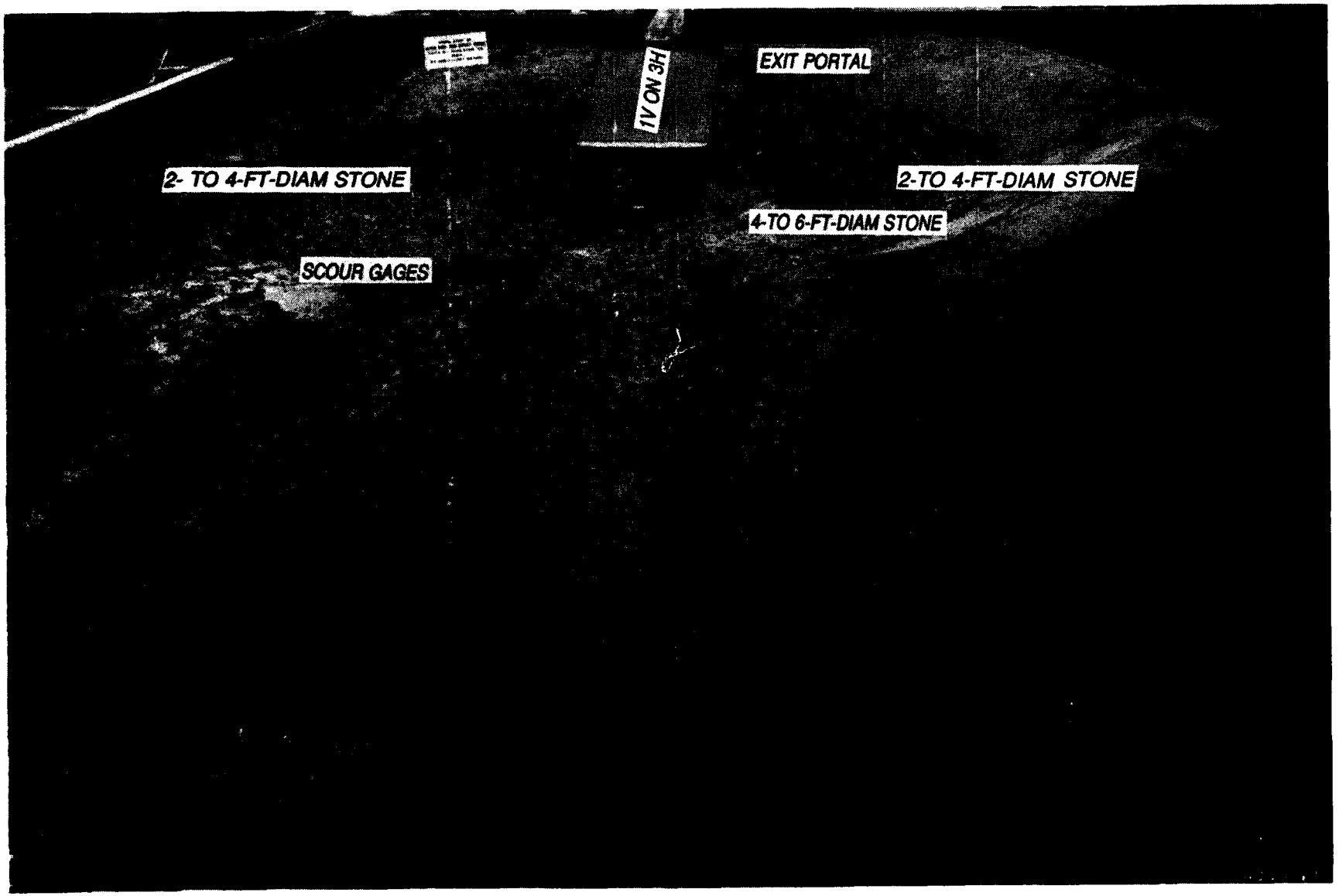

Photo 23. Scour, type 10 design energy dissipator/preformed scour; discharge 8,000 cfs; pool el 2580; 5 hr (prototype)

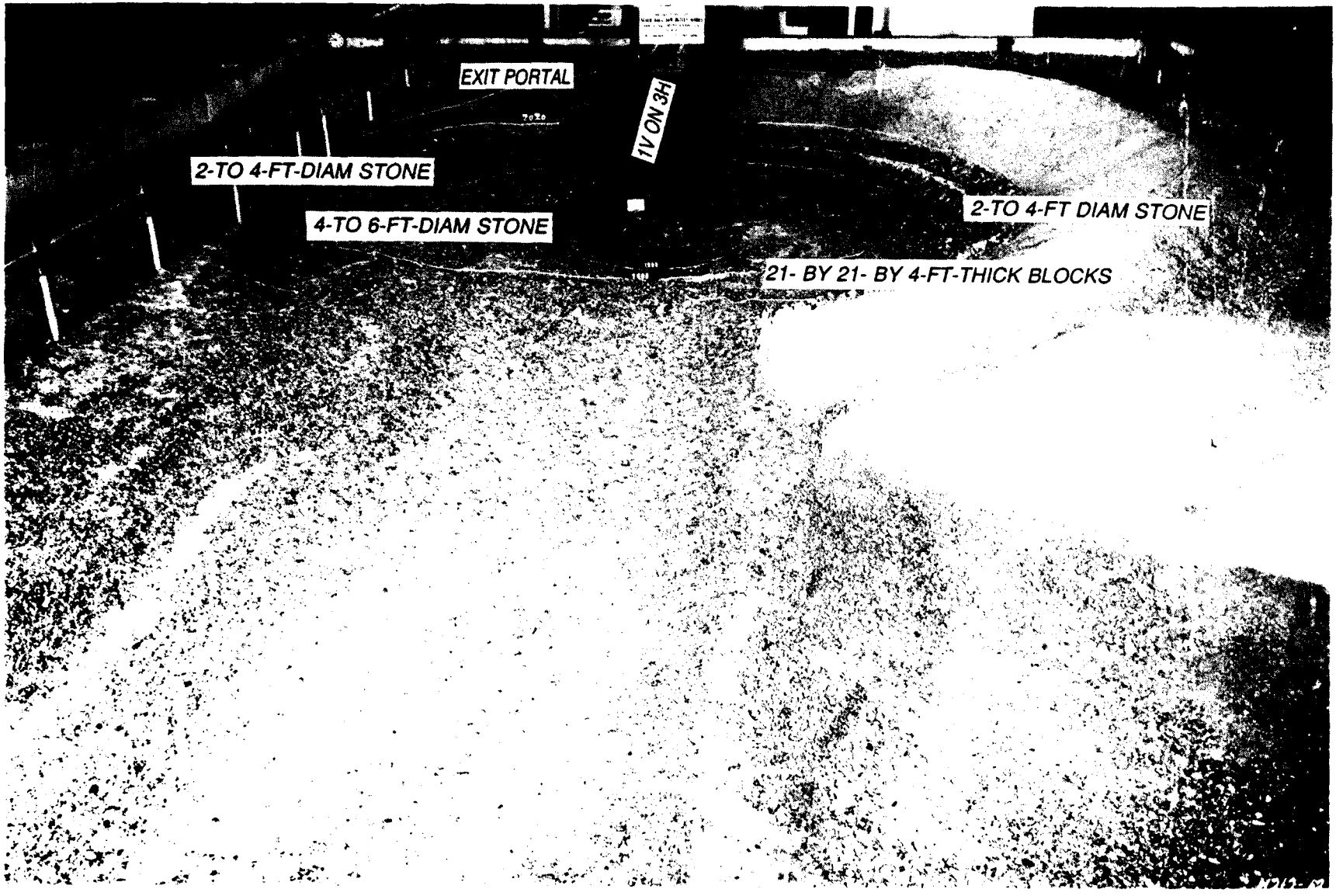

Photo 24. Type 1 design apron mat, discharge 8,000 cfs; pool el 2580; 5 hr (prototype)

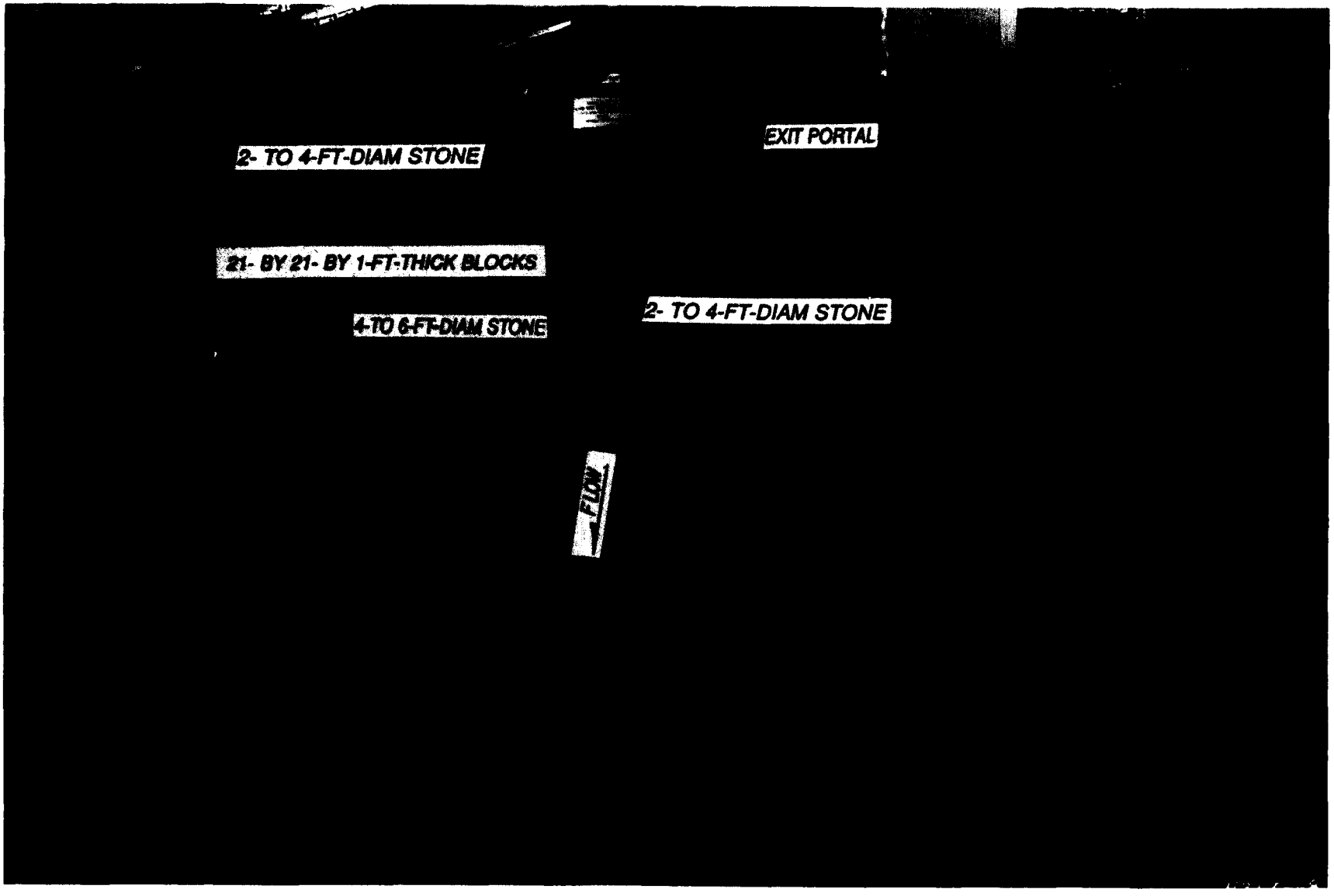

Photo 25. Failure of type 2 design apron mat, 21-ft-long by 21-ft-wide by 1-ft-thick blocks; discharge 400 cfs; pool el 2300

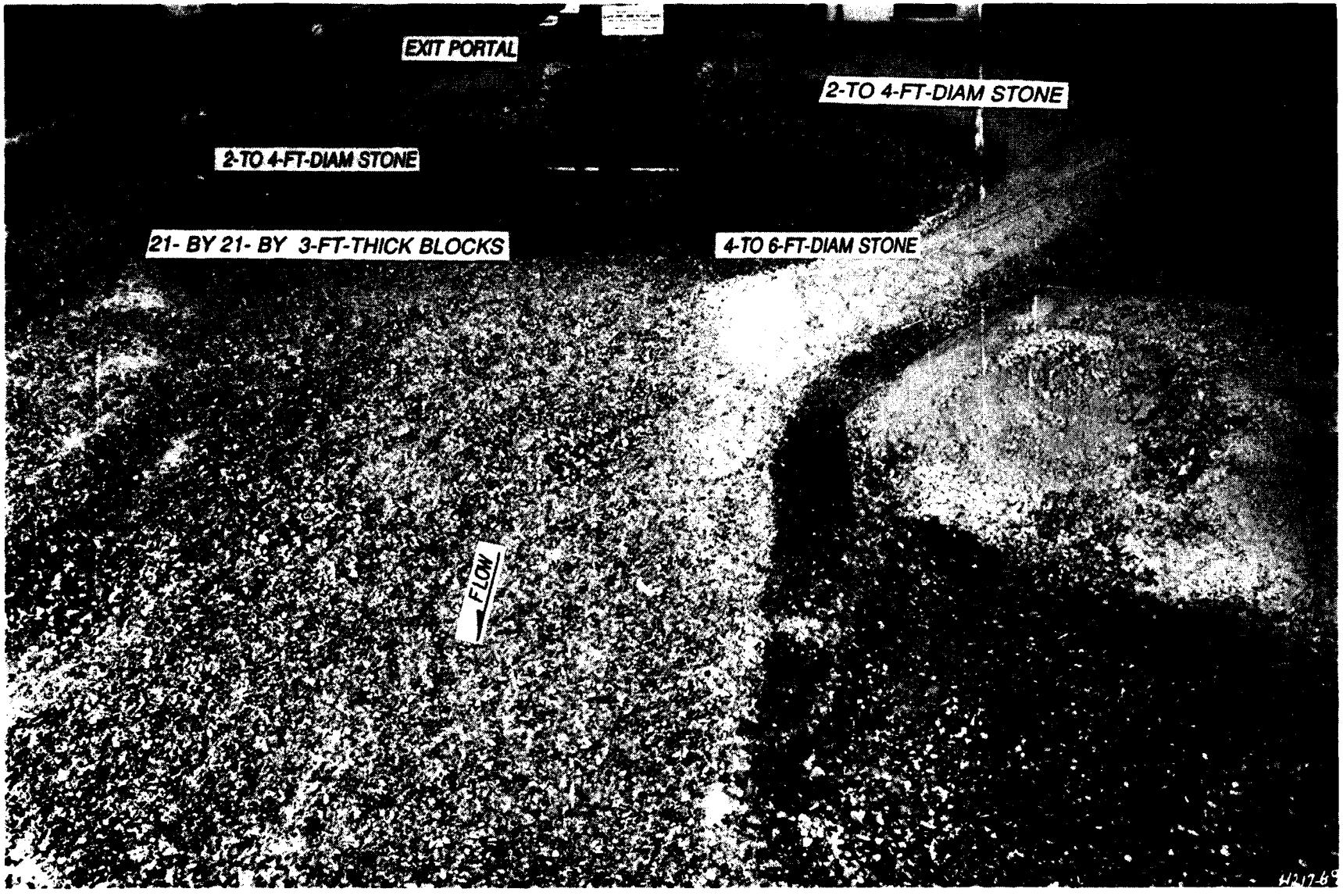

Photo 26. Failure of type 3 design apron mat, discharge 2,000 cfs; pool el 2300

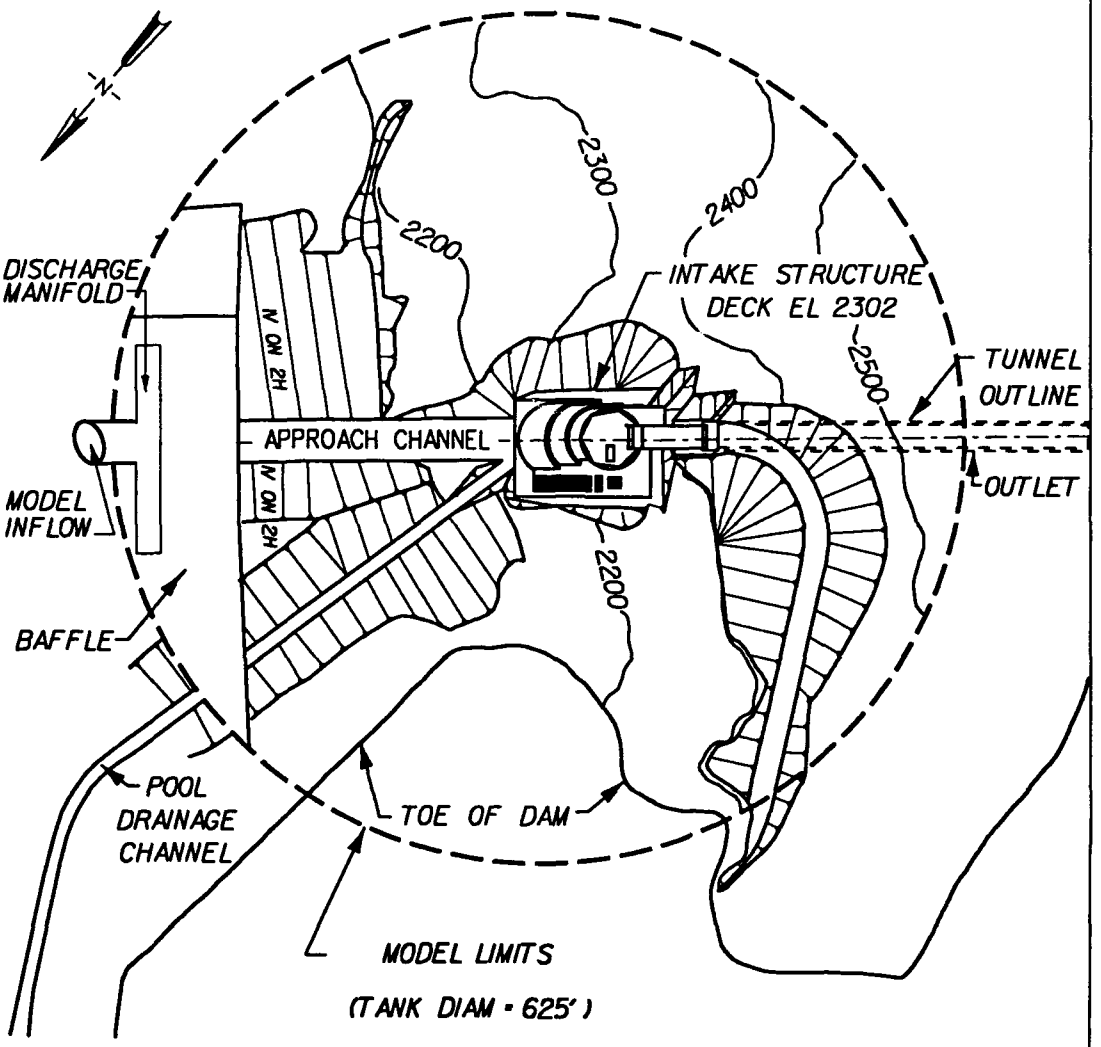

SCALE
30 0 30 60 90 120 FT

INTAKE TOWER
AND
UPSTREAM TOPOGRAPHY

PLATE 1

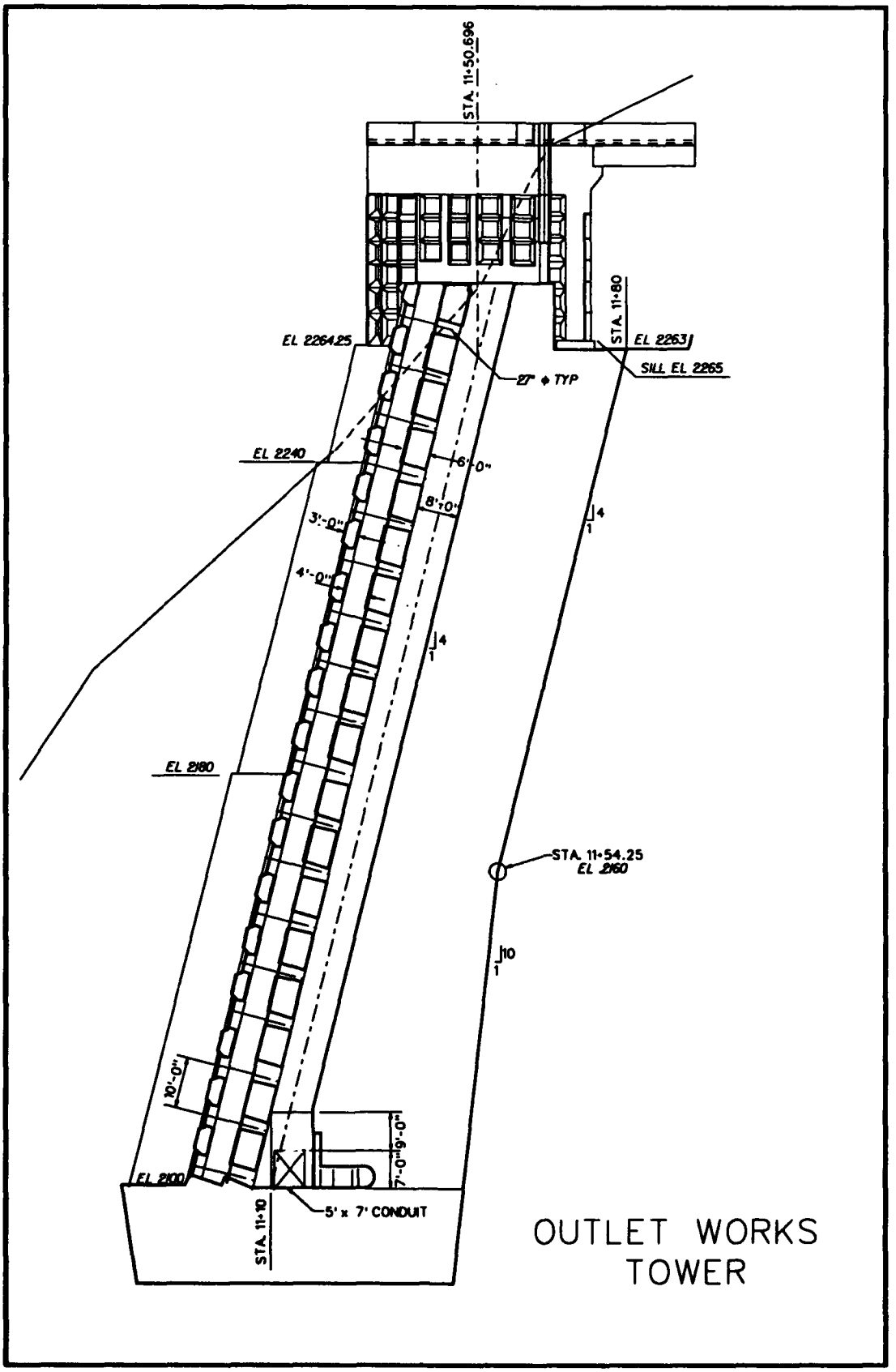
STA. 11+50.696
STA. 11+80
EL 2264.25
EL 2263
SILL EL 2265
27" ϕ TYP
EL 2240
6'-0"
8'-0"
3'-0"
4'-0"
4
1
4
1
EL 2180
STA. 11+54.25
EL 2160
10
1
10'-0"
7'-0"
9'-0"
EL 2100
5' x 7' CONDUIT
STA. 11+10
OUTLET WORKS
TOWER

PLATE 2

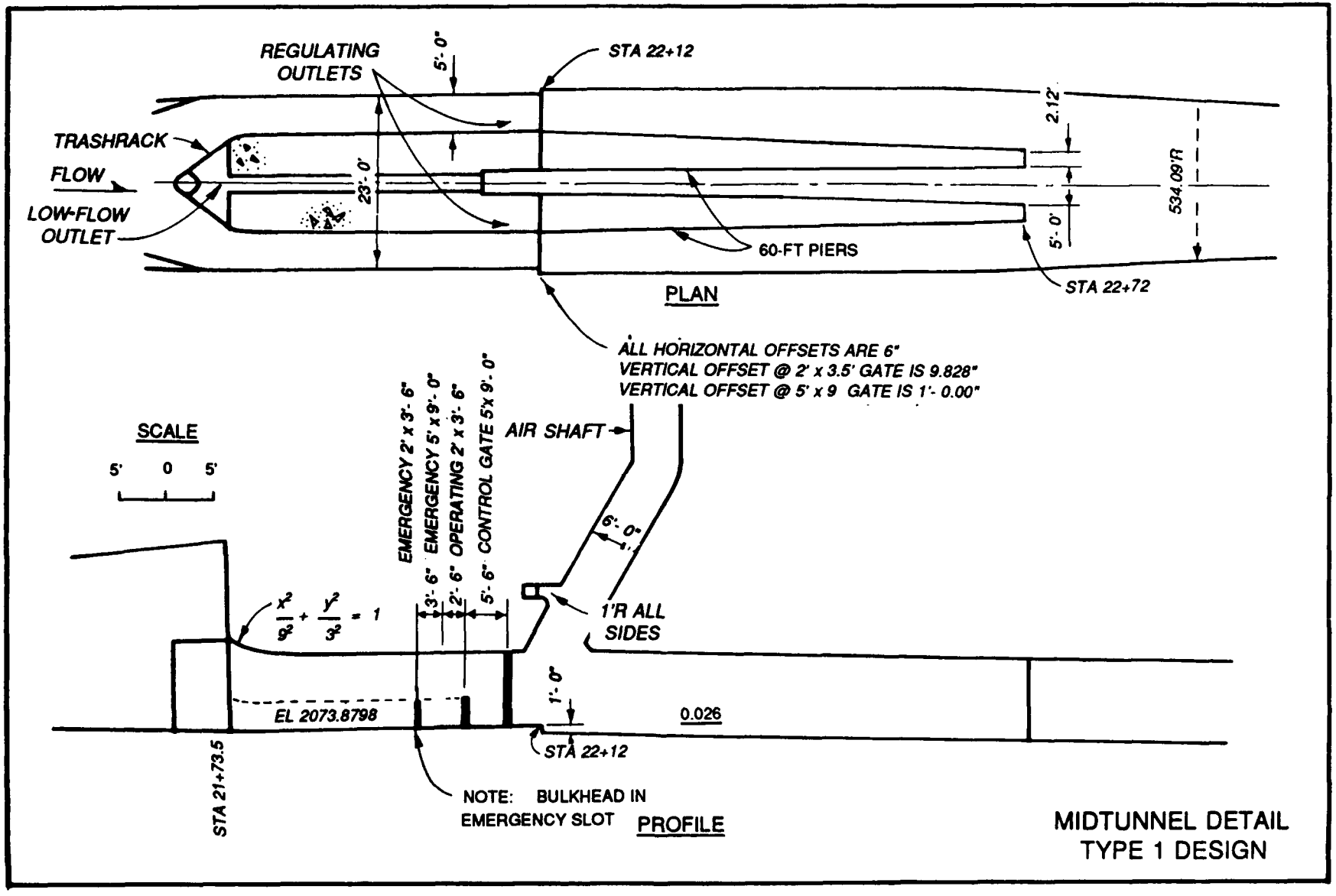
REGULATING OUTLETS
5'- 0"
STA 22+12
TRASHRACK
FLOW
LOW-FLOW OUTLET
23'- 0"
2.12'
5'- 0"
534.09'R
60-FT PIERS
STA 22+72
PLAN
ALL HORIZONTAL OFFSETS ARE 6"
VERTICAL OFFSET @ 2' x 3.5' GATE IS 9.828"
VERTICAL OFFSET @ 5' x 9 GATE IS 1'- 0.00"
SCALE
5' 0 5'
AIR SHAFT
EMERGENCY 2' x 3'- 6"
EMERGENCY 5' x 9'- 0"
OPERATING 2' x 3'- 6"
CONTROL GATE 5'x 9'- 0"
6'- 0"
1'R ALL SIDES
$\frac{x^2}{9^2} + \frac{y^2}{3^2} = 1$
3'- 6"
2'- 6"
5'- 6"
1'- 0"
EL 2073.8798
0.026
STA 21+73.5
STA 22+12
NOTE: BULKHEAD IN EMERGENCY SLOT
PROFILE
MIDTUNNEL DETAIL
TYPE 1 DESIGN

PLATE 3

PLATE 4

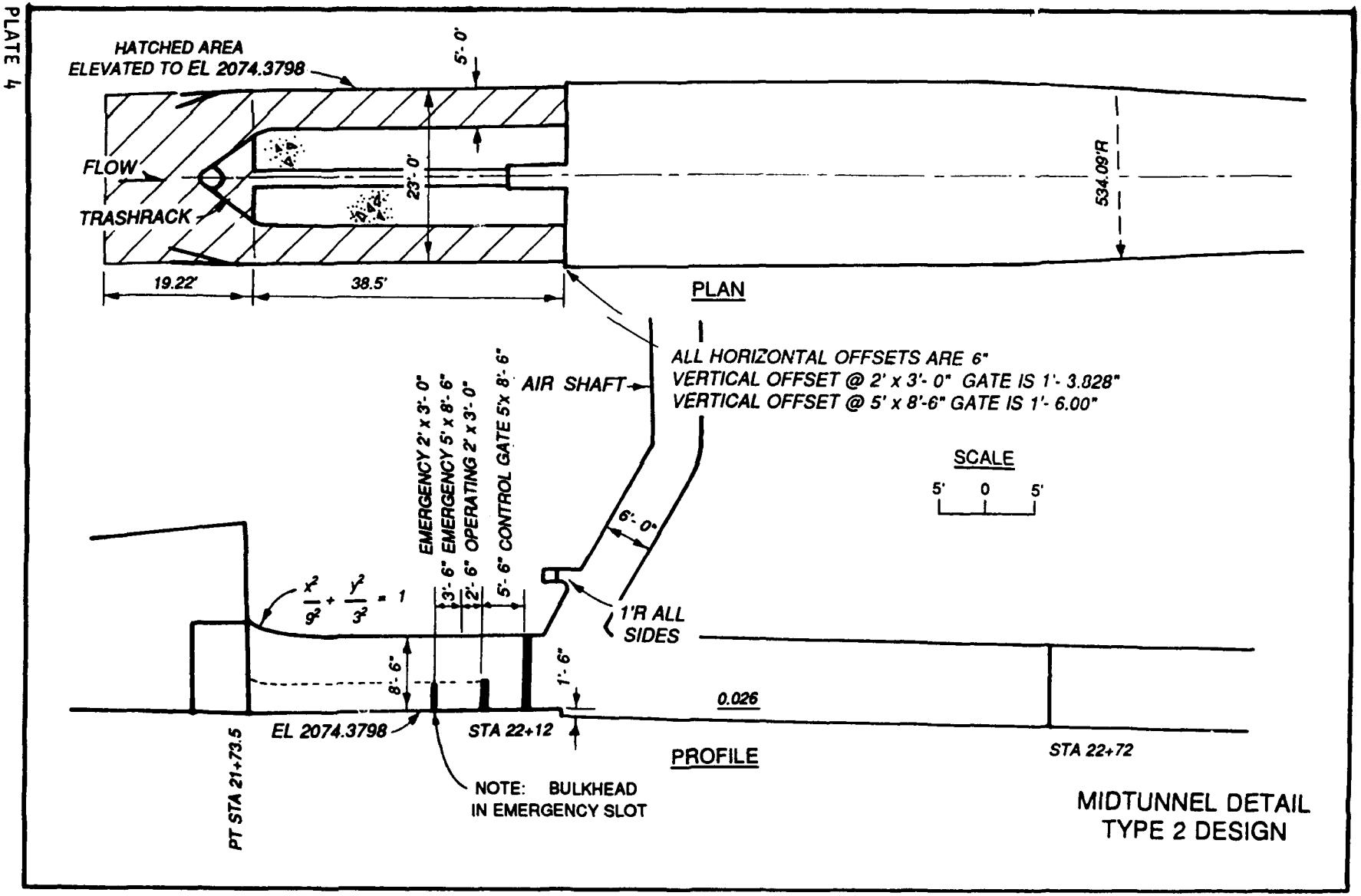

MIDTUNNEL DETAIL
TYPE 2 DESIGN

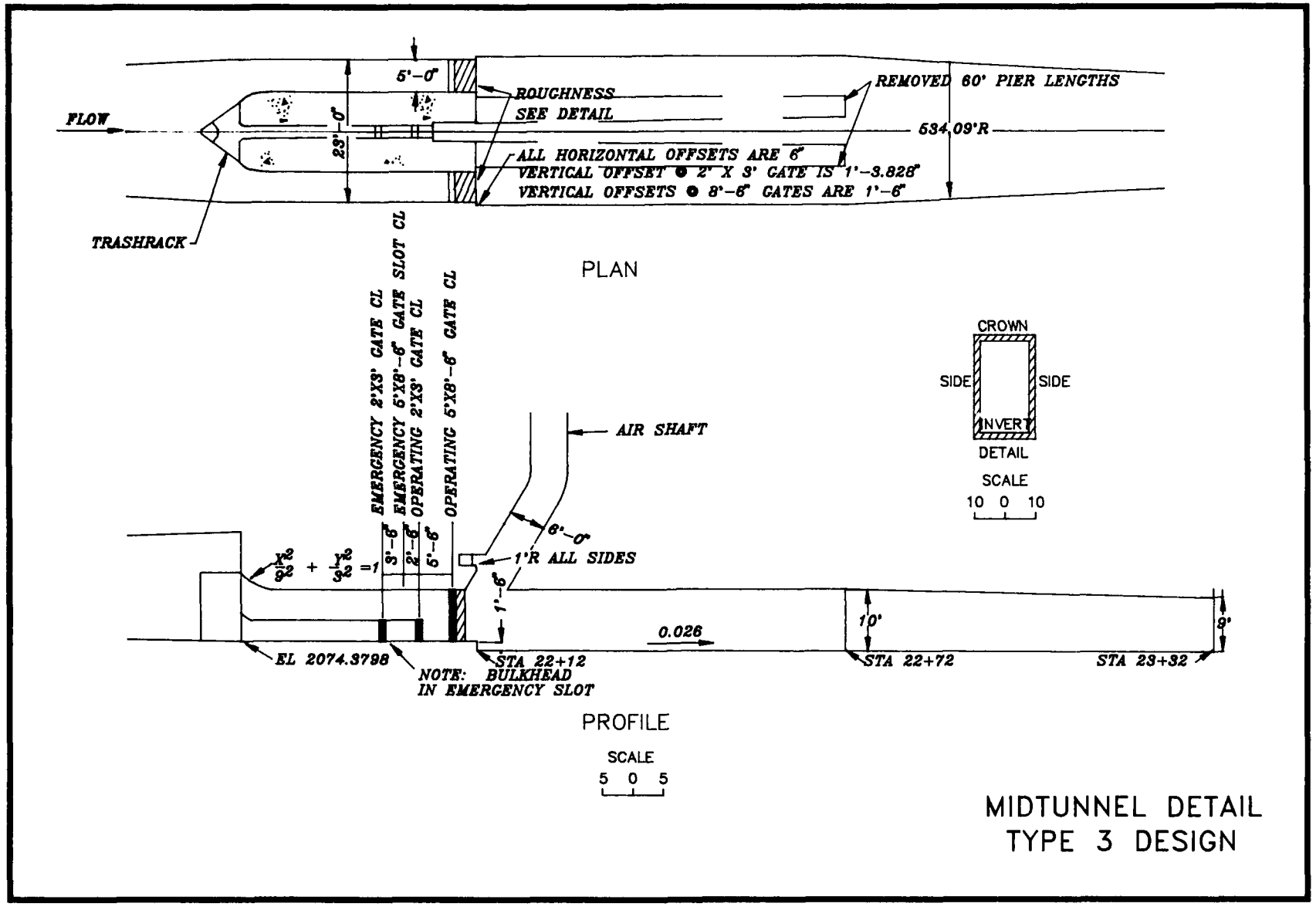
5'-0"
ROUGHNESS
SEE DETAIL
REMOVED 60' PIER LENGTHS
FLOW
23'-0"
534.09'R
ALL HORIZONTAL OFFSETS ARE 6"
VERTICAL OFFSET @ 2" X 3' GATE IS 1'-3.828"
VERTICAL OFFSETS @ 8'-6" GATES ARE 1'-6"
TRASHRACK
PLAN
EMERGENCY 2'X3' GATE CL
EMERGENCY 6'X8'-6" GATE SLOT CL
OPERATING 2'X3' GATE CL
OPERATING 6'X8'-6" GATE CL
AIR SHAFT
CROWN
SIDE
SIDE
INVERT
DETAIL
SCALE
10 0 10
3'-6"
2'-6"
6'-6"
6'-0"
1'R ALL SIDES
1'-6"
0.026
10'
9'
EL 2074.3798
NOTE: BULKHEAD
IN EMERGENCY SLOT
STA 22+12
STA 22+72
STA 23+32
PROFILE
SCALE
5 0 5
MIDTUNNEL DETAIL
TYPE 3 DESIGN

PLATE 5

PLATE 6

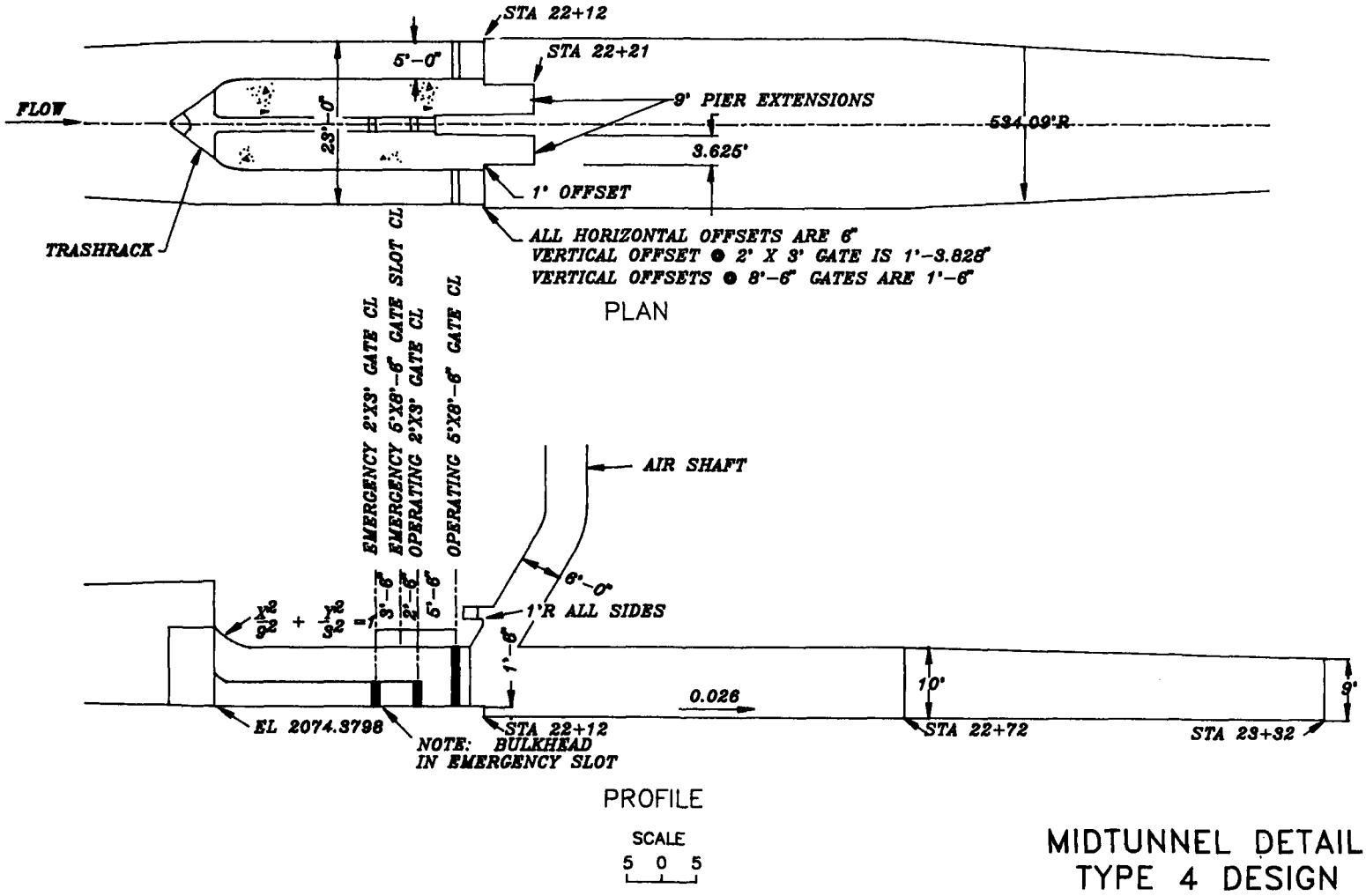

MIDTUNNEL DETAIL TYPE 4 DESIGN

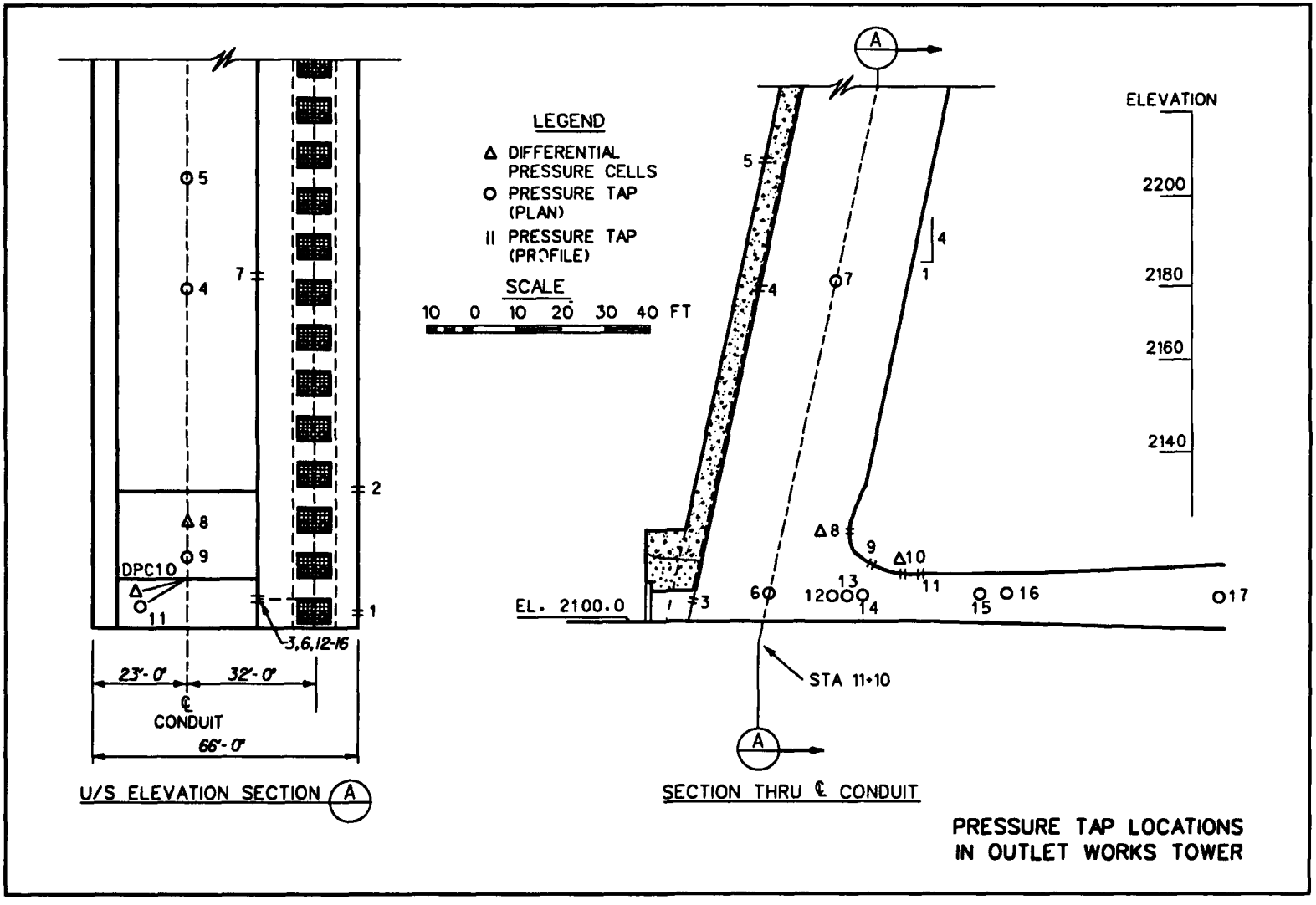
LEGEND
Δ DIFFERENTIAL PRESSURE CELLS
O PRESSURE TAP (PLAN)
II PRESSURE TAP (PROFILE)
SCALE
10 0 10 20 30 40 FT
ELEVATION
2200
2180
2160
2140
EL. 2100.0
DPC10
3,6,12-16
23'-0"
32'-0"
℄ CONDUIT
66'-0"
STA 11+10
U/S ELEVATION SECTION A
SECTION THRU ℄ CONDUIT
PRESSURE TAP LOCATIONS IN OUTLET WORKS TOWER

PLATE 7

PLATE 8

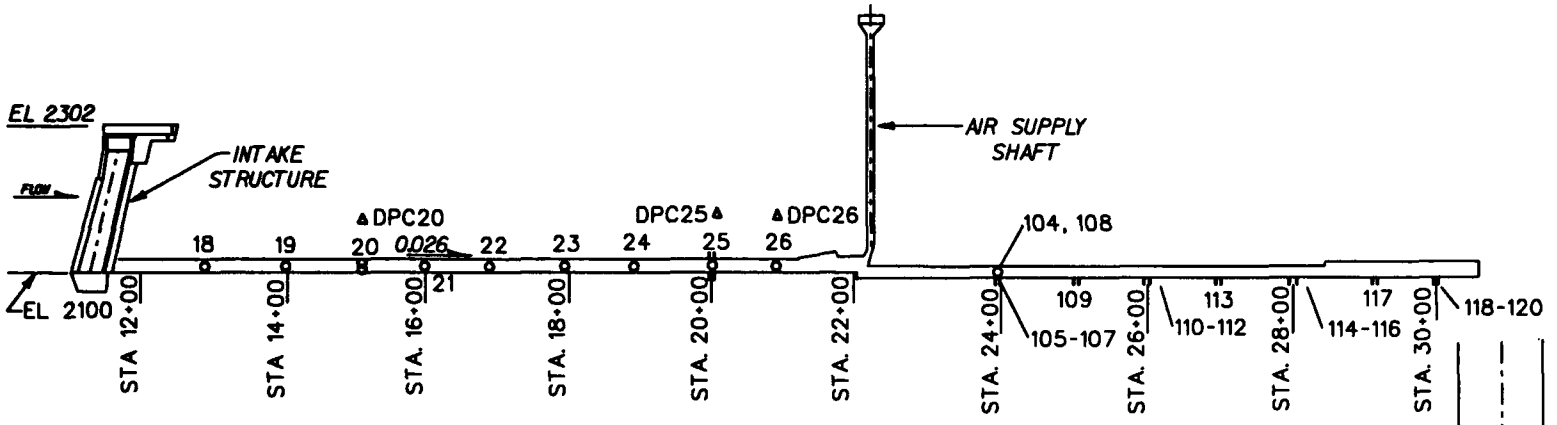

PROFILE - OUTLET WORKS

LEGEND

■ & ○ PRESSURE TAP

▲ DIFFERENTIAL PRESSURE CELL (DPC)

PRESSURE TAP LOCATIONS

STA	PRESSURE TAP NO.	TYPE
13+12.5	18	1S
14+00	19	1S
14+00	21	1S
17+00	22	1S
18+00	23	1S
19+00	24	1S
21+00	26	1S
15+00	20	3T
20+00	25	3T

1S CONFIGURATION

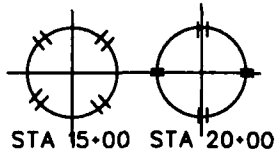

3T CONFIGURATION

PRESSURE TAP LOCATIONS

STA	PRESSURE TAP NO.	TYPE
26+00	110-112	3B
24+00	104-108	5B
28+00	114-116	3B
30+00	118-120	3B
25+00	109	1B
27+00	113	1B
29+00	117	1B

SCALE

20' 0' 20' 40'

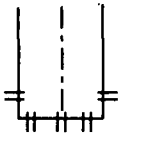

5B CONFIGURATION

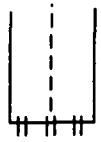

3B CONFIGURATION

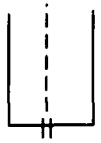

1B CONFIGURATION

PRESSURE TAP LOCATIONS IN CONDUIT

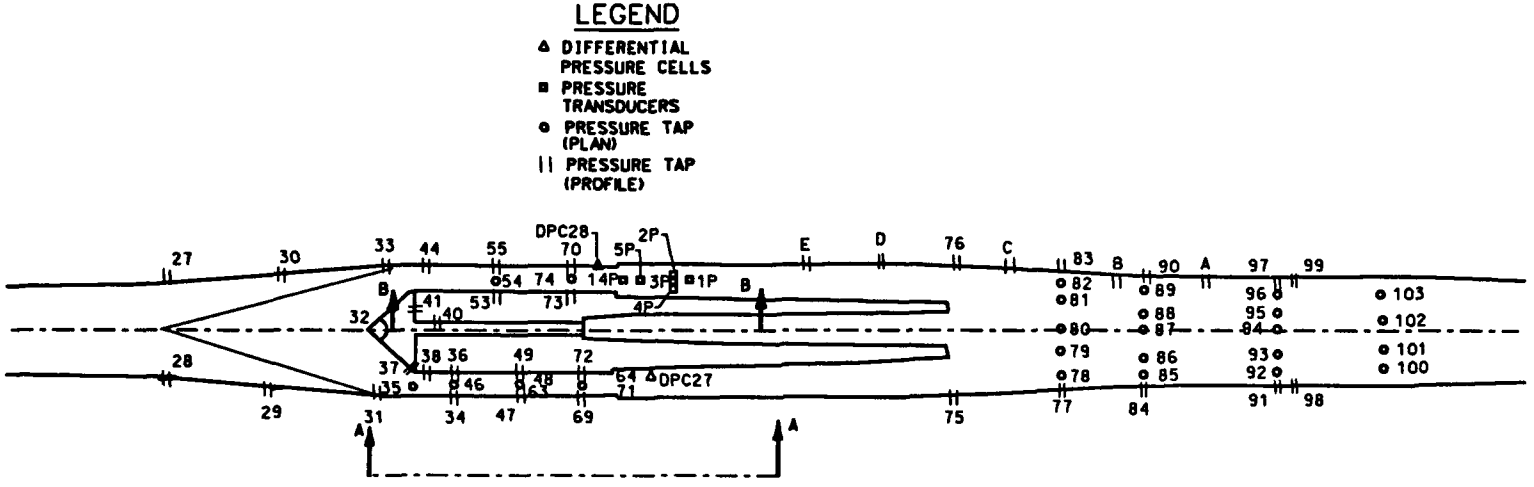

PRESSURE TAP
AND PRESSURE TRANSDUCER
LOCATIONS IN MIDTUNNEL

PLATE 9
(Sheet 1 of 3)

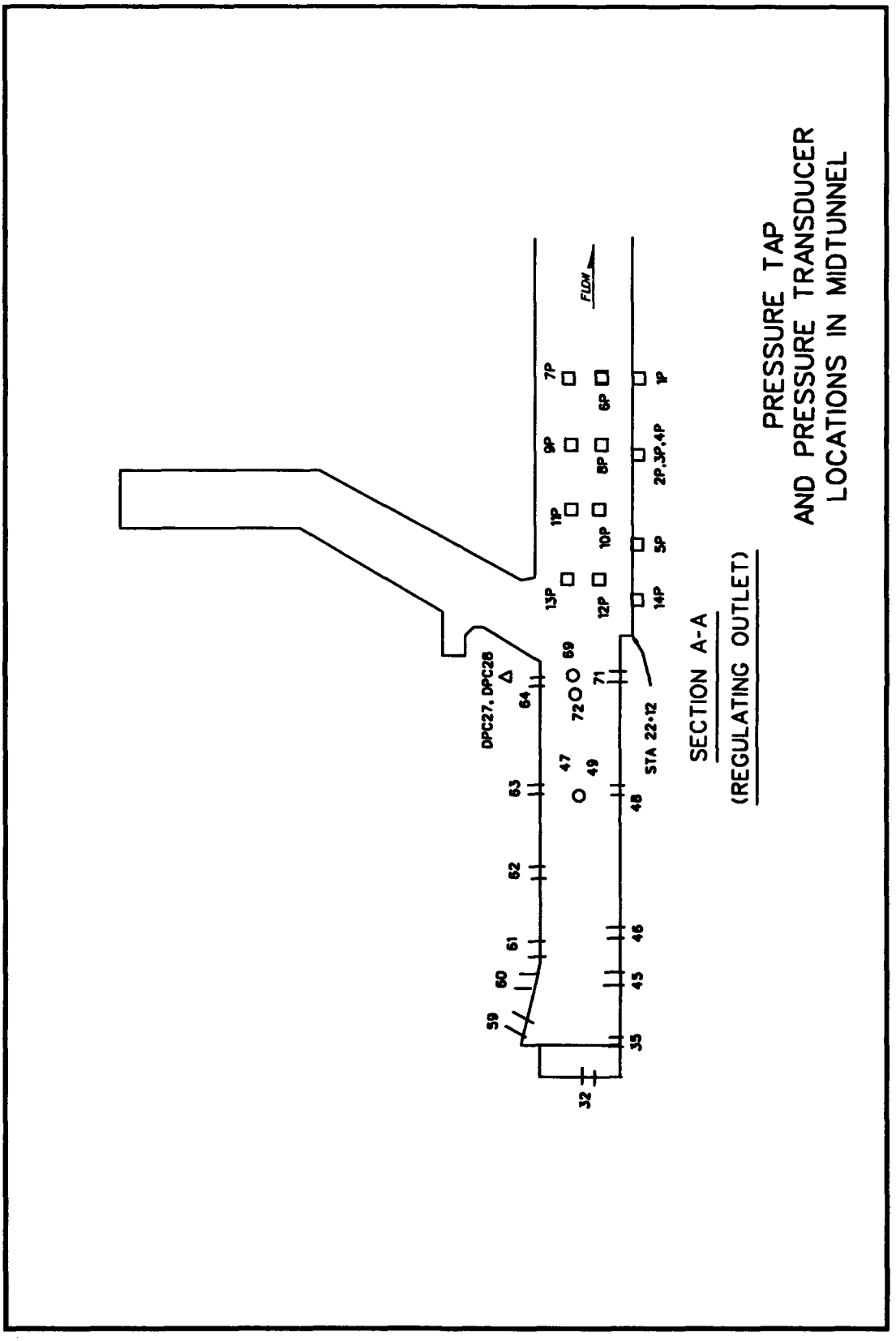

PLATE 9
(Sheet 2 of 3)

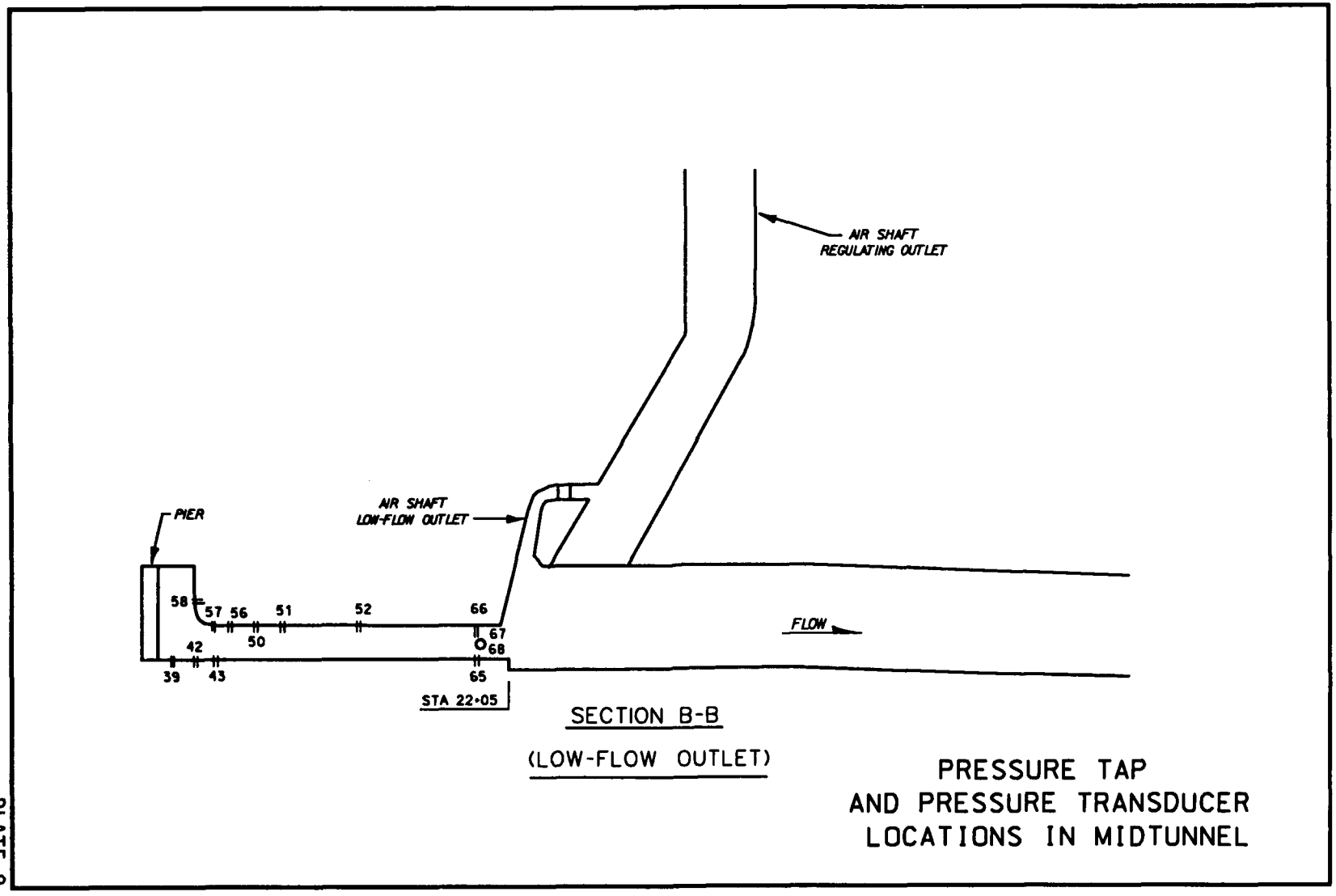

SECTION B-B

(LOW-FLOW OUTLET)

PRESSURE TAP
AND PRESSURE TRANSDUCER
LOCATIONS IN MIDTUNNEL

PLATE 9
(Sheet 3 of 3)

PLATE 10

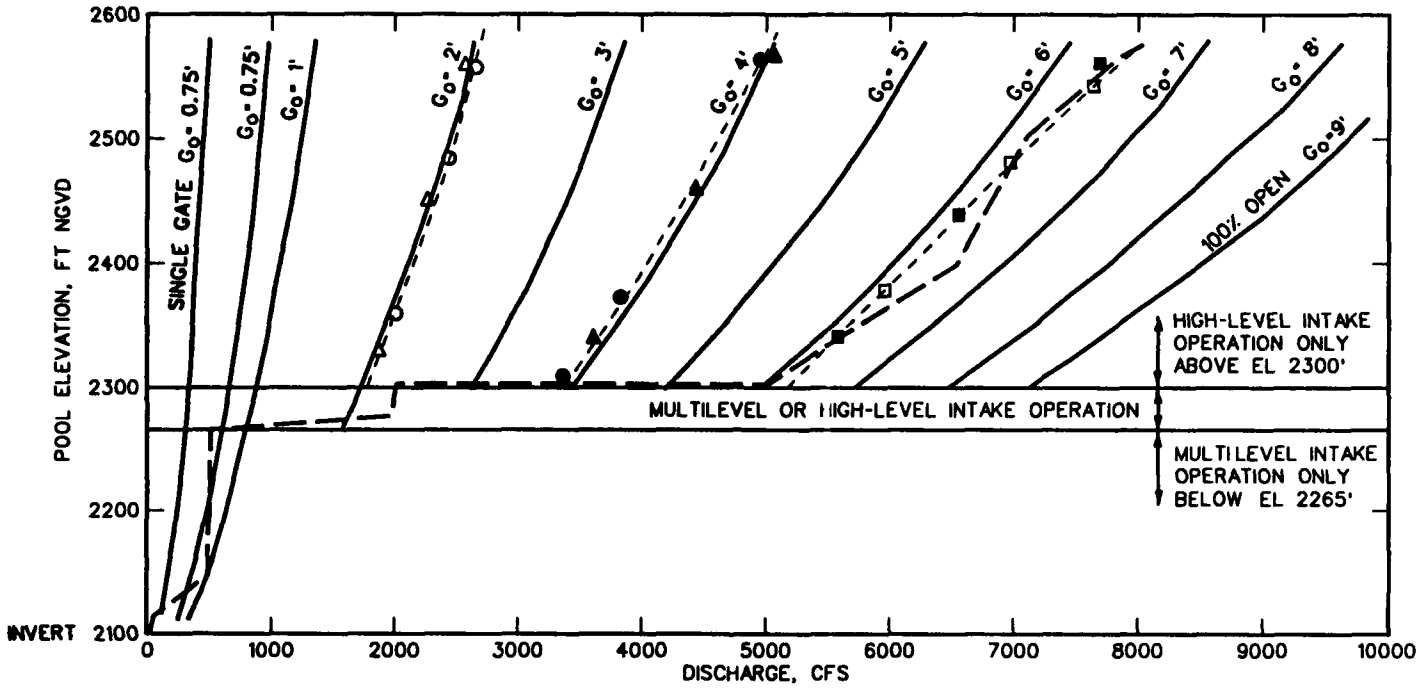

LEGEND

G_o- GATE OPENING, FT

——— COMPUTED CURVE (PORTLAND DISTRICT)

– – – MAXIMUM OPERATION SCHEDULE

– – – WES CALIBRATION CURVE

TYPE 1 DESIGN

○ G_o- 2.0' ● G_o- 4.0' □ G_o- 6.0'

TYPE 2 DESIGN

△ G_o- 2.0' ▲ G_o- 4.0' ■ G_o- 6.0'

GATE RATING

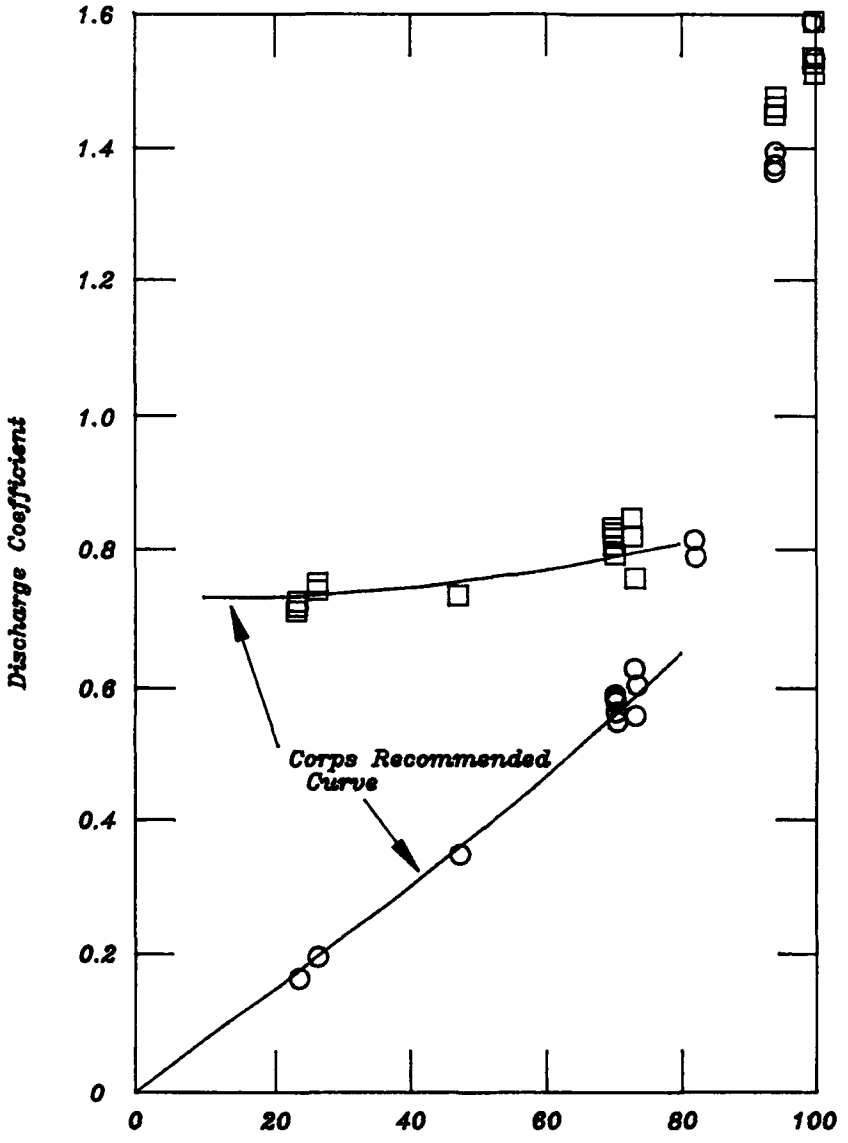

Legend

○ *Based on Full Gate opening*

□ *Based on Actual Gate Opening*

MODEL GATE COEFFICIENTS

PLATE 11

PLATE 12

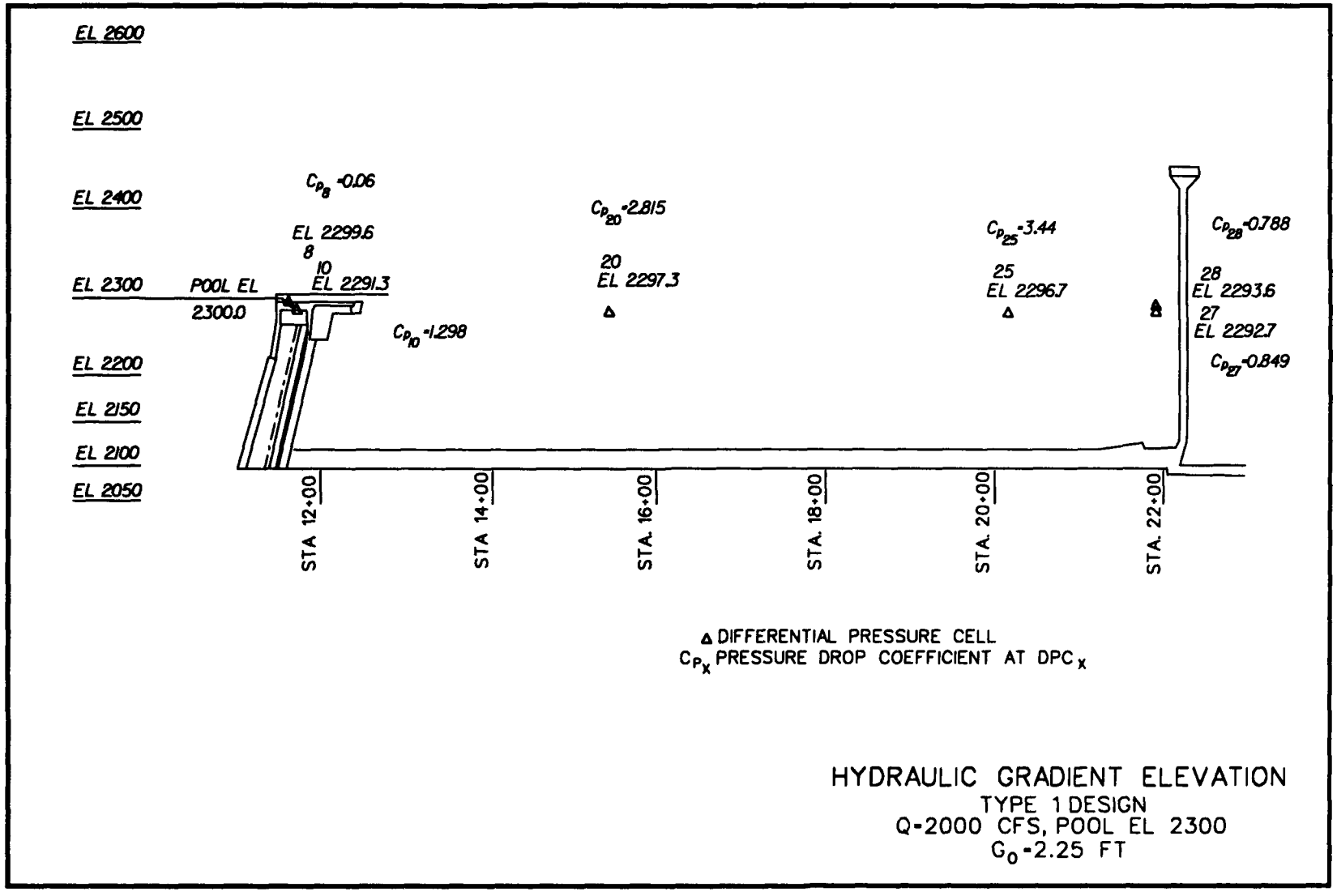

HYDRAULIC GRADIENT ELEVATION
TYPE 1 DESIGN
Q-2000 CFS, POOL EL 2300
G_0-2.25 FT

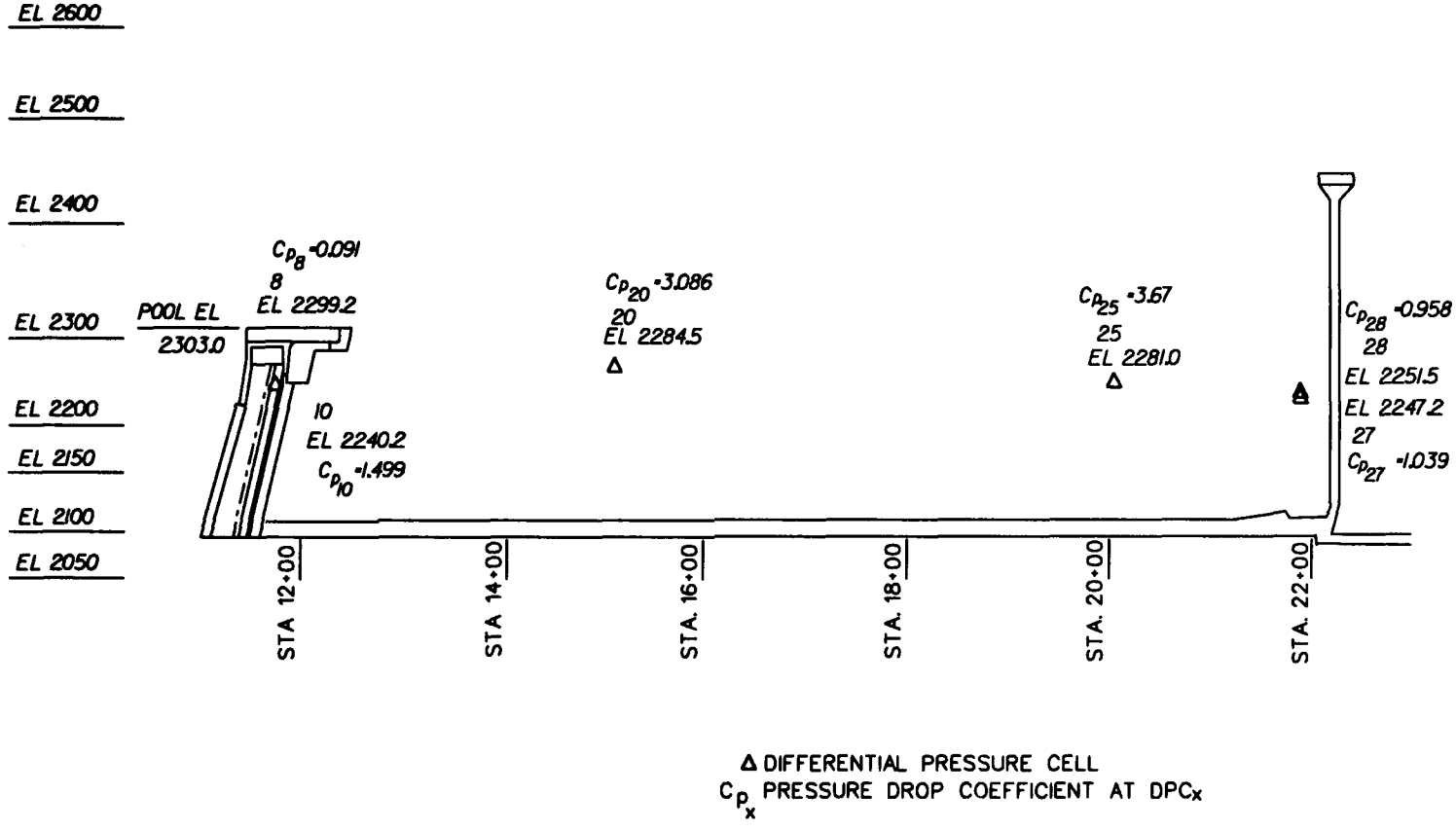

Δ DIFFERENTIAL PRESSURE CELL
C_{p_x} PRESSURE DROP COEFFICIENT AT DPCx

HYDRAULIC GRADIENT ELEVATION

TYPE 1 DESIGN
Q-5000 CFS, POOL EL 2303.0
G_o -6.0 FT

PLATE 13

PLATE 14

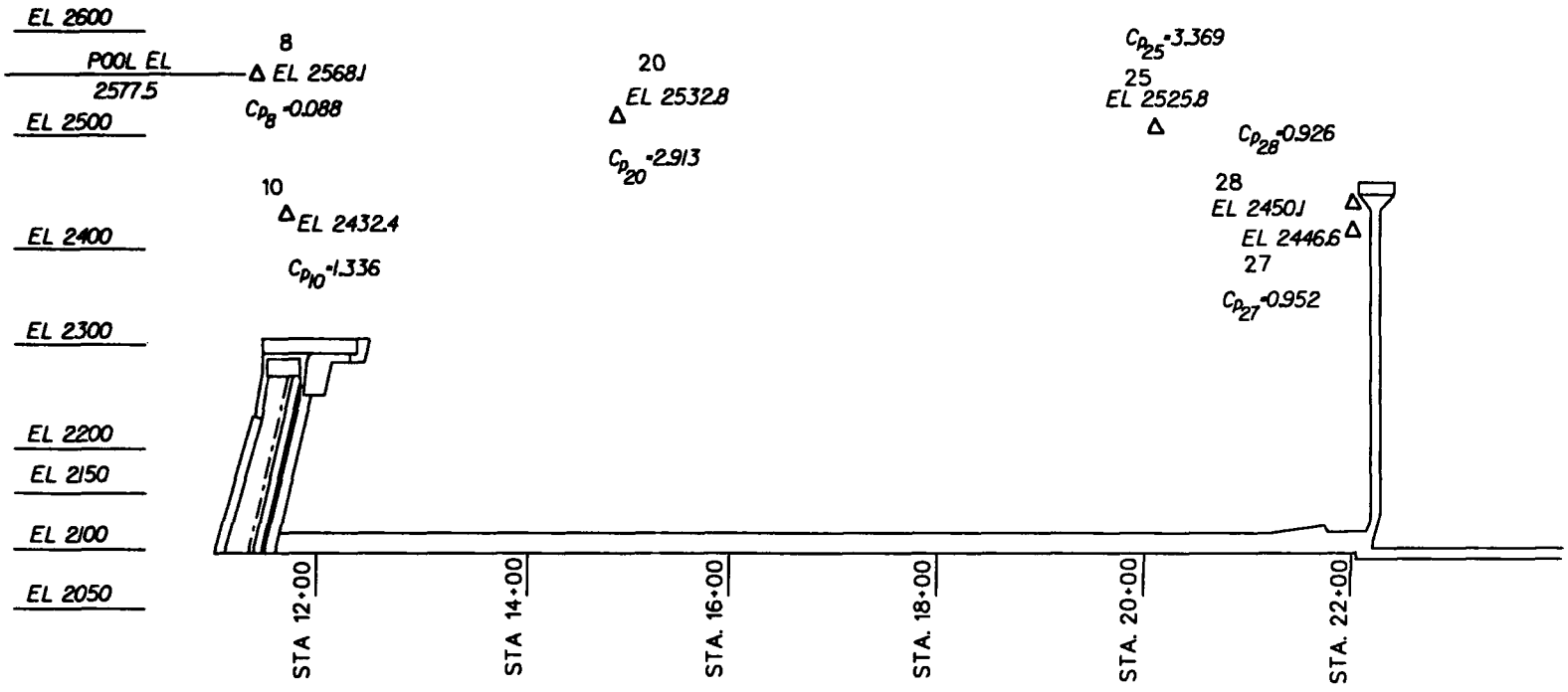

Δ DIFFERENTIAL PRESSURE CELL

C_{p_x} PRESSURE DROP COEFFICIENT AT DPC x

HYDRAULIC GRADIENT ELEVATION

TYPE 1 DESIGN

Q-8000 CFS, POOL EL 2577.5

G_o-6.25 FT

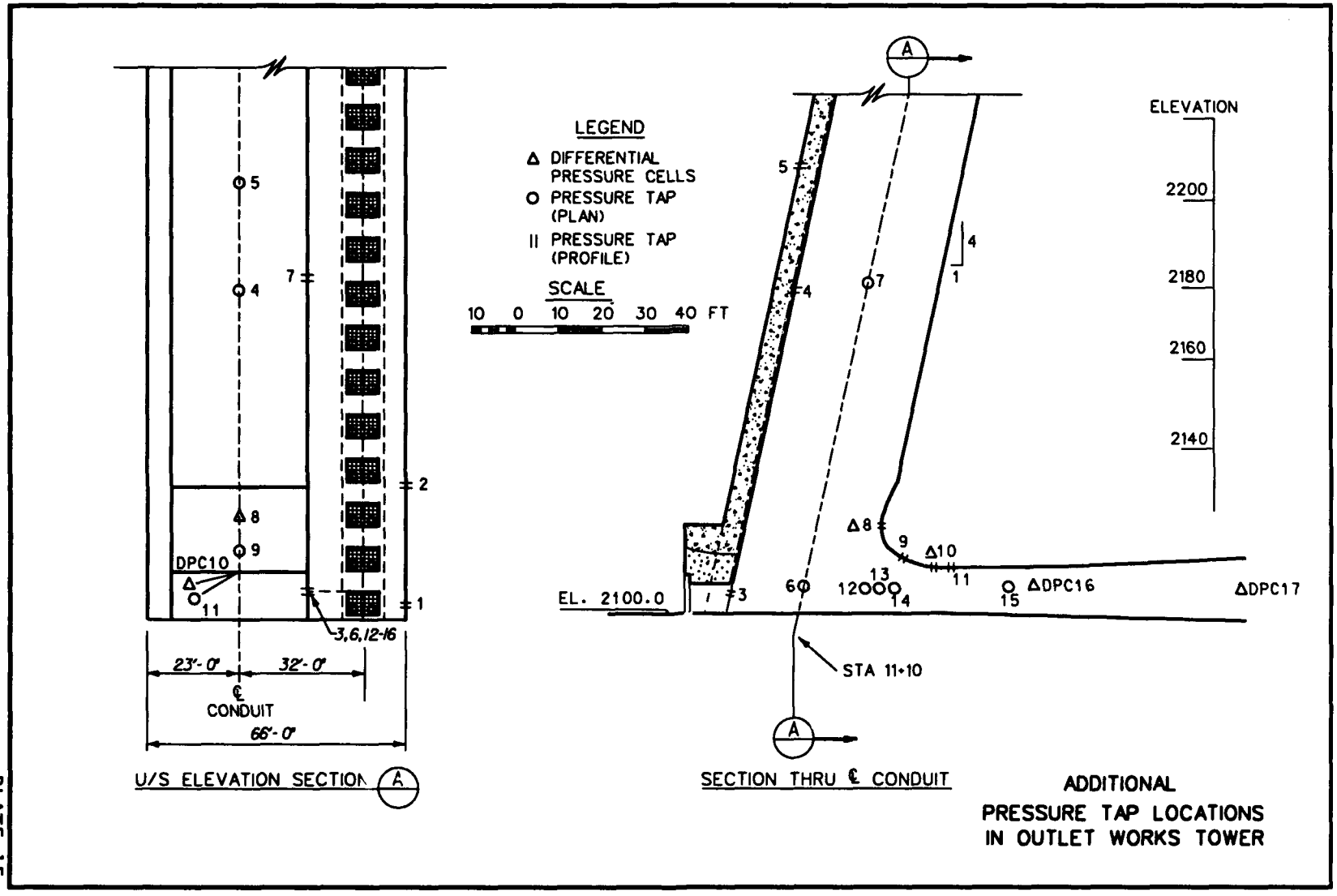

PLATE 15

ADDITIONAL PRESSURE TAP LOCATIONS IN OUTLET WORKS TOWER

PLATE 16

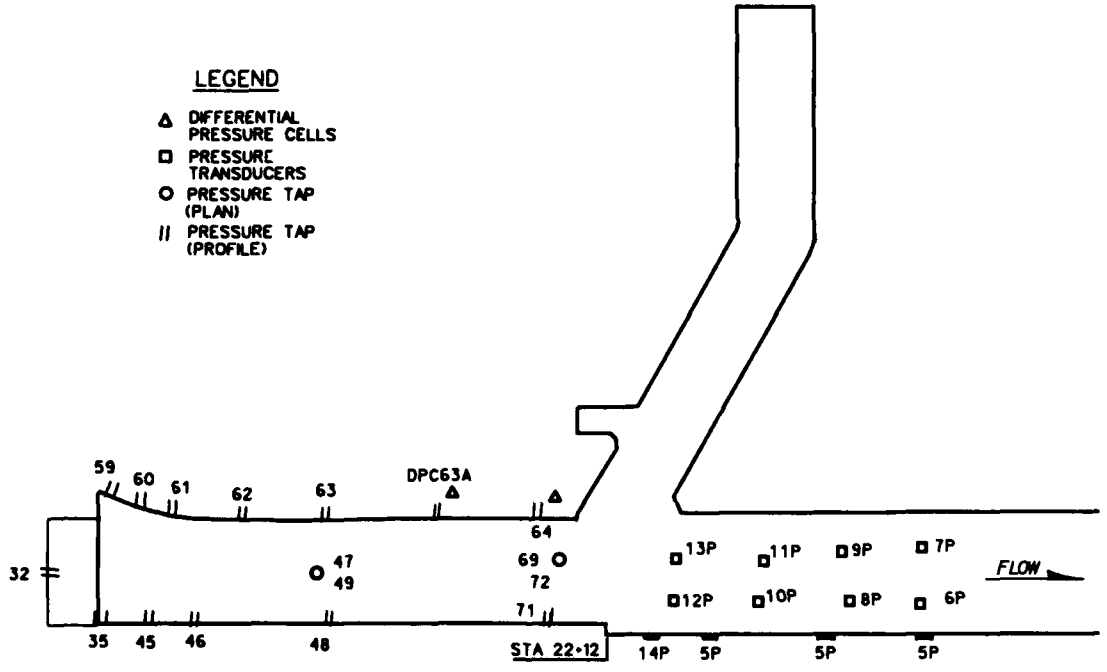

PRESSURE TAP AND PRESSURE TRANSDUCER LOCATIONS IN REGULATING OUTLET

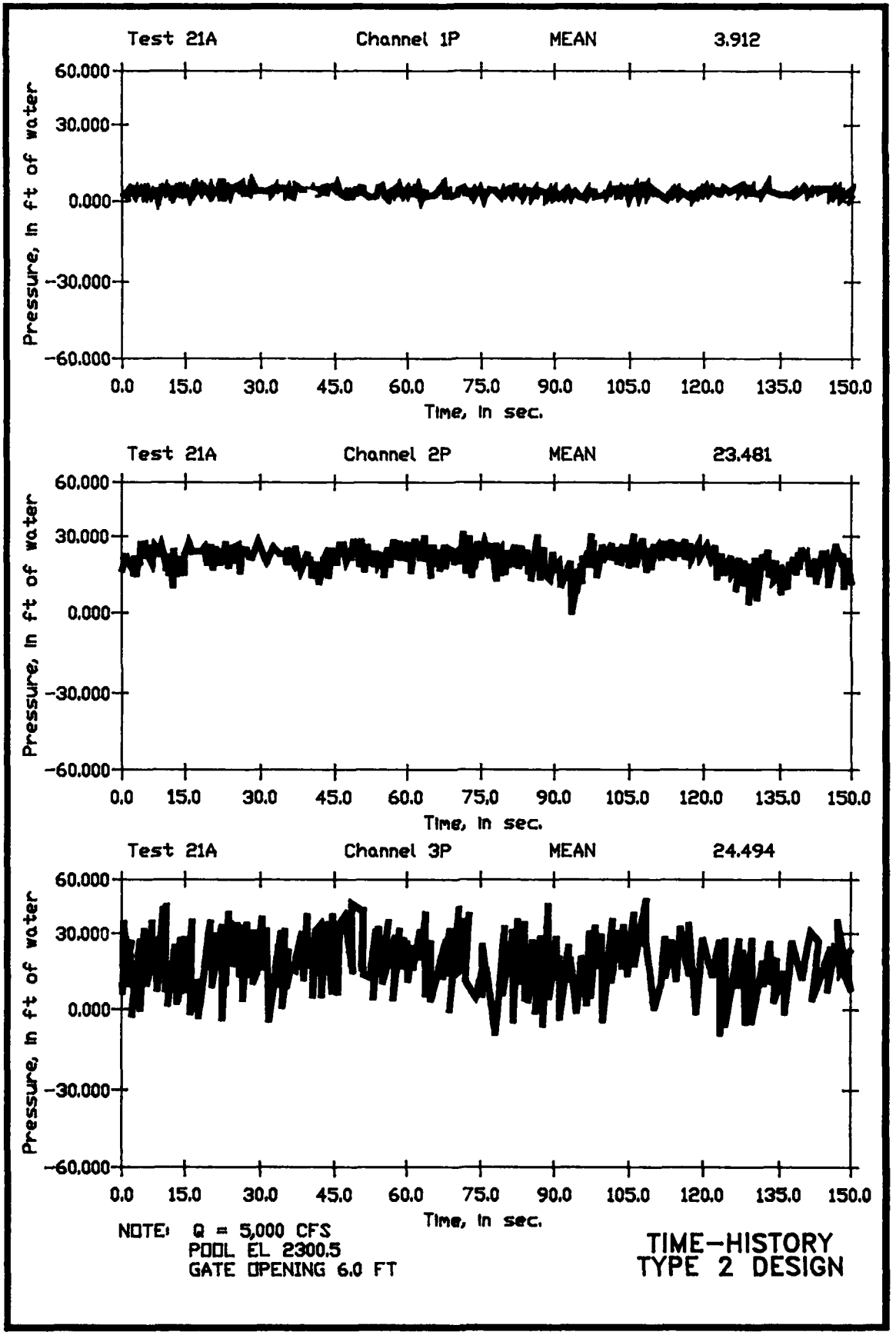

PLATE 17
(Sheet 1 of 5)

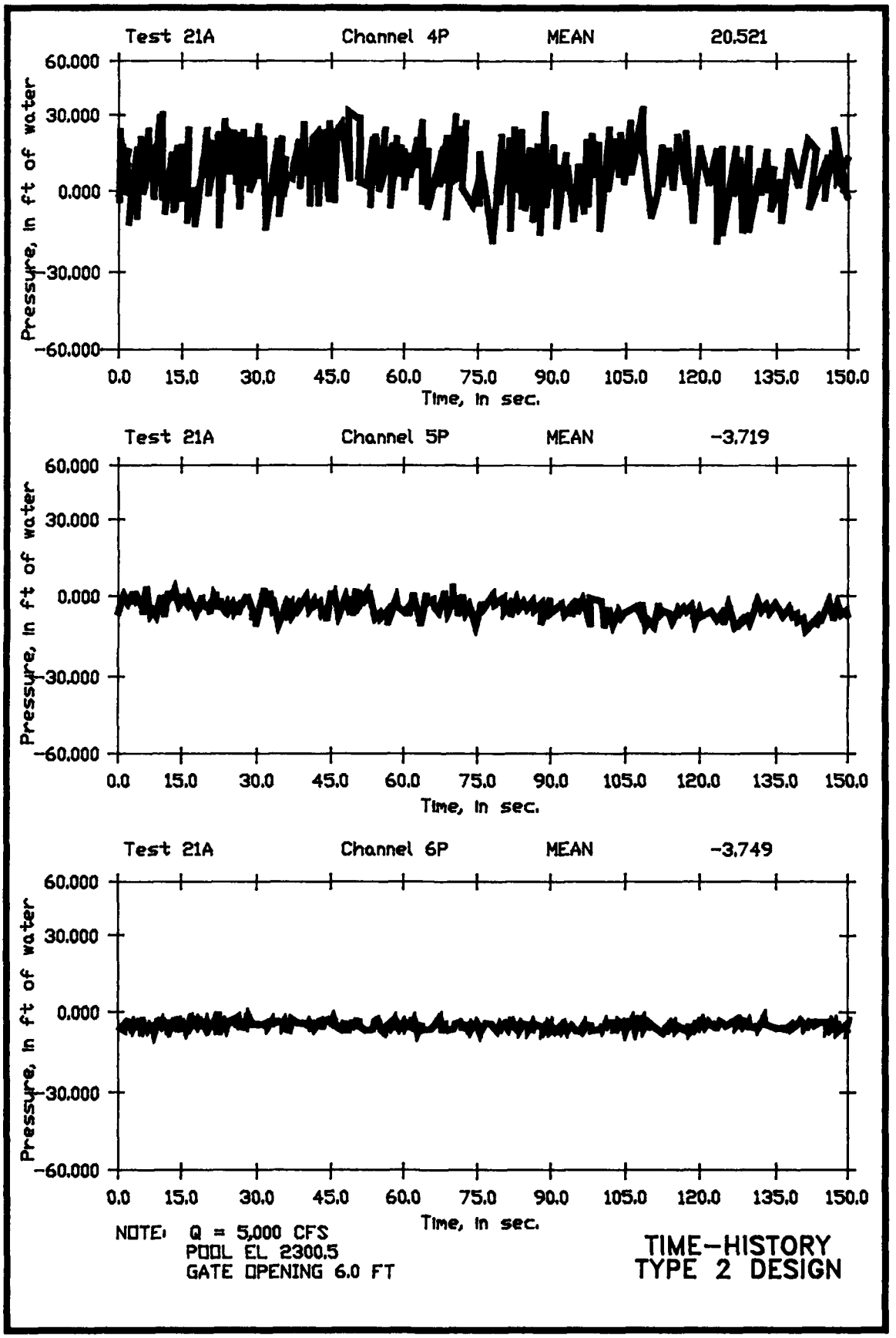

PLATE 17
(Sheet 2 of 5)

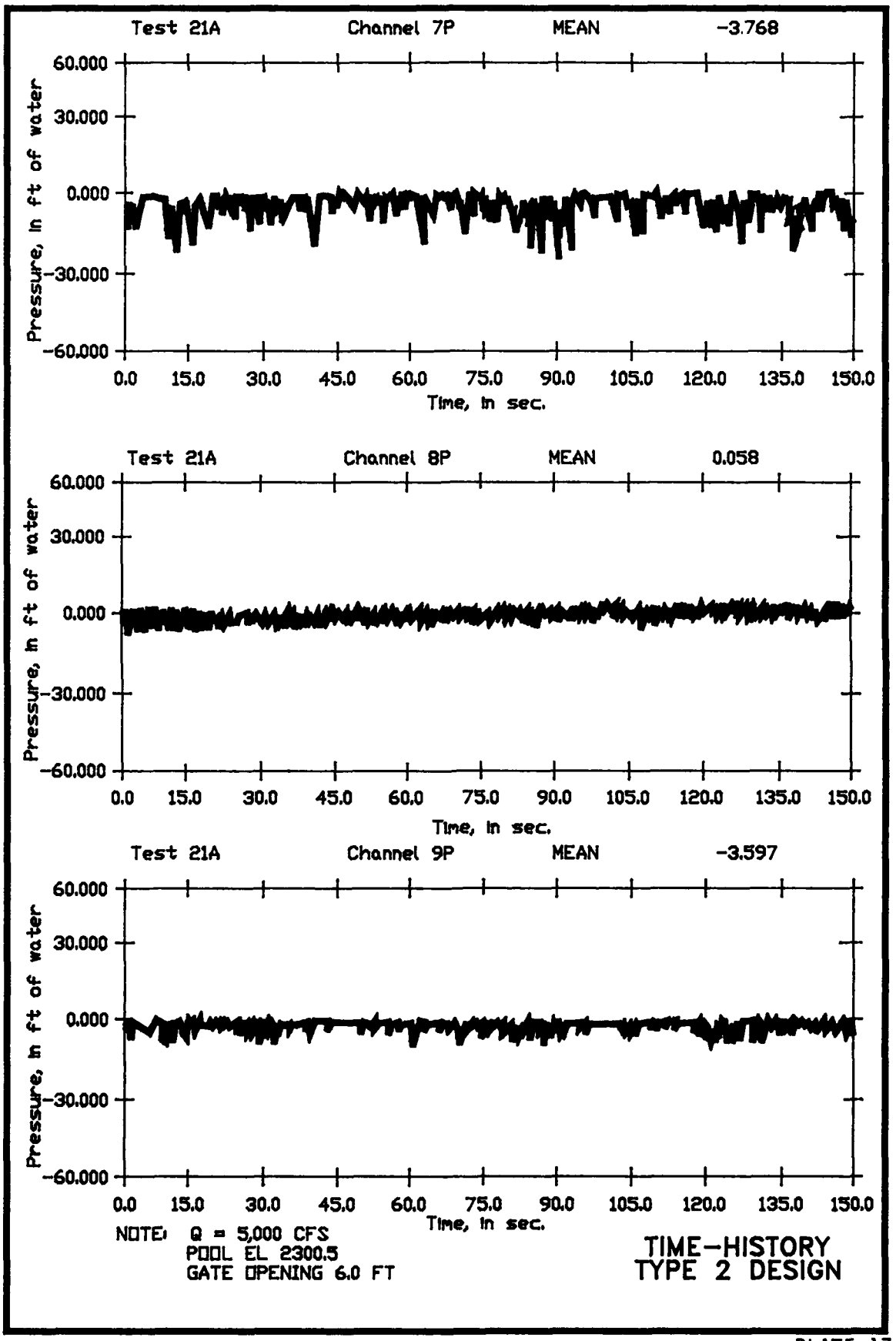

PLATE 17
(Sheet 3 of 5)

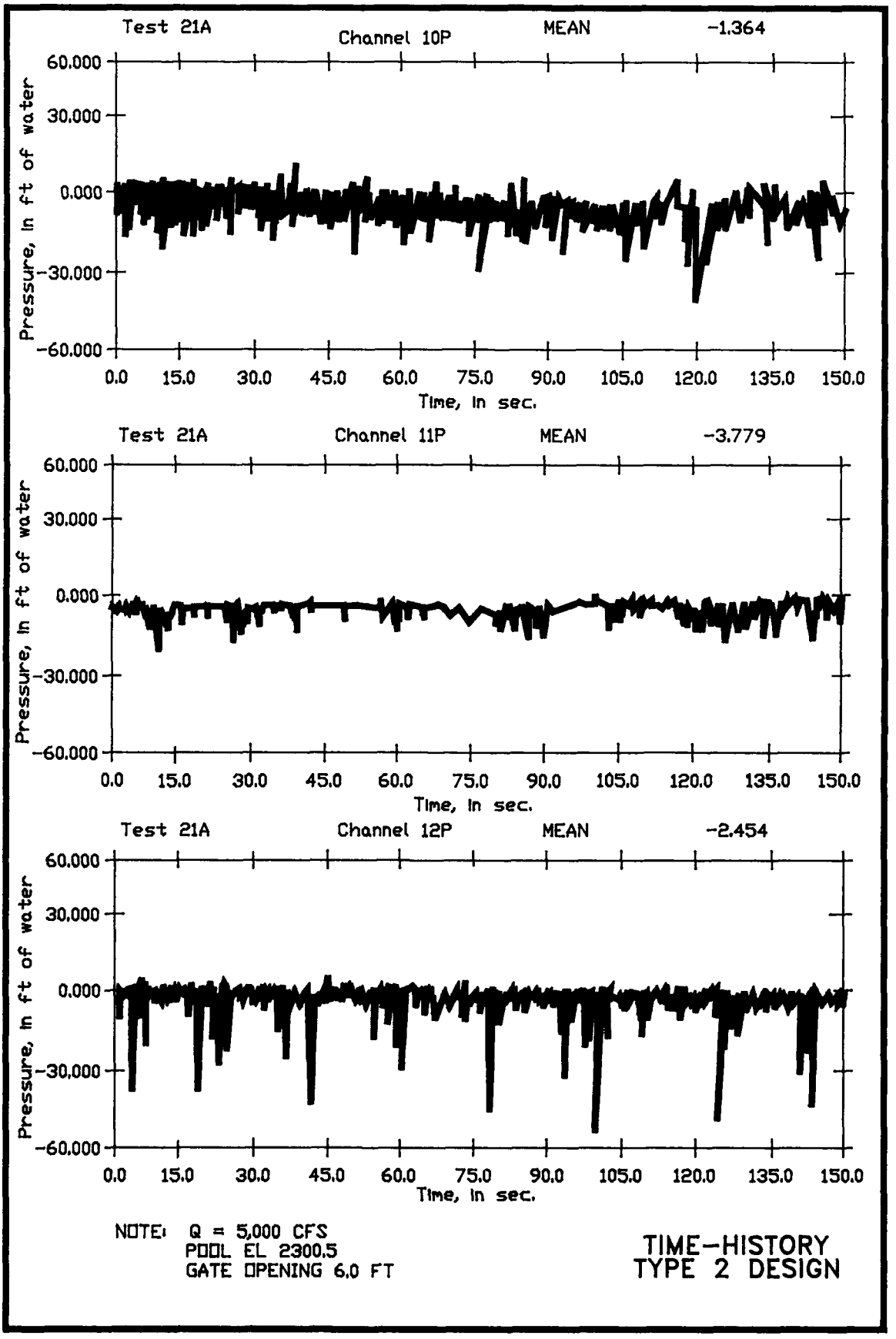

PLATE 17
(Sheet 4 of 5)

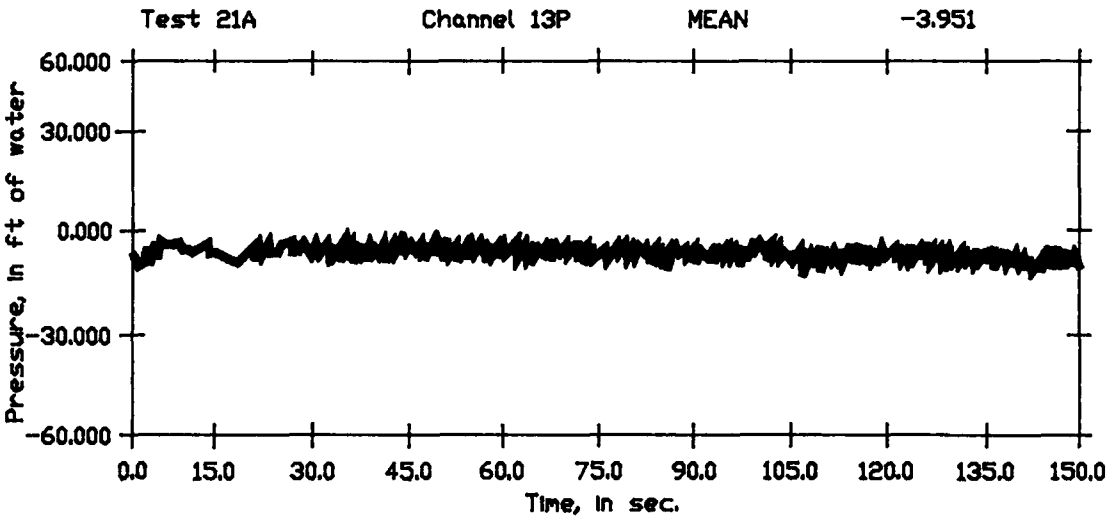

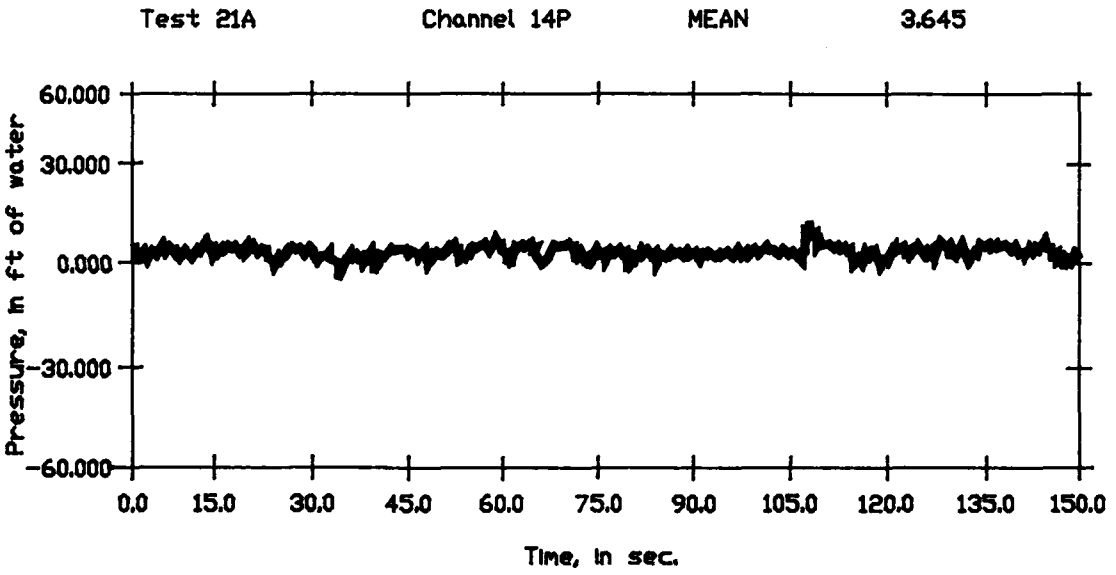

NOTE: Q = 5,000 CFS
POOL EL 2300.5
GATE OPENING 6.0 FT

TIME-HISTORY
TYPE 2 DESIGN

PLATE 17
(Sheet 5 of 5)

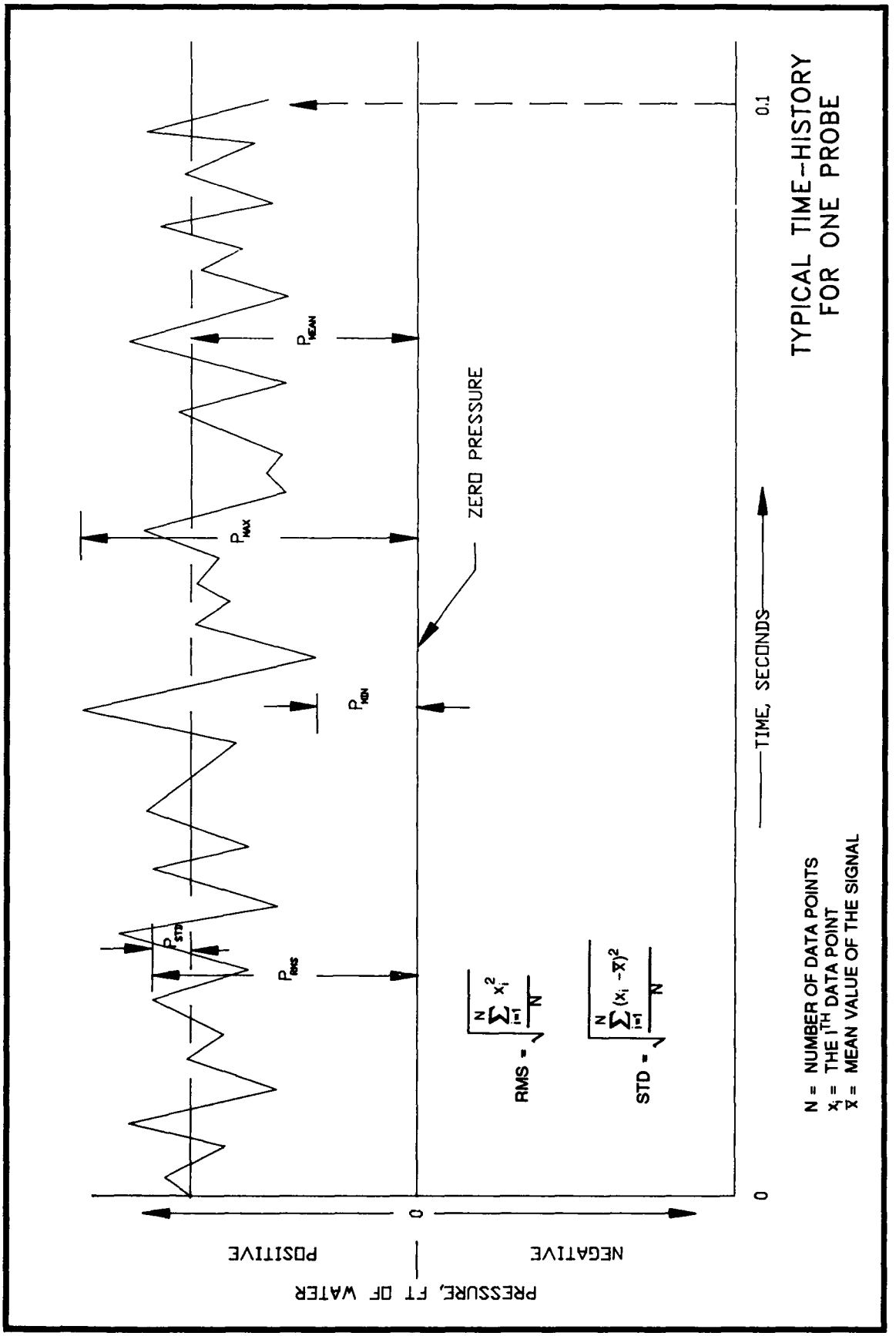
TYPICAL TIME-HISTORY
FOR ONE PROBE
PRESSURE, FT OF WATER
POSITIVE
NEGATIVE
0
TIME, SECONDS
0.1
ZERO PRESSURE
P_{MAX}
P_{MEAN}
P_{MIN}
P_{RMS}
P_{STD}
$RMS = \sqrt{\frac{\sum_{i=1}^{N} x_i^2}{N}}$
$STD = \sqrt{\frac{\sum_{i=1}^{N} (x_i - \bar{x})^2}{N}}$
N = NUMBER OF DATA POINTS
x_i = THE i^{TH} DATA POINT
$\bar{x}$ = MEAN VALUE OF THE SIGNAL

PLATE 18

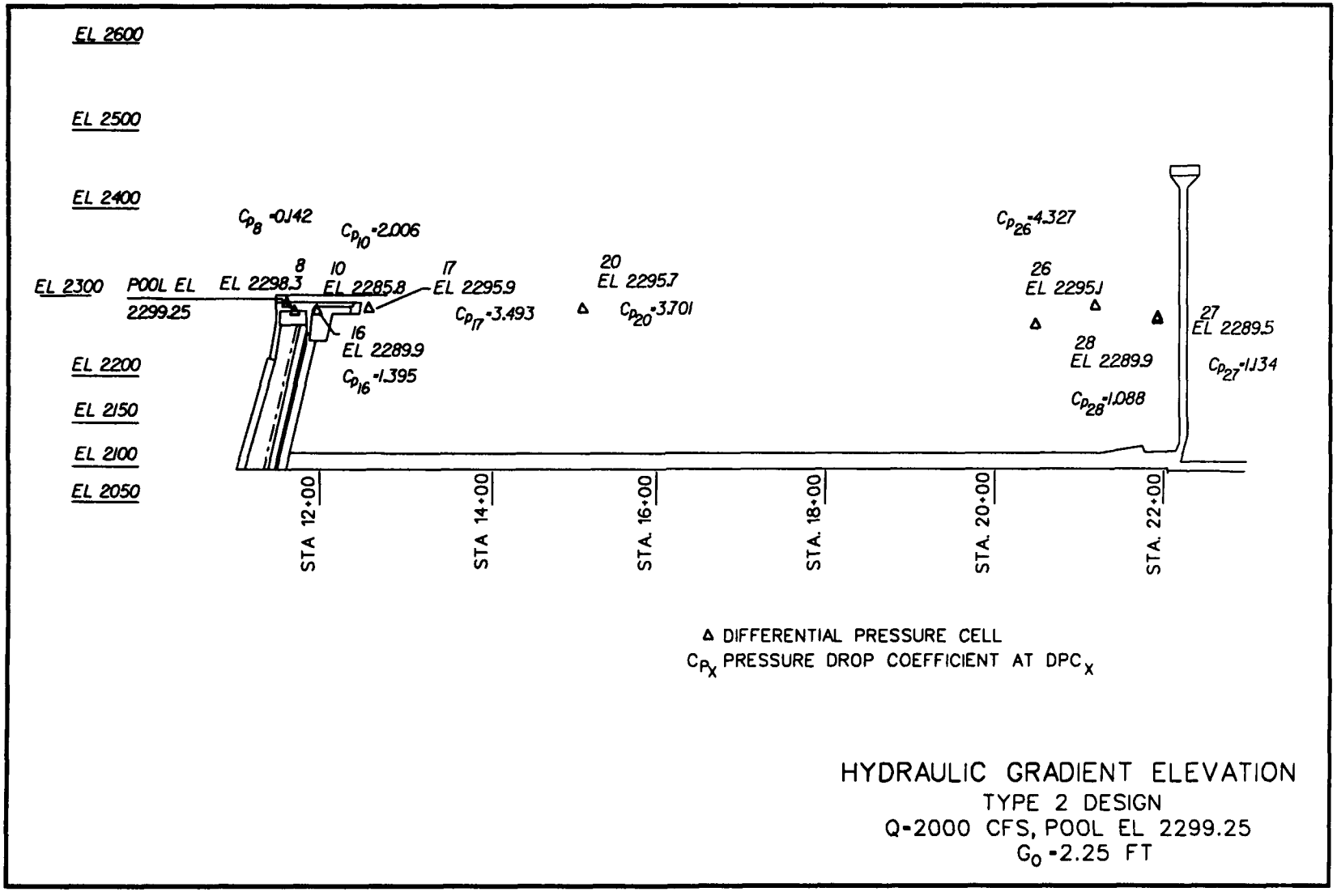

HYDRAULIC GRADIENT ELEVATION
TYPE 2 DESIGN
Q-2000 CFS, POOL EL 2299.25
G_0 -2.25 FT

PLATE 19

PLATE 20

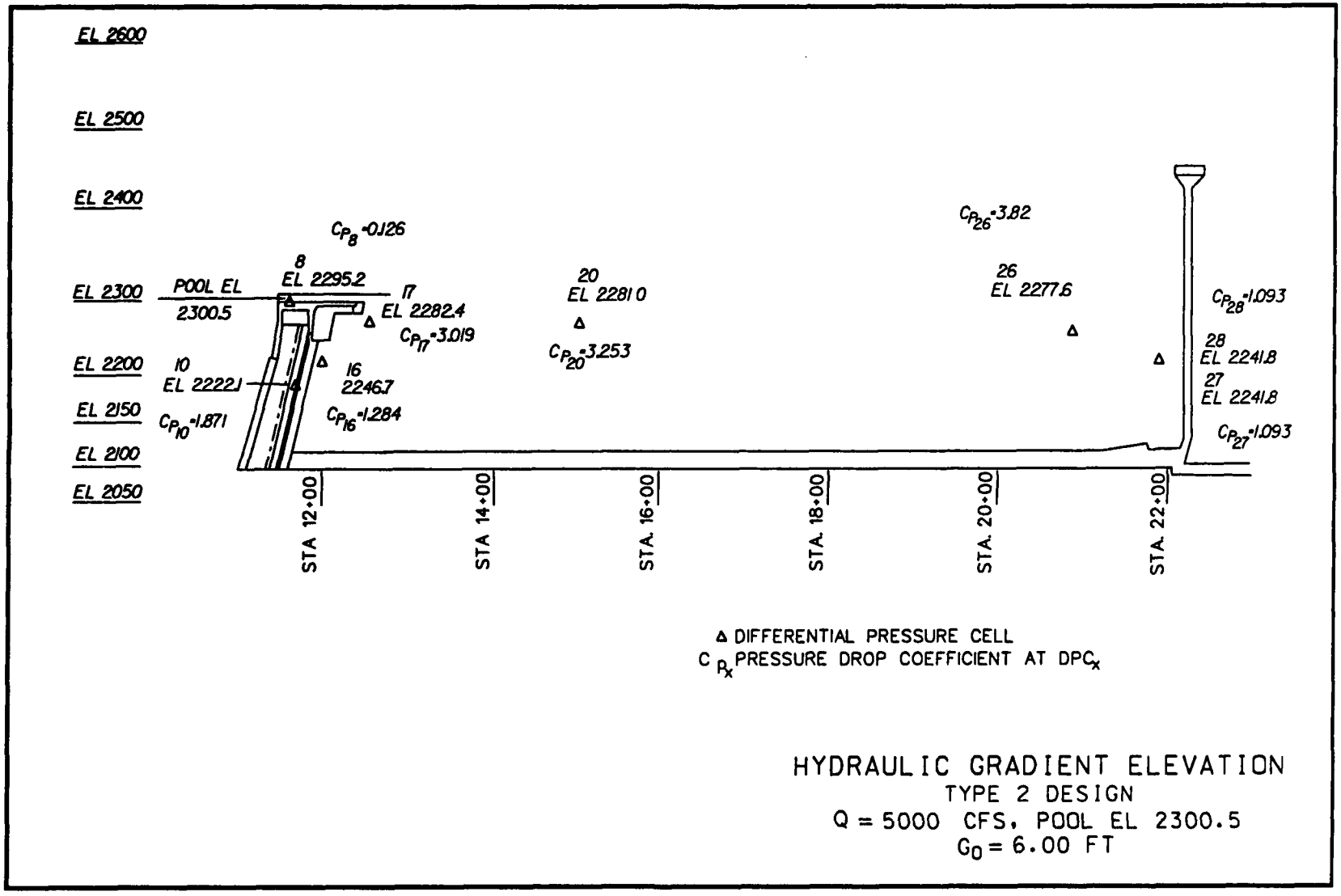

HYDRAULIC GRADIENT ELEVATION

TYPE 2 DESIGN

Q = 5000 CFS, POOL EL 2300.5

G_0 = 6.00 FT

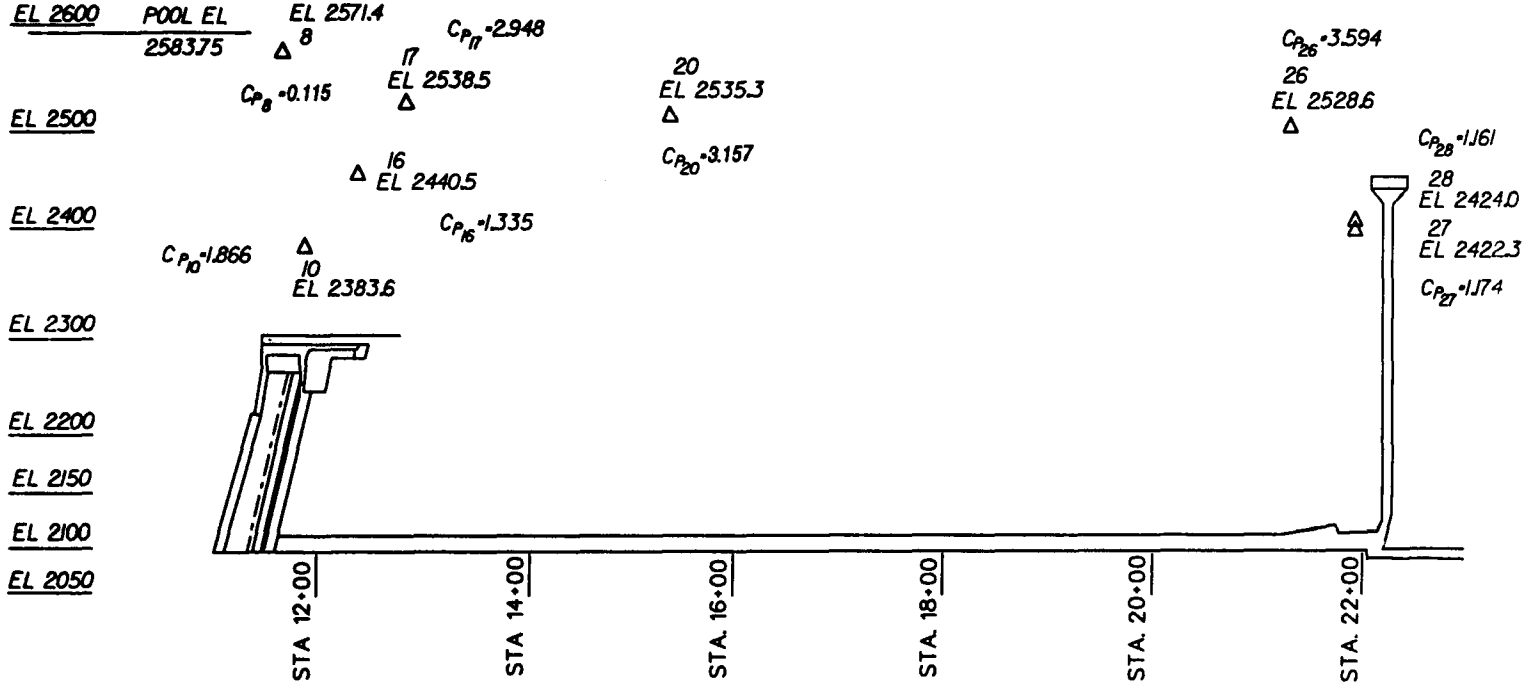

Δ DIFFERENTIAL PRESSURE CELL

C_{P_x} PRESSURE DROP COEFFICIENT AT DPC $_x$

HYDRAULIC GRADIENT ELEVATION

TYPE 2 DESIGN

Q = 8000 CFS, POOL EL 2583.75

G_D = 6.25 FT

PLATE 21

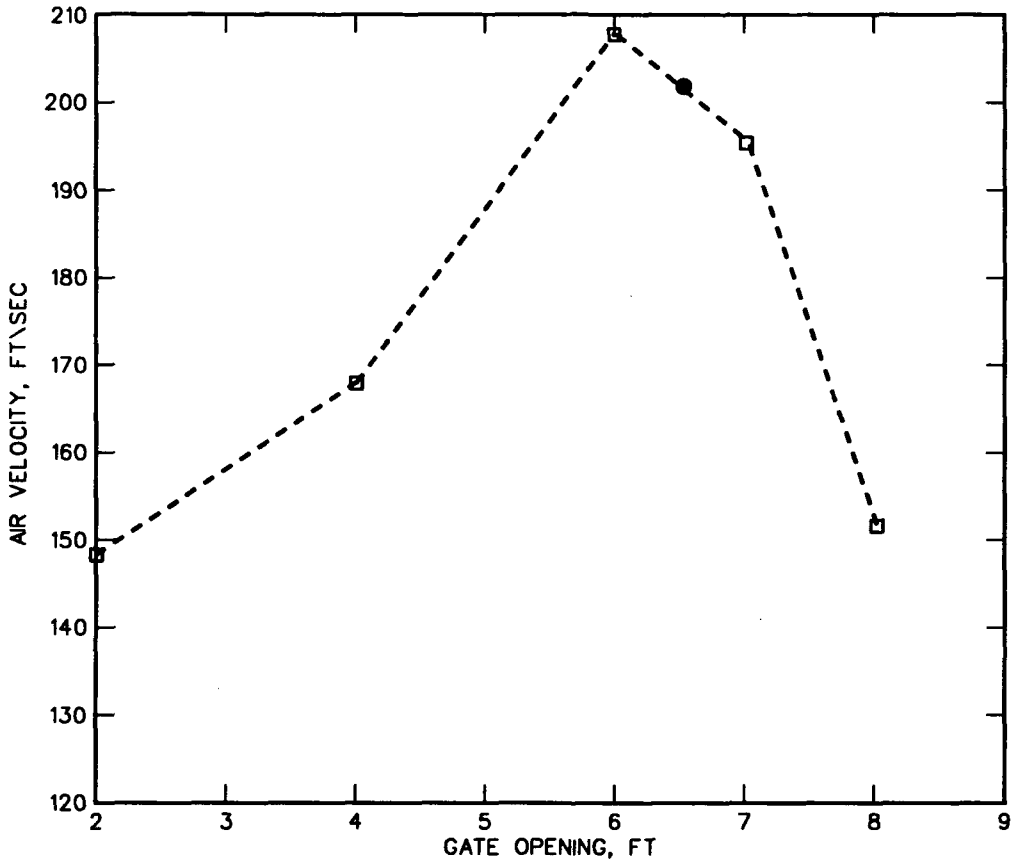

LEGEND

TYPE 2 DESIGN

TYPE 3 DESIGN

AIR VELOCITY IN AIR SHAFT

PLATE 22

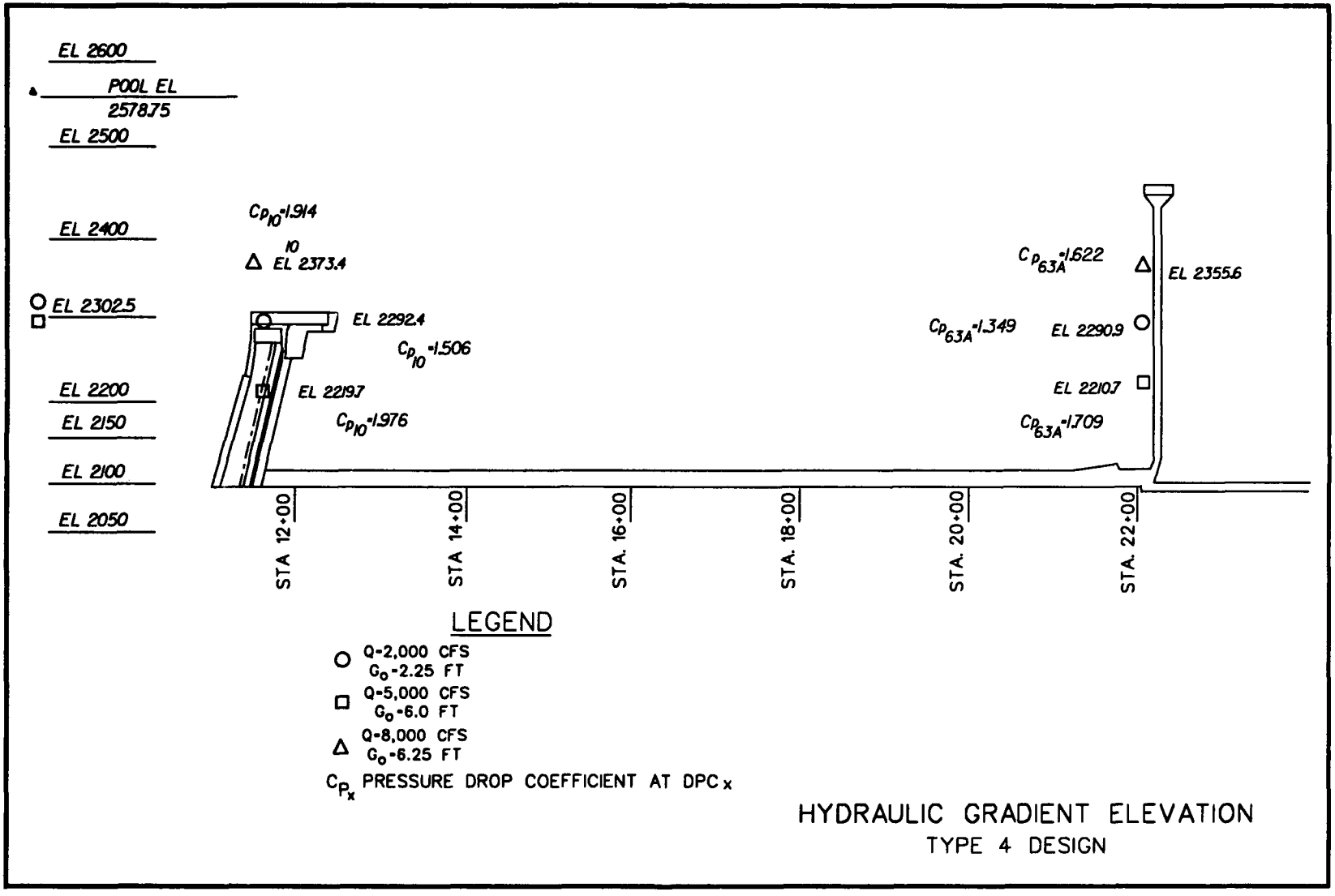

HYDRAULIC GRADIENT ELEVATION
TYPE 4 DESIGN

PLATE 23

PLATE 24

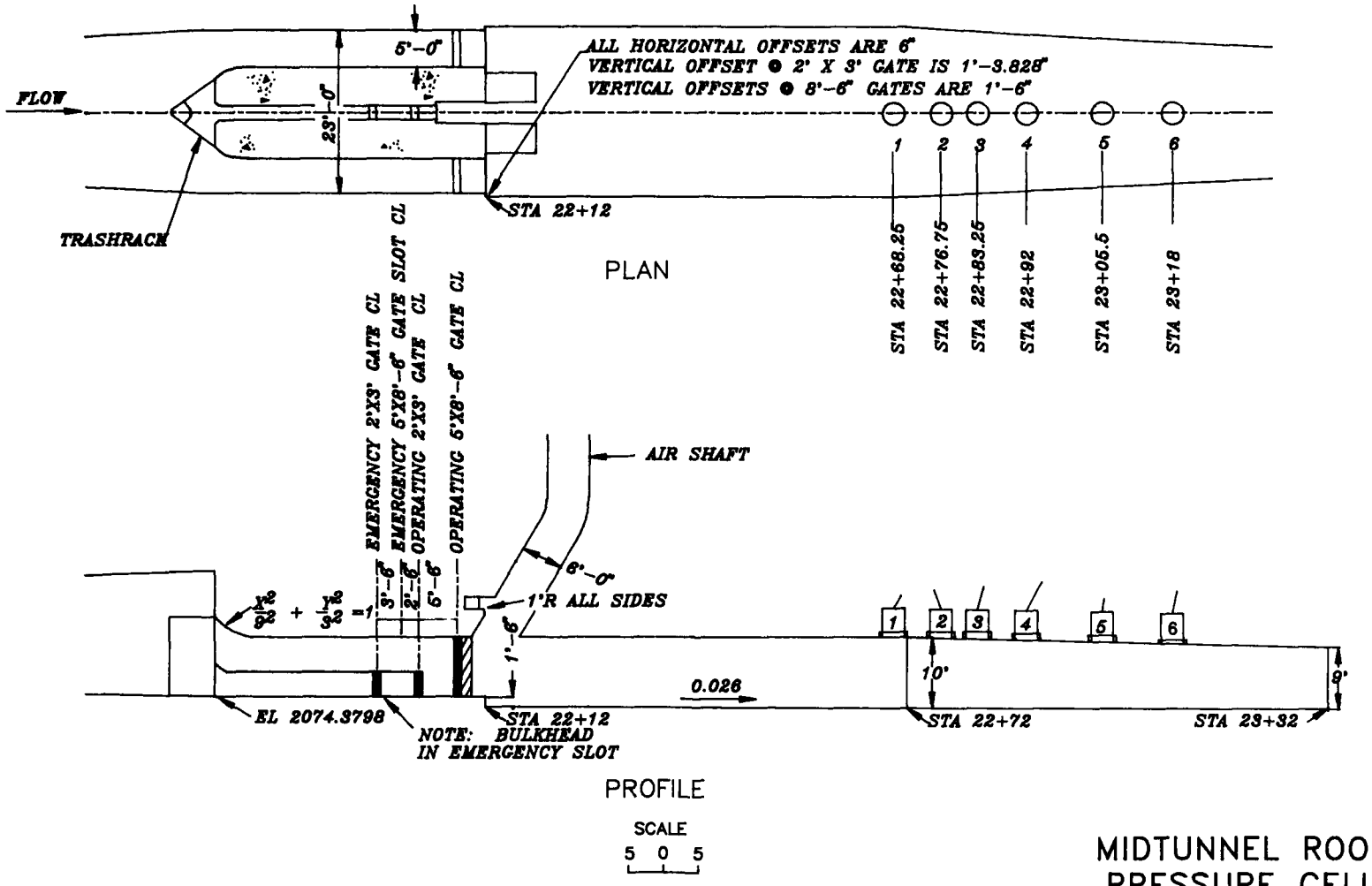

MIDTUNNEL ROOF PRESSURE CELL DETAIL

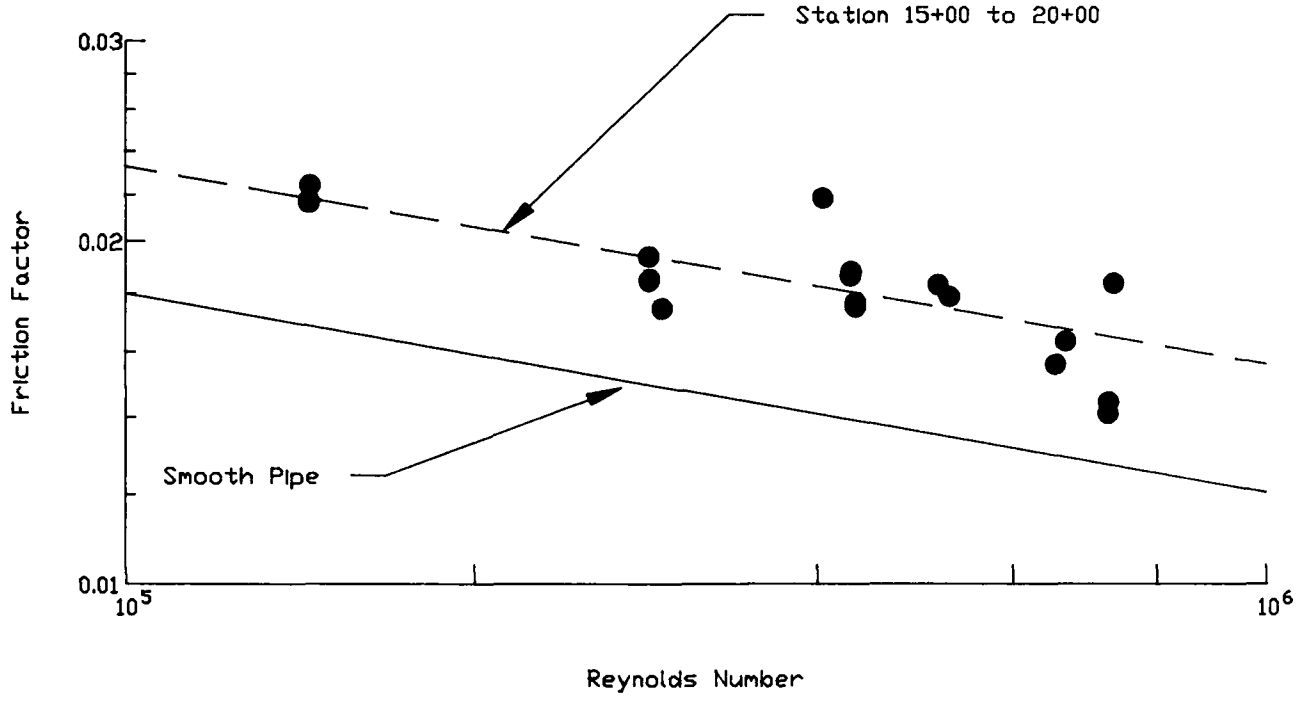

FRICTION FACTORS IN
MODEL TUNNEL

PLATE 25

PLATE 26

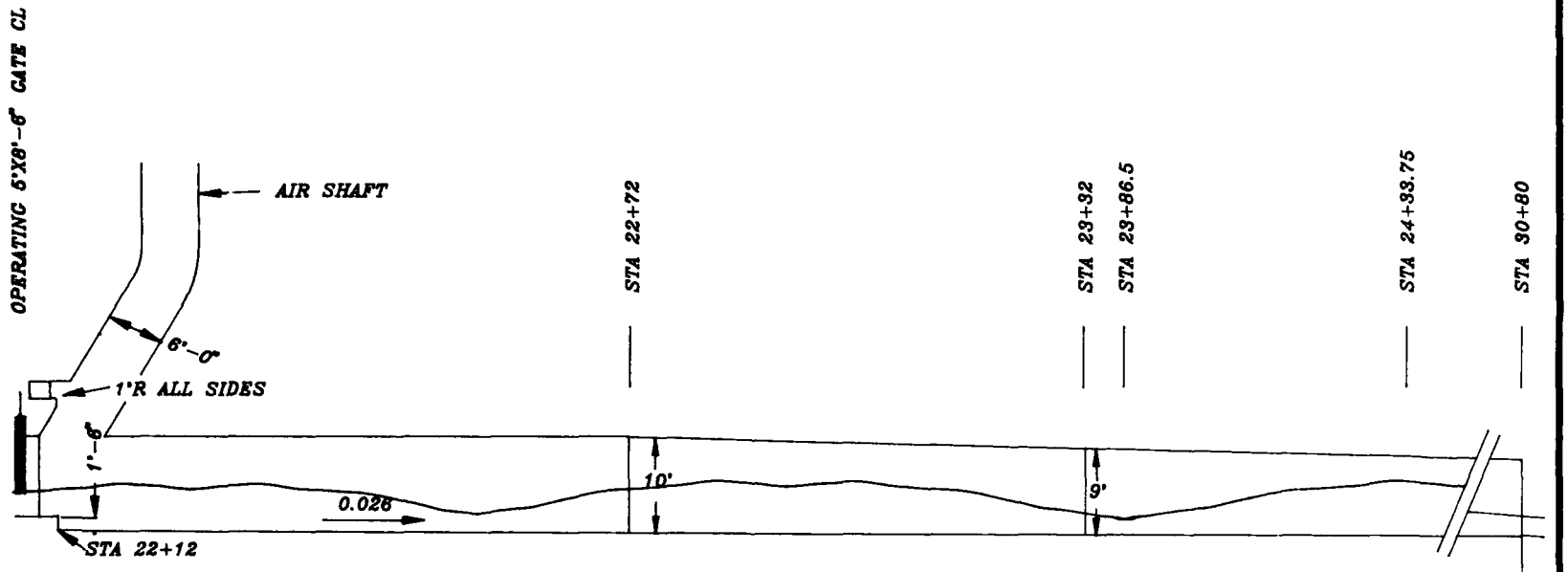

PROFILE

SCALE
5 0 5

LOCATIONS OF TYPICAL CRITICAL CROSS SECTIONS FOR OPEN CHANNEL VELOCITIES

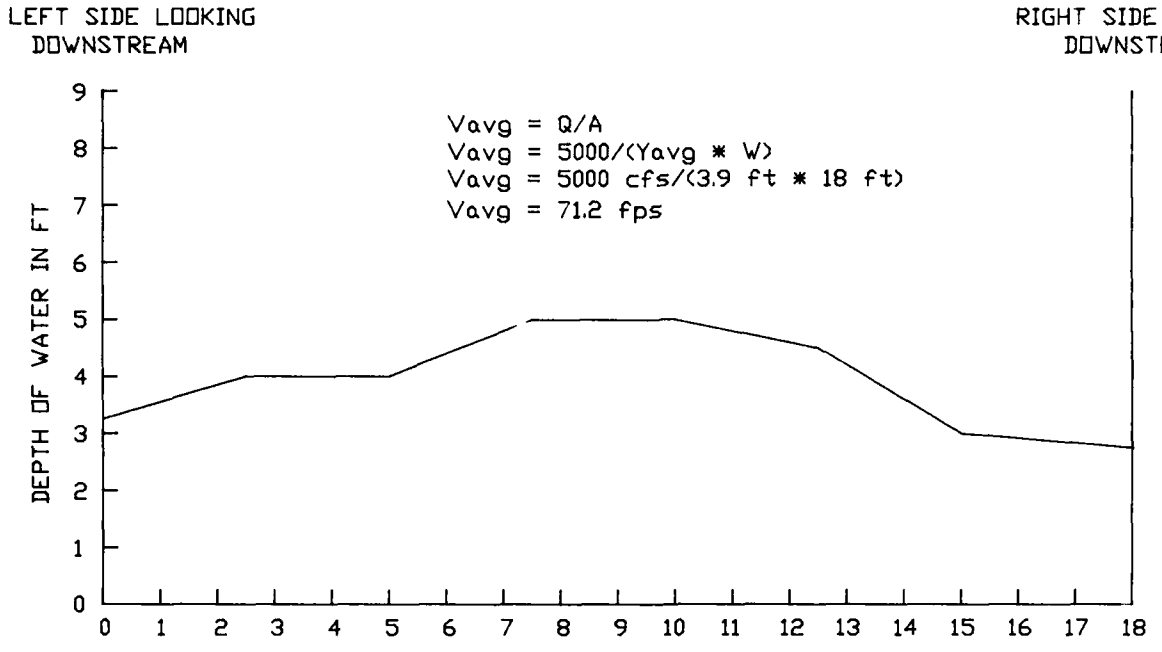

STA 24+41.25

WATER–SURFACE
CROSS SECTION
Q = 5,000 CFS
POOL EL 2300
LOW POINT OF FLOW

PLATE 27

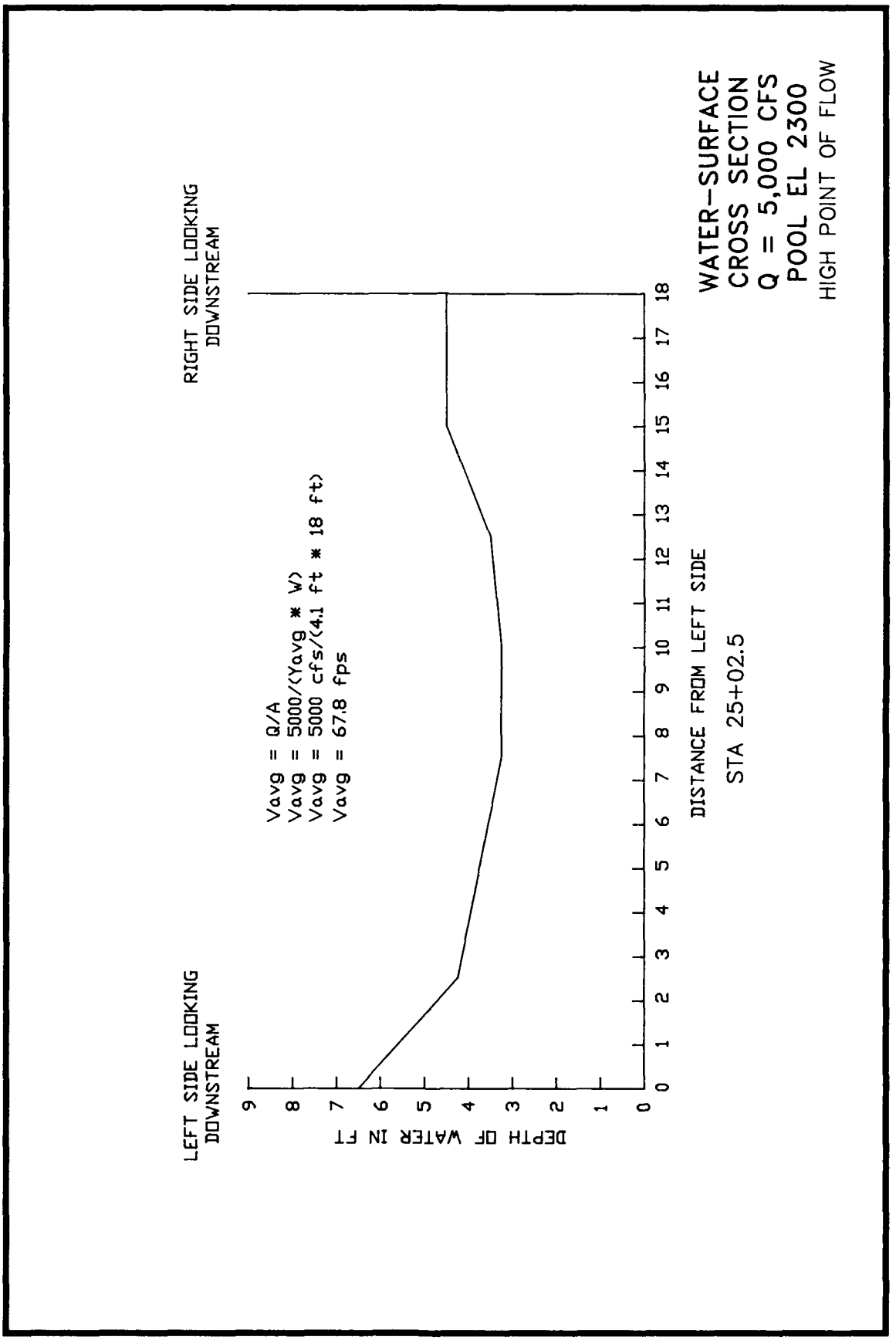
WATER-SURFACE
CROSS SECTION
Q = 5,000 CFS
POOL EL 2300
HIGH POINT OF FLOW
RIGHT SIDE LOOKING
DOWNSTREAM
LEFT SIDE LOOKING
DOWNSTREAM
Vavg = Q/A
Vavg = 5000/(Yavg * W)
Vavg = 5000 cfs/(4.1 ft * 18 ft)
Vavg = 67.8 fps
DEPTH OF WATER IN FT
0
1
2
3
4
5
6
7
8
9
DISTANCE FROM LEFT SIDE
STA 25+02.5
0
1
2
3
4
5
6
7
8
9
10
11
12
13
14
15
16
17
18

PLATE 28

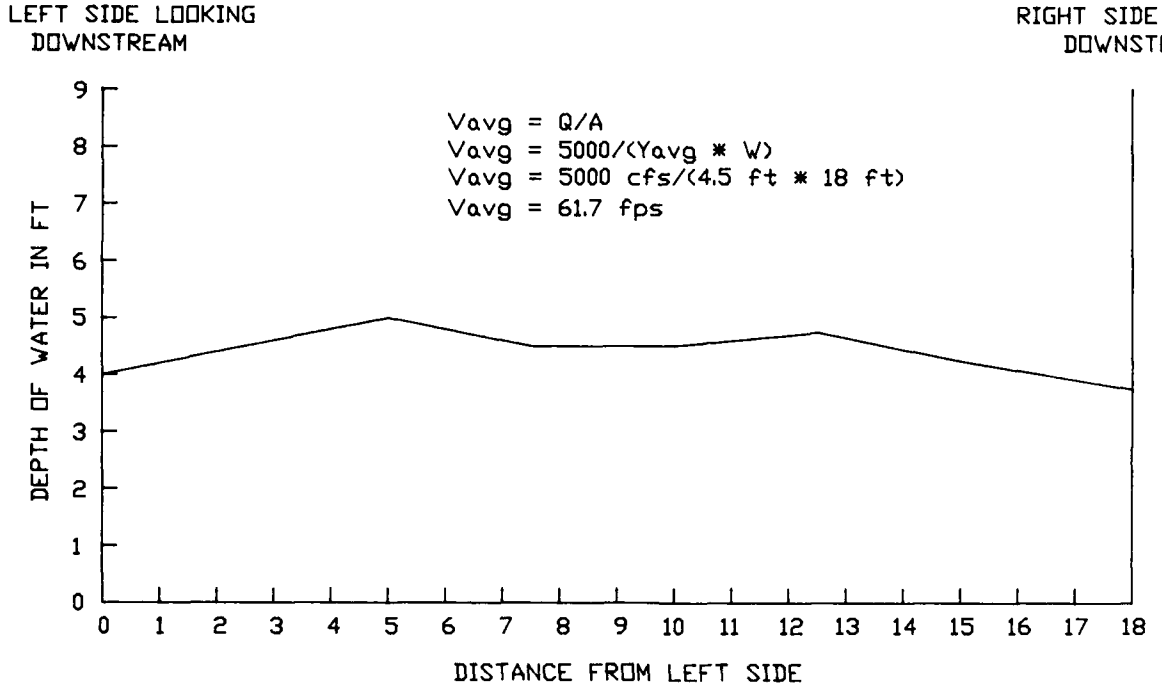

STA 30+80

WATER-SURFACE
CROSS SECTION
Q = 5,000 CFS
POOL EL 2300
AT THE EXIT

PLATE 29

PLATE 30

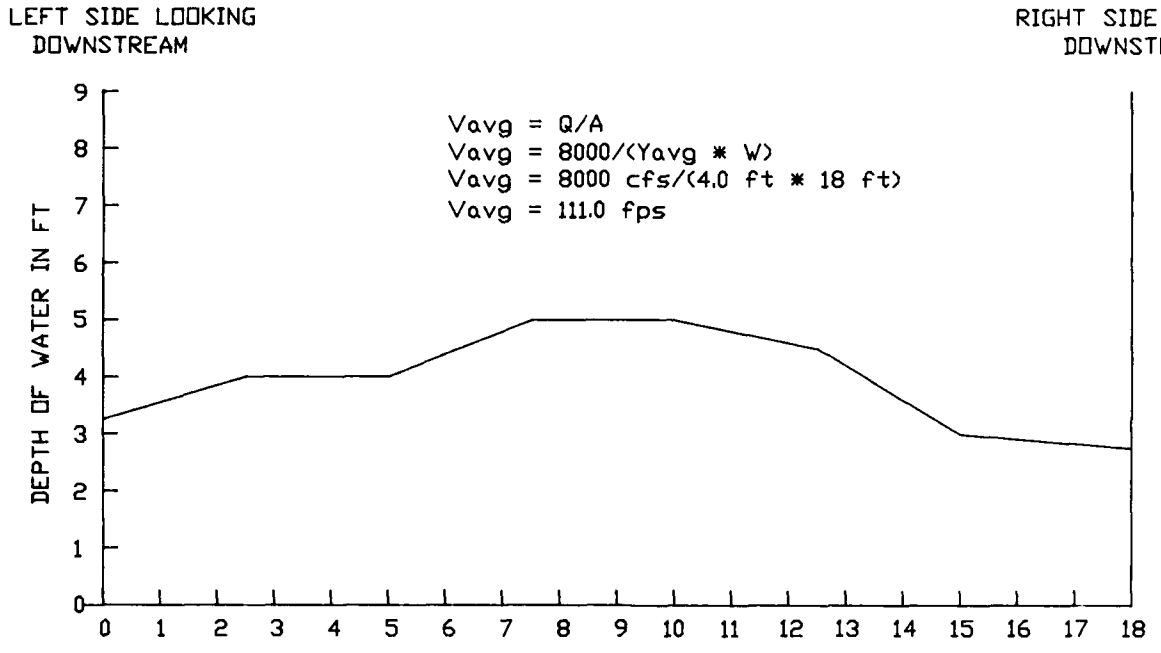

STA 24+41.2

WATER-SURFACE
CROSS SECTION
Q = 8,000 CFS
POOL EL 2580
LOW POINT OF FLOW

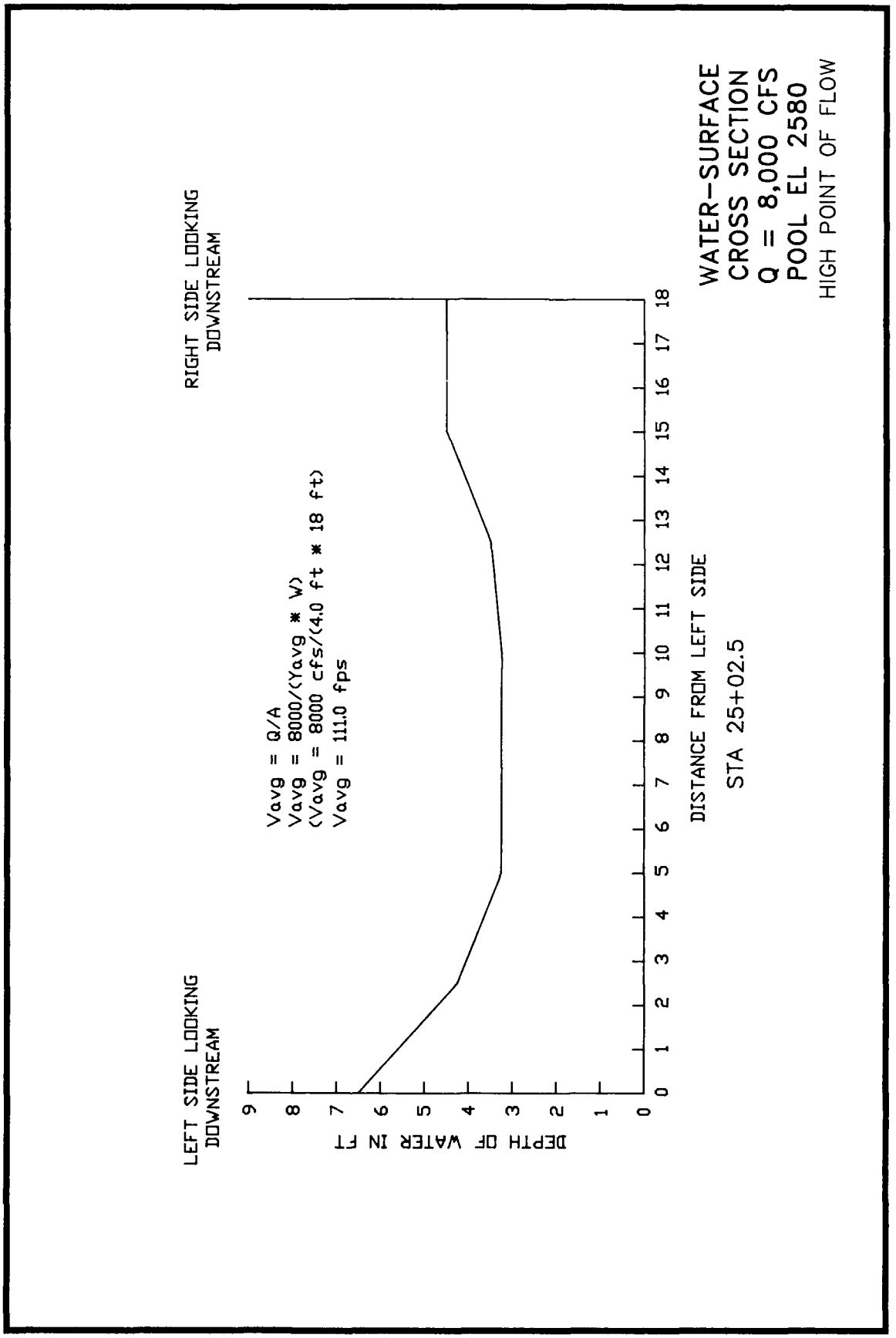
WATER-SURFACE
CROSS SECTION
Q = 8,000 CFS
POOL EL 2580
HIGH POINT OF FLOW
RIGHT SIDE LOOKING
DOWNSTREAM
LEFT SIDE LOOKING
DOWNSTREAM
Vavg = Q/A
Vavg = 8000/(Yavg * W)
(Vavg = 8000 cfs/(4.0 ft * 18 ft)
Vavg = 111.0 fps
DEPTH OF WATER IN FT
0
1
2
3
4
5
6
7
8
9
DISTANCE FROM LEFT SIDE
0
1
2
3
4
5
6
7
8
9
10
11
12
13
14
15
16
17
18
STA 25+02.5

PLATE 31

PLATE 32

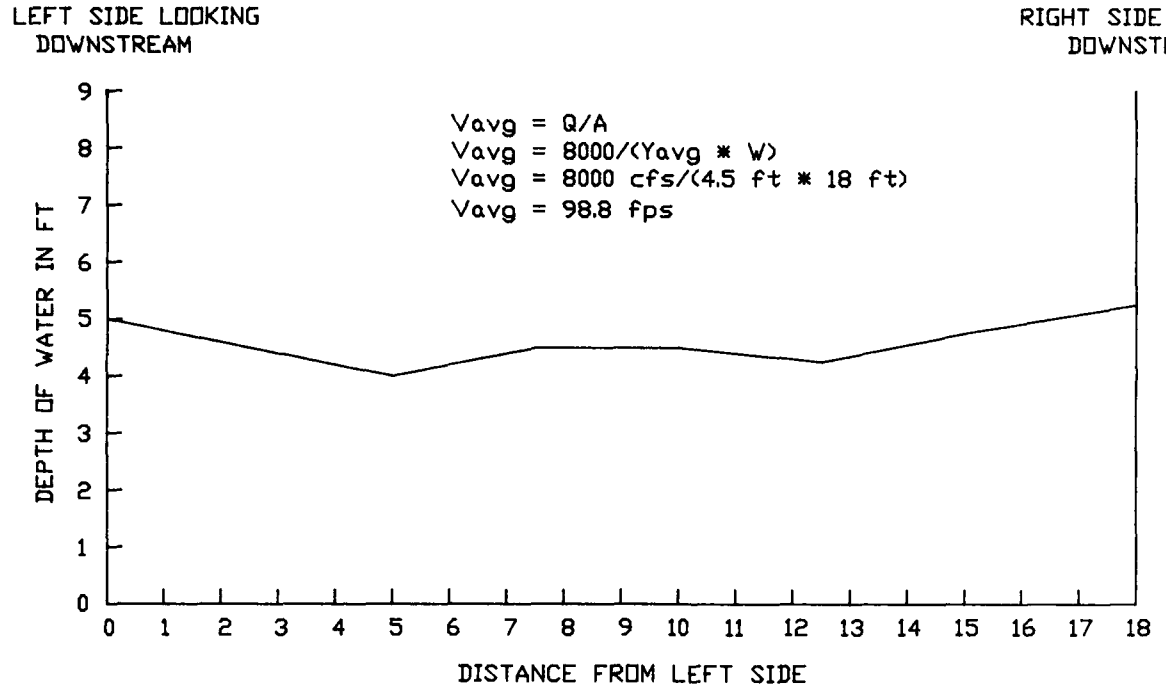

STA 30+80

WATER-SURFACE
CROSS SECTION
Q = 8,000 CFS
POOL EL 2580
AT THE EXIT

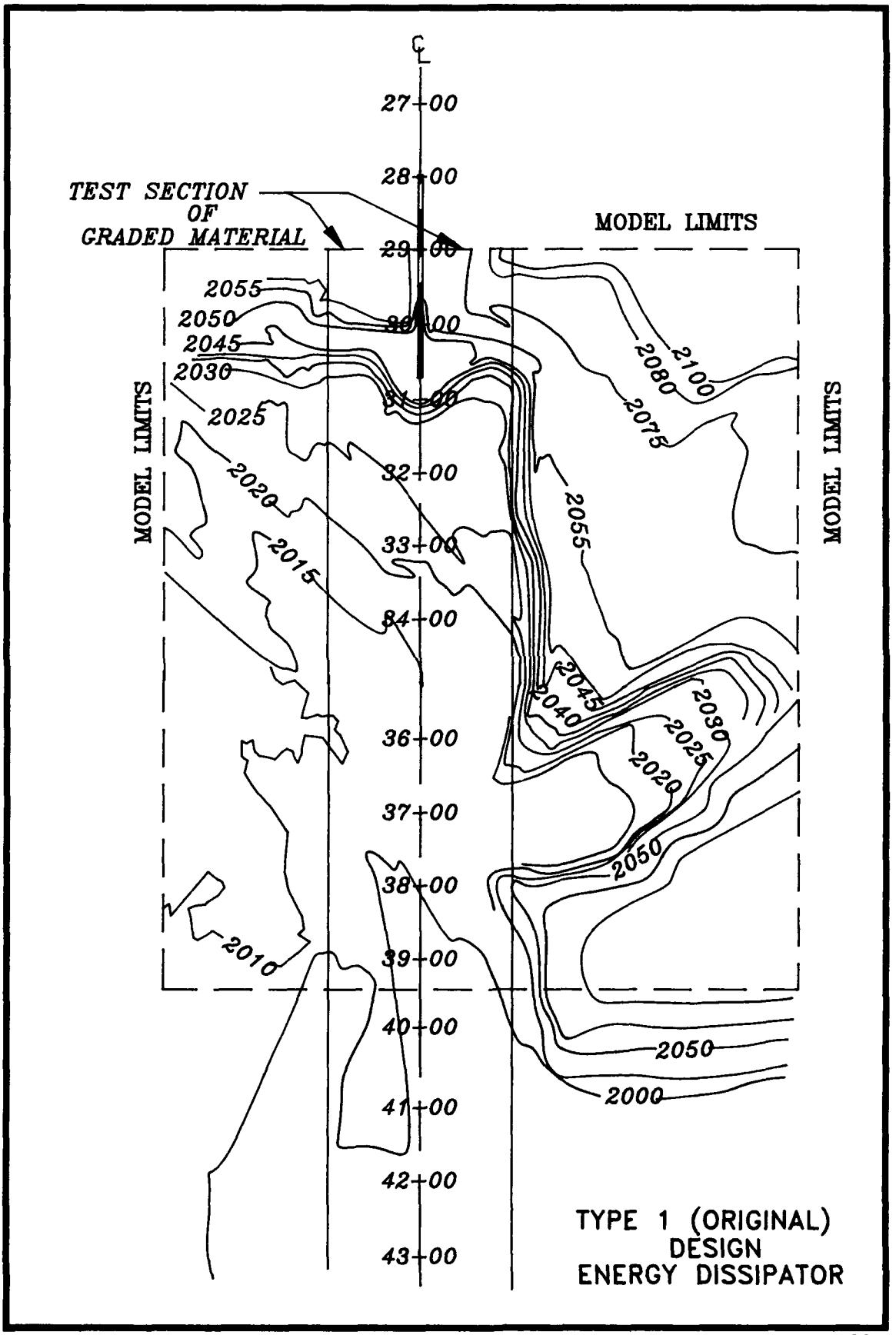
℄
27+00
28+00
29+00
30+00
31+00
32+00
33+00
34+00
36+00
37+00
38+00
39+00
40+00
41+00
42+00
43+00
TEST SECTION OF GRADED MATERIAL
MODEL LIMITS
MODEL LIMITS
MODEL LIMITS
2055
2050
2045
2030
2025
2020
2015
2010
2100
2080
2075
2055
2045
2040
2030
2025
2020
2050
2050
2000
TYPE 1 (ORIGINAL) DESIGN ENERGY DISSIPATOR

PLATE 33

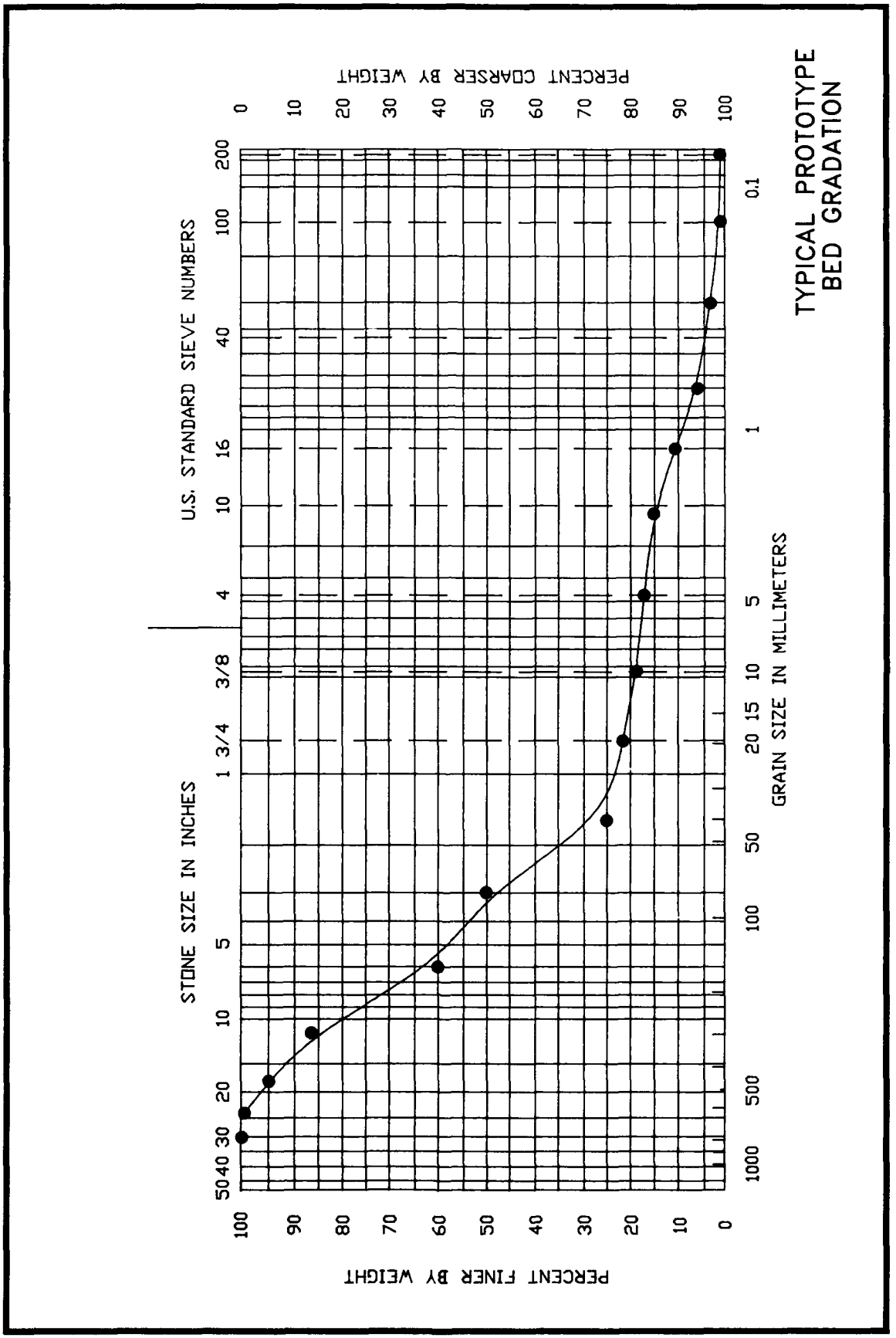
TYPICAL PROTOTYPE
BED GRADATION
PERCENT FINER BY WEIGHT
PERCENT COARSER BY WEIGHT
0
10
20
30
40
50
60
70
80
90
100
STONE SIZE IN INCHES
5
40
30
20
10
5
1 3/4
3/8
U.S. STANDARD SIEVE NUMBERS
4
10
16
40
100
200
GRAIN SIZE IN MILLIMETERS
1000
500
100
50
20
15
10
5
1
0.1

PLATE 34

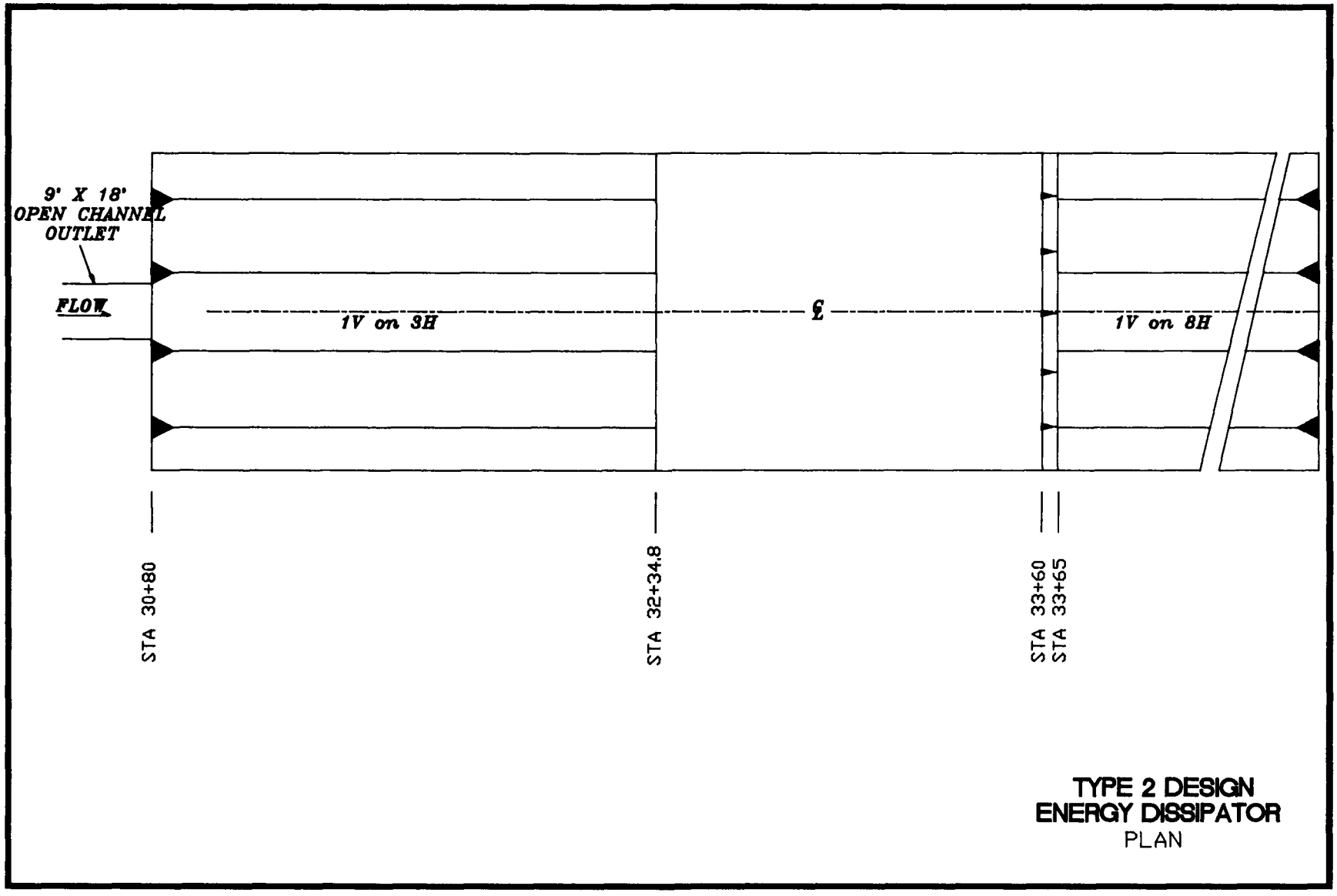

TYPE 2 DESIGN
ENERGY DISSIPATOR
PLAN

PLATE 35

PLATE 36

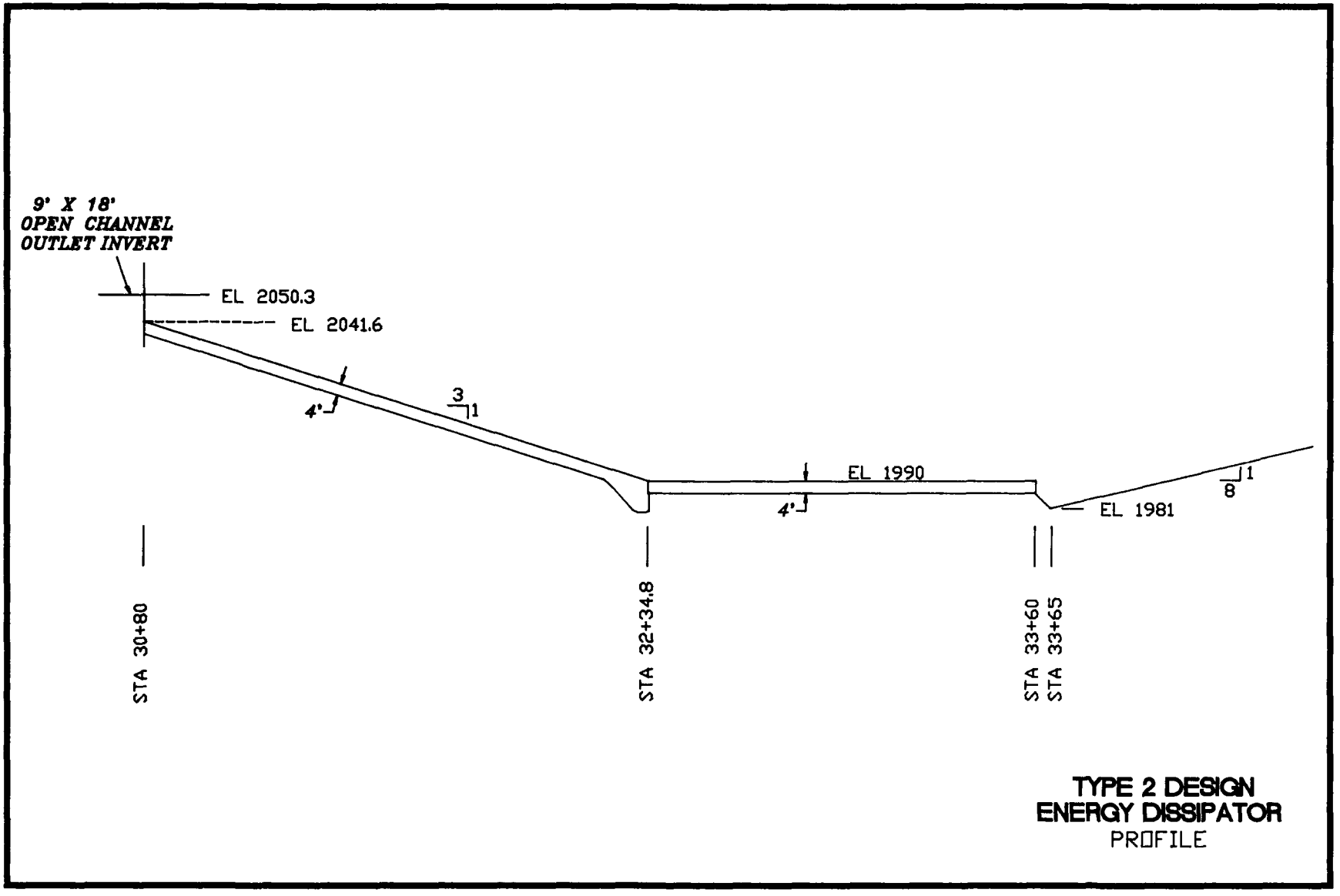

TYPE 2 DESIGN
ENERGY DISSIPATOR
PROFILE

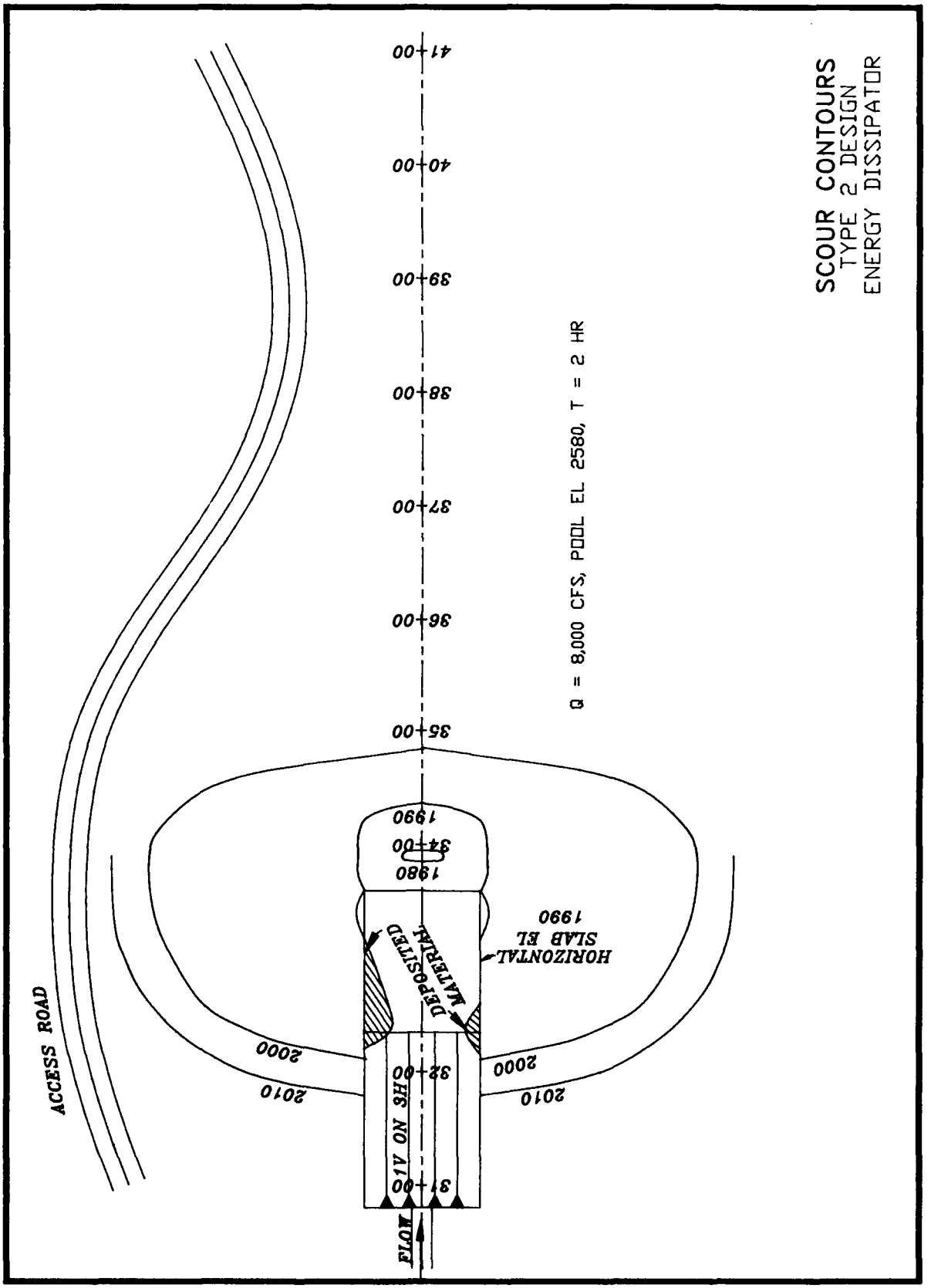
SCOUR CONTOURS
TYPE 2 DESIGN
ENERGY DISSIPATOR
Q = 8,000 CFS, POOL EL 2580, T = 2 HR
41+00
40+00
39+00
38+00
37+00
36+00
35+00
34+00
32+00
31+00
1990
1980
2000
2010
HORIZONTAL SLAB EL 1990
DEPOSITED MATERIAL
SHS ON A1
ACCESS ROAD
FLOW

PLATE 37

PLATE 38

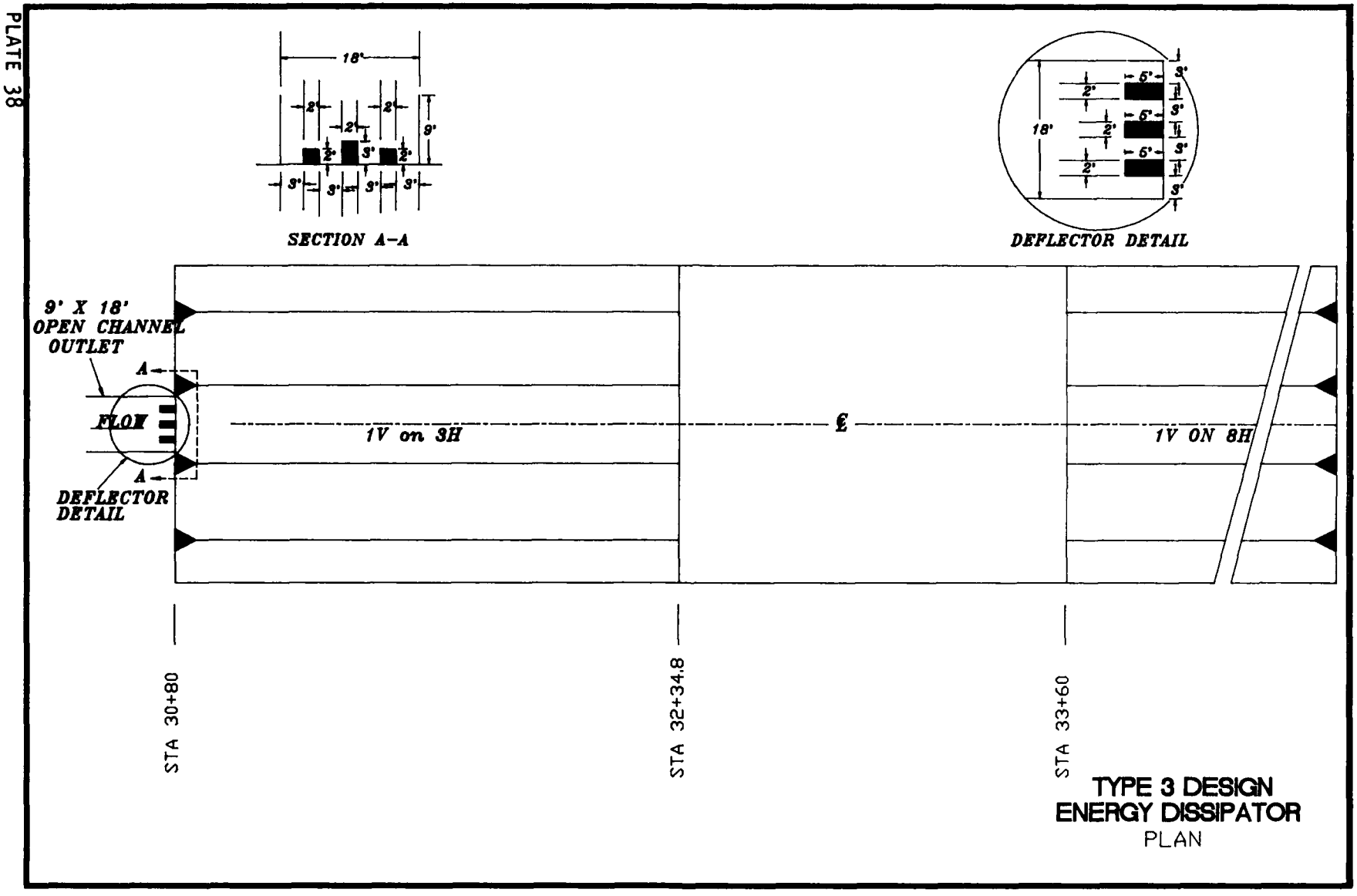

TYPE 3 DESIGN
ENERGY DISSIPATOR
PLAN

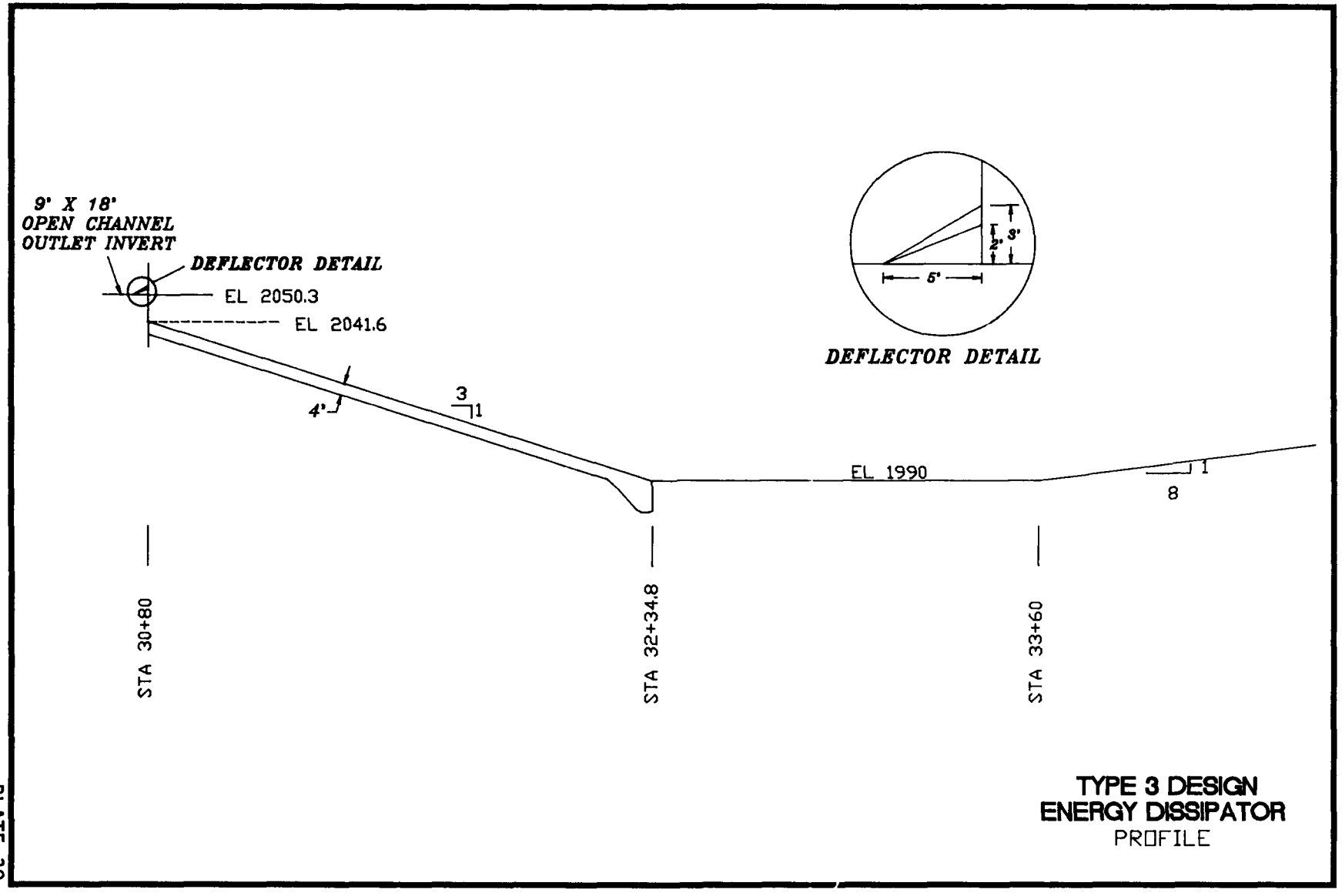

TYPE 3 DESIGN
ENERGY DISSIPATOR
PROFILE

PLATE 39

PLATE 40

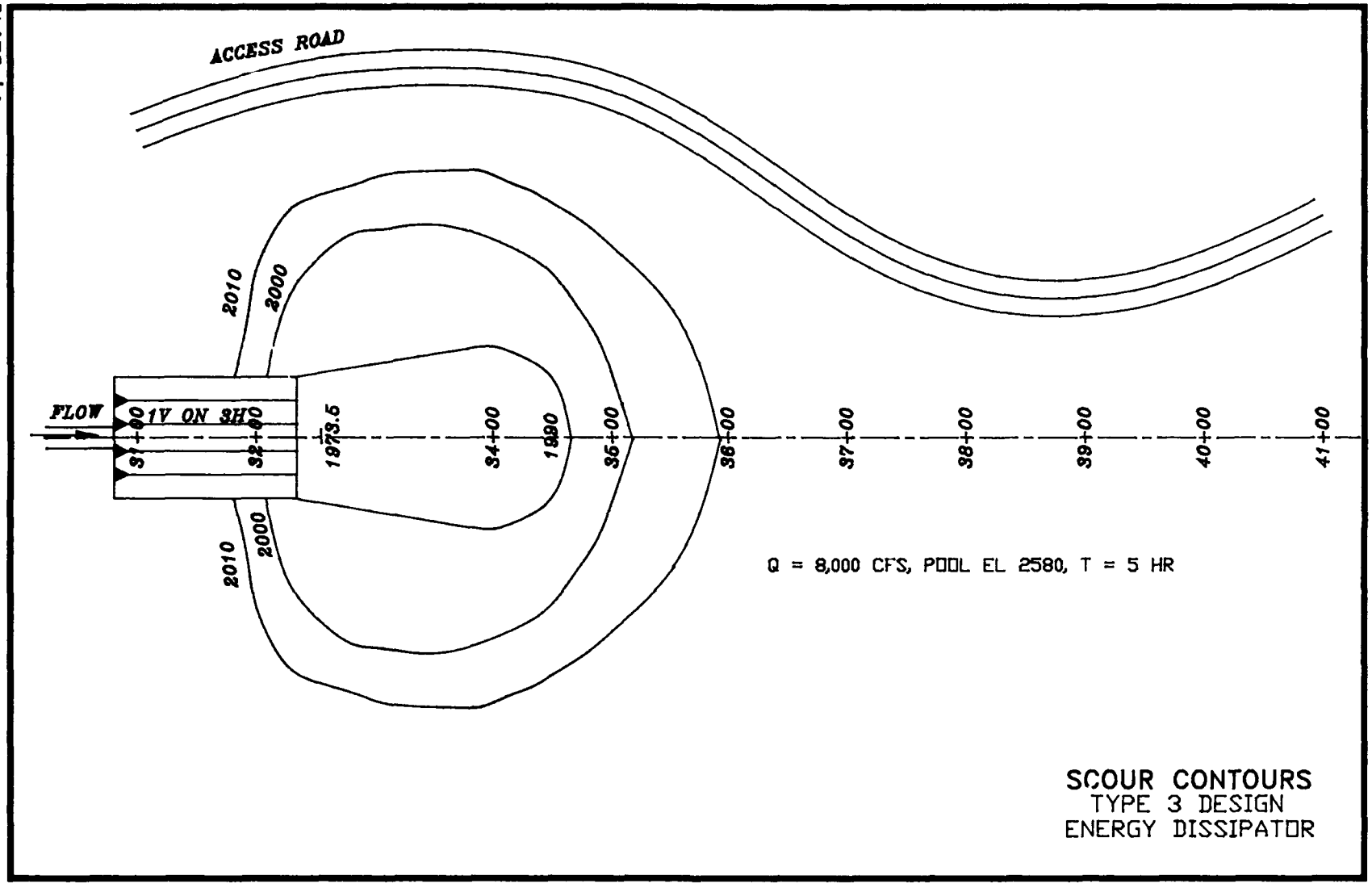

SCOUR CONTOURS
TYPE 3 DESIGN
ENERGY DISSIPATOR

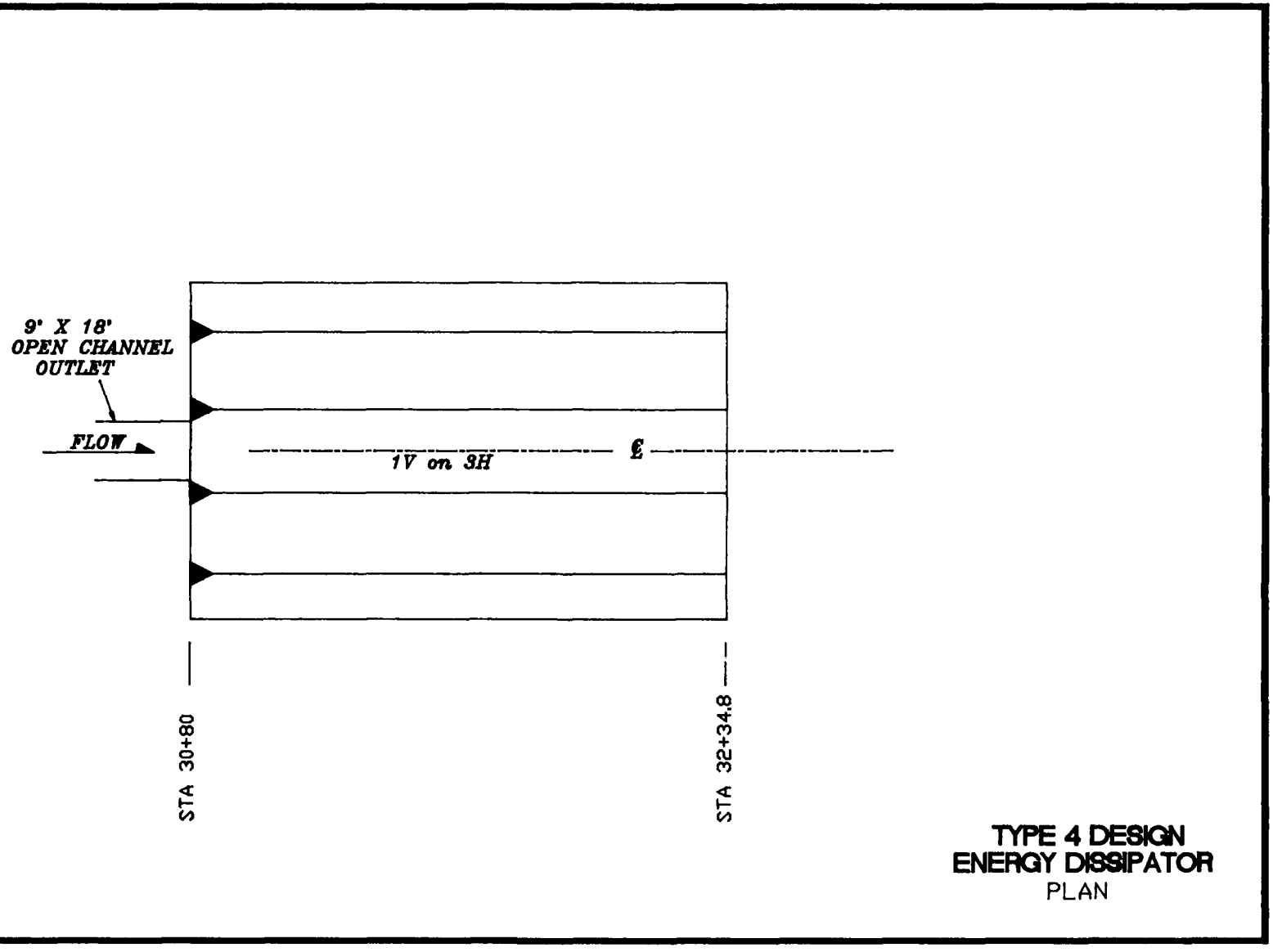

TYPE 4 DESIGN
ENERGY DISSIPATOR
PLAN

PLATE 41

PLATE 42

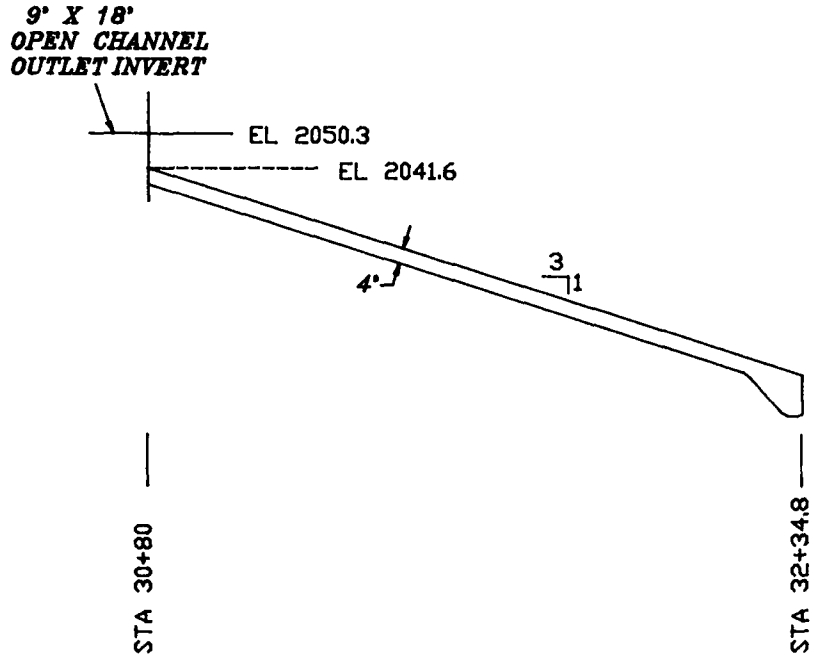

TYPE 4 DESIGN
ENERGY DISSIPATOR
PROFILE

SCOUR CONTOURS
TYPE 4 DESIGN
ENERGY DISSIPATOR
Q = 8,000 CFS, POOL EL 2580, T = 1 HR
41+00
40+00
39+00
38+00
37+00
36+00
35+00
1890
1880
34+00
1884.5
2000
2010
2000
2010
32+00
HB NO A10
31+00
FLOW
ACCESS ROAD

PLATE 43

PLATE 44

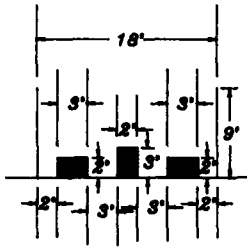

SECTION A–A

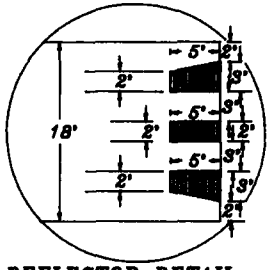

DEFLECTOR DETAIL

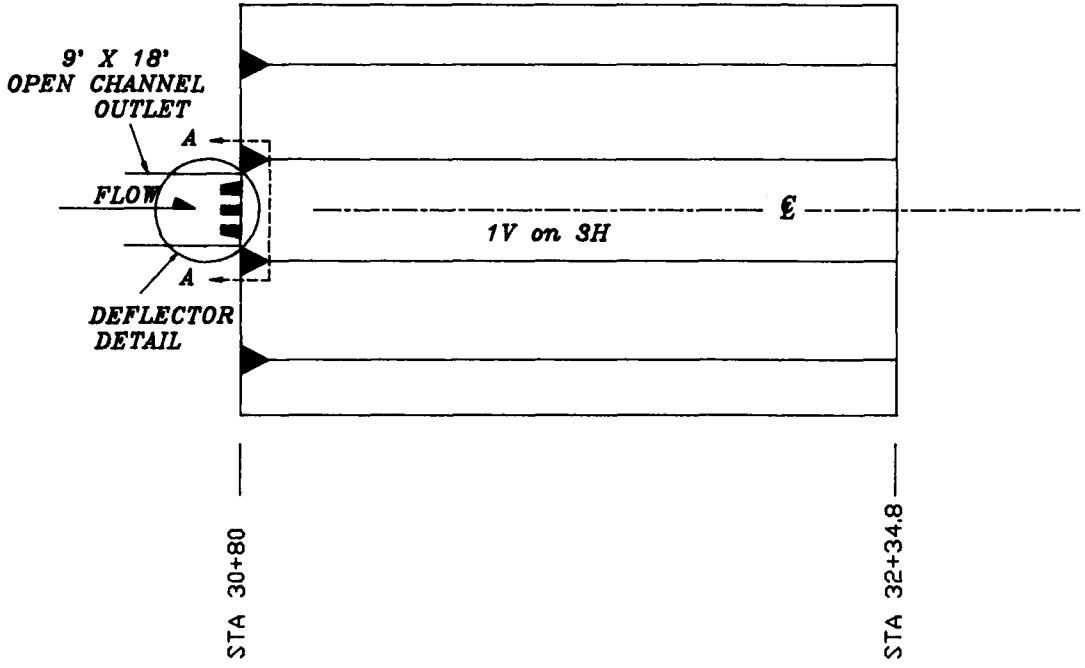

TYPE 5 DESIGN
ENERGY DISSIPATOR
PLAN

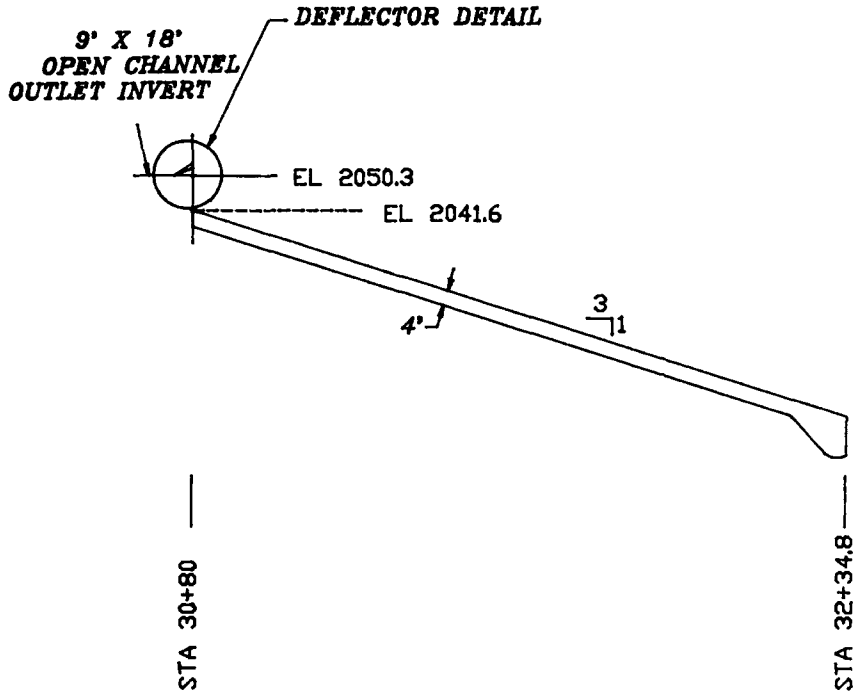

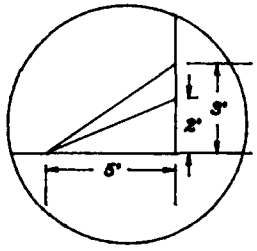

DEFLECTOR DETAIL

TYPE 5 DESIGN
ENERGY DISSIPATOR
PROFILE

PLATE 45

SCOUR CONTOURS
TYPE 5 DESIGN
ENERGY DISSIPATOR
Q = 8,000 CFS, POOL EL 2580, T = 1 HR
41+00
40+00
39+00
38+00
37+00
36+00
1890
1980
84+00
1885
2000
2010
2000
2010
32+00
3H ON 1V
31+00
ACCESS ROAD
FLOW

PLATE 46

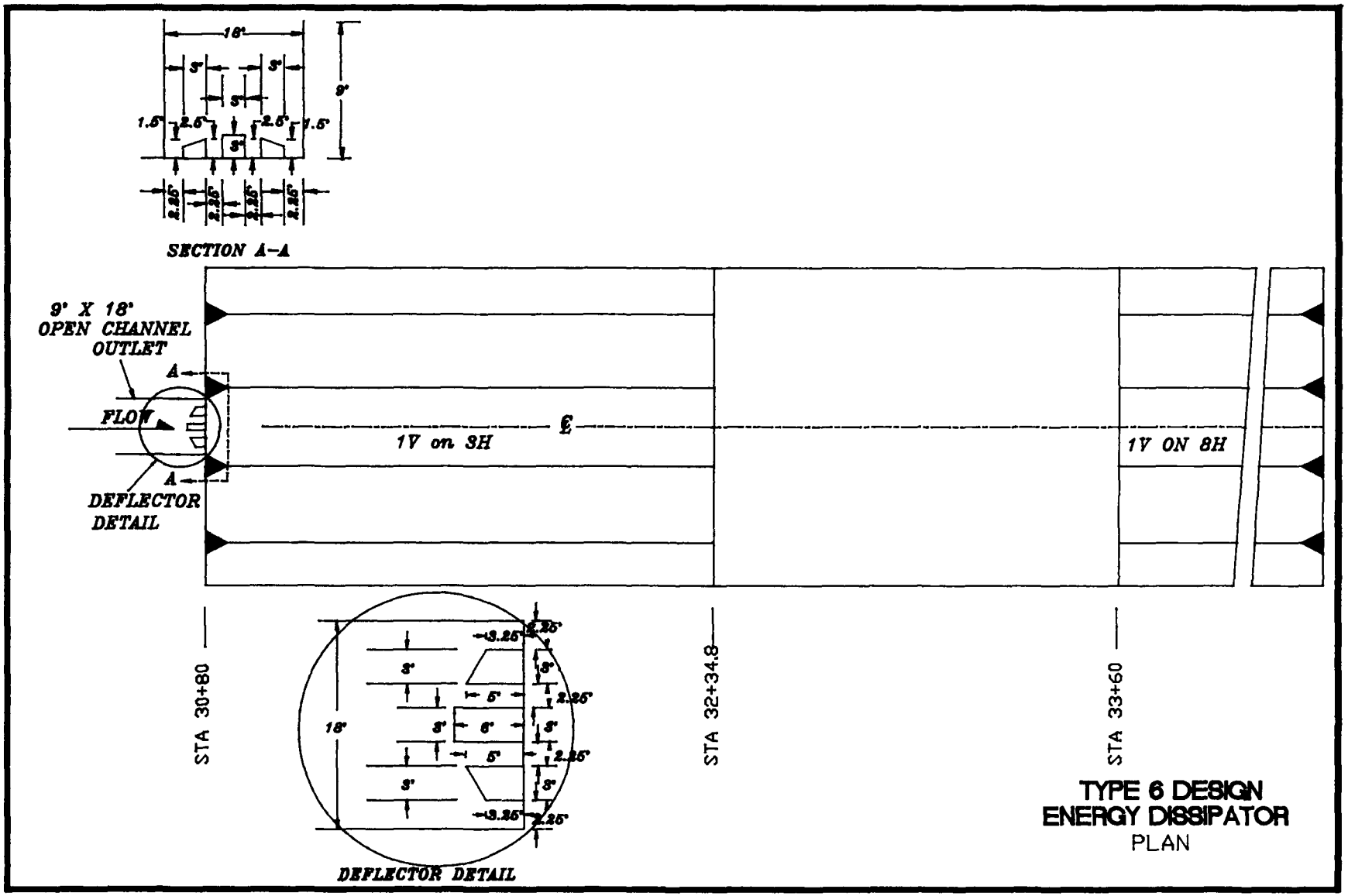

TYPE 6 DESIGN
ENERGY DISSIPATOR
PLAN

PLATE 47

PLATE 48

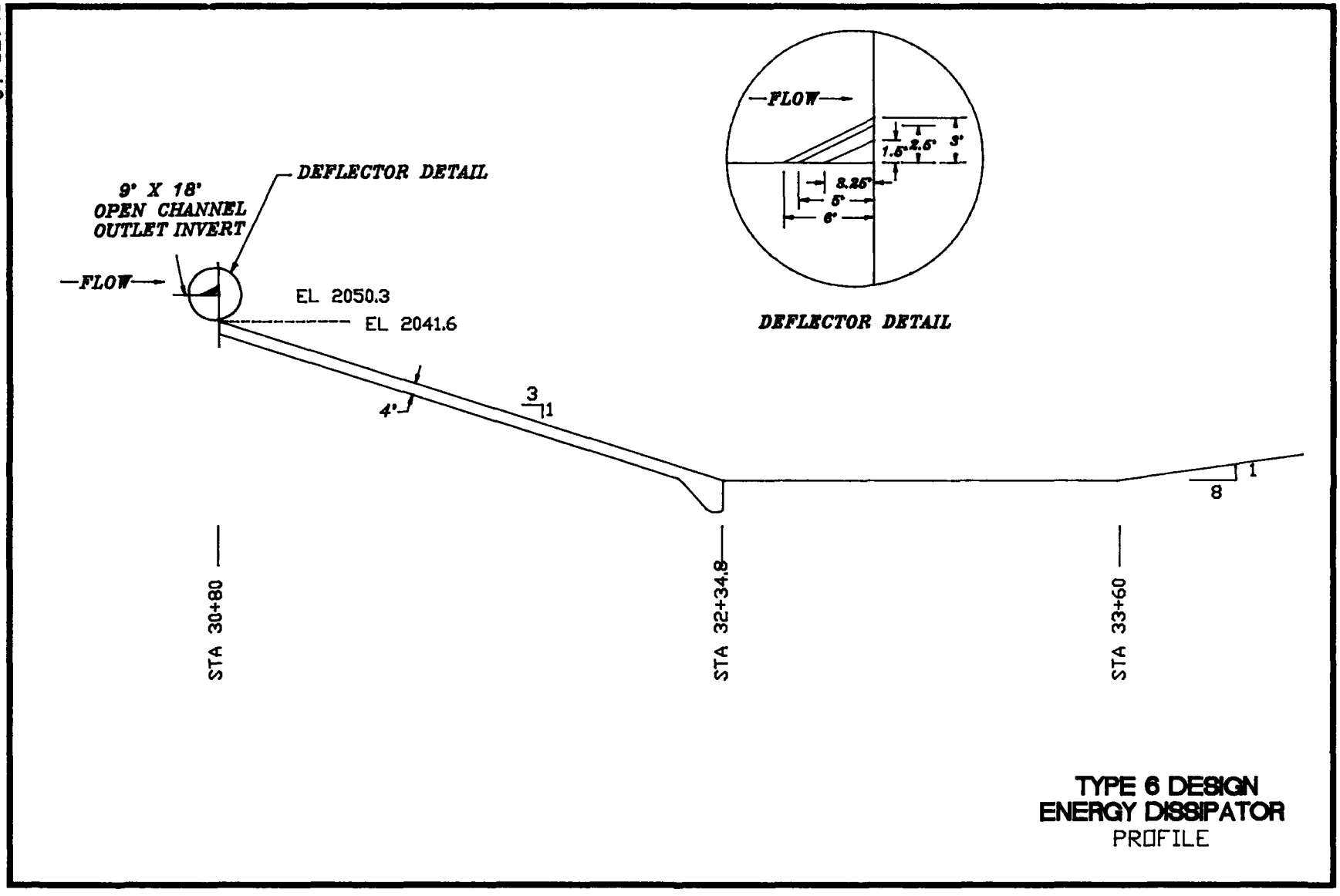

TYPE 6 DESIGN
ENERGY DISSIPATOR
PROFILE

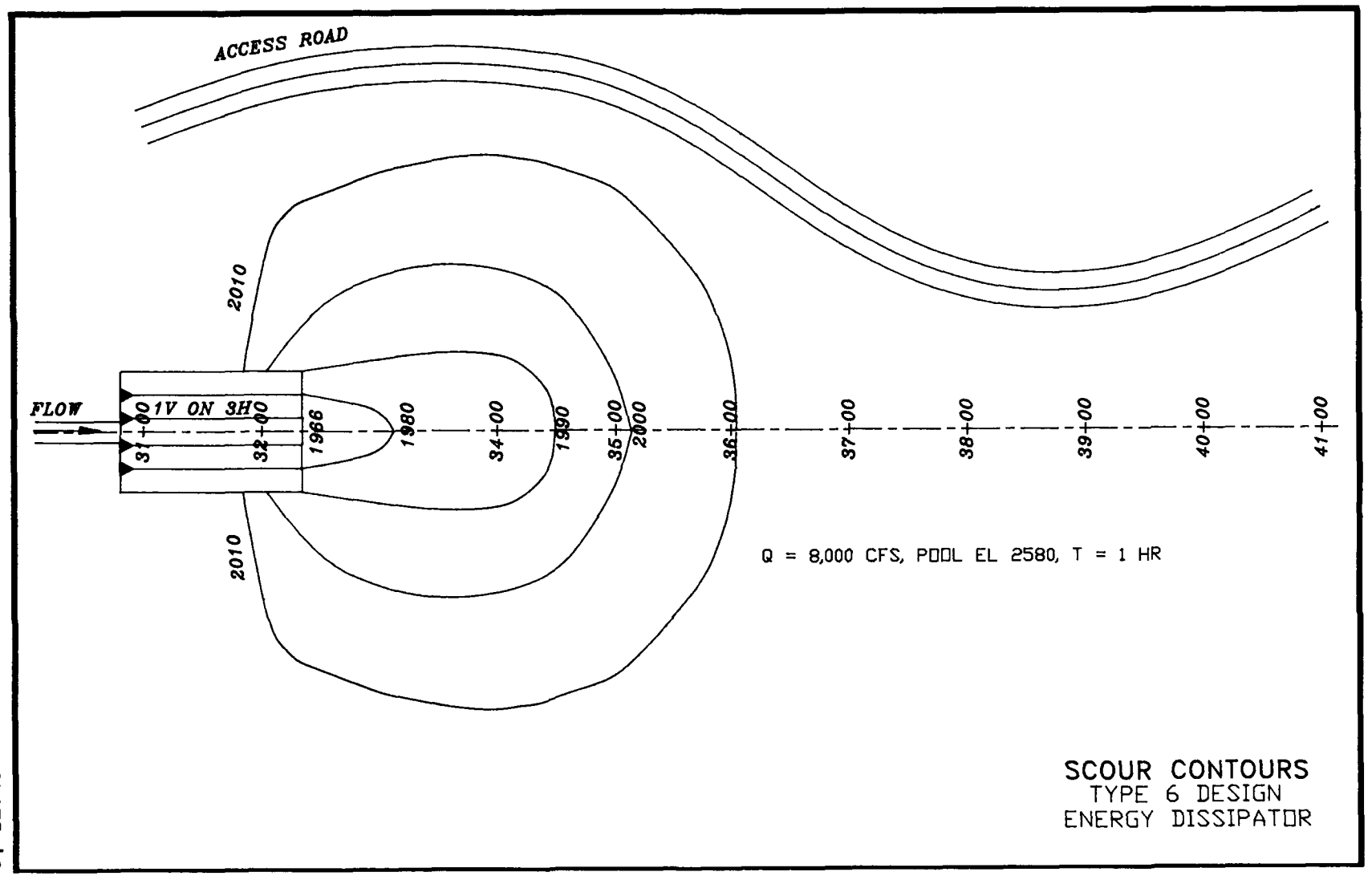

SCOUR CONTOURS
TYPE 6 DESIGN
ENERGY DISSIPATOR

PLATE 49

PLATE 50

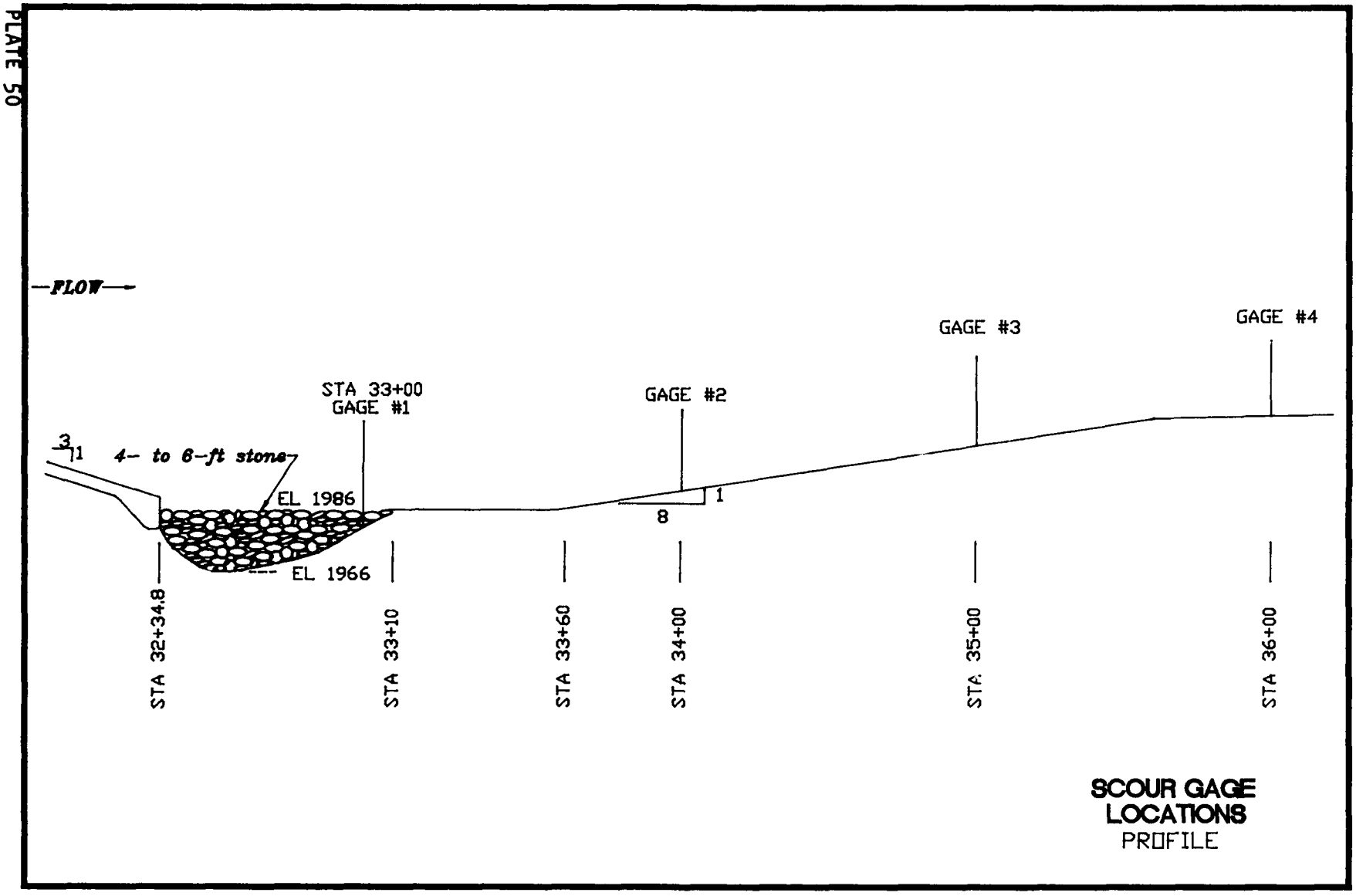

SCOUR GAGE LOCATIONS
PROFILE

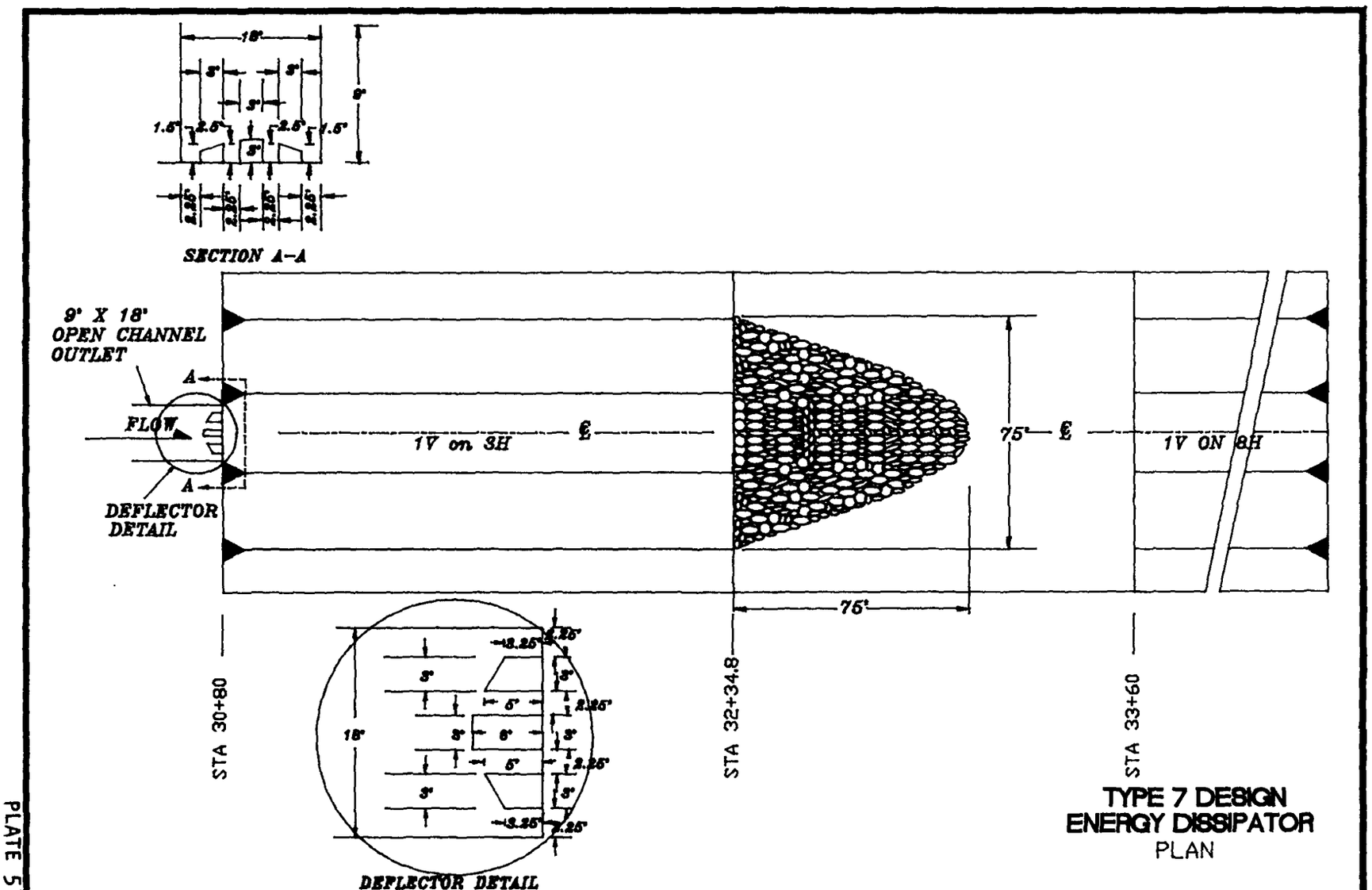

PLATE 51

TYPE 7 DESIGN
ENERGY DISSIPATOR
PLAN

PLATE 52

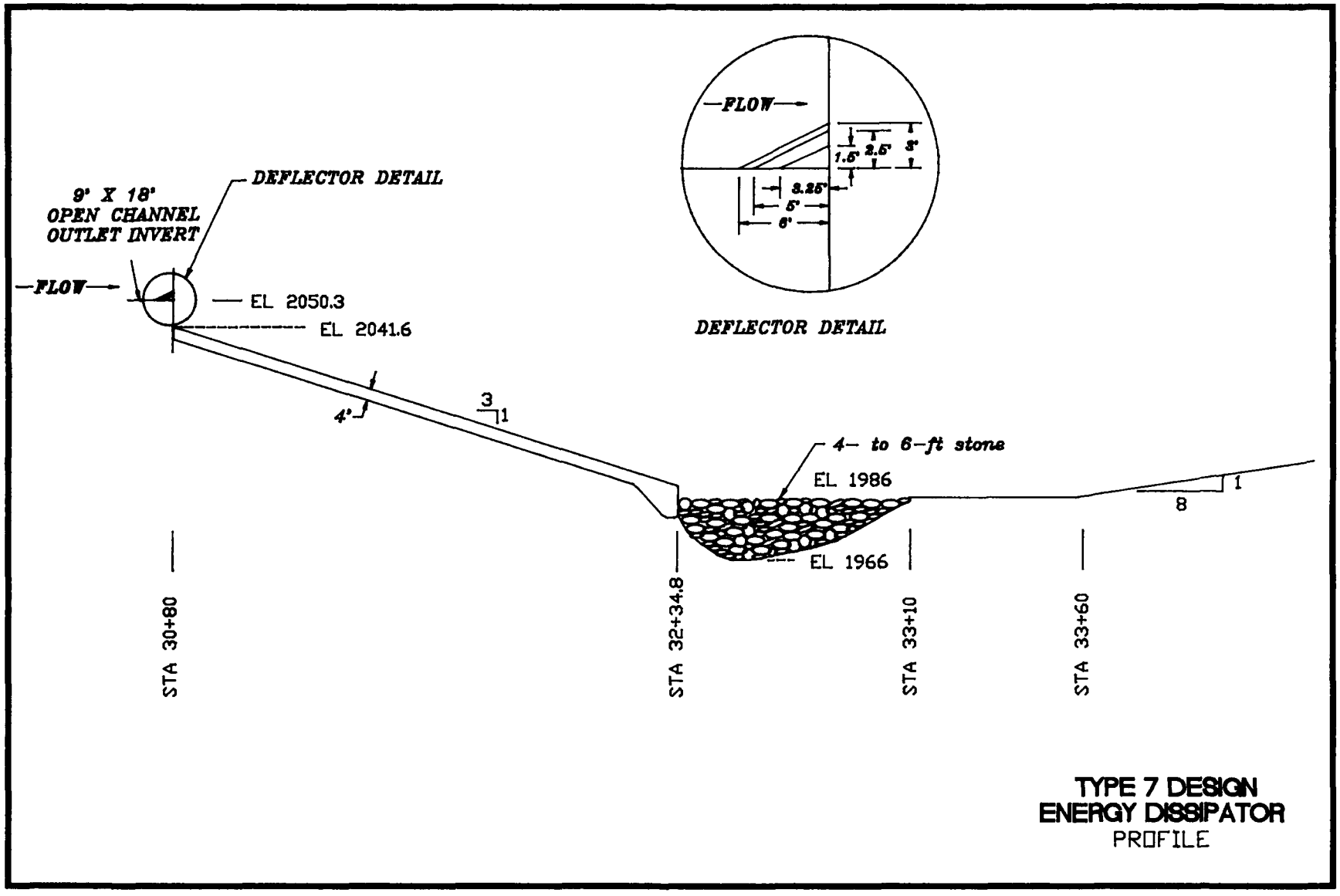

TYPE 7 DESIGN
ENERGY DISSIPATOR
PROFILE

SCOUR CONTOURS
TYPE 7 DESIGN
ENERGY DISSIPATOR
Q = 8,000 CFS, POOL EL 2580, T = 1 HR
41+00
40+00
39+00
38+00
37+00
36+00
35+00
2000
1990
34+00
ROCK
32+00
31+00
1V ON 3H
2010
2010
ACCESS ROAD
FLOW

PLATE 53

PLATE 54

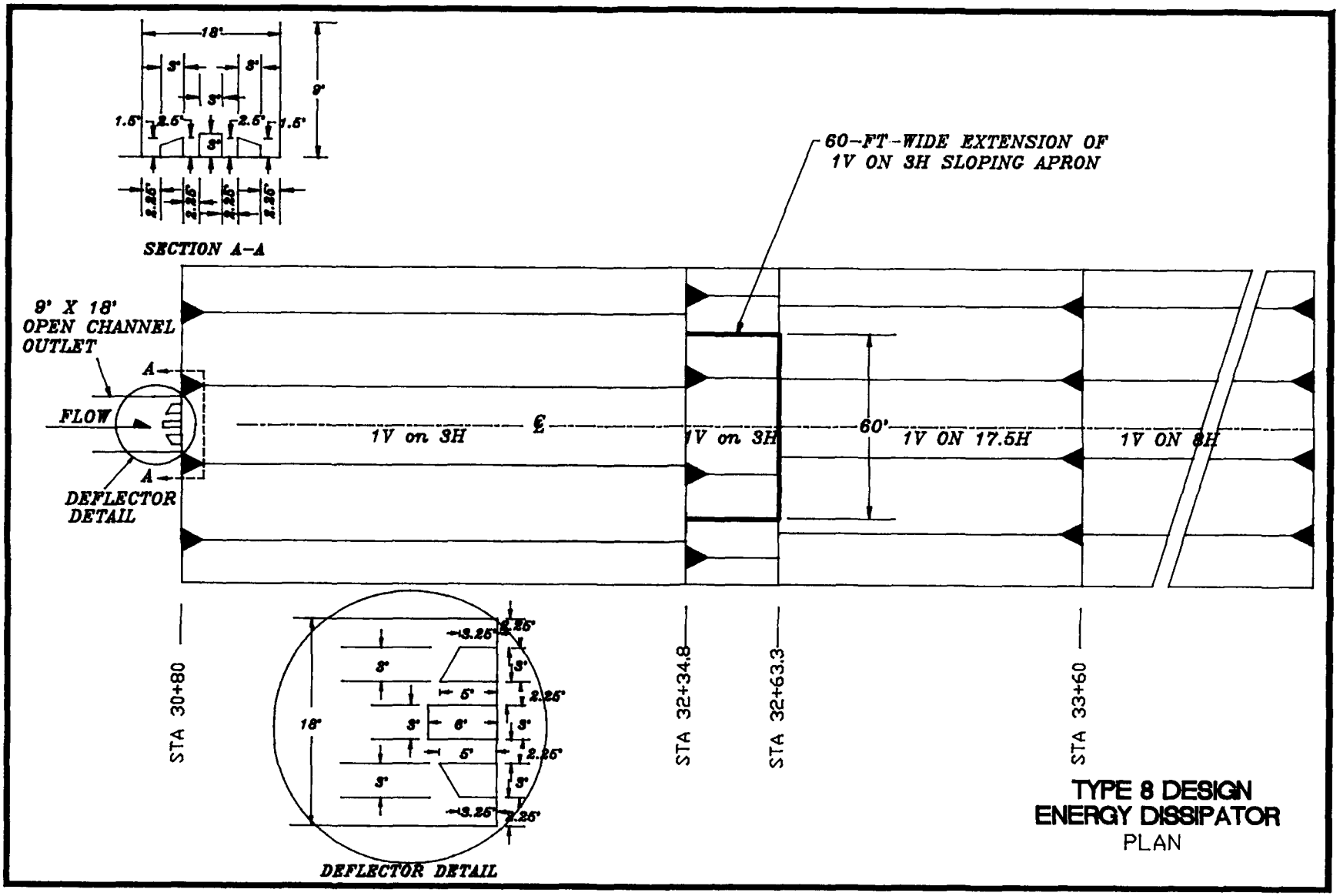
18'
9'
3'
3'
3'
1.5'
2.5'
2.5'
1.5'
9'
2.25'
2.25'
2.25'
2.25'
SECTION A-A
60-FT-WIDE EXTENSION OF
1V ON 3H SLOPING APRON
9' X 18'
OPEN CHANNEL
OUTLET
A
FLOW
A
DEFLECTOR
DETAIL
1V on 3H
℄
1V on 3H
60'
1V ON 17.5H
1V ON 8H
STA 30+80
STA 32+34.8
STA 32+63.3
STA 33+60
18'
3.25'
2.25'
3'
5'
2.25'
3'
6'
3'
5'
2.25'
3'
3.25'
2.25'
DEFLECTOR DETAIL
TYPE 8 DESIGN
ENERGY DISSIPATOR
PLAN

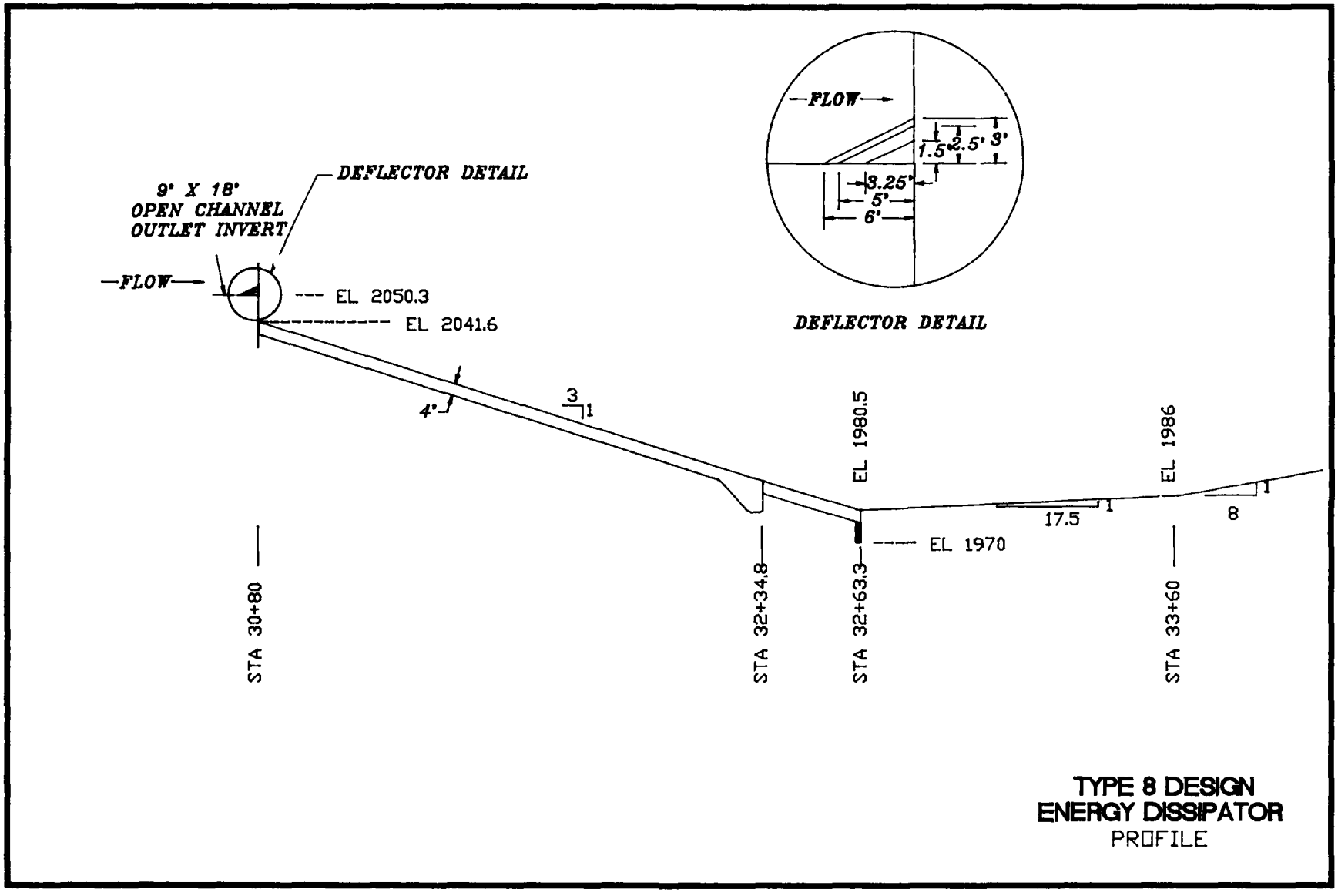
9' X 18'
OPEN CHANNEL
OUTLET INVERT
DEFLECTOR DETAIL
FLOW
EL 2050.3
EL 2041.6
4°
3
1
EL 1980.5
EL 1986
17.5
1
8
EL 1970
STA 30+80
STA 32+34.8
STA 32+63.3
STA 33+60
FLOW
1.5
2.5'
3'
3.25'
5'
6'
DEFLECTOR DETAIL
TYPE 8 DESIGN
ENERGY DISSIPATOR
PROFILE

PLATE 55

PLATE 56

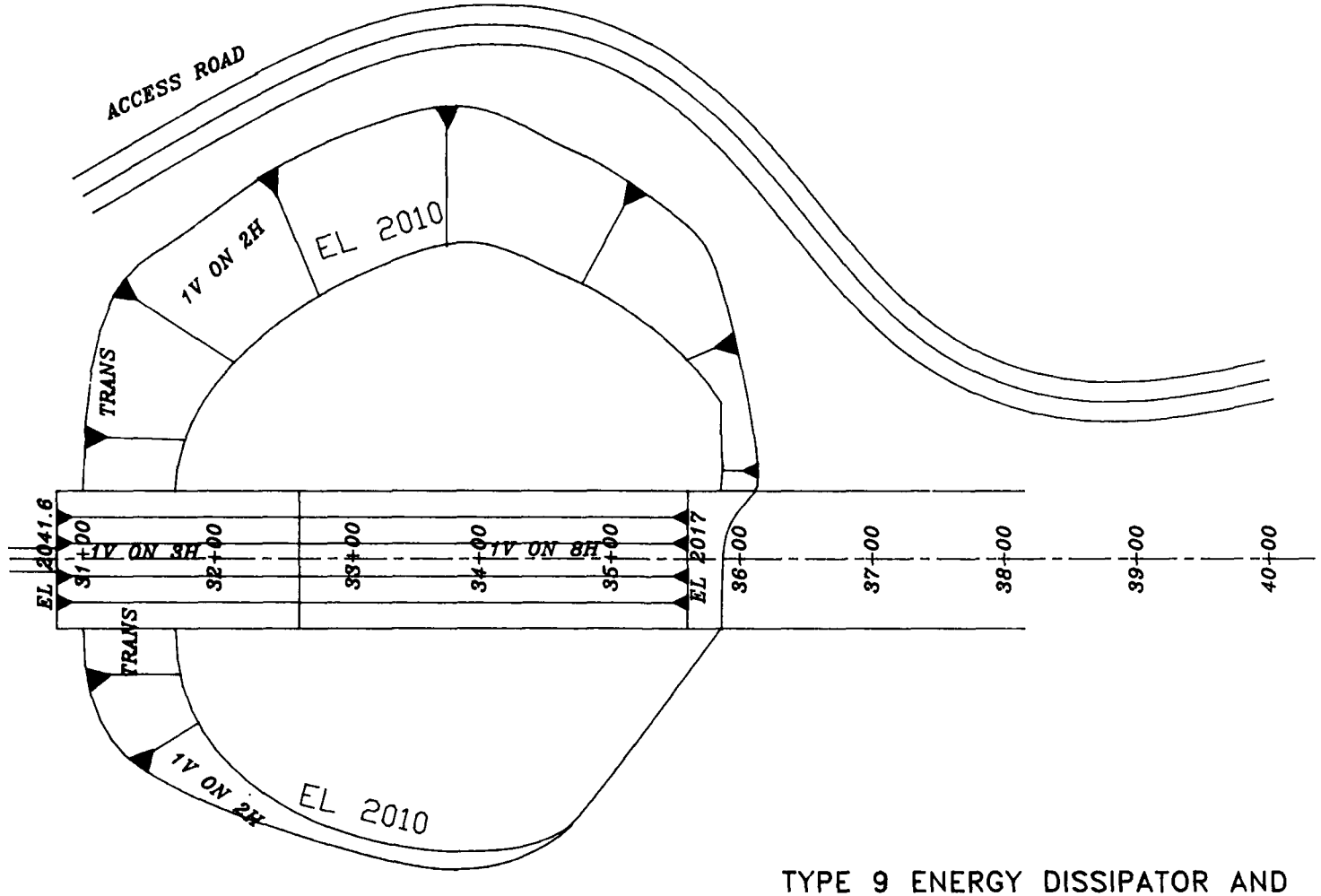

TYPE 9 ENERGY DISSIPATOR AND
PREFORMED SCOUR HOLE
PLAN

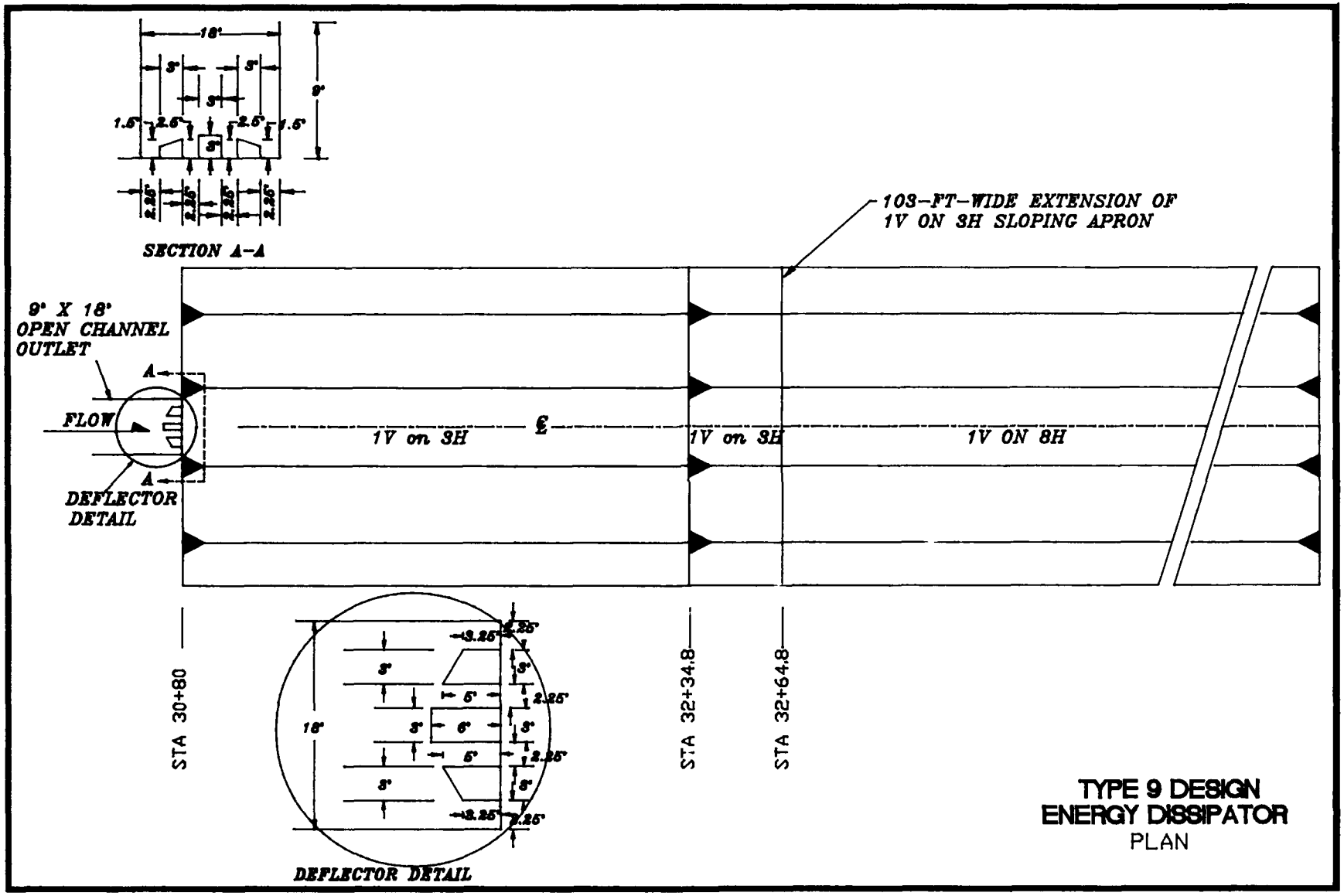
18'
3'
3'
3'
9'
1.5'
2.5'
2.5'
1.5'
3'
2.25'
2.25'
2.25'
2.25'
SECTION A-A
103-FT-WIDE EXTENSION OF
1V ON 3H SLOPING APRON
9' X 18'
OPEN CHANNEL
OUTLET
A
FLOW
A
DEFLECTOR
DETAIL
1V on 3H
℄
1V on 3H
1V ON 8H
STA 30+80
STA 32+34.8
STA 32+64.8
18'
3.25'
2.25'
3'
5'
2.25'
3'
6'
3'
5'
2.25'
3'
3.25'
2.25'
DEFLECTOR DETAIL
TYPE 9 DESIGN
ENERGY DISSIPATOR
PLAN

PLATE 57

PLATE 58

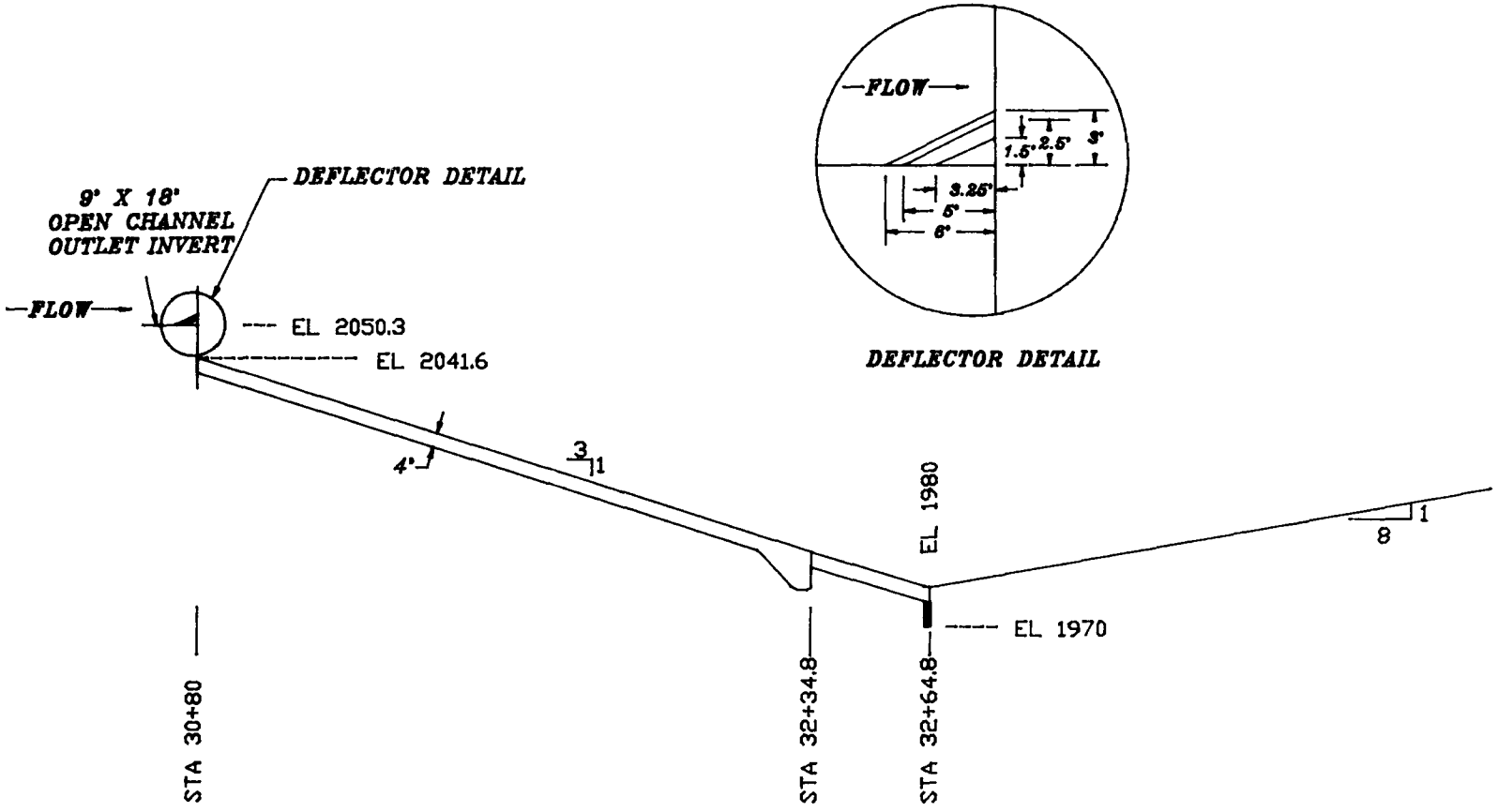

TYPE 9 DESIGN
ENERGY DISSIPATOR
PROFILE

SCOUR CONTOURS
TYPE 9 DESIGN
ENERGY DISSIPATOR
Q = 8,000 CFS, POOL EL 2580, T = 5 HR
40+00
39+00
38+00
37+00
36+00
35+00
2000
1990
34+00
33+00
1980
1976
DEPOSITION
6.25'
32+00
THE NO AI
31+00
2010
2010
10' TO 11'
OF SCOUR
ACCESS ROAD
FLOW

PLATE 59

PLATE 60

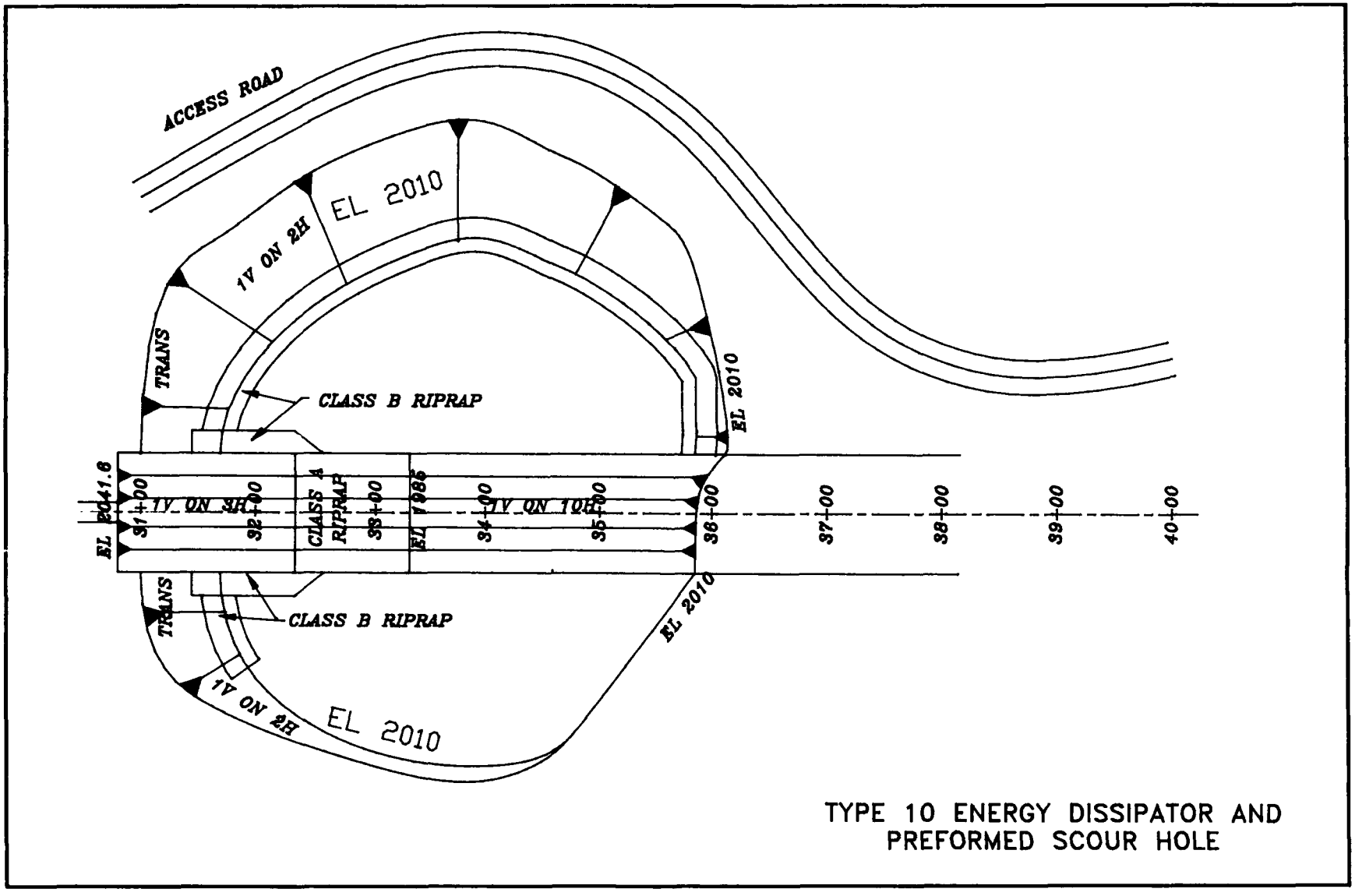

TYPE 10 ENERGY DISSIPATOR AND PREFORMED SCOUR HOLE

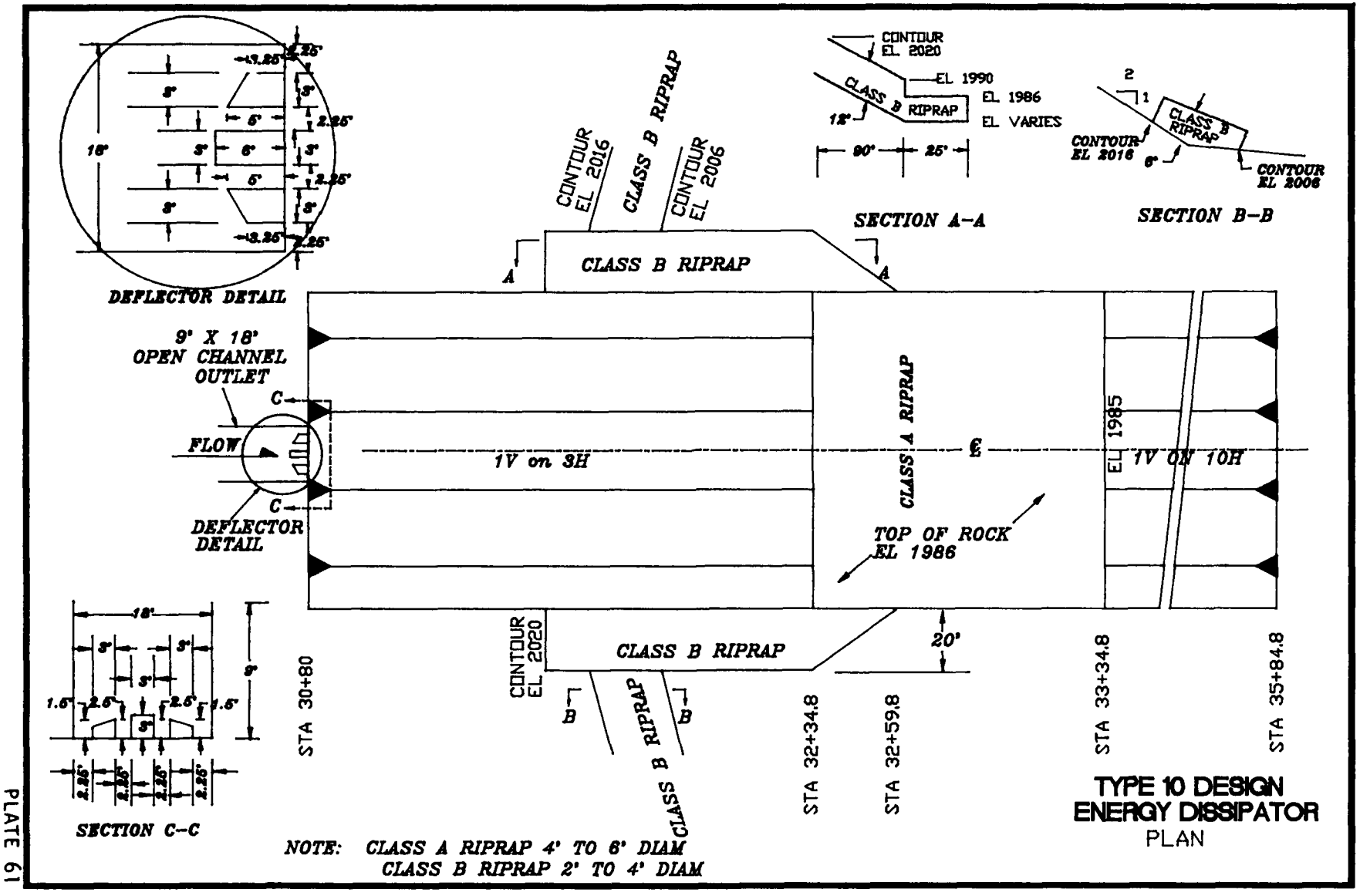
DEFLECTOR DETAIL
9' X 18'
OPEN CHANNEL
OUTLET
FLOW
DEFLECTOR
DETAIL
SECTION C-C
CONTOUR
EL 2016
CLASS B RIPRAP
CONTOUR
EL 2006
CONTOUR
EL 2020
EL 1990
EL 1986
EL VARIES
SECTION A-A
SECTION B-B
CLASS B RIPRAP
CONTOUR
EL 2016
CONTOUR
EL 2006
1V on 3H
CLASS A RIPRAP
EL 1985
1V ON 10H
TOP OF ROCK
EL 1986
CONTOUR
EL 2020
CLASS B RIPRAP
CLASS B RIPRAP
20'
STA 30+80
STA 32+34.8
STA 32+59.8
STA 33+34.8
STA 35+84.8
NOTE: CLASS A RIPRAP 4' TO 6' DIAM
CLASS B RIPRAP 2' TO 4' DIAM
TYPE 10 DESIGN
ENERGY DISSIPATOR
PLAN

PLATE 61

PLATE 62

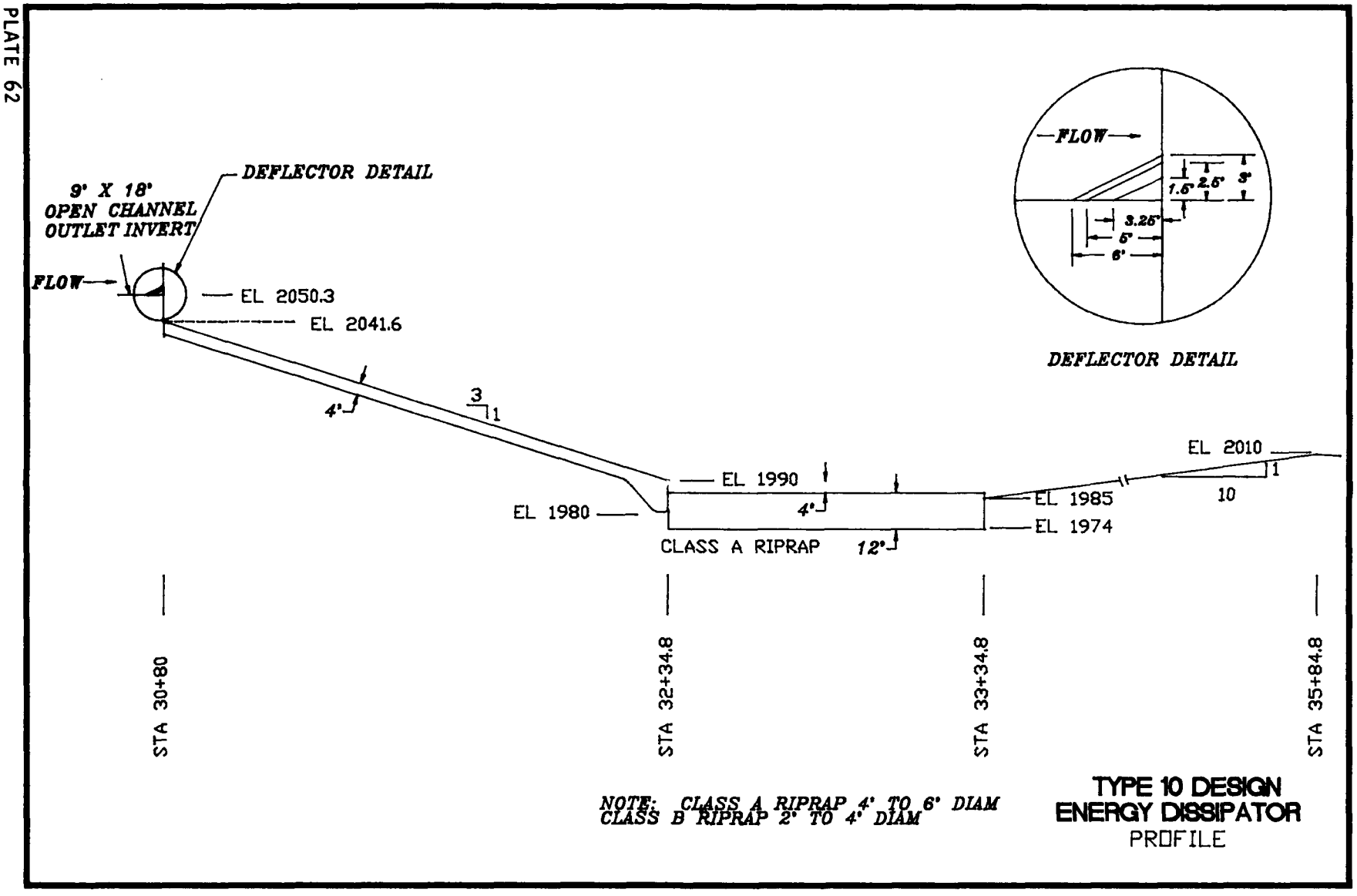
9" X 18"
OPEN CHANNEL
OUTLET INVERT
DEFLECTOR DETAIL
FLOW
EL 2050.3
EL 2041.6
4"
3
1
EL 1990
EL 1980
4"
CLASS A RIPRAP
12"
EL 1985
EL 1974
EL 2010
1
10
STA 30+80
STA 32+34.8
STA 33+34.8
STA 35+84.8
FLOW
1.6"
2.6"
3"
3.25"
5"
6"
DEFLECTOR DETAIL
NOTE: CLASS A RIPRAP 4" TO 6" DIAM
CLASS B RIPRAP 2" TO 4" DIAM
TYPE 10 DESIGN
ENERGY DISSIPATOR
PROFILE

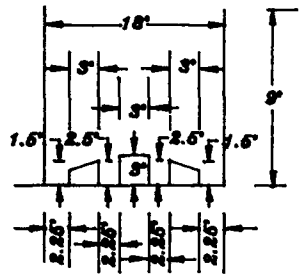

SECTION A–A

9' X 18' OPEN CHANNEL OUTLET

FLOW

A

A

DEFLECTOR DETAIL

1V on 3H

5	10	15	20	25	30	35	40
4	9	14	19	24	29	34	39
3	8	13	18	23	28	33	38
2	7	12	17	22	27	32	37
1	6	11	16	21	26	31	36

4' to 6' diam riprap

CLASS A RIPRAP

105'

℄

100'

STA 30+80

STA 32+34.8

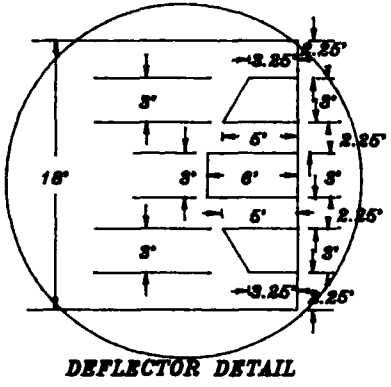

DEFLECTOR DETAIL

NOTE: BLOCKS 1 THROUGH 5 ARE 21' WIDE BY 16.2' LONG BY 4' THICK
ALL OTHER BLOCKS ARE 21' WIDE BY 21' LONG BY 4' THICK

TYPE 1 DESIGN APRON

PLAN

PLATE 63

PLATE 64

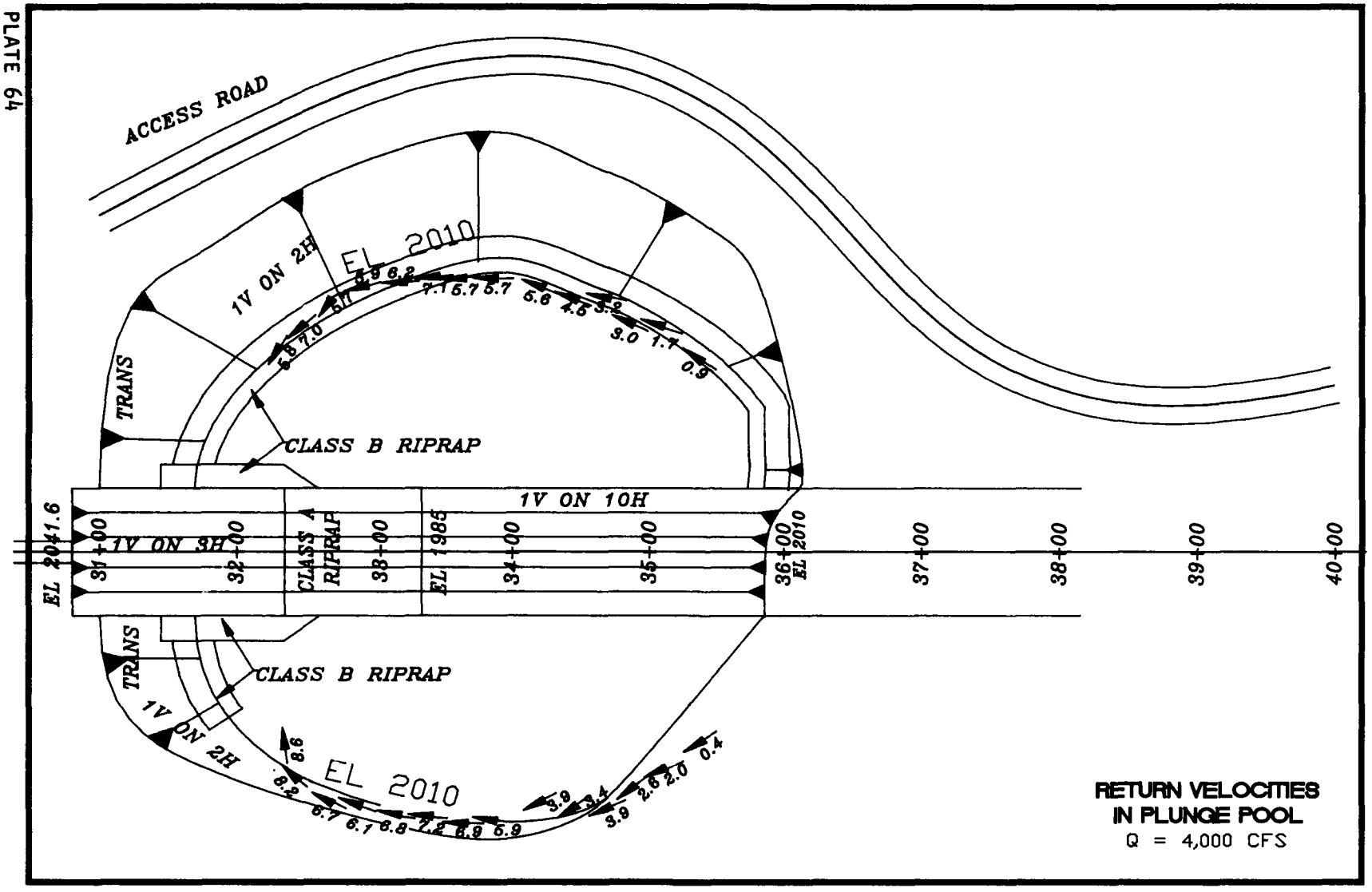
ACCESS ROAD
1V ON 2H
EL 2010
6.9 6.2 7.1 6.7 6.7 5.8 4.6 3.2 3.0 1.7 0.9
5.8 7.0 6.1
TRANS
CLASS B RIPRAP
1V ON 10H
EL 2041.6
30+00
1V ON 3H
32+00
CLASS A RIPRAP
33+00
EL 1985
34+00
35+00
36+00
EL 2010
37+00
38+00
39+00
40+00
TRANS
CLASS B RIPRAP
1V ON 2H
8.6
8.6
EL 2010
6.7 6.1 6.8 7.2 6.9 6.9
3.9 3.4 3.9 2.6 2.0 0.4
RETURN VELOCITIES
IN PLUNGE POOL
Q = 4,000 CFS

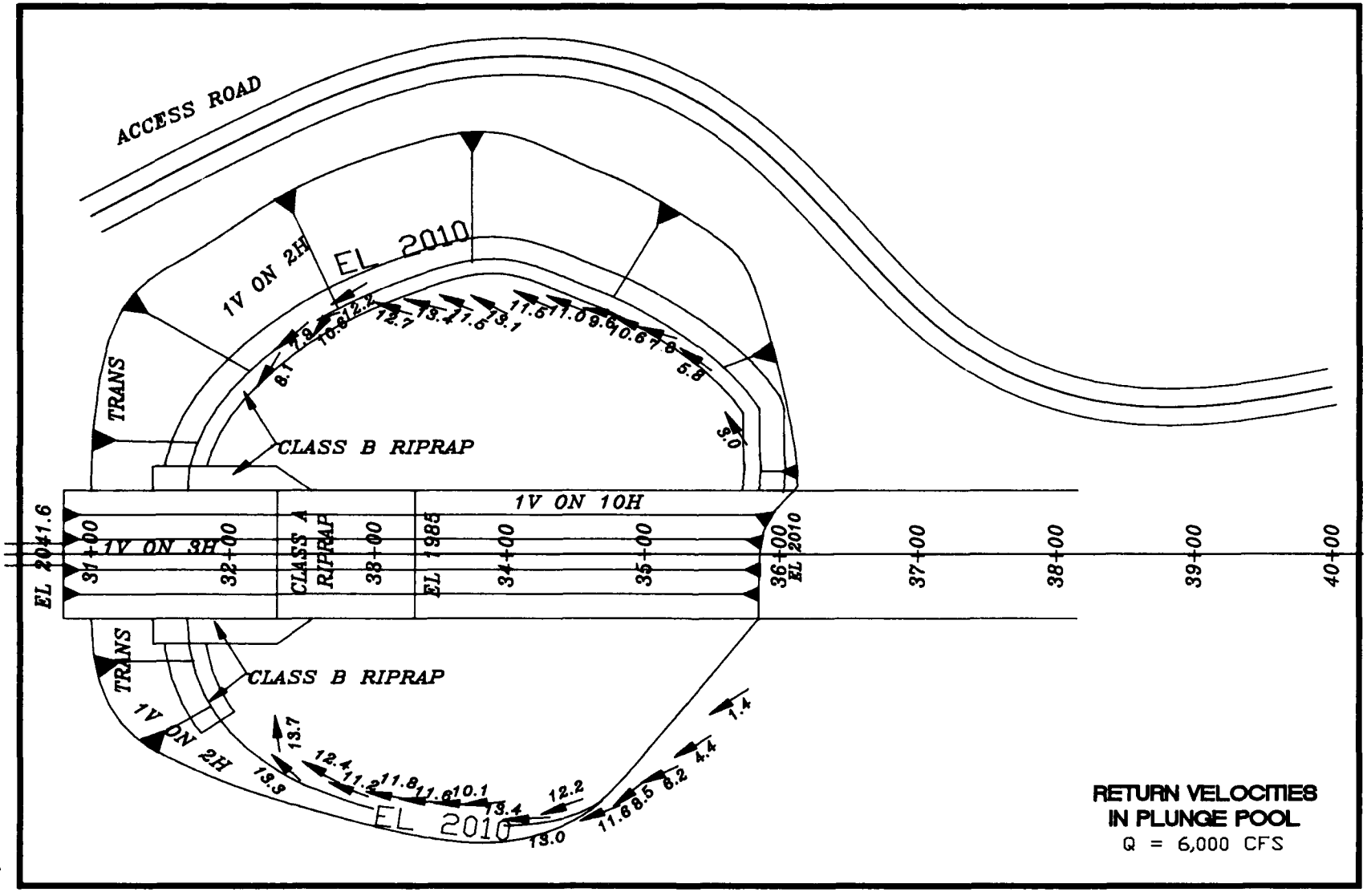
ACCESS ROAD
1V ON 2H
EL 2010
TRANS
CLASS B RIPRAP
1V ON 10H
EL 2041.6
1V ON 3H
31+00
32+00
CLASS A RIPRAP
33+00
EL 1985
34+00
35+00
36+00
EL 2010
37+00
38+00
39+00
40+00
TRANS
CLASS B RIPRAP
1V ON 2H
EL 2010
RETURN VELOCITIES
IN PLUNGE POOL
Q = 6,000 CFS

PLATE 65

PLATE 66

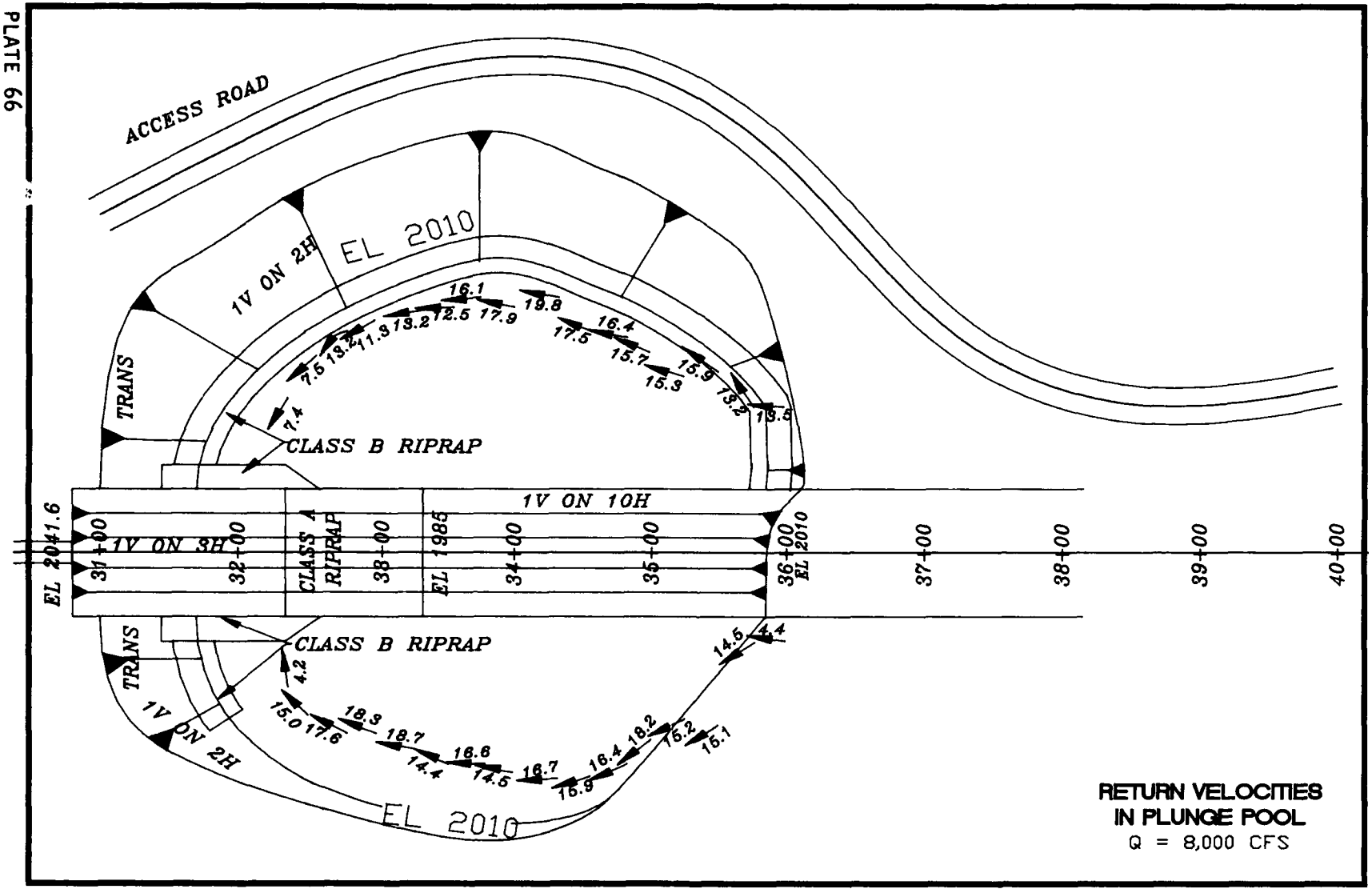
ACCESS ROAD
EL 2010
1V ON 2H
TRANS
7.5 13.2 11.3 13.2 12.5 17.9 16.1 19.8 17.5 16.4 15.7 15.3 15.9 13.2 13.5
7.4
CLASS B RIPRAP
1V ON 10H
EL 2041.6
1V ON 3H
31+00
32+00
CLASS A RIPRAP
33+00
EL 1985
34+00
35+00
36+00
EL 2010
37+00
38+00
39+00
40+00
CLASS B RIPRAP
4.2
TRANS
1V ON 2H
15.0 17.6 18.3 18.7 14.4 16.6 14.5 16.7 16.9 16.4 18.2 15.2 15.1 14.6 4.4
EL 2010
RETURN VELOCITIES
IN PLUNGE POOL
Q = 8,000 CFS

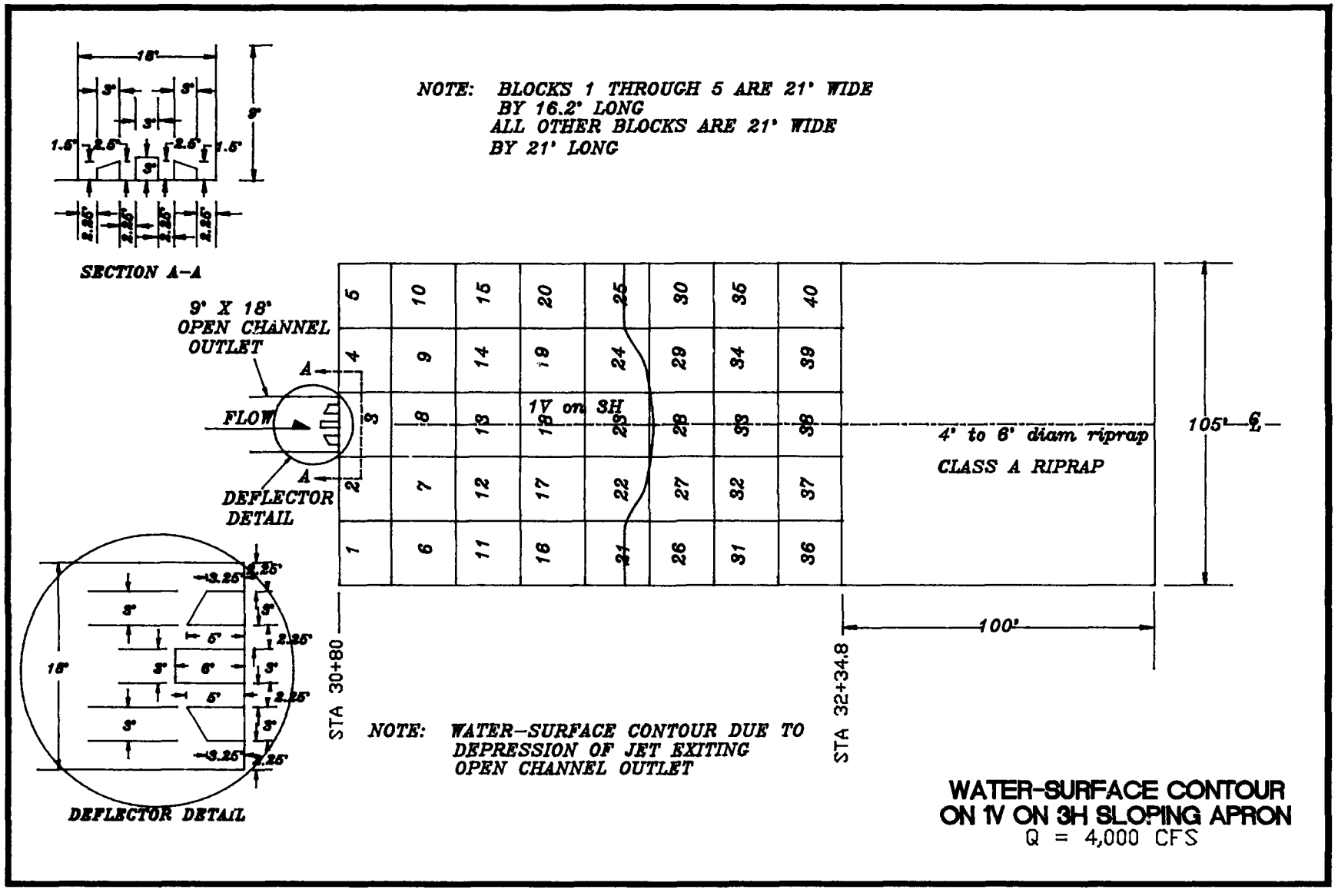

WATER-SURFACE CONTOUR ON 1V ON 3H SLOPING APRON

Q = 4,000 CFS

PLATE 67

PLATE 68

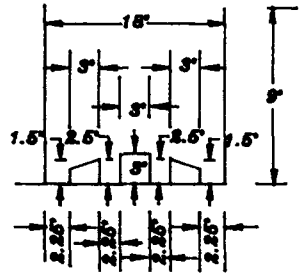

SECTION A-A

NOTE: BLOCKS 1 THROUGH 5 ARE 21' WIDE BY 16.2' LONG
ALL OTHER BLOCKS ARE 21' WIDE BY 21' LONG

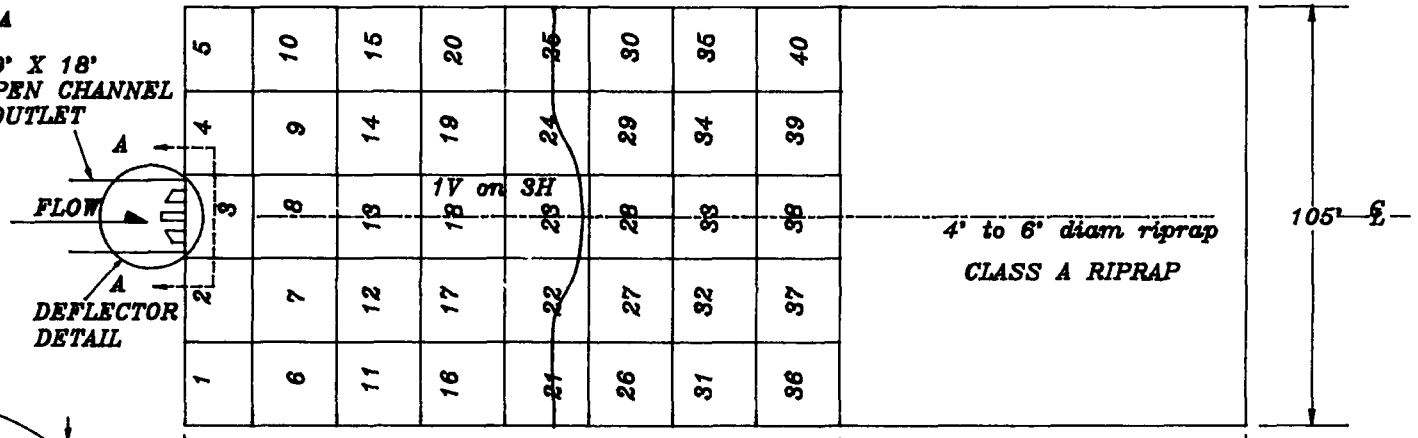

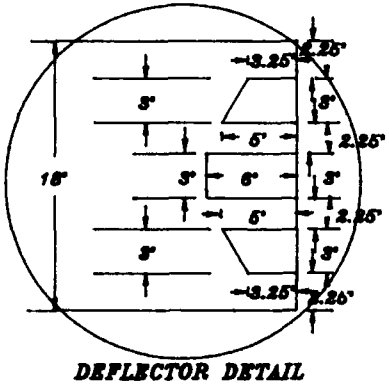

DEFLECTOR DETAIL

NOTE: WATER-SURFACE CONTOUR DUE TO DEPRESSION OF JET EXITING OPEN CHANNEL OUTLET

WATER-SURFACE CONTOUR ON 1V ON 3H SLOPING APRON

Q = 5,000 CFS

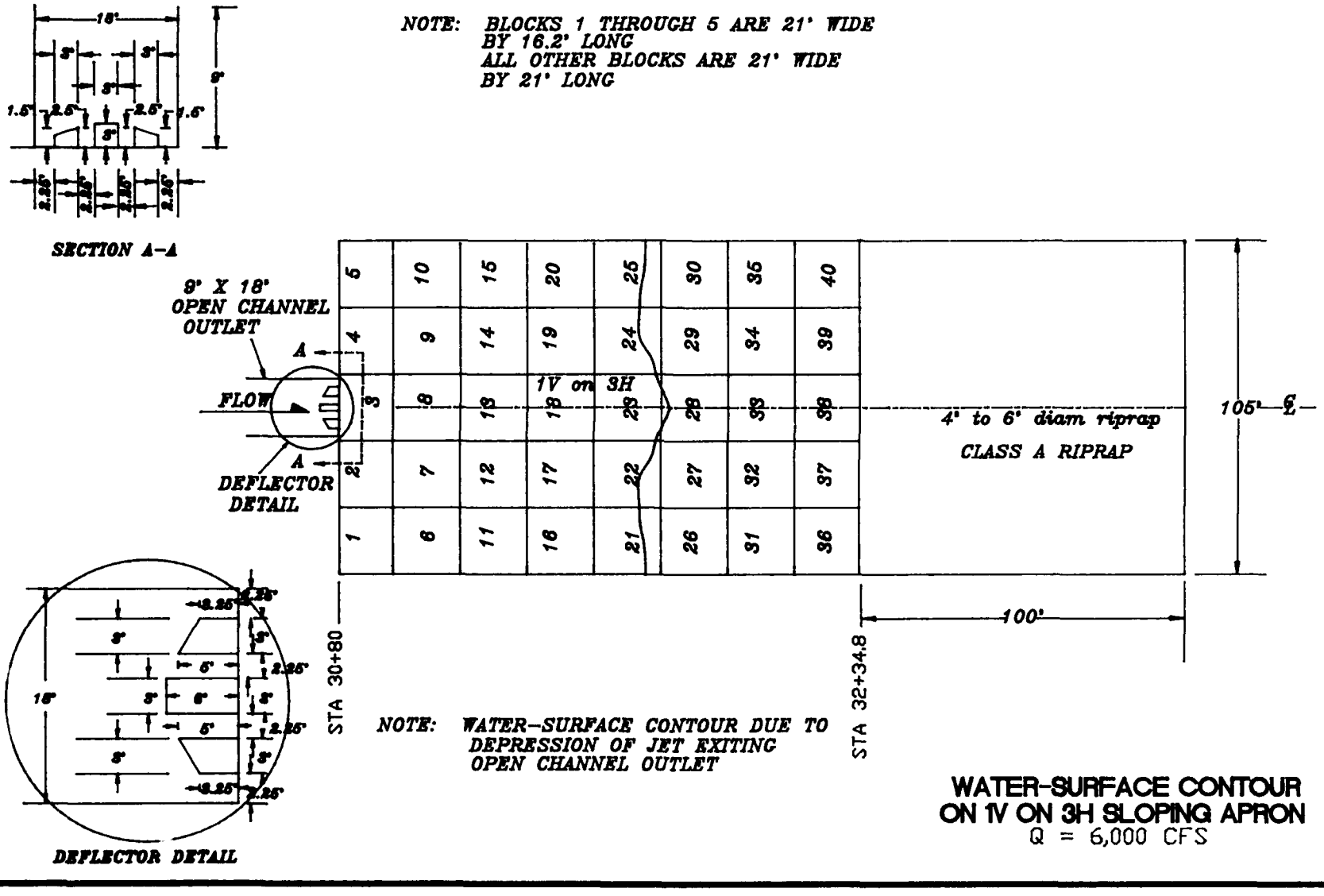

WATER-SURFACE CONTOUR ON 1V ON 3H SLOPING APRON

Q = 6,000 CFS

PLATE 69

PLATE 70

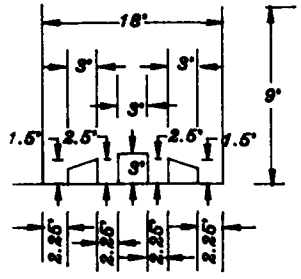

SECTION A-A

NOTE: BLOCKS 1 THROUGH 5 ARE 21' WIDE BY 16.2' LONG
ALL OTHER BLOCKS ARE 21' WIDE BY 21' LONG

9' X 18' OPEN CHANNEL OUTLET

FLOW

A

A

DEFLECTOR DETAIL

1V on 3H

4' to 6' diam riprap

CLASS A RIPRAP

105'

℄

100'

STA 30+80

STA 32+34.8

NOTE: WATER-SURFACE CONTOUR DUE TO DEPRESSION OF JET EXITING OPEN CHANNEL OUTLET

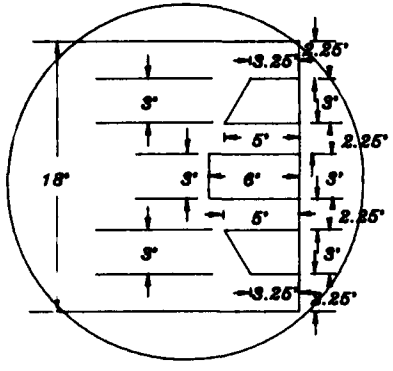

DEFLECTOR DETAIL

WATER-SURFACE CONTOUR ON 1V ON 3H SLOPING APRON

Q = 7,000 CFS

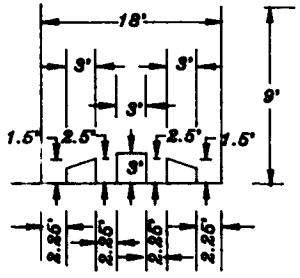

SECTION A-A

NOTE: BLOCKS 1 THROUGH 5 ARE 21' WIDE BY 16.2' LONG
ALL OTHER BLOCKS ARE 21' WIDE BY 21' LONG

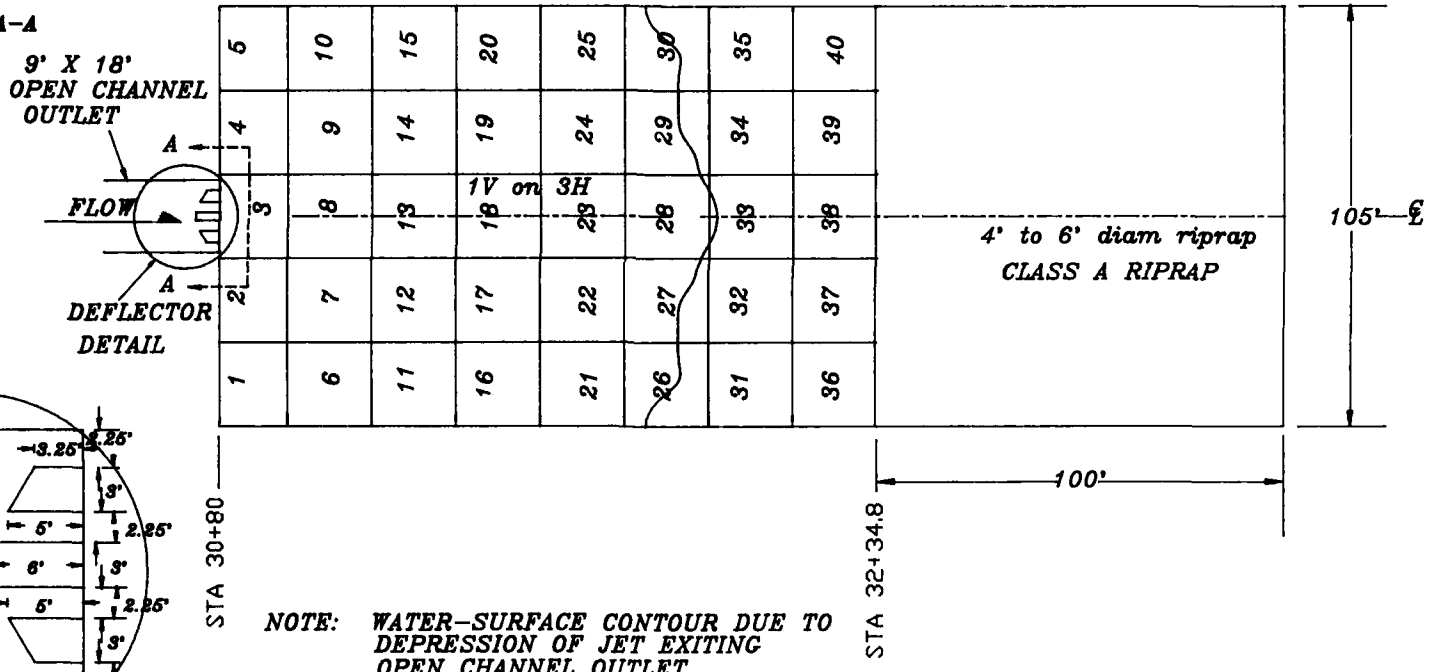

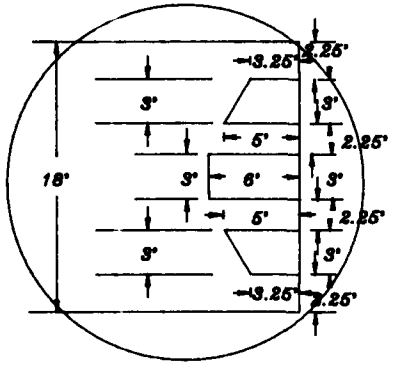

DEFLECTOR DETAIL

NOTE: WATER-SURFACE CONTOUR DUE TO DEPRESSION OF JET EXITING OPEN CHANNEL OUTLET

WATER-SURFACE CONTOUR ON 1V ON 3H SLOPING APRON

Q = 8,000 CFS

PLATE 71

Waterways Experiment Station Cataloging-in-Publication Data

Cooper, Deborah R.
Outlet works for Seven Oaks Dam, Santa Ana River, San Bernardino County, California : hydraulic model investigation / by Deborah R. Cooper ; prepared for US Army Engineer District, Los Angeles.
188 p. : ill. ; 28 cm. — (Technical report ; HL-92-14)
Includes bibliographical references.
1. Dams — California — San Bernardino County -- Environmental aspects — Testing. 2. Scour (Hydraulic engineering) 3. Seven Oaks Dam (Calif) — Models. 4. Hydraulic models. I. United States. Army. Corps of Engineers. Los Angeles District. II. U.S. Army Engineer Waterways Experiment Station. III. Title. IV. Series: Technical report (U.S. Army Engineer Waterways Experiment Station) ; HL-92-14.
TA7 W34 no.HL-92-14